https://doi.org/10.35662/unine-thesis-3064

Faculty of Science

Institute of Biology

Plant Physiology Laboratory

The atypical kinase ABC1K1 / PGR6 allocates geranylgeranyl diphosphate to the carotenoid biosynthesis pathway

A dissertation submitted to the
University of Neuchâtel
For the degree of
Doctor ès Sciences

Presented by

Wayne ZITA

Thesis committee:

Prof. Dr. Felix Kessler (Thesis Director) – University of Neuchâtel, Switzerland

Dr. Shanmugabalaji Ventakasalam (Thesis supervisor) – University of Neuchâtel, Switzerland

Prof. Dr. Theodoor Turlings – University of Neuchâtel, Switzerland

Prof. Dr. Christophe Rothan – University of Bordeaux, France

Defended on May 24th, 2023

Université de Neuchâtel
Faculté des sciences

Rue Emile-Argand 11
CH-2000 Neuchâtel
doctorat.sciences@unine.ch

IMPRIMATUR POUR THÈSE DE DOCTORAT

La Faculté des sciences de l'Université de Neuchâtel autorise l'impression de la présente thèse soutenue par

Monsieur Wayne ZITA

Titre :

"The atypical kinase ABC1K1 / PGR6 allocates geranylgeranyldiphosphate to the carotenoid biosynthesis pathway"

sur le rapport des membres du jury composé comme suit :

- Prof. Felix Kessler, directeur de thèse, Université de Neuchâtel, Suisse
- Dr Shanmugabalaji Venkatasalam, Université de Neuchâtel, Suisse
- Prof. Théodoor Turlings, Université de Neuchâtel, Suisse
- Dr Christophe Rothan, INRAE, Bordeaux, France

Neuchâtel, le 5 juin 2023

Le Doyen, Prof. R. Bshary

Abstract

Crop fruit species play an important role in life on Earth. Indeed, fruits provide essential nutrients and vitamins which are not synthesized by humans but are necessary for their health. The synthesis of these essential nutrients occurs during the complex process of fruit maturation and ripening, orchestrated by regulatory genes, transcription factors, and hormones. During this process, many biological, and physiological events lead to fruit changes and are indispensable for the fruit color, flavor, aroma and quality. In tomato fruit, many of these biological events occur in a colored plastid specialized in carotenoid biosynthesis and sequestration, the chromoplast. The hallmark red color of tomato fruit is due to the synthesis and accumulation of lycopene in a lipoprotein sub-organellar compartment of chloroplasts and chromoplasts called plastoglobule (PG). The hydrophobic core of chloroplast and chromoplast plastoglobules serves as a reservoir and biosynthetic compartment of phytyl esters, prenyl lipids and carotenoids. In the first chapter entitled "Plastoglobules: A hub of lipid metabolism in the chloroplast" (Shanmugabalaji *et al.,* 2022) we reviewed plastoglobule functions and metabolism in different plastid types.

In the second chapter "Chapter II: Chromoplast plastoglobules recruit the carotenoid biosynthetic pathway and contribute to carotenoid accumulation during tomato fruit maturation" (Zita *et al.,* 2022), we used a proteomic approach to investigate plastoglobule proteome remodeling during the chloroplast to chromoplast transition in tomato fruit. This proteomic study revealed that the tomato plastoglobule contains around 30 proteins and members of different enzyme families including fibrillins (FBNs), the activity of BC1 complex kinase (ABC1Ks), tocopherol cyclase (VTE1), NAD(P)H-ubiquinone oxidoreductase C1 (NDC1). The study revealed the presence of the complete carotenoid biosynthesis pathway in chromoplast plastoglobules: phytoene synthase 1 (PSY1), phytoene desaturase (PDS), zeta carotene desaturase (ZDS), carotenoid isomerase (CRTISO), and lycopene beta cyclase (LYC-B). The results show that the plastoglobule becomes a platform for carotenoid biosynthesis during the chloroplast to chromoplast transition. In addition, the lipidomes of chloroplast and chromoplast plastoglobule undergo remodeling during progressive fruit ripening stages. Specifically, β-carotene and lycopene were highly enriched in chromoplast plastoglobules compared to chloroplast plastoglobules. Overall, the chapter demonstrates that the plastoglobule plays a central role in the ripening process.

The third chapter "A quantitative method to measure geranylgeranyl diphosphate (GGPP) and geranylgeranyl monophosphate (GGP) in tomato (*Solanum lycopersicum*) fruit" (Zita *et al.,* 2023), a method to quantify GGPP from tomato fruit tissue was developed using ultra-high performance liquid chromatography coupled with tandem mass spectrometry (UHPLC-MS/MS). The method has been validated by using a wild-type (WT) and mutant matrices defective in GGPP synthesis. In addition, this chapter highlight the importance of sample preparation to preserve the GGPP and limited its conversion to GGP (hydrolyzed product). This method is essential for further analysis in my thesis.

Finally, in the fourth chapter of my thesis “An atypical kinase ABC1K1 allocates geranylgeranyl diphosphate to the carotenoid biosynthesis pathway in plastoglobules of chromoplasts”, I investigate the role of SlABC1K1 in tomato fruit carotenoid metabolism. The CRISPR-Cas9 mutant of SlABC1K1 (*slabc1k1*) showed the photosynthetic PGR6 phenotype in leaves that had previously been observed in Arabidopsis. Surprisingly, *slabc1k1* fruit had an orange phenotype. The *slabc1k1* phenotype was linked to reduced lycopene accumulation as well as that of its phytoene precursor. Based on our results, I propose two possible scenarios for the function of SlABC1K1 in tomato fruit plastoglobules. SlABC1K1 may acts as a key regulator for geranylgeranyl diphosphate (GGPP) allocation to the carotenoid pathway or as a co-regulator of carotenoid biosynthesis enzymes in plastoglobules. The discovery that SlABC1K1 is required for the GGPP allocation to plastoglobule is the principal result of my thesis.

Keywords: Atypical bc1 complex like Kinases (ABC1Ks), Carotenoid pathway, Geranylgeranyl diphosphate (GGPP), Metabolite flux, Plastoglobules (PG), Lycopene.

Résumé

Les espèces fruitières cultivées jouent un rôle important dans la vie sur Terre. En effet, les fruits fournissent des nutriments et des vitamines essentiels qui ne sont pas synthétisés par l'homme mais qui sont nécessaires à sa santé. La synthèse de ces nutriments essentiels a lieu au cours du processus complexe de maturation et de mûrissement des fruits, orchestré par des gènes régulateurs, des facteurs de transcription et des hormones. Au cours de ce processus, de nombreux événements biologiques et physiologiques entraînent des changements dans les fruits et sont indispensables pour la couleur, la saveur, l'arôme et la qualité des fruits. Dans le fruit de la tomate, nombre de ces événements biologiques se produisent dans un plaste coloré spécialisé dans la biosynthèse et la séquestration des caroténoïdes, le chromoplaste. La couleur rouge caractéristique des fruits de la tomate est due à la synthèse et à l'accumulation de lycopène dans un compartiment lipoprotéique sous-organellaire des chloroplastes et des chromoplastes appelé plastoglobule (PG). Le noyau hydrophobe des plastoglobules des chloroplastes et des chromoplastes sert de réservoir et de compartiment de biosynthèse des esters de phytyle, des lipides prényliques et des caroténoïdes. Dans le premier chapitre intitulé "Plastoglobules : A hub of lipid metabolism in the chloroplast" (Shanmugabalaji *et al.,* 2022), nous avons passé en revue les fonctions et le métabolisme des plastoglobules dans différents types de plastes. Dans le deuxième chapitre "Chapter II : Les plastoglobules du chromoplaste recrutent la voie de biosynthèse des caroténoïdes et contribuent à l'accumulation des caroténoïdes pendant la maturation du fruit de la tomate " (Zita *et al.,* 2022), nous avons utilisé une approche protéomique pour étudier le remodelage du protéome des plastoglobules pendant la transition chloroplaste-chromoplaste dans le fruit de la tomate. Cette étude protéomique a révélé que le plastoglobule de la tomate contient environ 30 protéines et des membres de différentes familles d'enzymes dont les fibrillines (FBNs), l'activité du complexe BC1 kinase (ABC1Ks), la tocophérol cyclase (VTE1), la NAD(P)H-ubiquinone oxydoréductase C1 (NDC1). L'étude a révélé la présence de la voie complète de biosynthèse des caroténoïdes dans les plastoglobules du chromoplaste : phytoène synthase 1 (PSY1), phytoène désaturase (PDS), zeta carotène désaturase (ZDS), caroténoïde isomérase (CRTISO), et lycopène beta cyclase (LYC-B). Les résultats montrent que le plastoglobule devient une plateforme pour la biosynthèse des caroténoïdes pendant la transition chloroplaste-chromoplaste. En outre, les lipidomes du chloroplaste et du plastoglobule du chromoplaste subissent un remodelage au cours des étapes de maturation progressive du fruit. En particulier, le β-carotène et le lycopène sont fortement enrichis dans les plastoglobules du chromoplaste par rapport aux plastoglobules du chloroplaste. Dans l'ensemble, ce chapitre démontre que le plastoglobule joue un rôle central dans le processus de maturation. Dans le troisième chapitre "A quantitative method to measure geranylgeranyl diphosphate (GGPP) and geranylgeranyl monophosphate (GGP) in tomato (Solanum lycopersicum) fruit" (Zita *et al.,* 2023), une méthode de quantification du GGPP à partir de tissus de fruits de tomates a été mise au point en utilisant la chromatographie liquide à ultra-haute performance couplée à la spectrométrie de masse en tandem (UHPLC-MS/MS). La méthode a été validée en utilisant un type sauvage (WT) et des matrices mutantes défectueuses dans la synthèse du GGPP. En outre, ce chapitre souligne l'importance de la préparation des échantillons pour préserver le GGPP et limiter sa conversion en GGP (produit hydrolysé). Cette méthode est essentielle pour la suite de l'analyse dans ma thèse. Enfin, dans le quatrième chapitre de ma thèse "An atypical kinase ABC1K1 allocates geranylgeranyl diphosphate to the carotenoid biosynthesis pathway in plastoglobules of chromoplasts", j'étudie le rôle de SlABC1K1 dans le métabolisme des caroténoïdes du fruit de la tomate. Le mutant CRISPR-Cas9 de SlABC1K1 (*slabc1k1*) présente le phénotype photosynthétique PGR6 dans les feuilles qui avait été observé précédemment chez Arabidopsis. De manière surprenante, les fruits de *slabc1k1* présentaient un phénotype orange. Le phénotype *slabc1k1* est lié à une accumulation réduite de lycopène et de son précurseur, le phytoène. Sur la base de nos résultats, je propose deux scénarios possibles pour la fonction de SlABC1K1 dans les plastoglobules des fruits de tomate. SlABC1K1 peut agir comme un régulateur clé pour l'allocation du géranylgéranyl diphosphate (GGPP) à la voie des caroténoïdes ou comme un co-régulateur des enzymes de biosynthèse des caroténoïdes dans les plastoglobules. La découverte que SlABC1K1 est nécessaire pour l'allocation du GGPP au plastoglobule est le principal résultat de ma thèse.

Mots-clés : Kinases atypique similaires au complexe bc1 (ABC1Ks), Caroténoïdes, Geranylgeranyl diphosphate (GGPP), Flux de métabolites, Plastoglobules (PG), Lycopène.

Table of contents

5. An atypical kinase ABC1K1 allocates geranylgeranyl diphosphate to the carotenoid biosynthesis pathway in plastoglobules of chromoplasts 121

Abbreviations

ATP	adenosine triphosphate
ABC1K	activity of bc1 complex 1-like kinase
CRTISO	carotenoid isomerase
CO_2	carbon dioxide
Cyt	cytochrome
DGDG	digalactosyldiacylglycerol
DMPBQ	dimethylphytylbenzoquinone
ET	ethylene
ETC	electron transport chain
e-	electron
FAPE	fatty acid phytyl
FAR	far-red
FM	maximum fluorescence in dark-adapted state
F0	minimum fluorescence in dark-adapted state
FV	variable fluorescence in dark-adapted state
FM’	maximum fluorescence in light
FS	steady-state chlorophyll fluorescence in light
FNR	ferredoxin NADP+ reductase
GGP	geranylgeranyl monophosphate
GGPP	geranylgeranyl diphosphate
H2O	water
HL	high light
HPLC	high-performance liquid chromatography
kDa	kilodaltons
LCYB	lycopene beta-cyclase
LHC	light-harvesting complex
MGDG	monogalactosyldiacylglycerol
ML	moderate light
NADP(H)	nicotinamide adenine dinucleotide phosphate
NPQ	non-photochemical quenching
O2	molecular oxygen
PC-8	plastochromanol-8
PDS	phytoene desaturase
PG	plastoglobule
PGR	proton gradient regulation
PQ	plastoquinone
PQH2	plastoquinol
PQ-OH	hydroxyplastoquinone
PSI	photosystem I
PSII	photosystem II
PSY1	phytoene desaturase 1
PTOX	plastid terminal oxidase

P680	photosystem II special chlorophyll *a* pair
P700	photosystem I special chlorophyll *a* pair
QA	plastoquinone strongly bounds to photosystem II reaction center
QB	plastoquinone exchange site at photosystem II reaction center
qE	energy- or pH-dependent quenching
qI	photoinhibitory quenching
qZ	zeaxanthin-dependent quenching
ROS	reactive oxygen species
TAG	triacylglycerol
TF	transcription factor
TMPBQ	trimethylphytylbenzoquinone
α-TQ	alpha-tocopherol quinone
WT	wild type
ZEP	zeaxanthin epoxidase
Z-ISO	zeta carotene isomerase
ΦMAX	maximum photosystem II efficiency
ΦPSII	photosystem II quantum yield

1. General Introduction

1.1 Plastids: a versatile organelle family

The Earth as we know it could have been very different without the presence of plastids. In fact, oxygen-depending life would have been simply impossible.

There is general agreement about the ancient endosymbiotic origin of plastids, which originated from a cyanobacterial ancestor and a eukaryotic host cell, approximately 1.5 billion years ago. Plastids are ubiquitously found in algae and plant cells. Whereas plants only have a primary plastid, three categories of plastids, primary, secondary, and tertiary, can be distinguished in certain protists which differ in the number of surrounding membranes resulting from sequential endosymbiotic events (Larkum *et al.,* 2007). Plastids may take on various sizes, shapes, and functions (Jarvis and López-Juez, 2013; W W Thomson and Whatley, 1980) (FIG 1). They are responsible for many biological, molecular, and biochemical processes, providing a wide variety of compounds essential to life (Bartley and Scolnik, 1995). Apart from their endosymbiotic origin, plastids share several common aspects with mitochondria, in that both are semi-autonomous organelles containing their own genome together with a genetic machinery and are surrounded by a double membrane (Allen, 2003).

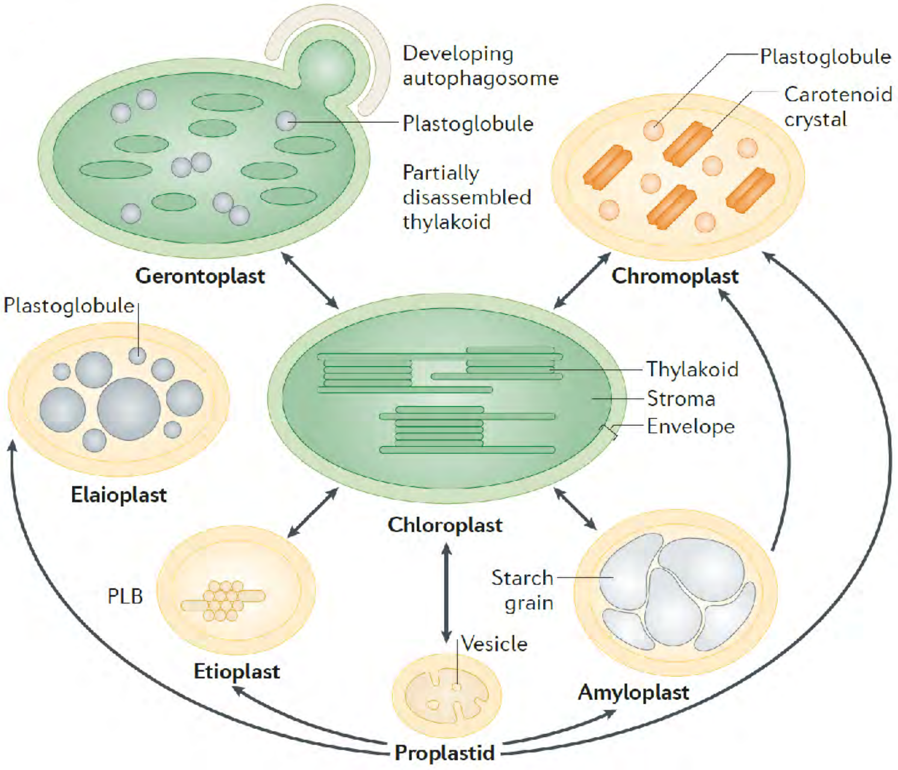

FIG 1| **Interconversion of plastid types.** Plastids adopt various forms and types, according to the developmental stage and environmental conditions. The solid arrows indicate plastid conversions. PLB: prolamellar body. Figure and legend were adapted from (Jarvis and López-Juez, 2013).

1.2 Plastid types: differentiation and conversions

Proplastids are malleable organelles that have the capacity to develop into specialized plastid types depending on plant developmental stage, environment, and tissue (FIG 1). Specialized plastid types are **chloroplasts** (performing photosynthesis), **chromoplasts** (containing carotenoids), **gerontoplasts** (senescing chloroplast), **amyloplasts** (storing starch), **elaioplasts** (storing lipids), and **etioplasts** (differentiating chloroplast in the dark) development derived from the **proplastid** (undifferentiated plastid) (Howe *et al.,* 2008; Jarvis and López-Juez, 2013; Whatley, 1979). In many fruit types, chloroplasts are converted to chromoplast during ripening.

1.3 The chloroplast: the photosynthetic plastid

The chloroplast is the photosynthetic organelle found in plant and algal cells and is probably the most-studied plastid type. Photosynthesis is their primary energy source. It consists of the conversion of sunlight into chemical energy and assimilated carbon. Light energy from the sun is used to oxidize water to ultimately form carbohydrates as described in the following equation:

$$CO_2 + H_2O \rightarrow C(H_2O) + O_2 \qquad (1)$$

This bioenergetic process, at the origin of aerobic life on Earth, takes place exclusively in chloroplasts of plants and algae as well as free-living cyanobacteria (Schmetterer, 1994). The chloroplast contains pigments that allow the capture of light at specific wavelengths in the visible light range. The most common ones in plants are chlorophyll a/b, xanthophylls, and carotenoids. Chlorophylls are the main pigments involved in light-harvesting and drive photosynthesis (Guaus *et al.,* 2017).

Chloroplasts have three distinct membrane systems. The envelope consists of two lipid bilayers, forming an outer and inner membrane. The outer membrane is composed of 48% phospholipids, 46% galactolipids, and 6% sulfolipids, the inner membrane contains 16% phospholipids, 79% galactolipids, and 5% sulfolipids (Block *et al.,* 1983). An extensive internal network of membranes known as thylakoid membranes is surrounded by a liquid phase, the stroma.

1.4 Thylakoids: a membrane network involved in photosynthesis

The thylakoid membrane consists of 70-80% galactolipids, 4% sulfolipids, and 10% phospholipids (Mechela *et al.,* 2019; Nielsen *et al.,* 1979). The thylakoid membrane hosts the primary light-driven reactions of photosynthesis which involve photosystem II (PSII) and photosystem I (PSI), as well as the Cyt b_6f complex. Intersystem electron transport relies free electron carriers: plastoquinone (PQ), a small hydrophobic quinone in the thylakoid membrane and plastocyanin (PC), a soluble, copper-containing protein in the thylakoid lumen (Rochaix, 2011). Two distinct light reactions are sequentially mediated by the photosystems II and I and require red and far red light, respectively (Emerson *et al.,* 1957)(FIG 2). The PSII complex core consists of two reaction center proteins (D1 (PsbA) and D2 (PsbD)), and two core antenna proteins CP43 (PsbC) and CP47 (PsbB). The three hydrophilic subunits of the oxygen-evolving complex (PsbO, PsbP and PsbQ) are associated with membrane-extrinsic lumenal side of PSII (Ifuku *et al.,* 2010). The PSI reaction center has two major subunits at its core (PsaA and PsaB), around 90 chlorophyll-*a* molecules, 1 phylloquinone (vitamine K1) molecule and iron sulfur cluster (2Fe-2S, Fe-S protein ferredoxin). PSII and PSI reaction centers have special reaction center chlorophyll a molecules, P680 and P700 respectively. The two photosystems are physically separated, PSII being located mainly in the grana membrane stacks, while PSI is found predominantly in stroma lamellae. Electron flow is initiated by light-induced water oxidation by the oxygen evolving complex and results in the reduction of the electron carrier plastoquinone to plastoquinol at PSII (Johnson, 2016; Rochaix, 2011). Plastoquinol delivers electrons to the cytochrome b_6f complex which in the following reduces plastocyanin in the thylakoid lumen. Plastocyanin in turn is oxidized by PSI, the electrons ultimately being used to reduce the stromal electron carrier ferredoxin (Fd). Fd in turn is used by the ferredoxin $NADP^+$reductase (FNR) to reduce nicotinamide adenine dinucleotide phosphate ($NADP^+$) to NADPH in the final electron transfer reaction. These electron transfer reactions due to the water-splitting and PQH_2 oxidation result in a H+ gradient across the thylakoid membrane. The ATP synthase, another complex of the thylakoid membrane exploits this gradient by coupling the flux of H^+ from the thylakoid lumen to the stroma to ATP synthesis from adenosine diphosphate (ADP^+) and inorganic phosphate (Pi). This phosphorylation step is mechanistically similar to oxidative phosphorylation occurring in the inner mitochondrial membrane during respiration (Johnson, 2016). In the context of my thesis it is important to note that much of the plastoquinone is stored in and allocated to the thylakoid membrane by a lipid droplet-like sub-compartment known as plastoglobule (PG). The plastoglobule and the associated atypical kinases ABC1K1 and -K3 contribute to plastoquinone homeostasis (see below 5.2) and have a crucial role in photosynthesis (Pralon *et al.,* 2019).

1.4.1 NPQ: regulatory mechanisms of photosynthesis

Plants are sessile photosynthetic organisms that need light for growth, and to survive. They have to quickly adapt to environmental change. Thus, the photoprotection via the non-photochemical chlorophyll fluorescence quenching (NPQ), is a vital and dynamic control mechanism of light harvesting adopted by photosynthetic organisms to prevent damage to their photosynthetic apparatus in oxygenic photosynthesis. Under excess light, NPQ dissipates excess energy as heat (Külheim *et al.,* 2002; Rochaix, 2011; Ruban and Murchie, 2012). At least three components of NPQ have been identified, according to different timescales of induction and relaxation. The qE (very fast activation and relaxation: dissipation of excess energy as heat) which is triggered by the transthylakoid proton gradient. The mechanism of NPQ implicates chemical changes of carotenoids at the level of light-harvesting complex LHCII antenna that are triggered by a variation in pH (ΔpH) (P. Horton *et al.,* 1996; Strand and Kramer, 2014). Excess light leads to an acidification of the thylakoid lumen which leads to protonation of PsbS acting as a sensor allowing a prompt response to increasing ΔpH and initiating qE (Ruban and Murchie, 2012). Meanwhile, as a result of PsbS protonation, the xanthophyll cycle is activated by the conversion of violaxanthin to antheraxanthin and zeaxanthin by the violaxanthin de-epoxidase (Ruban, 2012; Ruban and Murchie, 2012). Violaxanthin and zeaxanthin, known as quencher pigments, dissipate the energy harvested by the LHCII antenna in the form of heat (Ruban, 2012). This mechanism assures retro-control over light harvesting efficiency in the photosynthetic membrane (Strand and Kramer, 2014). The qT (moderate relaxation: also known as state transitions), relaxes within minutes, and qI (slowest relaxation: known as photoinhibitory quenching) relaxes very slowly (Külheim *et al.,* 2002; Nilkens *et al.,* 2010; Zhao *et al.,* 2016).

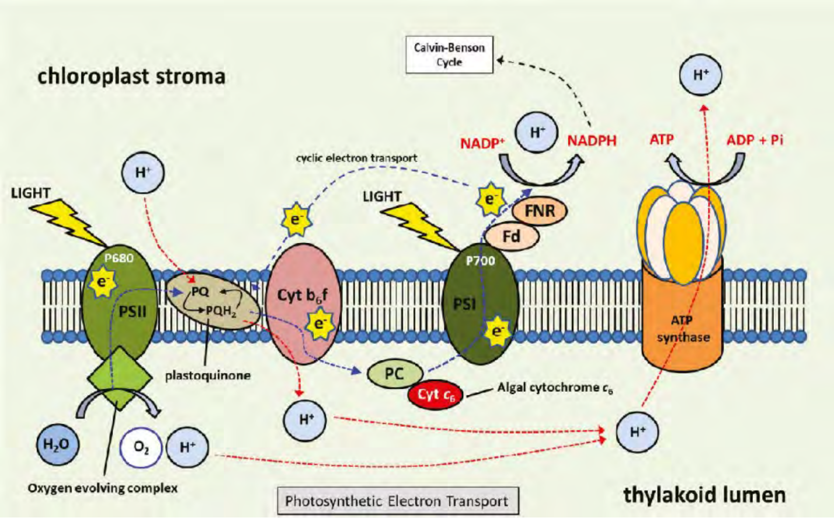

FIG 2| **Schematic illustration of photosynthetic electron transport.** Photosystem II, I (PSII andPSI), plastoquinone (PQ), plastoquinol (PQH2), ferredoxin (Fd), ferredoxin-NADP+ reductase (FNR), cytochrome b6f complex (Cyt b6f), plastocyanin (Rodríguez-Concepción et al.), cytochrome c6 (Cyt c6). Figure 2 was adapted from (Simkin et al., 2019).

1.4.2 Plastoglobules, lipoprotein particles in plastids

PG consist of a core of neutral lipids surrounded by a membrane lipid monolayer studded with a small number of proteins. Chloroplast PG are primarily associated with the thylakoid membranes and function in metabolism and storage of thylakoid lipids (Rey *et al.,* 2000). Regarding their chemical composition, chloroplast PG contain different types of prenyl lipids as well as other neutral lipids. These include α-tocopherol, plastoquinone, phylloquinone, fatty acid phytol esters, and triacylglycerol (Gaude *et al.,* 2007; Lohscheider *et al.,* 2016; van Wijk and Kessler, 2017). PG are not simply passive lipid storage sites but also contribute to lipid metabolism owing to the presence of specific enzymes (Austin *et al.,* 2006; Lundquist *et al.,* 2012; Peltier *et al.,* 2004; Vidi *et al.,* 2006).

PG also plays an active role in plastid differentiation, i.e, chloroplast to chromoplast transition. The enzymes are part of a PG core proteome that is composed of about 30 proteins (Lundquist *et al.,* 2012; Vidi *et al.,* 2006). The PG proteome consists essentially of three groups of proteins:

1) **Structural proteins:** fibrillins (FBNs) also known as plastoglobulins.

2) **Enzymes** involved in wide range of lipid metabolic pathways (plastochromanol and tocopherol biosynthesis (VTE1); phylloquinone biosynthesis (NDC1); fatty acid phytyl ester synthesis (PES1 and -2); and carotenoid metabolism, CCD4, ZDS and LYC-β (see below 4.4).

3) **Regulatory proteins** (ABC1Ks, Activity of BC1 complex-like kinases).

There are a total of 13 fibrillins (FBN), also called plastoglobulins amongst them FBN1a. FBN1a is also known as chromoplast-specific carotenoid-associated protein (CHRC) or Plastoglobulin 35 (PGL35) and is a widely accepted PG marker (Vishnevetsky *et al.,* 1996). FBN are thought to participate in the formation and structural stabilization of PG. The presence of a conserved lipocalin-like motif suggests a role of fibrillins in the binding or trafficking of small hydrophobic metabolites. It is important to note that not all fibrillins are associated with PG and FBN5, for instance, plays an essential role in activating solanesyl diphosphate synthase 1 and 2 (required for plastoquinone biosynthesis) in the stroma. In apple, the *fbn4* knock-down, showed a dramatic decrease of plastoquinone in PG, which directly affected stress sensitivity of the *fbn4* knock-down (Singh *et al.,* 2012). The highly conserved lipocalin domain in FBN4 and other FBN family members, might therefore play important roles in the trafficking of plastoquinone and other lipids (Singh *et al.,* 2012).

During senescence, PG contribute to dismantling of the thylakoid membrane network by the action of phytyl ester synthases PES1 and -2 which are responsible for the formation of FAPE and TAG accumulate in PG in Arabidopsis (Lippold *et al.,* 2012). In tomato, PALE YELLOW PETAL 1 (PYP1), a PES homologo, is required for the synthesis of colored carotenoid esters in petal chromoplasts (Ariizumi *et al.,* 2014).

CAROTENOID CLEAVAGE DIOXYGENASE 4 (CCD4) cleaves carotenoids during senescence in chloroplasts and seed development.

The tocopherol cyclase (VTE1, vitamin E deficient 1) is a key enzyme in vitamin E synthesis. VTE1 catalyzes the formation of the chromanol ring in 2,3-dimethyl-5-phytyl-1,4-hydroquinol (DMPQ) resulting in γ-tocopherol (Porfirova *et al.,* 2002).

NDC1 is a multifunctional NAD(P)H-dependent quinone reductase. This enzyme belongs to the green cut and has been conserved from cyanobacteria. It plays a role in maintaining plastoquinone in a reduced state and has also been shown to be essential for phylloquinone biosynthesis (Eugeni Piller *et al.,* 2011).

The Activity of BC1 complex-like kinases are conserved from bacteria (UbiB) to plants (ABC1Ks and animals (COQ8) and form a small family of proteins (see chapter 5 for a detailed description). Plants possess mitochondrial as well as chloroplast homologs. A majority of the chloroplast ABC1Ks are associated with plastoglobules (FIG 3).

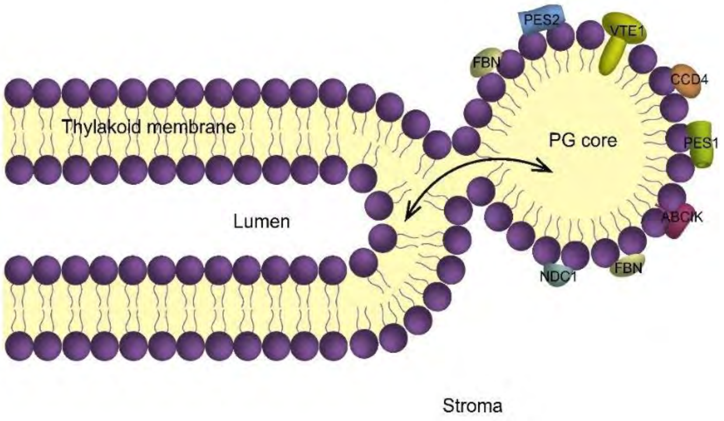

FIG 3| **Schematic representation of the thylakoid membrane and an associated plastoglobule.** Plastoglobule bud from the external lipid layer of the thylakoid membrane. Fibrillin (FBN), phytyl ester synthase 1 and 2 (PES1 and PES2), tocopherol cyclase (VTE1), carotenoid cleavage dioxygenase 4 (CCD4), the activity of BC1 complex like kinases (ABC1K) and NAD(P)H-oxidoreductase C1 (NDC1). Adapted from (Rottet *et al.,* 2015).

1.5 The chromoplast: a plastid specializing in carotenoid biosynthesis.

Chromoplasts are specialized non-photosynthetic plastids that have the ability to synthesize and accumulate high amounts of carotenoids and xanthophylls, responsible for the yellow, orange and red color of flowers, certain roots, and fruits (Lopez-Juez and Pyke, 2005).

1.5.1 Fruit ripening

Fruit development in tomato (*Solanum lycopersicum*) is a good model to investigate the ripening process. The ripening processes in climacteric fruits is characterized by observable changes in shape, size, flavor, and color. All these events are finely orchestrated by several hormonal signaling pathways including auxin, gibberellic acid (GA), cytokinin (CK), abscisic acid methyl-jasmonate (Valenta et al.), brassinosteroids (BRs), but also requiring ethylene (ET) for ripening (Davey and Van Staden, 1978; de Jong *et al.,* 2015; Dorcey *et al.,* 2009; Fenn and Giovannoni, 2021; Giovannoni, 2004; Kumar *et al.,* 2014; Osorio *et al.,* 2013). Ethylene synthesis is essential for normal climacteric fruit ripening and softening. The level of ET is determined by the fruit developmental stage. This regulation consists of two distinct systems. In the first phase, which occurs during the transition from immature green (IMG) fruit to breaker stage (BS), the synthesis of the ET is auto-inhibited (system 1 ethylene), followed by a rapid boost of ET emission. However, in the autocatalytic phase (system 2 ethylene) corresponding to the transition from BS to red ripe fruit RF the ET synthesis, sensitivity and response are decreased (Fenn and Giovannoni, 2021; Klee and Tieman, 2002). In addition, the tomato MADS-box transcription factor (TF) RIPENING INHIBITOR (RIN), NON-RIPENING (NOR), and COLORLESS NON-RIPENING (CNR) were identified as the major TF genes in the regulation of fruit ripening (Giovannoni, 2007; Klee and Giovannoni, 2011; Wang *et al.,* 2020). In tomatoes, the transcription factor *RIN* has been reported as a regulator of carotenoid gene expression and ET response (Fujisawa and Ito, 2013; Li *et al.,* 2020). Fruits of the rin mutant have a yellow-orange phenotype due to low lycopene synthesis (Li *et al.,* 2020). The production of volatile organic compounds (VOCs) emission is impaired in *rin* mutant fruit, resulting in a loss of quality, flavor, and aroma (Li *et al.,* 2020). nor mutant fruits are green in color, due to altered thylakoid membrane remodeling. The ET production has been reported to be low in the nor mutant. The *cnr* mutant have green-yellow fruit phenotype, due to a lack of lycopene accumulation and chlorophyll degradation (Kovács *et al.,* 2009; Wang *et al.,* 2020).

1.5.2 Primary and secondary metabolites in fruit

In the tomato fruit ripening process, in the early stage known as immature green, the fruits are partially photosynthetic and then follow remodeling stages known as mature green, breaker and ripe fruit that is completely red (FIG4). During these steps of fruit ripening, important events occur that determine fruit quality and nutritional value (Bauchet *et al.,* 2017; Beauvoit *et al.,* 2014; Biais *et al.,* 2014; Carrari and Fernie, 2006). Cell division, cell enlargement and ripening contribute to fruit development. Along these three stages sugars accumulate (Schaffer and Petreikov, 1997). Moreover, fruit pigments, organic acids (malate and citrate), amino acids, and volatiles are produced and are the main contributors to the taste, aroma, and quality of tomato fruit (Bastías *et al.,* 2011; Biais *et al.,* 2014; Bucheli *et al.,* 1999; Kader, 2008; Lobit *et al.,* 2003).

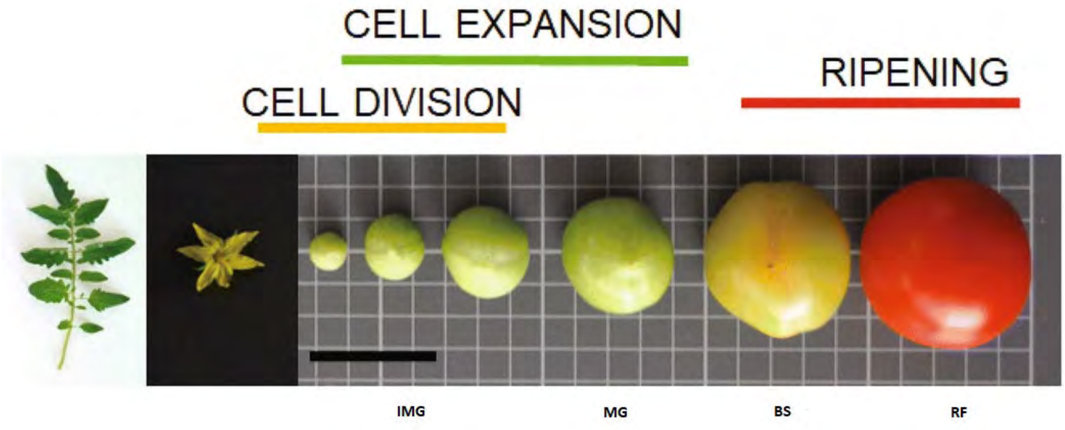

FIG 4| **Moneymaker (MM) tomato fruits during ripening process**. Representative examples of the tomatoes analysed in different development stages, immature green (IMG), mature green (MG), breaker (BS) and red ripe (RF). Adapted from (Renau-Morata *et al.,* 2020).

1.5.3 Primary metabolism in tomato:

Sugars in Fruit

Carbohydrate metabolites, as well as metabolites based on other carbon skeletons are key components which influence the favor and quality of fruit by affecting the sweet taste (Malundo *et al.,* 1995). In tomato fruit, the most common soluble sugars are sucrose, fructose, and glucose, which are transported from leaves and derived from starch during the development and ripening processes (BERTIN *et al.,* 2003; Gautier *et al.,* 2001; Heuvelink, 1997). The role of fruit photosynthesis in fruit metabolism and development has been largely studied, but the extent of its contribution to fruit biomass is unclear (BLANKE and LENZ, 1989; Carrara *et al.,* 2001). It has been estimated that approximately 20% of the total carbon of the fruit is the result of photosynthetic activity in the fruit itself, while the remaining 80% of carbon is imported from leaves via the phloem (Fernie *et al.,* 2020; Hetherington *et al.,* 1998; Pesaresi *et al.,* 2014). In green fruit (cell division stage) (FIG 4), starch accumulation in pericarp and columella tissues is a key factor for the total soluble sugar contents in the final red ripe stage (Carrari and Fernie, 2006). The breaker stage (chloroplast to chromoplast conversion) begins with the breakdown of starch and the lysis of thylakoid membranes. Starches are transient and serve as carbohydrate reservoir for soluble hexoses in the red ripe fruit (Schaffer and Petreikov, 1997). Concomitantly, enzymes involved in glycolysis and the tricarboxylic acid (TCA) cycle show a high activity. Sucrose metabolism acts as a key regulator in sugar accumulation and is under the control of sucrose-phosphate synthase (SPS), sucrose synthase (SS), and invertase (Ivr) (Dali *et al.,* 1992). SPS catalyzes sucrose phosphate synthesis from uridine diphosphate glucose (UDPG) and fructose 6-phosphate which then is hydrolyzed by sucrose phosphate phosphatase (SPP) to produce sucrose (Dali *et al.,* 1992). In sucrose synthase1 (SuSy1) mutant, a reduction of sucrose unloading capacity, as well as a decrease of starch accumulation, has been demonstrated that affect fruit development (D’Aoust *et al.,* 1999). Ivr catalyzes the conversion of sucrose into glucose and fructose. During the ripening process, glucose and fructose mainly accumulate in fruit pericarp, whereas organic acids decrease (Carrari and Fernie, 2006).

Organic acids

In contrast to glucose and fructose, the organic acids which are accumulated in the fruit are *de-novo* synthesized during the cell division phase (Beauvoit *et al.,* 2014). Citric and malic acid are the two main organic acid found in fruit, and are the intermediate products of the TCA cycle and phosphoenolpyruvate carboxylase (PEPC), a key enzyme in organic acid biosynthesis (Carrari *et al.,* 2003; Guillet *et al.,* 2012). Citric and malic acid contribute mainly to the acidic taste of tomatoes (Schauer *et al.,* 2004).

Amino acids

In tomato fruit pericarp, free amino acids increase significantly during fruit ripening. But not all amino acids increase to the same extent. In developing tomato fruit pericarp, approximately 70% of the total amino acid content belongs to the glutamate family (Boggio *et al.,* 2000; Valle *et al.,* 1998). Glutamate also plays a central role as a precursor for chlorophyll synthesis in developing leaves (FORDE and WALCH-LIU, 2009; Yaronskaya *et al.,* 2006). Glutamate is also responsible for the umami taste (the fifth basic flavors along with sweet, sour, bitter and salty) in tomato fruits.

1.5.4 Secondary metabolism in tomato:

Carotenoids

The ripening process in tomato is accompanied by a change of color in the pericarp, largely resulting from an intense accumulation of carotenoids (Shinozaki *et al.,* 2018). The red color of tomato is mainly due to the accumulation of the linear carotenoid lycopene. During tomato ripening the concentration of lycopene increases ~14 fold (Tamasi *et al.,* 2019). The carotenoid pathway has been studied extensively in tomato, and the major steps of this biosynthetic pathway are reviewed (see below 4.4).

Flavonoids

Flavonoid metabolites are mainly derived from phenylalanine and synthesized via the phenylpropanoid pathway and contribute to lesser degree to pigmentation (Shinozaki *et al.,* 2018b). Flavonoids constitute a large family grouped into six classes, which are the flavones, flavonols, flavanones, flavanols, anthocyanidins, and isoflavones (Bovy *et al.,* 2007; Tohge *et al.,* 2017). In tomato fruits, flavonoids are mainly found at the level of exocarp, which represent 5% of the whole fruit (Ballester *et al.,* 2016; Bovy *et al.,* 2010; Schijlen *et al.,* 2008).

Volatile organic compounds (VOC)

Plants and their fruit are capable of synthesizing and releasing a wide range of volatile organic compounds derived from fatty acids, terpenes (including the carotenoids) and amino acids (Klee, 2010; Klee and Giovannoni, 2011; Shen *et al.,* 2014; Vogel *et al.,* 2010). Volatiles play an important role in many aspects of plant biology, such as defense, communication, the attraction of pollinators and disseminators and also contribute to fruit quallity and nutritional value (Arimura *et al.,* 2009; Christensen and Kolomiets, 2011; Dicke and Baldwin, 2010; Mann *et al.,* 2021; Tieman *et al.,* 2012). VOCs are an indicator of fruit quality and often make up complex mixtures of terpenes, aldehydes, alcohols, esters and ketones and others (Zhu *et al.,* 2022). The ripening process increases the catabolism of polyunsaturated fatty acids (PUFAs) derived from dismantled thylakoid membranes, which leads to emission of PUFA derived degradation products via the jasmonic acid (JA) pathway. Thereby the ripening tomato fruit becomes a sink of free fatty acids important for fruit quality. Linoleic acid (C18:2) is the most abundant PUFA catabolized in tomato fruit during the BS to RF stage (Saini *et al.,* 2017). LOXC is involved in the formation of C5, C6 flavor volatiles derived from linoleic acid which include 1-penten-3-one, (E)-2-pentenal, 3-pentanone, 1-pentanol, (Z)-3-hexenal, hexenal, 3-hexen-1-ol, and hexyl alcohol).

1.6 Chromoplasts

Chromoplasts are divided into three main groups based on their ultrastructure (Ben-Shaul and Klein, 1965). One of these groups is characterized by the carotene bodies of the carrot root, containing chromoplasts evolve from a colorless proplastid (Ben-Shaul and Naftali, 1969; Frey-Wyssling and Schwegler, 1965; Toyama, 1980). The two other groups are differentiated from chloroplasts, carotenoid containing pigments in “globular bodies” or “filamentous components” and are derived from senescing chloroplasts. However, in certain circumstances, proplastids can also give rise to chromoplasts.

In tomato, chromoplasts develop from fully developed chloroplasts (Pyke, 2007; Wang *et al.,* 2013). The tomato chloroplast to chromoplast conversion passes through different observable steps during the ripening period. These steps are associated with chlorophyll breakdown, turning yellow and then red. Concomitantly, physiological and biochemical changes occur. In tomato fruit, chloroplast to chromoplast conversion is under the control of different factors that depend on gene expression and hormone regulation (Egea *et al.,* 2010). STAY GREEN (*SGR*) is a plastid-localized protein involved in the regulation of chlorophyll degradation during senescence (Cheung *et al.,* 1993; Luo *et al.,* 2013; Sakuraba *et al.,* 2015). Recent studies have indicated that SGR1 plays an important role in the process of chlorophyll degradation by modulating Pheophorbide *a* Oxygenase activity (Kuai *et al.,* 2018; Sakuraba *et al.,* 2015). In tomatoes, SGR1 may regulate lycopene and beta-carotene accumulation, due to its direct interaction with the enzyme Phytoene Synthase 1 (PSY1) and its role in the induction of ethylene signaling (Luo *et al.,* 2013).

In most cases, the nature of the fruit type reflects an evolutionary strategy that plays out at the level of seed dissemination by water, wind, or animals (Wang *et al.,* 2015). Colored fruit can be seen as part of a commensal relationship between plants and animals attracted for the reason of seed dispersal. Color appears also as one of the survival advantages of species colonizing their environment (Valenta *et al.,* 2018). However, the color can also be a signal of danger to animals and humans who eat the fruit. In addition, the color is also an indicator of antioxidants, nutrients, and minerals in the fruit that are beneficial to human health. Fruits may take on a wide range of colors, shapes, sizes, textures, and flavors depending on their developmental stage and environment (Wang *et al.,* 2015). The diverse fruit colors are due to the intrinsic composition and content of carotenoids, xanthophylls, chlorophylls, and flavonoids.

The Solanaceae family presents a rich variety of fruit types and distinct colors, resulting from the conversion of chloroplasts to chromoplasts during ripening and massive sequestration of carotenoids (Jeong *et al.,* 2020; Knapp, 2002). In tomato, bell pepper, and eggplant, the mature fruit color is regulated by several genes and enzymes (Rodriguez-Uribe *et al.,* 2011).

Carotenoid biosynthesis is a complex pathway derived from the elementary building blocks isopentenyl diphosphate, and its isomer dimethylallyl diphosphate (DMAPP) in higher plants, produced by two pathways, the mevalonic acid (MVA) and 2C-methyl-D-erythritol-4-phosphate (MEP) (Chappell *et al.,* 1995; Enfissi *et al.,* 2005; Rodriguez-Uribe *et al.,* 2011). The MVA pathway is localized in the cytosol, and the MEP pathway in plastids and is responsible for carotenoid biosynthesis in chromoplasts (Eisenreich *et al.,* 2001; Lichtenthaler, 1999). The nuclear genome codes for all the carotenoid biosynthetic enzymes that are located in the plastids (Lee, 2005).

The MEP pathway provides the first block for the synthesis of terpenoids and isoprene. In the early step of carotenogenesis, fruit ripening is regulated and catalyzed by 1-deoxy-D-xylulose 5-phosphate synthase (DXS), 1-deoxy-D-xylulose 5-phosphate (DXP) and hydroxymethylbutenyl diphosphate reductase (HDR) encoded by the nucleus. The first step is followed by the conversion of DXP to MEP by the enzyme 1-deoxy-D-xylulose- 5-phosphate reductoisomerase (DXR) (Rodríguez-Concepción *et al.,* 2001). Thereafter, MEP is converted to methylerythritol 2,4-cyclodiphosphate (MEcDP) into three subsequent enzymatic steps involving cytidylation (CTP-dependent), phosphorylation (ATP-dependent), and cyclization, Methyl Erythritol 4-phosphate (MEP) Pathway Metabolic Regulation (FIG 5) (Lois *et al.,* 2000; Wolfertz *et al.,* 2004). MEcDP is then converted into hydroxymethylbutenyl diphosphate (HMBDP), catalyzed by HMBDP synthase (HDS), which is reduced to IPP and DMAPP by HMBDP reductase (HDR) (Lois *et al.,* 2000).

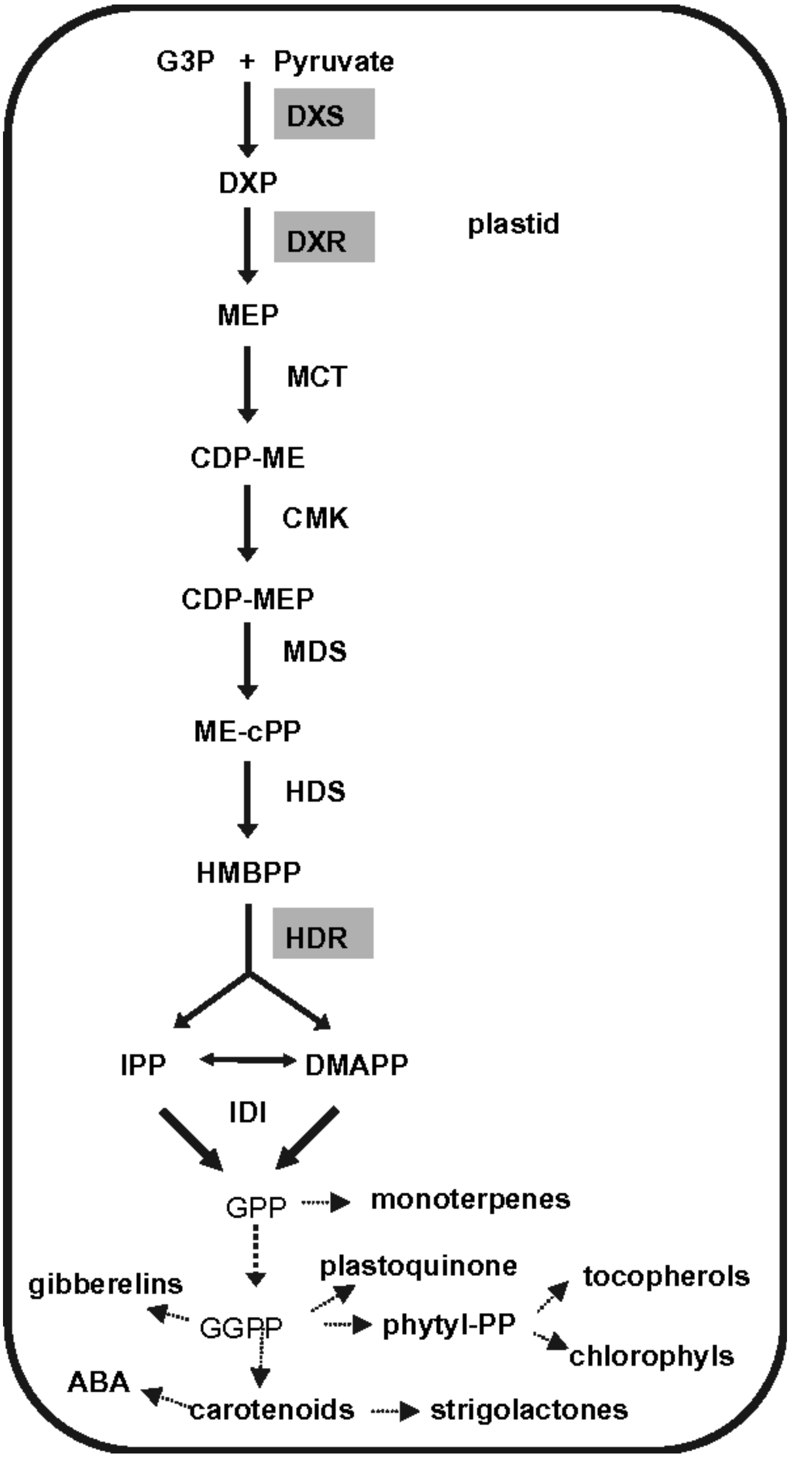

FIG 5| **Schematic representation of MEP pathway in tomato plant and fruits**. Here, we represented the main enzymes of the MEP pathway required for lycopene accumulation in tomato. Enzymes: 1-deoxy-D-xylulose-5-phosphate synthase (DXS), 1-deoxy-D-xylulose-5-phosphate reductoisomerase (DXR), 4-(cytidine 5'-diphospho)-2-C-methyl-D-erythritol synthase (MCT), 4-(cytidine 5'-diphospho)-2-C-methyl-D-erythritol kinase (CMK), 2-C-methyl-D-erythritol 2,4-cyclodiphosphate synthase (MDS), 4-hydroxy-3-methylbut-2-enyl diphosphate synthase (HDS), 4-hydroxy-3-methylbut-2-enyl diphosphate reductase (HDR), isopentenyl diphosphate isomerase (IDI), geranylgeranyl diphosphate synthase (GGPPs), geranyl diphosphate synthase (GPPs). Products: glyceraldehyde 3-phosphate (GA-3P), 1-deoxy-D-xylulose 5-phosphate (DXP), 2-C-methyl-D-erythritol 4-phosphate (MEP), 4-(cytidine 5'-diphospho)-2-C-methyl-D-erythritol (CDP-ME), 2-phospho-4-(cytidine 5'-di-phospho)-2-C-methyl-D-erythritol (CDP-MEP), 2-C-methyl-D-erythritol 2,4-cyclodiphosphate (ME-cPP), 4-hydroxy-3-methylbut-2-enyl diphosphate (HMBPP), isopentenyl diphosphate (IPP), dimethylallyl diphosphate (DMAPP), geranyl diphosphate (GPP), geranylgeranyl diphosphate (GGPP). Adapted from (Cordoba *et al.,* 2009).

IPP and DMAPP are converted into GGPP by the GGPP synthase (GGDS), for the synthesis of plastid isoprenoid end compounds such as carotenoids (FIG 6) (Rodríguez-Concepción *et al.,* 2001). Phytoene synthase (PSY), produces phytoene through the condensation of two molecules of geranylgeranyl diphosphate. Then, the phytoene desaturase (PDS) and zeta-carotenoid desaturase (ZDS) introduce subsequently four double bonds in phytoene to produce zeta-carotene and cis-trans lycopene. The carotenoid isomerase (CRTISO), converts prolycopene/zeta-carotene (poly-*cis*-lycopene) to all-*trans*-lycopene (Eckardt, 2002; Giuliano *et al.,* 2002). Beta-carotene and α-carotene are synthesized respectively from the cyclization of lycopene by the lycopene-beta cyclase (LCY-b), and lycopene-epsilon cyclase (LCY-e). Hydroxylation of α-carotene and β-carotene by beta-carotene hydroxylase (BCH) and e-hydroxylase (eOHase), produce respectively the lutein and the xanthophylls. Zeaxanthin is the first xanthophyll resulting from the hydroxylation of β-carotene. Violaxanthin is produced from zeaxanthin by zeaxanthin epoxidase (ZEP) and can be reversed into zeaxanthin again by the violaxanthin de-epoxidase (VDE). Finally, neoxanthin is a product by conversion from violaxanthin by neoxanthin synthase (NXS) (Sun *et al.,* 2018). Different mutated genes in the carotenoid biosynthetic pathway were characterized and led to variations in carotenoid pigments stored in chromoplasts of fruit pericarp. In tomato and pepper, a mutation in the *Psy1* gene (*psy1*) is responsible for yellow or orange-yellow fruit color named *yellow flesh* (*r*), resulting in geranylgeranyl diphosphate accumulation (Fray and Grierson, 1993; Kachanovsky *et al.,* 2012; Kim *et al.,* 2010; Tan *et al.,* 2017). The *CrtISO* gene mutant was also characterized by an orange phenotype in tomato fruit *tangerine* (*t*), as a consequence of prolycopene accumulation (Kachanovsky *et al.,* 2012; Sacks *et al.,* 2018). The carotenoid genes are regulated by transcription factors, post-transcriptional mechanisms, and several co-factors such as hormone signaling.

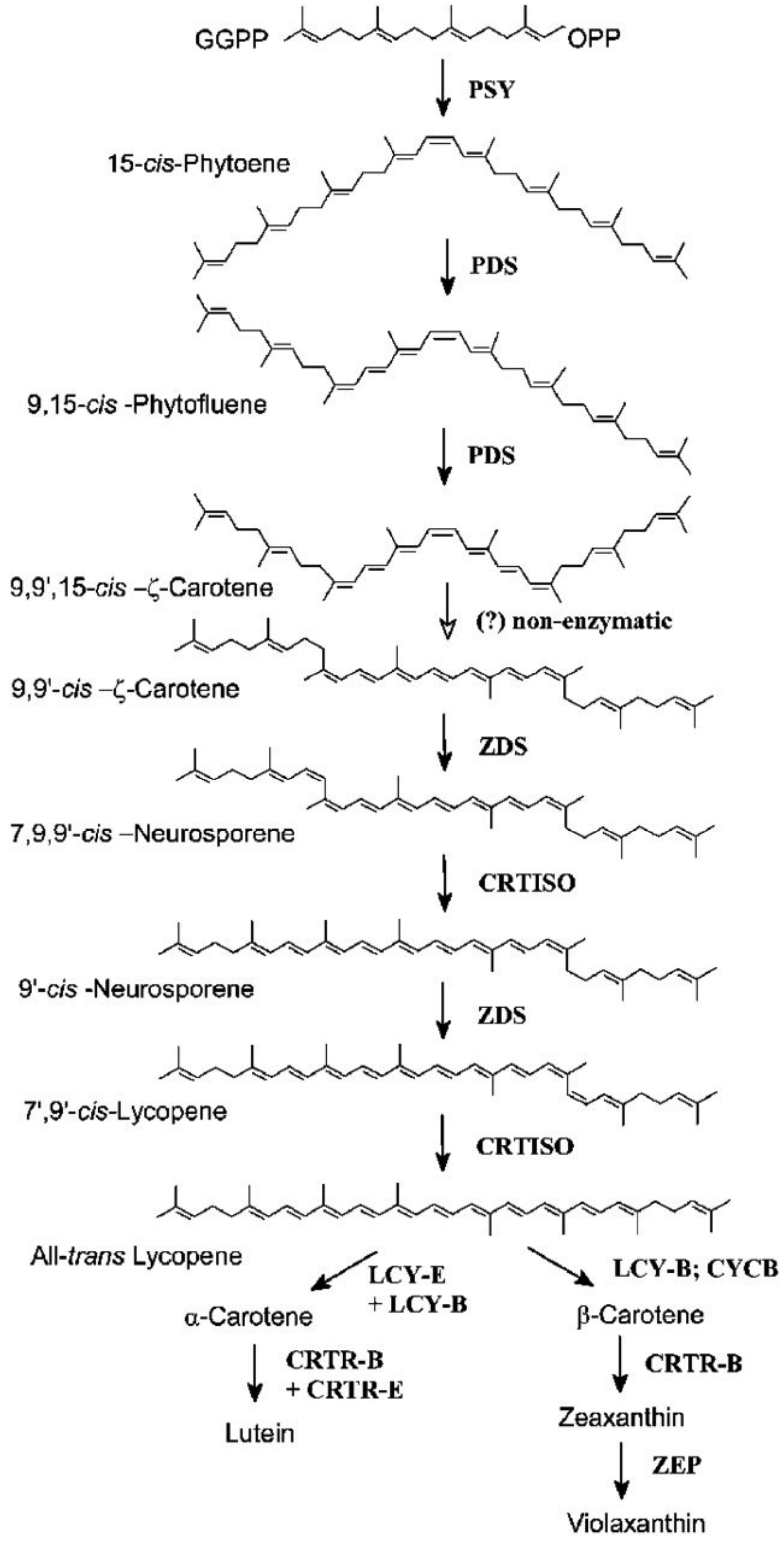

FIG 6| **Simplified illustration of the carotenoid pathway in plants and fruits**. The carotenoid pathway starts with the methylerythritol phosphate (MEP) necessary for the production of geranylgeranyl pyrophosphate (GGPP), the precursor of carotenoids and chlorophyll synthesis. The scheme illustrates the main enzymes of the pathway and the most accumulated carotenoids in plant and fruit models discussed throughout this thesis. Enzymes: phytoene synthase (PSY), phytoene desaturase (PDS), zeta-carotenoid desaturase (ZDS), zeta carotene isomerase (Z-ISO), carotenoid isomerase (CRTISO), lycopene-beta cyclase (LCYB or CYCB), lycopene-epsilon cyclase (LCYE), beta-carotene hydroxylase (CRTR-B or CHYB), carotene e-hydroxylase (CRTR-E or CHYE), violaxanthin de-epoxidase (VDE) and zeaxanthin epoxidase (ZEP). Adapted from (Isaacson *et al.,* 2004).

1.6.1 Chromoplast plastoglobules and role in carotenoid biosynthesis

Analysis of chromoplasts by transmission electron microscopy (TEM) revealed that, during chloroplast to chromoplast transition, plastid ultrastructure changes considerably (Nogueira *et al.,* 2013; Suzuki *et al.,* 2015) (FIG7). The chlorophylls and thylakoid membranes are degraded, leaving thylakoid remnants and simultaneously large and numerous PG as well as carotenoid crystals emerge. Carotenoids are accumulated and stored in the large PG, carotenoid-containing structures (Cheung *et al.,* 1993; Egea *et al.,* 2010; Zeng *et al.,* 2015). In chromoplasts TEM images, the PGs were observed to be detached from the membranes and floating in the stroma (Pozueta-Romero *et al.,* 1997; Vidi *et al.,* 2006; Ytterberg *et al.,* 2006; Zeng *et al.,* 2015) (FIG 7). They are larger than those in the chloroplasts due to the increased accumulation of osmophilic compounds (Zeng *et al.,* 2015). In bell pepper (*Capsicum annuum*), chromoplast PG have been characterized revealing a common PG core protein shared with Arabidopsis, pea, and Citrus (Ytterberg *et al.,* 2006; Zeng *et al.,* 2015). In the context of my thesis it is important to note that PG have been identified as a potential site of carotenoid biosynthesis due to the presence of carotenoid biosynthetic enzymes (Ytterberg *et al.,* 2006).

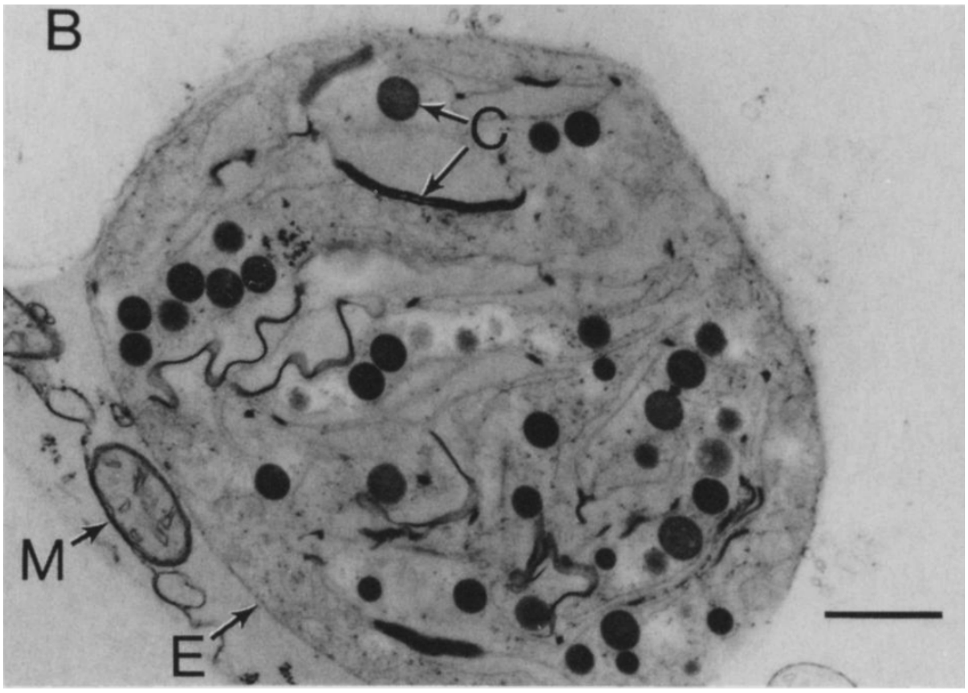

FIG 7| **Ultrastructure of a chromoplast with a large number of PG from the flesh of tomato *Solanum lycopersicum* cv Micro-Tom.** C, carotenoid-containing structures upper arrow pointing to an electron-dense, globular PG and lower arrow to a membranous, carotenoid-containing structure; E, plastid envelope; M, Mitochondria; Adapted from (Cheung *et al.,* 1993).

1.7 UbiB/ABC1-like kinase family

The activity of bc(1) complex kinase (ABC1K) protein family, is a member of the subgroup of atypical Protein Kinases (aPKs), which are themselves part of the Protein Kinase-like superfamily (PKL). In yeast and animals the ABC1K homologs are contained inside mitochondria. In plants somel homologs are also in mitochondria but several others are localized in plastids, most of them associated with PG. The ABC1K gene family (also named UbiB in E. coli, “ABC1 domain–containing kinases” ADCKs in humans) are well conserved throughout the kingdoms (archaea, bacteria, and eukaryotes).

1.7.1 Roles of the UbiB /ABC1-like kinases in different organisms

E. coli UbiB i, yeast (Saccharomyces cerevisiae) mitochondrial ABC1 (also known as COQ8) and human mitochondrial ADCK3 and -4 homologs are implicated in the the aerobic biosynthesis of ubiquinone (Do *et al.,* 2001; Poon *et al.,* 2000).

In yeast, the lack of ubiquinone in the coq8 mutant diminishes the mitochondrial bc1 complex (hence absence of bc1, ABC1) and aerobic metabolic activity. It has been suggested that COQ8 catalyzes, possibly through phosphorylation, the assembly of a large biosynthetic multi-enzyme complex (Bousquet *et al.,* 1991; Do *et al.,* 2001).

In humans, the ADCK3 and -4 homologs both contribute to ubiquinone synthesis in the mitochondria. Defects of the kind have been linked to cerebellar ataxia, epilepsy, muscle symptoms and hereditary diseases in humans (Hikmat *et al.,* 2016).

Two mitochondrial proteins members of the UbiB family in *Saccharomyces cerevisiae*, identified as Ypl109c (Cqd1) and Ylr253w (Cqd2), affected CoQ distribution in mitochondria and widely in the cell (Kemmerer *et al.,* 2021). It has been showed that Cqd1 and Cqd2 homologs are not involved in ubiquinone biosynthesis, but in its trafficking and play a central role in a form of regulated cell death known as ferroptosis. Collectively, the study of (Kemmerer *et al.,* 2021), revealed that the CQD1 mediated the redistribution of the extramitochondrial CoQ relies on atypical kinase/ATPase activity (Kemmerer *et al.,* 2021). The mutant of CQD1 showed a accumulation of CoQ in the extramitochondrial cell compartment. It has been demonstrated that CQD2 activity counteracts CQD1 function. In absence of CQD2, the CoQ component is accumulated at the inner mitochondrial membrane (IMM), and is insufficiently export to the extramitochondrial compartment. This result support the model that CQD1/CQD2 couple ATPase activity allowing the trafficking of CoQ across the extramitochondrial from outer mitochondrial membrane (OMM) to the IMM (Kemmerer *et al.,* 2021).

ABC1Ks have expanded to greater numbers specifically in photosynthetic organisms(Lundquist *et al.,* 2012). The ABC1K family represents the majority of known or predicted kinases in plastids and mitochondria; however, relatively little is known about this family in plants. In the last decade, the studies of this gene family have revealed that Arabidopsis contains seventeen members, nine of which are identified in plastids with six assigned to plastoglobules (Lundquist *et al.,* 2012; Vidi *et al.,* 2006). The proteomic studies of purified plastoglobules from Arabidopsis chloroplasts demonstrated the presence of ABC1K1, -3, -5, -6, -7, -9 (Lundquist *et al.,* 2012; Vidi *et al.,* 2006). A seventh, ABC1K8, has been localized in the inner envelope of plastids (Manara *et al.,* 2015). ABC1K2, and -4, have been predicted to be localized in the plastids but without known sublocalization. ABC1K10a-b, -11, -12a-b, -13, -14, -15, have been located in the mitochondria (van Wijk and Kessler, 2017b). Functional studies of PG-localized ABC1K1, -3, -7 and plastid ABC1K8 have been initiated in Arabidopsis, and the role of ABC1K3 has also been studied in rice (Li *et al.,* 2015). PG-localized ABC1K7 contributes to cadmium tolerance, oxidative stress response, iron distribution, lipid metabolism, and to crosstalk between abscisic acid and ROS signaling (Manara *et al.,* 2015; Manara *et al.,* 2014). The Chlamydomonas homolog of ABC1K6 (EYE3) is located in the eyespot and involved in the biogenesis of pigment granules (Boyd *et al.,* 2011).

Apart from its association with PG, ABC1K1 was identified in two independent genetic screens. In a screen for mutants with reduced non-photochemical quenching (NPQ) (Shikanai *et al.,* 1999), PGR6 (Proton Gradient Regulation 6) was identified and later found to be identical with ABC1K1. In a screen for mutants defective in seedling growth under continuous red light, ABC1K1 was identified as BDR1 (bleaching and dwarf under red light 1) (Yang *et al.,* 2016). Under continuous red light, *abc1k1/bdr1* seedlings exhibited an albino and dwarf phenotype. To identify additional components involved in ABC1K1/BDR1 function, a suppressor screen was carried out in *abc1k1-2* and resulted in the isolation of *rbd1* (repressor of *bdr1-2*) which turned out to be identical with ABC1K3 (Huang *et al.,* 2015). This work provided the evidence for a role of atypical ABC1Ks in cellular signaling. The data suggested that ABC1K3 in the *abc1k1* background interfered with red light signaling acting downstream of PhyB and HY5 and affecting the expression of PIF genes.

1.7.2 ABC1K1, a regulator of prenyl quinone metabolism and distribution in plants

abc1k1 has a photosynthetic phenotype characterized by strong photoinhibition and reduced NPQ upon high light exposure (Martinis *et al.,* 2014; Pralon *et al.,* 2019). In addition, metabolic perturbations were observed in *abc1k1*: Tocopherol concentrations remained low under high light stress and carotenoid concentrations were diminished even under moderate light conditions (Martinis *et al.,* 2013; Martinis *et al.,* 2014). After high light treatment, carbon-allocation shifted from starch to soluble sugars. In addition to their genetic interaction, ABC1K1 and ABC1K3 interact physically (Lundquist *et al.,* 2013). Moreover, recent research demonstrated that ABC1K1 and -3 together are involved in PQ-9 homeostasis (defined as the maintenance of sufficient PQ-9 in the photoactive pool in the thylakoids) (Pralon *et al.,* 2020; Pralon *et al.,* 2019). In the *abc1k1* mutant, the photoactive PQ-9 pool in the thylakoid membranes was selectively depleted under moderate high light stress. Importantly this phenotype of *abc1k1* was rescued in the *abc1k1/abc1k3* double mutant. Thus, ABC1K1 and ABC1K3 together appear to control the distribution of PQ-9 between the plastoglobule and thylakoid membrane pools (Havaux, 2020).

1.7.3 Prenyl lipid and nucleotide binding properties of UbiB/ABC1Ks

Recently, the crystal structure of mouse COQ8A has been determined and, due to its sequence similarity, has provided important new insight also into plant ABC1Ks (Stefely *et al.,* 2015). The structure reveals that a UbiB family-specific KxGQ domain both in the absence and presence of ATP blocks the typical peptide substrate-binding site and has been proposed to preclude protein phosphorylation in trans, meaning UbiB family members are unlikely to function as a protein kinase (FIG 9). The work also demonstrated that COQ8A functionality depends on a conserved ATPase active site and adenine nucleotide binding (Stefely *et al.,* 2016). Furthermore, recombinant COQ8 co-purified with membrane lipids and ubiquinone biosynthesis intermediates (Reidenbach *et al.,* 2018). While this research made important inroads, it did not reveal the molecular mechanisms of COQ8. Several "unorthodox" functional models that excluded a canonical kinase model were put forward and included COQ complex stabilizing interactions, specific lipid binding, or small molecule kinases. In yeast, this hypothesis is supported by the observation that the ABC1K1 homolog COQ8 is bound to lipids and ubiquinone pathway intermediates (Reidenbach *et al.,* 2018).

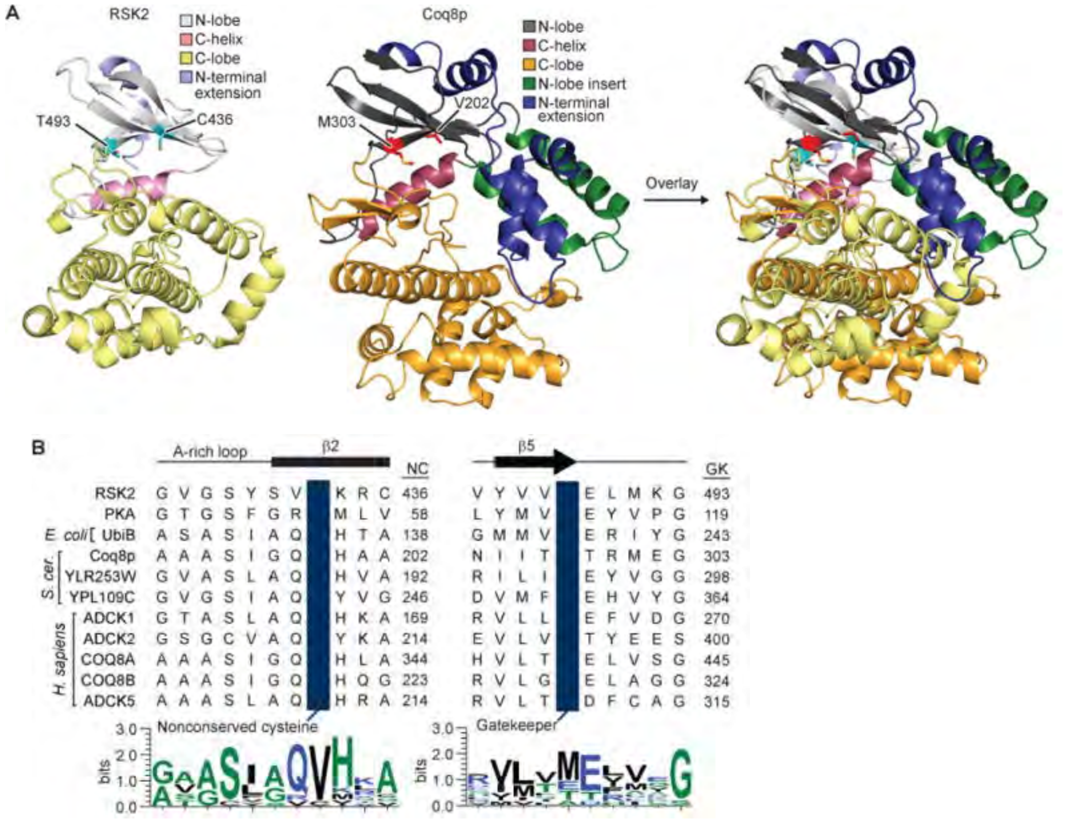

		NC		GK
RSK2	G V G S Y S V K R C	436	V Y V V E L M K G	493
PKA	G T G S F G R M L V	58	L Y M V E Y V P G	119
E. coli UbiB	A S A S I A Q H T A	138	G M M V E R I Y G	243
S. cer. Coq8p	A A A S I G Q H A A	202	N I I T T R M E G	303
S. cer. YLR253W	G V A S L A Q H V A	192	R I L I E Y V G G	298
S. cer. YPL109C	G V G S I A Q Y V G	246	D V M F E H V Y G	364
H. sapiens ADCK1	G T A S L A Q H K A	169	R V L L E F V D G	270
H. sapiens ADCK2	G S G C V A Q Y K A	214	E V L V T Y E E S	400
H. sapiens COQ8A	A A A S I G Q H L A	344	H V L T E L V S G	445
H. sapiens COQ8B	A A A S I G Q H Q G	223	R V L G E L A G G	324
H. sapiens ADCK5	A A A S L A Q H R A	214	R V L T D F C A G	315

FIG 8| **Structural and Primary sequence alignment of UbiB family**. A) Structural alignment of Coq8p homology model based on COQ8A (PDB: 5I35) with RSK2 (PDB: 4D9U). The nonconserved cysteine C436 and gatekeeper T493 residues are shown in cyan. The V202 and gatekeeper M303 residues of Coq8p are shown in red; B) Primary sequence alignment of the nonconserved cysteine and gatekeeper residues from human RSK2 (PDB: 4D9U), human PKA, and the UbiB family. Sequence logos are shown for the displayed amino acid sequences. NC, nonconserved cysteine; GK, gatekeeper. Adapted from (Reidenbach *et al.,* 2018).

In mitochondria, the COQ8 active site is essential for COQ complex stability and ubiquinone accumulation (Stefely *et al.,* 2016).

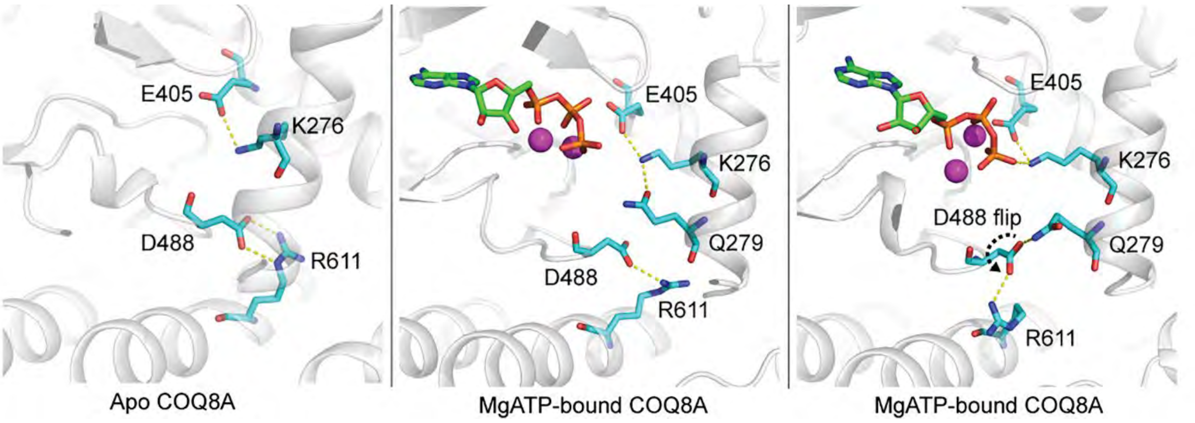

FIG 9| **Structure and Dynamics of Nucleotide-Bound COQ8A**. The residues K276, Q279, E405, D488, and R611 of protein COQ8A (PDB: 4PED) are given in blue color. COQ8A showing interactions of D488 with either R611 or the KxGQ motif. Left: apo; middle and right: MgATP-bound. Adapted from (Stefely *et al.,* 2016).

1.8 Aim of my thesis

Arabidopsis thaliana is considered a suitable plant model system for molecular genetic research. But it is irrelevant as a crop species. The aim of my thesis is therefore to translate ongoing research on Arabidopsis plastoglobules to the tomato (*Solanum lycopersicum* cv Micro Tom) crop model system. Tomato is one of the most consumed and commercially important crop species in the world. It is also potentially an excellent model system to study 'chromoplast' PG as they are known to be involved in carotenoid biosynthesis and accumulation, which are key determinants of fruit quality. My thesis has two main objectives.

- The first is to determine tomato fruit plastoglobule composition. The proteomes as well as the lipidomes of purified chloroplast and chromoplast plastoglobules in mature green and ripe red fruit, respectively will be determined.
- The second is the study of the tomato SlABC1K1 homolog that was expected to be present in the proteome of tomato fruit plastoglobules. In collaboration with the Rothan lab at the University of Bordeaux, we have engineered tomato (Micro-Tom variety) PG mutants *slabc1k1* (SlABC1K1, Solyc08g074560). With the intention of expanding our research results to the tomato crop species and a view toward metabolic engineering of tomato nutrient contents, I will explore the role of the SlABC1K protein in chromoplast PG and their potential contribution to pigmentation and nutrient content. Based on the state of the art I will investigate the potential metabolite trafficking function of ABC1K1, associated with the kinase/ATPase activity (Reidenbach *et al.,* 2018; Stefely *et al.,* 2015).

1.9 References

1. Allen, J.F. (2003). Why chloroplasts and mitochondria contain genomes. Comp Funct Genomics *4*, 31-36. 10.1002/cfg.245.

2. Ariizumi, T., Kishimoto, S., Kakami, R., Maoka, T., Hirakawa, H., Suzuki, Y., Ozeki, Y., Shirasawa, K., Bernillon, S., Okabe, Y., et al. (2014). Identification of the carotenoid modifying gene PALE YELLOW PETAL 1 as an essential factor in xanthophyll esterification and yellow flower pigmentation in tomato (Solanum lycopersicum). The Plant Journal *79*, 453-465. https://doi.org/10.1111/tpj.12570.

3. Arimura, G., Matsui, K., and Takabayashi, J. (2009). Chemical and molecular ecology of herbivore-induced plant volatiles: proximate factors and their ultimate functions. Plant Cell Physiol *50*, 911-923. 10.1093/pcp/pcp030.

4. Austin, J.R., 2nd, Frost, E., Vidi, P.A., Kessler, F., and Staehelin, L.A. (2006). Plastoglobules are lipoprotein subcompartments of the chloroplast that are permanently coupled to thylakoid membranes and contain biosynthetic enzymes. Plant Cell *18*, 1693-1703. 10.1105/tpc.105.039859.

5. Ballester, A.-R., Tikunov, Y., Molthoff, J., Grandillo, S., Viquez-Zamora, M., De Vos, R., De Maagd, R.A., Van Heusden, S., and Bovy, A.G. (2016). Identification of loci affecting accumulation of secondary metabolites in tomato fruit of a Solanum lycopersicum× Solanum chmielewskii introgression line population. Front Plant Sci *7*, 1428.

6. Bartley, G.E., and Scolnik, P.A. (1995). Plant carotenoids: pigments for photoprotection, visual attraction, and human health. Plant Cell *7*, 1027-1038. 10.1105/tpc.7.7.1027.

7. Bastías, A., López-Climent, M., Valcárcel, M., Rosello, S., Gómez-Cadenas, A., and Casaretto, J.A. (2011). Modulation of organic acids and sugar content in tomato fruits by an abscisic acid-regulated transcription factor. Physiologia Plantarum *141*, 215-226. https://doi.org/10.1111/j.1399-3054.2010.01435.x.

8. Bauchet, G., Grenier, S., Samson, N., Segura, V., Kende, A., Beekwilder, J., Cankar, K., Gallois, J.-L., Gricourt, J., Bonnet, J., et al. (2017). Identification of major loci and genomic regions controlling acid and volatile content in tomato fruit: implications for flavor improvement. New Phytologist *215*, 624-641. https://doi.org/10.1111/nph.14615.

9. Beauvoit, B.P., Colombié, S., Monier, A., Andrieu, M.H., Biais, B., Bénard, C., Chéniclet, C., Dieuaide-Noubhani, M., Nazaret, C., Mazat, J.P., and Gibon, Y. (2014). Model-assisted analysis of

sugar metabolism throughout tomato fruit development reveals enzyme and carrier properties in relation to vacuole expansion. Plant Cell *26*, 3224-3242. 10.1105/tpc.114.127761.

10. Ben-Shaul, Y., and Klein, S. (1965). Development and Structure of Carotene Bodies in Carrot Roots. Botanical Gazette *126*, 79-85.

11. Ben-Shaul, Y., and Naftali, Y. (1969). The development and ultrastructure of lycopene bodies in chromoplasts ofLycopersicum esculentum. Protoplasma *67*, 333-344.

12. BERTIN, N., BOREL, C., BRUNEL, B., CHENICLET, C., and CAUSSE, M. (2003). Do Genetic Make-up and Growth Manipulation Affect Tomato Fruit Size by Cell Number, or Cell Size and DNA Endoreduplication? Ann Bot *92*, 415-424. 10.1093/aob/mcg146.

13. Biais, B., Bénard, C., Beauvoit, B., Colombié, S., Prodhomme, D., Ménard, G., Bernillon, S., Gehl, B., Gautier, H., Ballias, P., et al. (2014). Remarkable reproducibility of enzyme activity profiles in tomato fruits grown under contrasting environments provides a roadmap for studies of fruit metabolism. Plant Physiol *164*, 1204-1221. 10.1104/pp.113.231241.

14. BLANKE, M.M., and LENZ, F. (1989). Fruit photosynthesis. Plant, Cell & Environment *12*, 31-46. https://doi.org/10.1111/j.1365-3040.1989.tb01914.x.

15. Block, M.A., Dorne, A.J., Joyard, J., and Douce, R. (1983). Preparation and characterization of membrane fractions enriched in outer and inner envelope membranes from spinach chloroplasts. II. Biochemical characterization. J Biol Chem *258*, 13281-13286.

16. Boggio, S.B., Palatnik, J.F., Heldt, H.W., and Valle, E.M. (2000). Changes in amino acid composition and nitrogen metabolizing enzymes in ripening fruits of Lycopersicon esculentum Mill. Plant Science *159*, 125-133. https://doi.org/10.1016/S0168-9452(00)00342-3.

17. Bousquet, I., Dujardin, G., and Slonimski, P.P. (1991). ABC1, a novel yeast nuclear gene has a dual function in mitochondria: it suppresses a cytochrome b mRNA translation defect and is essential for the electron transfer in the bc 1 complex. Embo j *10*, 2023-2031. 10.1002/j.1460-2075.1991.tb07732.x.

18. Bovy, A., Schijlen, E., and Hall, R.D. (2007). Metabolic engineering of flavonoids in tomato (Solanum lycopersicum): the potential for metabolomics. Metabolomics *3*, 399-412. 10.1007/s11306-007-0074-2.

19. Bovy, A.G., Gómez-Roldán, V., and Hall, R.D. (2010). Strategies to optimize the flavonoid content of tomato fruit. Recent advances in polyphenol research, Volume 2, 138-162.

20. Boyd, J.S., Mittelmeier, T.M., Lamb, M.R., and Dieckmann, C.L. (2011). Thioredoxin-family protein EYE2 and Ser/Thr kinase EYE3 play interdependent roles in eyespot assembly. Molecular Biology of the Cell *22*, 1421-1429. 10.1091/mbc.e10-11-0918.

21. Bucheli, P., Voirol, E., de la Torre, R., López, J., Rytz, A., Tanksley, S.D., and Pétiard, V. (1999). Definition of Nonvolatile Markers for Flavor of Tomato (Lycopersicon esculentum Mill.) as Tools in Selection and Breeding. Journal of Agricultural and Food Chemistry *47*, 659-664. 10.1021/jf980875l.

22. Carrara, S., Pardossi, A., Soldatini, G.F., Tognoni, F., and Guidi, L. (2001). Photosynthetic Activity of Ripening Tomato Fruit. Photosynthetica *39*, 75-78. 10.1023/A:1012495903093.

23. Carrari, F., and Fernie, A.R. (2006). Metabolic regulation underlying tomato fruit development. Journal of Experimental Botany *57*, 1883-1897. 10.1093/jxb/erj020.

24. Carrari, F., Nunes-Nesi, A., Gibon, Y., Lytovchenko, A., Loureiro, M.E., and Fernie, A.R. (2003). Reduced Expression of Aconitase Results in an Enhanced Rate of Photosynthesis and Marked Shifts in Carbon Partitioning in Illuminated Leaves of Wild Species Tomato. Plant Physiology *133*, 1322-1335. 10.1104/pp.103.026716.

25. Chappell, J., Wolf, F., Proulx, J., Cuellar, R., and Saunders, C. (1995). Is the Reaction Catalyzed by 3-Hydroxy-3-Methylglutaryl Coenzyme A Reductase a Rate-Limiting Step for Isoprenoid Biosynthesis in Plants? Plant Physiol *109*, 1337-1343. 10.1104/pp.109.4.1337.

26. Cheung, A.Y., McNellis, T., and Piekos, B. (1993). Maintenance of Chloroplast Components during Chromoplast Differentiation in the Tomato Mutant Green Flesh. Plant Physiol *101*, 1223-1229. 10.1104/pp.101.4.1223.

27. Christensen, S.A., and Kolomiets, M.V. (2011). The lipid language of plant-fungal interactions. Fungal Genet Biol *48*, 4-14. 10.1016/j.fgb.2010.05.005.

28. Cordoba, E., Salmi, M.L., and León, P. (2009). Unravelling the regulatory mechanisms that modulate the MEP pathway in higher plants. Journal of experimental botany *60 10*, 2933-2943.

29. D'Aoust, M.-A., Yelle, S., and Nguyen-Quoc, B. (1999). Antisense Inhibition of Tomato Fruit Sucrose Synthase Decreases Fruit Setting and the Sucrose Unloading Capacity of Young Fruit. The Plant Cell *11*, 2407-2418. 10.1105/tpc.11.12.2407.

30. Dali, N., Michaud, D., and Yelle, S. (1992). Evidence for the Involvement of Sucrose Phosphate Synthase in the Pathway of Sugar Accumulation in Sucrose-Accumulating Tomato Fruits 1. Plant Physiology *99*, 434-438. 10.1104/pp.99.2.434.

31. Davey, J.E., and Van Staden, J. (1978). Endogenous cytokinins in the fruits of ripening and non-ripening tomatoes. Plant Science Letters *11*, 359-364. https://doi.org/10.1016/0304-4211(78)90023-8.

32. de Jong, M., Wolters-Arts, M., Schimmel, B.C.J., Stultiens, C.L.M., de Groot, P.F.M., Powers, S.J., Tikunov, Y.M., Bovy, A.G., Mariani, C., Vriezen, W.H., and Rieu, I. (2015). Solanum lycopersicum AUXIN RESPONSE FACTOR 9 regulates cell division activity during early tomato fruit development. Journal of Experimental Botany *66*, 3405-3416. 10.1093/jxb/erv152.

33. Dicke, M., and Baldwin, I.T. (2010). The evolutionary context for herbivore-induced plant volatiles: beyond the 'cry for help'. Trends Plant Sci *15*, 167-175. 10.1016/j.tplants.2009.12.002.

34. Do, T.Q., Hsu, A.Y., Jonassen, T., Lee, P.T., and Clarke, C.F. (2001). A Defect in Coenzyme Q Biosynthesis Is Responsible for the Respiratory Deficiency in Saccharomyces cerevisiae abc1Mutants*. Journal of Biological Chemistry *276*, 18161-18168. https://doi.org/10.1074/jbc.M100952200.

35. Dorcey, E., Urbez, C., Blázquez, M.A., Carbonell, J., and Perez-Amador, M.A. (2009). Fertilization-dependent auxin response in ovules triggers fruit development through the modulation of gibberellin metabolism in Arabidopsis. The Plant Journal *58*, 318-332. https://doi.org/10.1111/j.1365-313X.2008.03781.x.

36. Eckardt, N.A. (2002). Tangerine dreams: cloning of carotenoid isomerase from Arabidopsis and tomato. Plant Cell *14*, 289-292. 10.1105/tpc.140210.

37. Egea, I., Barsan, C., Bian, W., Purgatto, E., Latché, A., Chervin, C., Bouzayen, M., and Pech, J.C. (2010). Chromoplast differentiation: current status and perspectives. Plant Cell Physiol *51*, 1601-1611. 10.1093/pcp/pcq136.

38. Eisenreich, W., Rohdich, F., and Bacher, A. (2001). Deoxyxylulose phosphate pathway to terpenoids. Trends Plant Sci *6*, 78-84. 10.1016/s1360-1385(00)01812-4.

39. Emerson, R., Chalmers, R., and Cederstrand, C. (1957). SOME FACTORS INFLUENCING THE LONG-WAVE LIMIT OF PHOTOSYNTHESIS. Proceedings of the National Academy of Sciences *43*, 133-143. doi:10.1073/pnas.43.1.133.

40. Enfissi, E.M., Fraser, P.D., Lois, L.M., Boronat, A., Schuch, W., and Bramley, P.M. (2005). Metabolic engineering of the mevalonate and non-mevalonate isopentenyl diphosphate-forming pathways for the production of health-promoting isoprenoids in tomato. Plant Biotechnol J *3*, 17-27. 10.1111/j.1467-7652.2004.00091.x.

41. Eugeni Piller, L., Besagni, C., Ksas, B., Rumeau, D., Bréhélin, C., Glauser, G., Kessler, F., and Havaux, M. (2011). Chloroplast lipid droplet type II NAD(P)H quinone oxidoreductase is essential for prenylquinone metabolism and vitamin K1 accumulation. Proc Natl Acad Sci U S A *108*, 14354-14359. 10.1073/pnas.1104790108.

42. Fenn, M.A., and Giovannoni, J.J. (2021). Phytohormones in fruit development and maturation. The Plant Journal *105*, 446-458. https://doi.org/10.1111/tpj.15112.

43. Fernie, A.R., Bachem, C.W.B., Helariutta, Y., Neuhaus, H.E., Prat, S., Ruan, Y.-L., Stitt, M., Sweetlove, L.J., Tegeder, M., Wahl, V., et al. (2020). Synchronization of developmental, molecular and metabolic aspects of source–sink interactions. Nature Plants *6*, 55-66. 10.1038/s41477-020-0590-x.

44. FORDE, B.G., and WALCH-LIU, P. (2009). Nitrate and glutamate as environmental cues for behavioural responses in plant roots. Plant, Cell & Environment *32*, 682-693. https://doi.org/10.1111/j.1365-3040.2008.01927.x.

45. Fray, R.G., and Grierson, D. (1993). Identification and genetic analysis of normal and mutant phytoene synthase genes of tomato by sequencing, complementation and co-suppression. Plant Molecular Biology *22*, 589-602. 10.1007/BF00047400.

46. Frey-Wyssling, A., and Schwegler, F. (1965). Ultrastructure of the chromoplasts in the carrot root. Journal of ultrastructure research *13*, 543-559.

47. Fujisawa, M., and Ito, Y. (2013). The regulatory mechanism of fruit ripening revealed by analyses of direct targets of the tomato MADS-box transcription factor RIPENING INHIBITOR. Plant Signaling & Behavior *8*, e24357. 10.4161/psb.24357.

48. Gaude, N., Bréhélin, C., Tischendorf, G., Kessler, F., and Dörmann, P. (2007). Nitrogen deficiency in Arabidopsis affects galactolipid composition and gene expression and results in accumulation of fatty acid phytyl esters. Plant J *49*, 729-739. 10.1111/j.1365-313X.2006.02992.x.

49. Gautier, H., Guichard, S., and Tchamitchian, M. (2001). Modulation of Competition between Fruits and Leaves by Flower Pruning and Water Fogging, and Consequences on Tomato Leaf and Fruit Growth. Ann Bot *88*, 645-652. https://doi.org/10.1006/anbo.2001.1518.

50. Giovannoni, J.J. (2004). Genetic Regulation of Fruit Development and Ripening. The Plant Cell *16*, S170-S180. 10.1105/tpc.019158.

51. Giovannoni, J.J. (2007). Fruit ripening mutants yield insights into ripening control. Curr Opin Plant Biol *10*, 283-289. 10.1016/j.pbi.2007.04.008.

52. Giuliano, G., Giliberto, L., and Rosati, C. (2002). Carotenoid isomerase: a tale of light and isomers. Trends in Plant Science *7*, 427-429. https://doi.org/10.1016/S1360-1385(02)02329-4.

53. Guaus, E., Torrent-Burgués, J., and Hoyo, J. (2017). Thylakoid Membrane Bioenergetics. In. 10.1016/B978-0-12-409547-2.13513-9.

54. Guillet, C., Aboul-Soud, M.A.M., Le Menn, A., Viron, N., Pribat, A., Germain, V., Just, D., Baldet, P., Rousselle, P., Lemaire-Chamley, M., and Rothan, C. (2012). Regulation of the Fruit-Specific PEP Carboxylase SlPPC2 Promoter at Early Stages of Tomato Fruit Development. PLOS ONE *7*, e36795. 10.1371/journal.pone.0036795.

55. Havaux, M. (2020). Plastoquinone In and Beyond Photosynthesis. Trends in Plant Science *25*, 1252-1265. https://doi.org/10.1016/j.tplants.2020.06.011.

56. Hetherington, S.E., Smillie, R.M., and Davies, W.J. (1998). Photosynthetic activities of vegetative and fruiting tissues of tomato. Journal of Experimental Botany *49*, 1173-1181. 10.1093/jxb/49.324.1173.

57. Heuvelink, E. (1997). Effect of fruit load on dry matter partitioning in tomato. Scientia Horticulturae *69*, 51-59. https://doi.org/10.1016/S0304-4238(96)00993-4.

58. Hikmat, O., Tzoulis, C., Knappskog, P.M., Johansson, S., Boman, H., Sztromwasser, P., Lien, E., Brodtkorb, E., Ghezzi, D., and Bindoff, L.A. (2016). ADCK 3 mutations with epilepsy, stroke-like episodes and ataxia: a POLG mimic? European journal of neurology *23*, 1188-1194.

59. Howe, C.J., Barbrook, A.C., Nisbet, R.E., Lockhart, P.J., and Larkum, A.W. (2008). The origin of plastids. Philos Trans R Soc Lond B Biol Sci *363*, 2675-2685. 10.1098/rstb.2008.0050.

60. Huang, H., Yang, M., Su, Y., Qu, L., and Deng, X.W. (2015). Arabidopsis Atypical Kinases ABC1K1 and ABC1K3 Act Oppositely to Cope with Photodamage Under Red Light. Mol Plant *8*, 1122-1124. 10.1016/j.molp.2015.04.003.

61. Ifuku, K., Ishihara, S., and Sato, F. (2010). Molecular Functions of Oxygen-Evolving Complex Family Proteins in Photosynthetic Electron Flow. Journal of Integrative Plant Biology *52*, 723-734. https://doi.org/10.1111/j.1744-7909.2010.00976.x.

62. Isaacson, T., Ohad, I., Beyer, P., and Hirschberg, J. (2004). Analysis in vitro of the enzyme CRTISO establishes a poly-cis-carotenoid biosynthesis pathway in plants. Plant Physiol *136*, 4246-4255. 10.1104/pp.104.052092.

63. Jarvis, P., and López-Juez, E. (2013). Biogenesis and homeostasis of chloroplasts and other plastids. Nature Reviews Molecular Cell Biology *14*, 787-802. 10.1038/nrm3702.

64. Jeong, H.B., Jang, S.J., Kang, M.Y., Kim, S., Kwon, J.K., and Kang, B.C. (2020). Candidate Gene Analysis Reveals That the Fruit Color Locus C1 Corresponds to PRR2 in Pepper (Capsicum frutescens). Front Plant Sci *11*, 399. 10.3389/fpls.2020.00399.

65. Johnson, M.P. (2016). Photosynthesis. Essays Biochem *60*, 255-273. 10.1042/ebc20160016.

66. Kachanovsky, D.E., Filler, S., Isaacson, T., and Hirschberg, J. (2012). Epistasis in tomato color mutations involves regulation of phytoene synthase 1 expression by cis-carotenoids. Proceedings of the National Academy of Sciences *109*, 19021-19026. 10.1073/pnas.1214808109.

67. Kader, A.A. (2008). Flavor quality of fruits and vegetables. Journal of the Science of Food and Agriculture *88*, 1863-1868. https://doi.org/10.1002/jsfa.3293.

68. Kemmerer, Z.A., Robinson, K.P., Schmitz, J.M., Manicki, M., Paulson, B.R., Jochem, A., Hutchins, P.D., Coon, J.J., and Pagliarini, D.J. (2021). UbiB proteins regulate cellular CoQ distribution in Saccharomyces cerevisiae. Nature Communications *12*, 4769. 10.1038/s41467-021-25084-7.

69. Kim, O.R., Cho, M.-C., Kim, B.-D., and Huh, J.H. (2010). A splicing mutation in the gene encoding phytoene synthase causes orange coloration in Habanero pepper fruits. Molecules and Cells *30*, 569-574. 10.1007/s10059-010-0154-4.

70. Klee, H., and Tieman, D. (2002). The tomato ethylene receptor gene family: Form and function. Physiol Plant *115*, 336-341. 10.1034/j.1399-3054.2002.1150302.x.

71. Klee, H.J. (2010). Improving the flavor of fresh fruits: genomics, biochemistry, and biotechnology. New Phytologist *187*, 44-56. https://doi.org/10.1111/j.1469-8137.2010.03281.x.

72. Klee, H.J., and Giovannoni, J.J. (2011). Genetics and control of tomato fruit ripening and quality attributes. Annu Rev Genet *45*, 41-59. 10.1146/annurev-genet-110410-132507.

73. Knapp, S. (2002). Tobacco to tomatoes: a phylogenetic perspective on fruit diversity in the Solanaceae. J Exp Bot *53*, 2001-2022. 10.1093/jxb/erf068.

74. Kovács, K., Fray, R.G., Tikunov, Y., Graham, N., Bradley, G., Seymour, G.B., Bovy, A.G., and Grierson, D. (2009). Effect of tomato pleiotropic ripening mutations on flavour volatile biosynthesis. Phytochemistry *70*, 1003-1008. https://doi.org/10.1016/j.phytochem.2009.05.014.

75. Kuai, B., Chen, J., and Hörtensteiner, S. (2018). The biochemistry and molecular biology of chlorophyll breakdown. J Exp Bot *69*, 751-767. 10.1093/jxb/erx322

76. Külheim, C., Agren, J., and Jansson, S. (2002). Rapid regulation of light harvesting and plant fitness in the field. Science *297*, 91-93. 10.1126/science.1072359.

77. Kumar, R., Khurana, A., and Sharma, A.K. (2014). Role of plant hormones and their interplay in development and ripening of fleshy fruits. Journal of Experimental Botany *65*, 4561-4575. 10.1093/jxb/eru277.

78. Larkum, A.W.D., Lockhart, P.J., and Howe, C.J. (2007). Shopping for plastids. Trends in Plant Science *12*, 189-195. https://doi.org/10.1016/j.tplants.2007.03.011.

79. Lee, D. (2005). Plant pigments and their manipulation. Annual Plant Reviews Vol 12. Davies KM, ed. 2004. Oxford/Boca Raton: Blackwell Publishing/CRC Press, Boca Raton. £110 (hardback). 352 pp. Ann Bot *96*, 1332-1333. 10.1093/aob/mci287.

80. Li, S., Zhu, B., Pirrello, J., Xu, C., Zhang, B., Bouzayen, M., Chen, K., and Grierson, D. (2020). Roles of RIN and ethylene in tomato fruit ripening and ripening-associated traits. New Phytologist *226*, 460-475. https://doi.org/10.1111/nph.16362.

81. Li, T., Jiang, J., Zhang, S., Shu, H., Wang, Y., Lai, J., Du, J., and Yang, C. (2015). OsAGSW1, an ABC1-like kinase gene, is involved in the regulation of grain size and weight in rice. J Exp Bot *66*, 5691-5701. 10.1093/jxb/erv160.

82. Lichtenthaler, H.K. (1999). THE 1-DEOXY-D-XYLULOSE-5-PHOSPHATE PATHWAY OF ISOPRENOID BIOSYNTHESIS IN PLANTS. Annual Review of Plant Physiology and Plant Molecular Biology *50*, 47-65. 10.1146/annurev.arplant.50.1.47.

83. Lippold, F., vom Dorp, K., Abraham, M., Hölzl, G., Wewer, V., Yilmaz, J.L., Lager, I., Montandon, C., Besagni, C., Kessler, F., et al. (2012). Fatty acid phytyl ester synthesis in chloroplasts of Arabidopsis. The Plant cell *24*, 2001-2014. 10.1105/tpc.112.095588.

84. Lobit, P., Génard, M., Wu, B.H., Soing, P., and Habib, R. (2003). Modelling citrate metabolism in fruits: responses to growth and temperature. Journal of Experimental Botany *54*, 2489-2501. 10.1093/jxb/erg264.

85. Lohscheider, J.N., Friso, G., and van Wijk, K.J. (2016). Phosphorylation of plastoglobular proteins in Arabidopsis thaliana. Journal of experimental botany *67*, 3975-3984. 10.1093/jxb/erw091.

86. Lois, L.M., Rodríguez-Concepción, M., Gallego, F., Campos, N., and Boronat, A. (2000). Carotenoid biosynthesis during tomato fruit development: regulatory role of 1-deoxy-D-xylulose 5-phosphate synthase. Plant J *22*, 503-513. 10.1046/j.1365-313x.2000.00764.x.

87. Lopez-Juez, E., and Pyke, K.A. (2005). Plastids unleashed: their development and their integration in plant development. Int J Dev Biol *49*, 557-577. 10.1387/ijdb.051997el.

88. Lundquist, P.K., Davis, J.I., and van Wijk, K.J. (2012a). ABC1K atypical kinases in plants: filling the organellar kinase void. Trends Plant Sci *17*, 546-555. 10.1016/j.tplants.2012.05.010.

89. Lundquist, P.K., Poliakov, A., Bhuiyan, N.H., Zybailov, B., Sun, Q., and van Wijk, K.J. (2012b). The functional network of the Arabidopsis plastoglobule proteome based on quantitative proteomics and genome-wide coexpression analysis. Plant physiology *158*, 1172-1192. 10.1104/pp.111.193144.

90. Lundquist, P.K., Poliakov, A., Giacomelli, L., Friso, G., Appel, M., McQuinn, R.P., Krasnoff, S.B., Rowland, E., Ponnala, L., Sun, Q., and van Wijk, K.J. (2013). Loss of Plastoglobule Kinases ABC1K1 and ABC1K3 Causes Conditional Degreening, Modified Prenyl-Lipids, and Recruitment of the Jasmonic Acid Pathway. The Plant Cell *25*, 1818-1839. 10.1105/tpc.113.111120.

91. Luo, Z., Zhang, J., Li, J., Yang, C., Wang, T., Ouyang, B., Li, H., Giovannoni, J., and Ye, Z. (2013). A STAY-GREEN protein SlSGR1 regulates lycopene and β-carotene accumulation by interacting directly with SlPSY1 during ripening processes in tomato. New Phytol *198*, 442-452. 10.1111/nph.12175.

92. Malundo, T.M.M., Shewfelt, R.L., and Scott, J.W. (1995). Flavor quality of fresh tomato (Lycopersicon esculentum Mill.) as affected by sugar and acid levels. Postharvest Biology and Technology *6*, 103-110. https://doi.org/10.1016/0925-5214(94)00052-T.

93. Manara, A., DalCorso, G., Guzzo, F., and Furini, A. (2015). Loss of the Atypical Kinases ABC1K7 and ABC1K8 Changes the Lipid Composition of the Chloroplast Membrane. Plant Cell Physiol *56*, 1193-1204. 10.1093/pcp/pcv046.

94. Manara, A., DalCorso, G., Leister, D., Jahns, P., Baldan, B., and Furini, A. (2014). AtSIA1 AND AtOSA1: two Abc1 proteins involved in oxidative stress responses and iron distribution within chloroplasts. New Phytologist *201*, 452-465. https://doi.org/10.1111/nph.12533.

95. Mann, L., Laplanche, D., Turlings, T.C.J., and Desurmont, G.A. (2021). A comparative study of plant volatiles induced by insect and gastropod herbivory. Scientific Reports *11*, 23698. 10.1038/s41598-021-02801-2.

96. Martinis, J., Glauser, G., Valimareanu, S., and Kessler, F. (2013). A Chloroplast ABC1-like Kinase Regulates Vitamin E Metabolism in Arabidopsis Plant Physiology *162*, 652-662. 10.1104/pp.113.218644.

97. Martinis, J., Glauser, G., Valimareanu, S., Stettler, M., Zeeman, S.C., Yamamoto, H., Shikanai, T., and Kessler, F. (2014). ABC1K1/PGR6 kinase: a regulatory link between photosynthetic activity and chloroplast metabolism. The Plant Journal *77*, 269-283. https://doi.org/10.1111/tpj.12385.

98. Mechela, A., Schwenkert, S., and Soll, J. (2019). A brief history of thylakoid biogenesis. Open Biol *9*, 180237-180237. 10.1098/rsob.180237.

99. Nielsen, N.C., Smillie, R.M., Henningsen, K.W., and Von Wettstein, D. (1979). Composition and Function of Thylakoid Membranes from Grana-rich and Grana-deficient Chloroplast Mutants of Barley. Plant physiology *63*, 174-182. 10.1104/pp.63.1.174.

100. Nilkens, M., Kress, E., Lambrev, P., Miloslavina, Y., Müller, M., Holzwarth, A.R., and Jahns, P. (2010). Identification of a slowly inducible zeaxanthin-dependent component of non-photochemical quenching of chlorophyll fluorescence generated under steady-state conditions in Arabidopsis. Biochimica et Biophysica Acta (BBA) - Bioenergetics *1797*, 466-475. https://doi.org/10.1016/j.bbabio.2010.01.001.

101. Nogueira, M., Mora, L., Enfissi, E.M., Bramley, P.M., and Fraser, P.D. (2013). Subchromoplast sequestration of carotenoids affects regulatory mechanisms in tomato lines expressing different carotenoid gene combinations. Plant Cell *25*, 4560-4579. 10.1105/tpc.113.116210.

102. Osorio, S., Scossa, F., and Fernie, A. (2013). Molecular regulation of fruit ripening. Front Plant Sci *4*. 10.3389/fpls.2013.00198.

103. P. Horton, A. V. Ruban, a., and Walters, R.G. (1996). REGULATION OF LIGHT HARVESTING IN GREEN PLANTS. Annual Review of Plant Physiology and Plant Molecular Biology *47*, 655-684. 10.1146/annurev.arplant.47.1.655.

104. Peltier, J.-B., Ytterberg, A.J., Sun, Q., and van Wijk, K.J. (2004). New Functions of the Thylakoid Membrane Proteome of Arabidopsis thaliana Revealed by a Simple, Fast, and Versatile Fractionation Strategy. *279*, 49367-49383. 10.1074/jbc.M406763200.

105. Pesaresi, P., Mizzotti, C., Colombo, M., and Masiero, S. (2014). Genetic regulation and structural changes during tomato fruit development and ripening. Front Plant Sci *5*. 10.3389/fpls.2014.00124.

106. Poon, W.W., Davis, D.E., Ha, H.T., Jonassen, T., Rather, P.N., and Clarke, C.F. (2000). Identification of Escherichia coli ubiB, a gene required for the first monooxygenase step in ubiquinone biosynthesis. J Bacteriol *182*, 5139-5146. 10.1128/jb.182.18.5139-5146.2000.

107. Porfirova, S., Bergmüller, E., Tropf, S., Lemke, R., and Dörmann, P. (2002). Isolation of an Arabidopsis mutant lacking vitamin E and identification of a cyclase essential for all tocopherol biosynthesis. Proceedings of the National Academy of Sciences *99*, 12495-12500. doi:10.1073/pnas.182330899.

108. Pozueta-Romero, J., Rafia, F., Houlne, G., Cheniclet, C., Carde, J.P., Schantz, M.L., and Schantz, R. (1997). A Ubiquitous Plant Housekeeping Gene, PAP, Encodes a Major Protein Component of Bell Pepper Chromoplasts. Plant Physiology *115*, 1185-1194. 10.1104/pp.115.3.1185.

109. Pralon, T., Collombat, J., Pipitone, R., Ksas, B., Shanmugabalaji, V., Havaux, M., Finazzi, G., Longoni, P., and Kessler, F. (2020). Mutation of the Atypical Kinase ABC1K3 Partially Rescues the PROTON GRADIENT REGULATION 6 Phenotype in Arabidopsis thaliana. Front Plant Sci *11*. 10.3389/fpls.2020.00337.

110. Pralon, T., Shanmugabalaji, V., Longoni, P., Glauser, G., Ksas, B., Collombat, J., Desmeules, S., Havaux, M., Finazzi, G., and Kessler, F. (2019). Plastoquinone homoeostasis by Arabidopsis proton gradient regulation 6 is essential for photosynthetic efficiency. Communications Biology *2*, 220. 10.1038/s42003-019-0477-4.

111. Pyke, K. (2007). Plastid biogenesis and differentiation. In Cell and Molecular Biology of Plastids, R. Bock, ed. (Springer Berlin Heidelberg), pp. 1-28. 10.1007/4735_2007_0226.

112. Reidenbach, A.G., Kemmerer, Z.A., Aydin, D., Jochem, A., McDevitt, M.T., Hutchins, P.D., Stark, J.L., Stefely, J.A., Reddy, T., Hebert, A.S., et al. (2018). Conserved Lipid and Small-Molecule Modulation of COQ8 Reveals Regulation of the Ancient Kinase-like UbiB Family. Cell Chem Biol *25*, 154-165.e111. 10.1016/j.chembiol.2017.11.001.

113. Renau-Morata, B., Carrillo, L., Cebolla-Cornejo, J., Molina, R.V., Martí, R., Domínguez-Figueroa, J., Vicente-Carbajosa, J., Medina, J., and Nebauer, S.G. (2020). The targeted overexpression of SlCDF4 in the fruit enhances tomato size and yield involving gibberellin signalling. Scientific Reports *10*, 10645. 10.1038/s41598-020-67537-x.

114. Rey, P., Gillet, B., Römer, S., Eymery, F., Massimino, J., Peltier, G., and Kuntz, M. (2000). Over-expression of a pepper plastid lipid-associated protein in tobacco leads to changes in plastid

ultrastructure and plant development upon stress. Plant J *21*, 483-494. 10.1046/j.1365-313x.2000.00699.x.

115. Rochaix, J.D. (2011). Regulation of photosynthetic electron transport. Biochim Biophys Acta *1807*, 375-383. 10.1016/j.bbabio.2010.11.010.

116. Rodríguez-Concepción, M., Ahumada, I., Diez-Juez, E., Sauret-Güeto, S., Lois, L.M., Gallego, F., Carretero-Paulet, L., Campos, N., and Boronat, A. (2001). 1-Deoxy-d-xylulose 5-phosphate reductoisomerase and plastid isoprenoid biosynthesis during tomato fruit ripening. The Plant Journal *27*, 213-222. https://doi.org/10.1046/j.1365-313x.2001.01089.x.

117. Rodriguez-Uribe, L., Guzman, I., Rajapakse, W., Richins, R.D., and O'Connell, M.A. (2011). Carotenoid accumulation in orange-pigmented Capsicum annuum fruit, regulated at multiple levels. Journal of Experimental Botany *63*, 517-526. 10.1093/jxb/err302.

118. Rottet, S., Besagni, C., and Kessler, F. (2015). The role of plastoglobules in thylakoid lipid remodeling during plant development. Biochimica et Biophysica Acta (BBA) - Bioenergetics *1847*, 889-899. https://doi.org/10.1016/j.bbabio.2015.02.002.

119. Ruban, A.V. (2012). The photosynthetic membrane: molecular mechanisms and biophysics of light harvesting (John Wiley & Sons).

120. Ruban, A.V., and Murchie, E.H. (2012). Assessing the photoprotective effectiveness of non-photochemical chlorophyll fluorescence quenching: A new approach. Biochimica et Biophysica Acta (BBA) - Bioenergetics *1817*, 977-982. https://doi.org/10.1016/j.bbabio.2012.03.026.

121. Sacks, D., Baxter, B., Campbell, B.C.V., Carpenter, J.S., Cognard, C., Dippel, D., Eesa, M., Fischer, U., Hausegger, K., Hirsch, J.A., et al. (2018). Multisociety Consensus Quality Improvement Revised Consensus Statement for Endovascular Therapy of Acute Ischemic Stroke. Int J Stroke *13*, 612-632. 10.1177/1747493018778713.

122. Saini, R.K., Zamany, A.J., and Keum, Y.S. (2017). Ripening improves the content of carotenoid, α-tocopherol, and polyunsaturated fatty acids in tomato (Solanum lycopersicum L.) fruits. 3 Biotech *7*, 43. 10.1007/s13205-017-0666-0.

123. Sakuraba, Y., Park, S.Y., and Paek, N.C. (2015). The Divergent Roles of STAYGREEN (SGR) Homologs in Chlorophyll Degradation. Mol Cells *38*, 390-395. 10.14348/molcells.2015.0039.

124. Schaffer, A.A., and Petreikov, M. (1997). Sucrose-to-Starch Metabolism in Tomato Fruit Undergoing Transient Starch Accumulation. Plant Physiology *113*, 739-746. 10.1104/pp.113.3.739.

125. Schauer, N., Zamir, D., and Fernie, A.R. (2004). Metabolic profiling of leaves and fruit of wild species tomato: a survey of the Solanum lycopersicum complex. Journal of Experimental Botany *56*, 297-307. 10.1093/jxb/eri057.

126. Schijlen, E., Beekwilder, J., Hall, R., and van der Meer, I. (2008). Boosting beneficial phytochemicals in vegetable crop plants. CAB Reviews: Perspectives in Agriculture, Veterinary Science, Nutrition and Natural Resources *3*.

127. Schmetterer, G. (1994). Cyanobacterial Respiration. In The Molecular Biology of Cyanobacteria, D.A. Bryant, ed. (Springer Netherlands), pp. 409-435. 10.1007/978-94-011-0227-8_13.

128. Shen, J., Tieman, D., Jones, J.B., Taylor, M.G., Schmelz, E., Huffaker, A., Bies, D., Chen, K., and Klee, H.J. (2014). A 13-lipoxygenase, TomloxC, is essential for synthesis of C5 flavour volatiles in tomato. Journal of Experimental Botany *65*, 419-428. 10.1093/jxb/ert382.

129. Shikanai, T., Munekage, Y., Shimizu, K., Endo, T., and Hashimoto, T. (1999). Identification and characterization of Arabidopsis mutants with reduced quenching of chlorophyll fluorescence. Plant Cell Physiol *40*, 1134-1142. 10.1093/oxfordjournals.pcp.a029498.

130. Shinozaki, Y., Nicolas, P., Fernandez-Pozo, N., Ma, Q., Evanich, D.J., Shi, Y., Xu, Y., Zheng, Y., Snyder, S.I., Martin, L.B.B., et al. (2018). High-resolution spatiotemporal transcriptome mapping of tomato fruit development and ripening. Nature Communications *9*, 364. 10.1038/s41467-017-02782-9.

131. Simkin, A.J., López-Calcagno, P.E., and Raines, C.A. (2019). Feeding the world: improving photosynthetic efficiency for sustainable crop production. J Exp Bot *70*, 1119-1140. 10.1093/jxb/ery445.

132. Singh, D.K., Laremore, T.N., Smith, P.B., Maximova, S.N., and McNellis, T.W. (2012). Knockdown of FIBRILLIN4 gene expression in apple decreases plastoglobule plastoquinone content. PLoS One *7*, e47547. 10.1371/journal.pone.0047547.

133. Stefely, J.A., Licitra, F., Laredj, L., Reidenbach, A.G., Kemmerer, Z.A., Grangeray, A., Jaeg-Ehret, T., Minogue, C.E., Ulbrich, A., Hutchins, P.D., et al. (2016). Cerebellar Ataxia and Coenzyme Q Deficiency through Loss of Unorthodox Kinase Activity. Mol Cell *63*, 608-620. 10.1016/j.molcel.2016.06.030.

134. Stefely, J.A., Reidenbach, A.G., Ulbrich, A., Oruganty, K., Floyd, B.J., Jochem, A., Saunders, J.M., Johnson, I.E., Minogue, C.E., Wrobel, R.L., et al. (2015). Mitochondrial ADCK3 employs an atypical

protein kinase-like fold to enable coenzyme Q biosynthesis. Mol Cell *57*, 83-94. 10.1016/j.molcel.2014.11.002.

135. Strand, D.D., and Kramer, D.M. (2014). Control of Non-Photochemical Exciton Quenching by the Proton Circuit of Photosynthesis. In Non-Photochemical Quenching and Energy Dissipation in Plants, Algae and Cyanobacteria, B. Demmig-Adams, G. Garab, W. Adams Iii, and Govindjee, eds. (Springer Netherlands), pp. 387-408. 10.1007/978-94-017-9032-1_18.

136. Sun, T., Yuan, H., Cao, H., Yazdani, M., Tadmor, Y., and Li, L. (2018). Carotenoid Metabolism in Plants: The Role of Plastids. Molecular Plant *11*, 58-74. https://doi.org/10.1016/j.molp.2017.09.010.

137. Suzuki, M., Takahashi, S., Kondo, T., Dohra, H., Ito, Y., Kiriiwa, Y., Hayashi, M., Kamiya, S., Kato, M., Fujiwara, M., et al. (2015). Plastid Proteomic Analysis in Tomato Fruit Development. PLoS One *10*, e0137266. 10.1371/journal.pone.0137266.

138. Tamasi, G., Pardini, A., Bonechi, C., Donati, A., Pessina, F., Marcolongo, P., Gamberucci, A., Leone, G., Consumi, M., Magnani, A., and Rossi, C. (2019). Characterization of nutraceutical components in tomato pulp, skin and locular gel. European Food Research and Technology *245*, 907-918. 10.1007/s00217-019-03235-x.

139. Tan, J., Zhongjing, Z., Niu, Y., Sun, X., and Deng, Z. (2017). Identification and Functional Characterization of Tomato CircRNAs Derived from Genes Involved in Fruit Pigment Accumulation. Scientific Reports *7*. 10.1038/s41598-017-08806-0.

140. Tieman, D., Bliss, P., McIntyre, Lauren M., Blandon-Ubeda, A., Bies, D., Odabasi, Asli Z., Rodríguez, Gustavo R., van der Knaap, E., Taylor, Mark G., Goulet, C., et al. (2012). The Chemical Interactions Underlying Tomato Flavor Preferences. Current Biology *22*, 1035-1039. https://doi.org/10.1016/j.cub.2012.04.016.

141. Tohge, T., de Souza, L.P., and Fernie, A.R. (2017). Current understanding of the pathways of flavonoid biosynthesis in model and crop plants. Journal of Experimental Botany *68*, 4013-4028. 10.1093/jxb/erx177.

142. Toyama, S. (1980). Electron microscope studies on the morphogenesis of plastids. X. Ultrastructural changes of chloroplasts in morning glory leaves exposed to ethylene. American Journal of Botany *67*, 625-635.

143. Valenta, K., Kalbitzer, U., Razafimandimby, D., Omeja, P., Ayasse, M., Chapman, C.A., and Nevo, O. (2018). The evolution of fruit colour: phylogeny, abiotic factors and the role of mutualists. Sci Rep *8*, 14302. 10.1038/s41598-018-32604-x.

144. Valle, E.M., Boggio, S.B., and Heldt, H.W. (1998). Free Amino Acid Composition of Phloem Sap and Growing Fruit of Lycopersicon esculentum. Plant and Cell Physiology *39*, 458-461. 10.1093/oxfordjournals.pcp.a029391.

145. van Wijk, K.J., and Kessler, F. (2017). Plastoglobuli: Plastid Microcompartments with Integrated Functions in Metabolism, Plastid Developmental Transitions, and Environmental Adaptation. Annual review of plant biology *68*, 253-289. 10.1146/annurev-arplant-043015-111737.

146. Vidi, P.-A., Kanwischer, M., Baginsky, S., Austin, J.R., Csucs, G., Dörmann, P., Kessler, F., and Bréhélin, C. (2006). Tocopherol Cyclase (VTE1) Localization and Vitamin E Accumulation in Chloroplast Plastoglobule Lipoprotein Particles. *281*, 11225-11234. 10.1074/jbc.M511939200.

147. Vishnevetsky, M., Ovadis, M., Itzhaki, H., Levy, M., Libal-Weksler, Y., Adam, Z., and Vainstein, A. (1996). Molecular cloning of a carotenoid-associated protein from Cucumis sativus corollas: homologous genes involved in carotenoid sequestration in chromoplasts. The Plant Journal *10*, 1111-1118. https://doi.org/10.1046/j.1365-313X.1996.10061111.x.

148. Vogel, J.T., Tieman, D.M., Sims, C.A., Odabasi, A.Z., Clark, D.G., and Klee, H.J. (2010). Carotenoid content impacts flavor acceptability in tomato (Solanum lycopersicum). Journal of the Science of Food and Agriculture *90*, 2233-2240.

149. W W Thomson, a., and Whatley, J.M. (1980). Development of Nongreen Plastids. Annual Review of Plant Physiology *31*, 375-394. 10.1146/annurev.pp.31.060180.002111.

150. Wang, L., Li, J., Zhao, J., and He, C. (2015). Evolutionary developmental genetics of fruit morphological variation within the Solanaceae. Front Plant Sci *6*, 248. 10.3389/fpls.2015.00248.

151. Wang, R., Lammers, M., Tikunov, Y., Bovy, A.G., Angenent, G.C., and de Maagd, R.A. (2020). The rin, nor and Cnr spontaneous mutations inhibit tomato fruit ripening in additive and epistatic manners. Plant Science *294*, 110436. https://doi.org/10.1016/j.plantsci.2020.110436.

152. Wang, Y.-Q., Yang, Y., Fei, Z., Yuan, H., Fish, T., Thannhauser, T.W., Mazourek, M., Kochian, L.V., Wang, X., and Li, L. (2013). Proteomic analysis of chromoplasts from six crop species reveals insights into chromoplast function and development. Journal of Experimental Botany *64*, 949-961. 10.1093/jxb/ers375.

153. Whatley, F.R. (1979). Standard reference work on the plastids. Nature *279*, 825-826. 10.1038/279825b0.

154. Wolfertz, M., Sharkey, T.D., Boland, W., and Kühnemann, F. (2004). Rapid regulation of the methylerythritol 4-phosphate pathway during isoprene synthesis. Plant Physiol *135*, 1939-1945. 10.1104/pp.104.043737.

155. Yang, M., Huang, H., Zhang, C., Wang, Z., Su, Y., Zhu, P., Guo, Y., and Deng, X.W. (2016). Arabidopsis atypical kinase ABC1K1 is involved in red light-mediated development. Plant Cell Rep *35*, 1213-1220. 10.1007/s00299-016-1953-7.

156. Yaronskaya, E., Vershilovskaya, I., Poers, Y., Alawady, A.E., Averina, N., and Grimm, B. (2006). Cytokinin effects on tetrapyrrole biosynthesis and photosynthetic activity in barley seedlings. Planta *224*, 700-709. 10.1007/s00425-006-0249-5.

157. Ytterberg, A.J., Peltier, J.B., and van Wijk, K.J. (2006). Protein profiling of plastoglobules in chloroplasts and chromoplasts. A surprising site for differential accumulation of metabolic enzymes. Plant Physiol *140*, 984-997. 10.1104/pp.105.076083.

158. Zeng, Y., Du, J., Wang, L., Pan, Z., Xu, Q., Xiao, S., and Deng, X. (2015). A Comprehensive Analysis of Chromoplast Differentiation Reveals Complex Protein Changes Associated with Plastoglobule Biogenesis and Remodeling of Protein Systems in Sweet Orange Flesh. Plant Physiol *168*, 1648-1665. 10.1104/pp.15.00645.

159. Zhao, X., Chen, T., Feng, B., Zhang, C., Peng, S., Zhang, X., Fu, G., and Tao, L. (2016). Non-photochemical Quenching Plays a Key Role in Light Acclimation of Rice Plants Differing in Leaf Color. Front Plant Sci *7*, 1968. 10.3389/fpls.2016.01968.

160. Zhu, F., Wen, W., Cheng, Y., and Fernie, A.R. (2022). The metabolic changes that effect fruit quality during tomato fruit ripening. Molecular Horticulture *2*, 2. 10.1186/s43897-022-00024-1.

2. Plastoglobules: A hub of lipid metabolism in the chloroplast

Venkatasalam Shanmugabalaji*, Wayne Zita, Joy Collombat, and Felix Kessler
Laboratoire de Physiologie Végétale, Université de Neuchâtel, Neuchâtel, Switzerland
*Corresponding author: e-mail address: shanmugabalaji.venkatasalam@unine.ch

2.1 Summary

Chloroplasts in plant and algae are the home of photosynthesis and many essential metabolic pathways. The photosynthetic light reactions occur at an extensive membrane system, the thylakoids. The main constituents of thylakoid membranes are the galactolipids, in particular monogalactosyldiacylglycerol (MGDG) and digalactosyldiacylglycerol (DGDG). Apart from these, thylakoid membranes contain a number of other lipid molecules that function as electron transporters (plastoquinone) or as lipid antioxidants (tocopherols) and that are free to diffuse in the membrane system. Others such as phylloquinone, carotenoids and chlorophylls are mostly associated with protein components of the photosystems that reside in the thylakoids. The thylakoids are extremely dynamic and rapidly respond to environmental stresses. Plastoglobules (PG), lipoprotein particles or lipid droplets associated with thylakoids, play a central role in these responses. PG are thought to allocate stored electron carriers as well as lipid antioxidants to the membranes. PG also contribute enzymatic capacity for antioxidant and electron carrier synthesis and metabolism. During senescence and under nitrogen deprivation PG actively participate in membrane catabolism. PG become supersized while absorbing triacylglycerols and fatty acid phytol esters resulting from galactolipid and chlorophyll degradation. This chapter aims at giving a broad overview of the role of PG in chloroplast lipid metabolism.

2.2 Introduction

2.2.1 Discovery and History

The advent of electron microscopy as a tool in cellular biology in the late 1950's and 1960's allowed a first glimpse inside the plant cell and its subcellular structures. Amongst other features within the chloroplast the electron micrographs revealed the presence of globular structures. Osmium tetroxide stained these structures intensely which hence were called osmiophile globules. Due to their presence in many plastid types the name was later changed to plastoglobules (abbreviated PG) (Greenwood *et al.,* 1963; Lichtenthaler, 1968a; Spurr and Harris, 1968). These early studies carried out on multiple species revealed a diversity of osmiophile globules which varied in size (30nm to several µm) and number under various environmental (for instance drought) or developmental conditions (for instance in older and younger leaves or fruit) (Lichtenthaler, 1968a; Thomson and Platt, 1973). Supersized PG, several µm in diameter, were readily observed in old and senescent leaves (Gaude *et al.,* 2007; Tevini and Steinmuller, 1985). It was also observed that numerous PG were contained in the prolamellar body of etiolated, dark grown seedlings. When exposed to light the thylakoid system rapidly emerged and the number of PG diminished during the greening process. The authors noted this correlation and suggested that PG may contribute (membrane) lipids to the developing photosynthetic membrane system (Lichtenthaler and Sprey, 1966).

It was quickly recognized that the globules were lipidic in nature and of low density, a property which allowed their isolation by flotation centrifugation. Isolated globules were subjected to biochemical analyses that revealed the presence of relatively large quantities of neutral lipids (mostly triacylglycerol (TAG), plastoquinone/plastoquinol (PQ/PQH_2) and tocopherol) as well as smaller quantities of polar galactolipids and traces of protein (Table 1) (Gaude *et al.,* 2007; Greenwood *et al.,* 1963; Leggett Bailey and Whyborn, 1963; Lichtenthaler and Peveling, 1966; Tevini and Steinmuller, 1985). A model emerged in which a monolayer of polar galactolipids surrounded a lipophilic core (FIG 1). The trace amounts of protein were not accounted for as individual proteins could not be identified at the time. The variations in size and number of PG in chloroplast and their correlation with the state of thylakoid membrane system suggested a dynamic relation between the two systems. The increase in PG size correlated with the disassembly of the thylakoid system during chloroplast senescence suggesting that PG function as a storage site for thylakoid membrane catabolites. Absent of further evidence PG were thought to function as passive lipid storage sites.

Table 1: Lipids enriched in plastoglobules of different plastid types

	Enriched Lipids	References
Chloroplast	Galactolipids; DAG (diacylglycerol) TAG (triacylglycerol) α-Tocopherol (Vitamin E) Phylloquinone (Vitamin K1) Plastoquinone/ol (PQ/PQH2) Fatty acid phytyl esters	Steinmüller and Tevini, (1985) Leggett Bailey and Whyborn, (1963) Lichtenthaler, (1968b) Lichtenthaler and Peveling, (1966) Lippold et al., 2012
Chromoplast	Triacylglycerol (TAG) Carotenoids Carotenoid esters Phytol α-Tocopherol (Vitamin E) Galactolipids	Hansmann and Sitte, (1982) Deruère et al., (1994) Arango and Heise, (1997) Whitaker, (1991) Tevini and Steinmüller, (1985) Deruère et al., (1994)
Gerontoplast	Fatty acid phytyl esters Triacylglycerol (TAG)	Gaude et al., (2007) Steinmüller and Tevini, (1985) Lippold et al., (2012)

This model started to evolve only recently with the discovery of the PG protein components (Table 2) (Deruère *et al.,* 1994; Kessler *et al.,* 1999; Vidi *et al.,* 2006; Ytterberg *et al.,* 2006). Ensuing studies revealed that PG contained a set of enzymatic activities and participated in a multitude of lipid metabolic pathways associated with PG and thylakoids. It has now been shown that PG even harbor regulatory functions (van Wijk and Kessler, 2017; Vidi *et al.,* 2006; Ytterberg *et al.,* 2006). To present these concepts, the present chapter will give an overview of the current state of knowledge on plastoglobules and their protein components. While most of the known functions pertain to prenyl lipids attention will also be given to the role of PG in galactolipid metabolism.

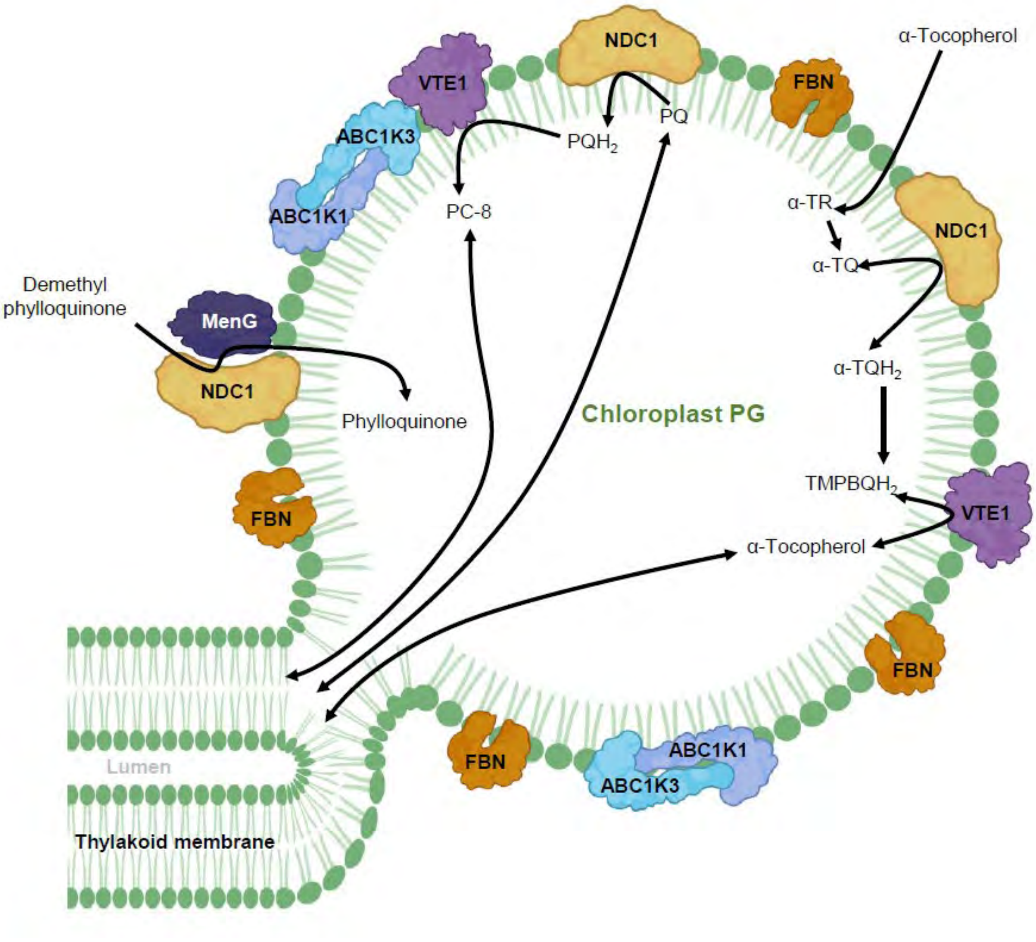

FIG. 1| **Prenyl lipid metabolism in the chloroplast plastoglobule**. Tocopherol cyclase (VTE1) catalyzes the biosynthesis of plastochromanol (PC8) from plastoquinol (PQH2) resulting from the prior reduction of PQ by type II NAD(P)H dehydrogenase C1 (NDC1). In addition, NDC1 derived trimethylbenzoquinol (TMPBQH2) is converted to α-tocopherol by VTE1. ACTIVITY OF BC1-LIKE 1/3 KINASE (ABC1K1/ABC1K3) have been implicated in the regulation of VTE1 activity and may do so by directly phosphorylating VTE1. NDC1 reduces demethylphylloquinone promoting methylation by MenG resulting in phylloquinone synthesis. Abundant fibrillins (FBNs) are thought to have mainly structural roles. The tocopherol repair and recycling involve NDC1 and VTE1, specifically to convert α-tocopherolquinone (α-TQ) to α-tocopherol (α-T) in PG. Abbreviations: α-TQH2, α-tocopherolquinol; α-TR, α-tocopheroxyl radical.

Table 2: PG core proteins based on proteome studies in *Arabidopsis thaliana* and *Capsicum annuum*

Protein name	**Accession**	**Functions**
Fibrillins		
Fibrillin 1a (FBN1a)	AT4G04020	Structural protein
Fibrillin 1b (FBN1b)	AT4G22240	
Fibrillin 2 (FBN2)	AT2G35490	
Fibrillin 4 (FBN4)	AT3G23400	
Fibrillin 7a (FBN7a)	AT3G58010	
Fibrillin 7b (FBN7b)	AT2G42130	
Fibrillin 8 (FBN8)	AT2G46910	
Enzymes		
Tocopherol cyclase VTE1	AT4G32770	Tocopherol metabolism
NAD(P)H dehydrogenase C1 NDC1	AT5G08740	Phylloquinone and PQ metabolism
Phytyl ester synthase PES1	AT1G54570	TAG and FAPEs biosynthesis
Phytyl ester synthase PES2	AT3G26840	
Regulatory kinases		
Activity of bc1-like kinase ABC1K1	AT4G31390	Metabolic regulation and PQ homeostasis
Activity of bc1-like kinase ABC1K3	AT1G79600	Metabolic regulation and PQ homeostasis
Activity of bc1-like kinase ABC1K5	AT1G71810	
Activity of bc1-like kinaseABC1K6	AT3G24190	
Activity of bc1-like kinase ABC1K7	AT3G07700	Metabolic regulation
Activity of bc1-like kinase ABC1K9	AT5G05200	
Other proteins		
SOUL heme binding protein 4 (SOUL 4)	AT3G10130	Heme metabolism
UbiE methyltransferase-related	AT1G78140	
UbiE methyltransferase-related	AT2G41040	
Aldo/keto reductase	AT1G06690	
plastoglobular protein 18 PG18	AT4G13200	Thylakoid biogenesis
PLAT/LH2–1	AT4G39730	
PGM48	AT3G27110	Protein homeostasis
Flavin reductase-related 1	AT1G32220	
Flavin reductase-related 2	AT2G34460	
DUF1350	AT3G43540	
alpha/beta hydrolase family protein	AT1G73750	
Esterase 1	AT5G41120	
Chromoplast PG carotenoid enzymes		
Carotenoid cleavage dioxygenase 4 CCD4	AT4G19170	Carotenoid metabolism
ζ-Carotene desaturase ZDS	gi|12643508 (Capsicum annuum)	Carotenoid biosynthesis
Lycopene β-cyclase LCY-β	gi|12643508 (Capsicum annuum)	
β-Carotene β-hydroxylase CrtR-β	gi|12643508 (Capsicum annuum)	

2.3 Metabolites and Proteins

2.3.1 The role of plastoglobules in thylakoid (prenyl) lipid metabolism

After their discovery by electron microscopy it quickly became clear that PG contain large and variable quantities of lipids that were in one way or the other linked to thylakoid function (Greenwood *et al.,* 1963; Tevini and Steinmuller, 1985). PG being lipid droplets contain neutral, hydrophobic lipids while the surface consists of a membrane lipid monolayer. Indeed, plastoquinone (large quantities) together with the tocopherols and phylloquinone (both in moderate quantities) were identified as major components (Leggett Bailey and Whyborn, 1963; Lichtenthaler, 1968b; Lichtenthaler and Peveling, 1966; Steinmüller and Tevini, 1985) (Table 1). All three belong to the prenyl quinone family and in part share biosynthetic pathways that are integrated at the PG (FIG 1, 2and 3). It is important to note that all three fulfill important functions at the thylakoid membrane and do not appear to carry out any specifically within PG. Plastoquinone is a membrane mobile electron carrier transferring electrons from Photosystem II to the cytochrome b6f complex (Tikhonov, 2013; Van Eerden *et al.,* 2017). It also "moonlights" as an anti-oxidant, the unsaturated prenyl tail able to react with and quench ROS whereby it is consumed (Apel and Hirt, 2004; Ksas *et al.,* 2018). Tocopherol is considered a membrane anti-oxidant quenching ROS via chromanol ring opening (Krieger-Liszkay and Trebst, 2006; Munné-Bosch, 2005; Neely *et al.,* 1988). The tocopherol oxidation product tocopherol quinone is known to be recycled to tocopherol (Kobayashi and DellaPenna, 2008), the process taking place at least in part at PG (Eugeni Piller *et al.,* 2014) (FIG 1). Phylloquinone is an electron carrier functioning within Photosystem I (Malkin, 1986; Santabarbara and Casazza, 2019; Schoeder and Lockau, 1986). Functions of free phylloquinone within the thylakoid membrane have to our knowledge not been described.

Other neutral lipids in PG are triacylglycerols that are present in large quantities and mostly derived from thylakoid galactolipid hydrolysis (Table 1). Free fatty acids were also detected and likely to be galactolipid hydrolysis products as well (Gaude *et al.,* 2007; Tevini and Steinmuller, 1985). In addition, PG of senescent chloroplasts accumulate large quantities of fatty acid phytyl esters (FIG 4) (Gaude *et al.,* 2007). Phytol is a product of chlorophyll breakdown and thought to be membrane toxic due to detergent-like properties (Krauß *et al.,* 2018). Esterification with free fatty acid detoxifies phytol and results in very hydrophobic fatty acid phytol esters that can be sequestered from the thylakoid membrane and deposited in PG (Hörtensteiner and Kräutler, 2011; Ischebeck *et al.,* 2006; Krauß and Vetter, 2018) (Table 1). Membrane lipids are present in minor quantities as they only constitute the membrane lipid monolayer at surface of the PG. They include monogalactosyl- and digalactosyldiacylglycerol (MGDG and DGDG) as well sulfoquinovosyldiacylglycerol which are the major membrane lipid components of the thylakoid membrane (Boudière *et al.,* 2014). Phospholipids have also been detected at trace levels. Electron microscopic images indicate that the membrane lipid monolayer surrounding the PG is contiguous with the outer membrane lipid layer of the thylakoid membrane (Austin *et al.,* 2006; Kessler *et al.,* 1999). This arrangement would allow for a lipid conduit from the PG interior to the thylakoid membrane. Such a conduit has been postulated to explain the lipid exchange processes that must occur between the thylakoid membrane and PG (Havaux, 2020a; Kirchhoff, 2019). However, such conduits have not been functionally demonstrated so far.

Interestingly, PG composition may vary with plastid type. Senescent chloroplasts, also known as gerontoplasts, accumulate very large amounts of TAG and fatty acid phytyl esters that result from thylakoid membrane catabolism and chlorophyll breakdown (FIG 4; Table 1)(Gaude *et al.,* 2007; Tevini and Steinmuller, 1985). This accumulation is directly linked to PG supersizing that can easily be observed by electron microscopy (Barton, 1966). During chloroplast-to-chromoplast transition thylakoid membranes are dismantled and large PG appear (Egea *et al.,* 2010; Spurr and Harris, 1968). In red pepper large PG transiently appear and are progressively replaced by carotenoid fibrils that are structurally related to PG (Deruère *et al.,* 1994). The PG and fibrils contain large quantities of carotenoids such as the linear lycopene in tomato and/or carotenoid esters that may constitute up to 90% of carotenoids in red pepper (Berry *et al.,* 2019; Deruère *et al.,* 1994) (Table 1). It is interesting to note here that the PG in chromoplasts recruit enzymes of the carotenoid biosynthesis pathway. Presumably, this enhances sequestration of these hydrophobic molecules within a hydrophobic metabolic sink (ie PG and/or fibrils).

2.3.2 The Plastoglobule Proteome

The first PG protein to be identified was called fibrillin due to its association with carotenoid fibrils (as well as PG) in red pepper fruit (Deruère *et al.,* 1994). Since then, a series of analyses have determined a proteome of around 30 *bona fide* PG proteins (Table 2) that may vary between plastid types and environmental conditions. Rather surprisingly, around a third of the proteins turned out be enzymes with known or predicted roles in lipid metabolism (Eugeni Piller *et al.,* 2011; Vidi *et al.,* 2006). Several members of the family of atypical ABC1K kinases were also present in the proteome suggesting that PG also had regulatory functions (FIG 1) (Lundquist *et al.,* 2013; Martinis *et al.,* 2014; Pralon *et al.,* 2020; Pralon *et al.,* 2019). Finally, members of the fibrillin (FBN) family constituted the largest portion of the mass of the PG proteome and have been attributed roles in PG structure and maintenance (FIG 1) (Kessler *et al.,* 1999; Pozueta-Romero *et al.,* 1997; Rey *et al.,* 2000; Simkin *et al.,* 2007; Singh *et al.,* 2012). Interestingly, the PG proteins partitioned to various degrees between thylakoid membranes, stroma and PGs, but there are few physical explanations for this. But, the distribution of the fibrillin proteins between the compartments correlated with their isoelectric points and hydrophobicity. Fibrillins that associated with PG tended to have a lower isoelectric point and be more hydrophobic (Lundquist *et al.,* 2012). While the precise functions of many PG components remain unknown, a genome-wide coexpression network of PG genes attributed PG proteins to four distinct “modules” (1 to 4) that were particulary enriched for senescence, carotenoid metabolism, redox regulation/”photoacclimation” and plastid biogenesis (Lundquist *et al.,* 2012). In the following paragraphs, we will discuss notable PG proteins and their functions.

2.3.3 The versatile but elusive fibrillin family

Quantitatively, the largest portion of the PG proteome is made up of members of the fibrillin/FBN family, sometimes also called plastoglobulins (PG) (Kessler *et al.,* 1999; Lundquist *et al.,* 2012). FBNs originated from a cyanobacterial chloroplast progenitor and are part of the green cut (Lohscheider and Río Bártulos, 2016; Merchant *et al.,* 2007). The first fibrillin was discovered in red pepper (*Capsicum annuum*) through its association with carotenoid-sequestering fibrils (Deruère *et al.,* 1994). Red pepper fibrillin protein allowed to reconstitute carotenoid fibrils from the fibril lipid components. This finding was taken as indication for a structural function of fibrillin (Deruère *et al.,* 1994). Additional support for this notion comes from the ability of FBN1a and -1b to dimerize *in vivo*. This may allow formation of a stabilizing FBN network around PG (Gámez-Arjona *et al.,* 2014). Overexpression of FBN in tobacco led to increased numbers and clustering of PG suggesting that FBN may form an interface at the surface of PG and prevent their coalescence (Rey *et al.,* 2000). FBNs share limited sequence homology with lipocalins, small proteins involved in the binding and transport of small hydrophobic compounds. The presence of a lipocalin signature suggested that some fibrillins may directly participate in lipid trafficking between PG and membrane compartments (Flower *et al.,* 2000; Laizet *et al.,* 2004; Singh and McNellis, 2011). The Arabidopsis genome encodes 14 FBNs, 7 of which (FBN1a, -1b, -2, -4, -7a, -7b, and -8) are considered PG core proteins (Vidi *et al.,* 2006; Ytterberg *et al.,* 2006). The other FBNs are associated with thylakoid membranes (FBN3a, -3b, -6, and -9 and FBN-like) or present in the chloroplast stroma (FBN5) (Kim *et al.,* 2015). The loss-of-function mutants for FBN1a, -1b, -2, and -4 in Arabidopsis as well as other species suggested the (direct or indirect) involvement of these FBNs in responses to biotic stresses, temperature, and excess light (Gillet *et al.,* 1998; Langenkämper *et al.,* 2001; Li *et al.,* 2019; Singh *et al.,* 2010; Youssef *et al.,* 2010). Arabidopsis FBN5 is not a PG component but a soluble stromal protein. FBN5 is required for the synthesis of solanesyl diphosphate, an essential step in the PQ-9 biosynthetic pathway (Kim *et al.,* 2015; Kim *et al.,* 2017; Otsubo *et al.,* 2018). FBN5 interacts directly with SPS1 and -2 (solanesyl diphosphate synthase 1 and -2) to stimulate the elongation of the prenyl chain resulting in the essential solanesyl moiety of PQ-9 (Kim *et al.,* 2015) (FIG 2). FBN4 has also been linked to PQ-9 metabolism .The PG of an apple FBN4 knockdown mutant had strongly reduced levels of PQ-9 while overall concentrations were comparable to WT suggesting that FBN4 participates in partitioning and/or trafficking of PQ-9 between PG and thylakoid membrane (Singh *et al.,* 2012). The current knowledge suggests that FBNs are highly versatile proteins contributing to PG structure as well as several metabolic pathways and metabolite trafficking. However, the functional mechanisms of the fibrillins remain elusive.

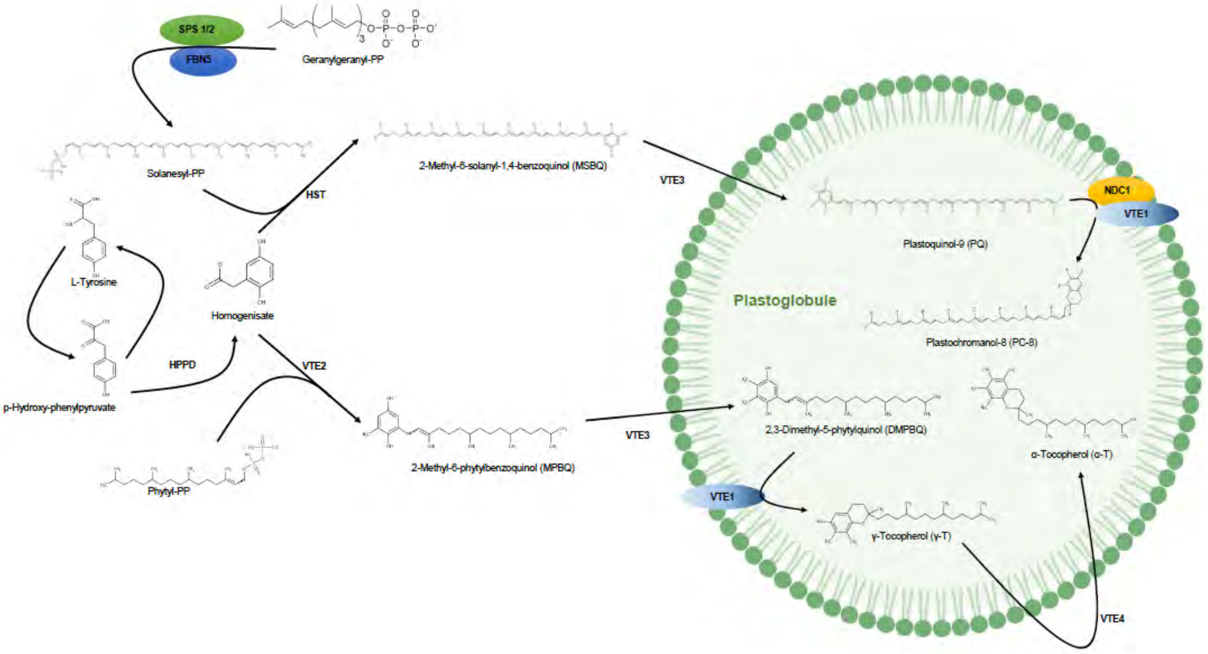

FIG 2| **Plastochromanol and tocopherol biosynthetic pathways in chloroplasts.** The tyrosine aminotransferase (TAT) converts the precursor L-tyrosine derived from the shikimate pathway into p-hydroxy-phenylpyruvate. The p-hydroxyphenyl-pyruvate dioxygenase (HPPD) converts p-hydroxy-phenylpyruvate into homogentisate. Homogentisate phytyltransferase (VTE2) adds the phytyl-pp tail to homogentisate resulting in 2,3-dimethyl-6-phytyl-1,4-benzoquinone (MPBQ). Alternatively, homogentisate solanesyltransferase (HST) adds a solanesyl-tail to homogentisate resulting in 2-methylmethyl-6-solanyl-1,4-benzoquinol (MSBQ). Solanesyl-PP is derived from geranylgeranyl-PP elongation catalysed by solanesyl diphosphate synthases 1 and 2 (SPS1 and 2) in conjunction with fibrillin 5 (FBN5). MPBQ methyltransferase (VTE3) methylates MPBQ resulting in DMPBQ as well as MSBQ resulting in plastoquinol-9 (PQ-9). Tocopherol cyclase (VTE1), localized at the plastoglobule (PG; shown as green lipid droplet) catalyzes the cyclization of DMPBQ generating γ-Tocopherol (γ-T). Also, at the PG, NDC1 reduces PQ-9 to PQH2-9 prior to conversion into plastochromanol-8 (PC-8) by VTE1. Tocopherol O-methyltransferase (VTE4) methylates γ-Tocopherol (γ-T) resulting in α-Tocopherol (α-T).

2.3.4 Members of the ABC1K family contribute to control of prenyl lipid metabolism and photosynthetic electron flow

Members of ABC1 (Activity of BC1 complex)-like kinase family (ABC1K) constitute the second most abundant family of proteins in PG (Lundquist *et al.,* 2012). The founding member of the ABC1K family [also called UbiB or ABC1 domain–containing kinases (ADCKs)] is UbiB from *E. coli*, which is required for the aerobic biosynthesis of ubiquinone (Poon *et al.,* 2000). The yeast (*Saccharomyces cerevisiae*) mitochondrial ABC1K, also known as coenzyme Q biosynthesis 8 (ScCOQ8), and the mammalian homologs ADCK3 and -4 are required for ubiquinone synthesis in the mitochondria of their respective organisms, possibly through phosphorylation-dependent assembly of a large biosynthetic multi-enzyme complex (Bousquet *et al.,* 1991; Do *et al.,* 2001; Lagier-Tourenne *et al.,* 2008; Mollet *et al.,* 2008). Due to the lack of ubiquinone, the *coq8* mutation compromises the mitochondrial bc1 complex and aerobic metabolic activity. Defects of the kind are linked to hereditary disease in humans (Gerards *et al.,* 2010).

Arabidopsis has 17 ABC1Ks, 8 of which are likely localized in mitochondria and 9 in plastids. Six of nine of the plastid ABC1Ks are localized in PGs (ABC1K1, -3, -5, -6, -7,-9) (Lundquist *et al.,* 2012). Notably, the ABC1K family represents the majority of known kinases in plastids and mitochondria; however, relatively little is known about this family in plants. Functional studies of PG-localized ABC1K1, -3 and -7, have been initiated in Arabidopsis, and the role of ABC1K3 has been addressed in rice (Li *et al.,* 2015). PG-localized ABC1K7 is involved in cadmium tolerance, oxidative stress response, iron distribution, lipid metabolism and in crosstalk between abscisic acid and ROS signaling (Manara *et al.,* 2015; Manara *et al.,* 2014). The Chlamydomonas homolog of ABC1K6 (EYE3) located in the eyespot, is involved in the biogenesis of pigment granules (Boyd *et al.,* 2011). Still, the modes of action of the ABC1K family members, for instance phosphorylation of proteins or metabolites, are quite unclear.

Apart from its association with PG, ABC1K1 was identified in at least two genetic screens. In a genetic screen to identify mutants defective in seedling growth under continuous red light, ABC1K1 was identified as BDR1 (bleaching and dwarf under red light 1) (Yang *et al.,* 2016). Under continuous red light *abc1k1/bdr1* exhibited an albino and dwarf phenotype and, while most photosynthetic proteins accumulated normally, the Photosystem II core protein D1 was diminished. To identify additional components required for ABC1K1/BDR1 function, a genetic to screen to find suppressors of *abc1k1-2* was carried out and resulted in the isolation of *rbd1* (*r*epressor of *bdr1-2*) that turned out to be identical with ABC1K3 (Huang *et al.,* 2015). It is thought that ABC1K3 in the *abc1k1* background interferes with red light signaling acting downstream of PhyB and HY5 and affects expression of PIF genes. This is supported by the observation that ABC1K3 overexpression produced a phenotype similar to that of the *abc1k1* mutant (Huang *et al.,* 2015).

In a second screen for mutants with reduced non-photochemical quenching (NPQ) of chlorophyll fluorescence (Shikanai *et al.,* 1999), PGR6 (Proton Gradient Regulation 6) was identified and found to be identical with ABC1K1. *abc1k1* has a photosynthetic phenotype characterized by strong photoinhibition and reduced NPQ after high light exposure (Martinis *et al.,* 2014; Pralon *et al.,* 2019). Prenyl lipid metabolism was affected in *abc1k1*: Tocopherol concentrations did not increase under high light stress and carotenoid concentrations were diminished even under moderate light conditions (Martinis *et al.,* 2013; Martinis *et al.,* 2014). After high light treatment, sugar metabolism was perturbed and carbon-allocation shifted from starch to soluble sugars. In addition to the genetic interaction between ABC1K1 and its closest homolog, ABC1K3, the two atypical kinases interact physically (FIG 1). (Lundquist *et al.,* 2013). Moreover, additional reports demonstrated that ABC1K1 and -3 together are involved in PQ-9 homeostasis (maintenance of sufficient PQ-9 in the photoactive thylakoid membrane pool) (Pralon *et al.,* 2020; Pralon *et al.,* 2019). In the *abc1k1* mutant, the photoactive PQ-9 pool in the thylakoid membranes was selectively depleted under moderate high light stress. The depleted photoactive PQ-9 pool phenotype of *abc1k1*is rescued in the *abc1k1/abc1k3* double mutant. Thus, ABC1K1 and ABC1K3 appear to regulate the distribution of PQ-9 between the plastoglobule and thylakoid membrane pools.

The perturbed plastoquinone homeostasis in the *abc1k1* mutant may explain the “proton gradient regulation”/PGR phenotype that is characterized by decreased NPQ: concomitantly with its role as an electron carrier plastoquinone transports protons from the stromal side of the thylakoid membrane to the lumenal side generating a ΔpH. An increasing ΔpH serves as a proxy for excess light and induces NPQ, to protect the photosynthetic apparatus. In *abc1k1*, plastoquinone levels in the electron chain are diminished under high light. These insufficient amounts of plastoquinone in *abc1k1* would limit not only electron transport but also the ΔpH across the thylakoid membrane. Therefore, induction of non-photochemical quenching, would be decreased and result in the observed PGR phenotype. Thus, ABC1K1 may be a very direct regulator of the proton gradient (Pralon *et al.,* 2019).

It remains unclear how the photosynthetic PGR phenotype relates to the cellular signaling phenotype also observed for ABC1K1 and -K3. It will be important to reconcile the two phenomena in the future. One possibility is that these two atypical kinases transmit signals emanating from the photosynthetic electron transport chain to the nucleus thereby affecting gene expression.

2.4 Role of PG proteins in the context of thylakoid lipid metabolism

2.4.1 NDC1 a new enzyme in phylloquinone biosynthesis

Phylloquinone mainly acts as an electron carrier in Photosystem I in the thylakoid membrane (Brettel *et al.,* 1986). But it has been demonstrated that about one-third of phylloquinone is present in PGs (Lohmann *et al.,* 2006; Spicher and Kessler, 2015). This suggests phylloquinone trafficking between PG and the thylakoid membrane. The MenG enzyme, a predicted methylase, catalyzes the final methylation step of the biosynthetic pathway from 2-phytyl-1,4-naphthoquinone (demethylphylloquinone) to phylloquinone (FIG 3). The AtmenG knockout mutant lacks phylloquinone but accumulates the precursor demethylphylloquinone instead. The lack of phylloquinone in *atmenG* has rather minor consequences resulting in reduced levels of Photosystem I and consequently a slight decrease of photosynthetic efficiency upon high light (HL) treatment (Eugeni Piller *et al.,* 2011; Lohmann *et al.,* 2006). Thus, it appears that the precursor of phylloquinone can functionally replace phylloquinone, at least under standard conditions. Surprisingly, the *ndc1* mutant in Arabidopsis mimics the *atmenG* phenotype and has identical phylloquinone and demethylphylloquinone profiles (Eugeni Piller *et al.,* 2011).

In Arabidopsis, NDC1 is one of seven NDH-2 (Type II NAD(P)H-dependent dehydrogenases). NDC1 appears to be localized mostly in chloroplast PG (FIG 3) whereas the remaining homologs have been localized in mitochondria. However, NDC1 was initially also found in mitochondria (Michalecka *et al.,* 2003) dual localization in mitochondria and chloroplasts cannot be excluded. NDC1 is evolutionarily conserved from cyanobacteria. In Chlamydomonas NDA2 NAD(P)H quinone oxidoreductase, the homolog of NDC1, is involved in cyclic electron flow and chlororespiration directly transferring electrons from NAD(P)H to plastoquinone (Desplats *et al.,* 2009). NDC1 in cyanobacteria is part of the MEN operon and its deletion also leads to loss of phylloquinone (Fatihi *et al.,* 2015). The mechanism of NDC1in the methylation step of phylloquinone synthesis has been solved: The NDC1-dependent reduction of demethylphylloquinone intermediate is essential for the subsequent methylation by MenG. NDC1 is therefore considered a *bona fide* enzyme of the phylloquinone biosynthesis pathway (FIG 3). (Eugeni Piller *et al.,* 2011; Fatihi *et al.,* 2015). Interestingly also Gross *et al.,* 2006 demonstrated that the PHYLLO metabolon (genetic fusion of MenF, MenD, MenC, and MenH) fused to a fluorescent marker resulted in a plastoglobuli-like fluorescence pattern inside chloroplasts (Gross *et al.,* 2006). The fluorescence pattern suggests that the PHYLLO metabolon may also be recruited to PG coupling the upstream portion of pathway with NDC1 and AtMenG activity (Gross *et al.,* 2006).

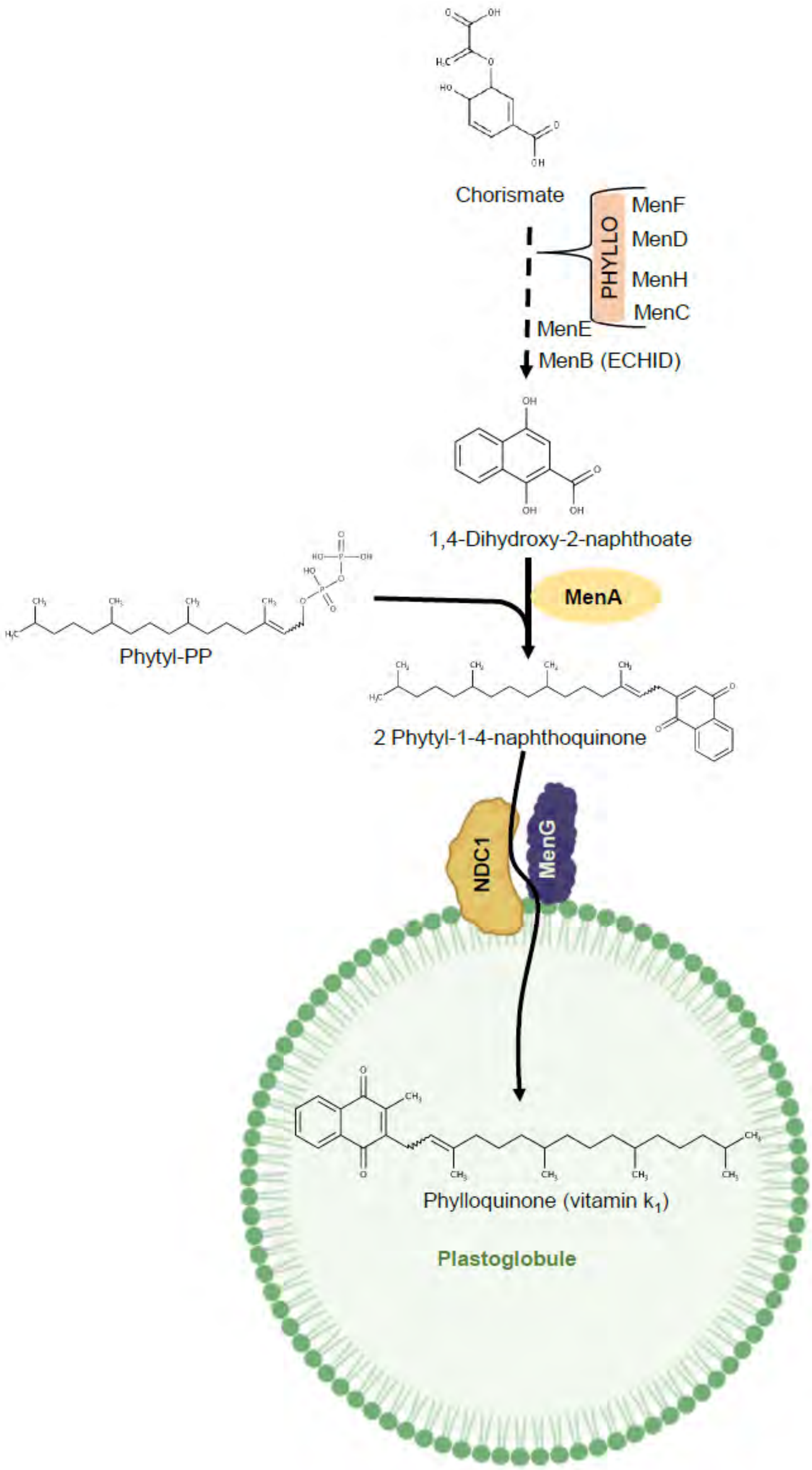

FIG 3| **Phylloquinone biosynthetic pathway in plants.** PHYLLO, a fusion protein of menaquinone synthesis enzymes (MenF, D, H, C) followed by MenE and MenB convert chorismate into 1,4-dihydroxydihydroxy-2-naphthoate (DHNA). DHNA phytyltransferase (MenA) converts DHNA to 2-phytyl-1,4-naphthoquinone (demethylphylloquinone). Next, the demethylphylloquinone is reduced by type II NAD(P)H dehydrogenase C1 (NDC1) resulting in demethylphylloquinol. Depending on the prior reduction of demethylphylloquinone by NDC1, MenG methylates demethylphylloquinol to complete the synthesis of phylloquinone.

2.4.2 NDC1 regulates the PQ-9 redox state and contributes to plastochromanol biosynthesis and tocopherol recycling

It has been demonstrated that recombinant NDC1 reduces decyl plastoquinone (a PQ-9 analog) in a NAD(P)H dependent fashion (Eugeni Piller *et al.,* 2011). However, NDC1 in Arabidopsis is not directly implicated in either linear or cyclic electron flow in Arabidopsis. In chloroplasts, plastoquinone is distributed between the thylakoids and PGs, constituting photoactive and non-photoactive pools, respectively. The non-photoactive pool may communicate with the photoactive plastoquinone pool to maintain adequate PQ-9 levels in the photoactive pool ("plastoquinone homeostasis") as seen in the earlier paragraphs on the ABC1K1 and -3 kinases. Total PQ-9 in *ndc1* was significantly more oxidized than in the wild-type while electron transport rates and other photosynthetic parameters were not affected. This suggested that NDC1 selectively reduces the photoinactive PQ-9 pool inside PG (Eugeni Piller *et al.,* 2011).

In an interesting twist, the *ndc1* mutant accumulates less plastochromanol-8 (PC-8) than WT (Eugeni Piller *et al.,* 2011). PC-8 is the product of tocopherol cyclase/VTE1 activity on reduced PQ-9 (PQH$_2$-9). VTE1 preferentially cyclizes reduced substrates, in this case PQH$_2$-9 contained in PG (FIG 2) (Woggon, 1999). In the absence of *ndc1* PQ-9 in PG is more oxidized impeding the action of VTE1 (FIG 2) and hence the biosynthesis of PC-8.

Under stress conditions, Photosystem II generates reactive oxygen species to which the thylakoid membranes are exposed. Tocopherols are one of the primary antioxidants able to quench ROS and protect the membrane lipids from oxidation (Munné-Bosch and Alegre, 2002). Scavenging of lipid peroxy radicals leads to chromanol ring opening in α-tocopherol and α-tocoquinone production (Muñoz and Munné-Bosch, 2019). α-tocoquinone can be "repaired" by a sequence of enzymatic steps culminating in chromanol ring formation by VTE1. This step occurs preferentially in the reduced substrate α-tocopherol quinol (α-TQH2) (Eugeni Piller *et al.,* 2014; Kobayashi and DellaPenna, 2008). In the *ndc1* mutant, α-tocopherol quinol is produced less efficiently leading to diminished α-tocopherol repair and increased concentrations of α-tocoquinone (Eugeni Piller *et al.,* 2014).

2.4.3 The tocopherol cyclase VTE1 (VITAMIN E DEFICIENT 1), the key enzyme in tocochromanol biosynthesis and metabolism

α-tocopherol is the primary tocochromanol protecting thylakoid membranes from lipid peroxidation under stress (Fryer, 1992; Liu *et al.,* 2008; Munné-Bosch and Alegre, 2002). Most of the enzymes of the tocopherol biosynthesis pathway, including tocopherol cyclase (VTE1), were originally localized at the inner envelope membrane of the chloroplast by activity measurements in isolated membrane fractions (Soll *et al.,* 1985). Tocopherol cyclase introduces the chromanol ring in DMPBQ, converting it to γ-tocopherol (FIG 2). Subsequently, VTE4 methylates γ-tocopherol resulting in α-tocopherol. Surprisingly, given the earlier results, VTE1 was discovered in the PG proteome (Vidi *et al.,* 2006; Ytterberg *et al.,* 2006). The majority of tocopherol cyclase VTE1 has been localized at PG using a variety of independent techniques VTE1-fluorescence tagging, immunoelectron microscopy, immunoelectron tomography and Western blotting of isolated chloroplast membrane fractions. Moreover, DMPBQ, the substrate of VTE1, accumulated in the PG of the *vte1* mutant, providing supporting evidence for the localization of VTE1 at PG (Austin *et al.,* 2006; Vidi *et al.,* 2006; Ytterberg *et al.,* 2006). The *vte1* mutant largely resembled the wild type suggesting that DMPBQ or other tocochromanols such as PC-8 can substitute for tocopherol as a functional antioxidant.

Together with plastochromanol-8 (PC-8), tocopherol protects seeds from oxidation and is required for seed longevity (Mène-Saffrané *et al.,* 2010). PC-8 is derived from plastoquinol (PQH_2-9) by tocopherol cyclase/VTE1 activity (FIG 2). PC-8 has the longer solanesyl side chain of plastoquinone but the chromanol-containing headgroup is identical to that of γ-tocopherol. The VTE1 overexpression lines resulted in a large increase of PC-8 that mainly accumulated in PG. It therefore appeared likely that VTE1 localized at PGs converted PQH_2-9 to PC-8 (Zbierzak *et al.,* 2009). Notably, the *ndc1* mutant accumulated less PC-8 likely due to the preference of VTE1 for reduced PQH_2-9 over PQ-9 (Eugeni Piller *et al.,* 2012).

2.5 Role of PG in thylakoid membrane remodeling under stress

Various abiotic environmental stresses (oxidative stress, high light intensity, nitrate starvation, drought) and plastid developmental transitions (chloroplast-to-chromoplast, chloroplast-to-gerontoplast) are associated with remodeling or even wholesale dismantling of thylakoid membranes and with increased accumulation of lipid antioxidants to cope with such conditions. Typically, PG numbers and size increase due to lipid deposition in PGs resulting from thylakoid membrane dismantling during chloroplast-to-gerontoplast transition or under nitrogen deprivation (Besagni and Kessler, 2013; Domínguez and Cejudo, 2021; Gaude *et al.,* 2007; Hörtensteiner and Kräutler, 2011). This process may result in supersized PG of several micrometers in diameter due to triacylglycerol and fatty acid phytyl ester accumulation. These products result from the combined simultaneous breakdown of galactolipids and chlorophyll in the presence of PG-localized enzymes (FIG 4) (Zechmann, 2019).

Phytol is released from chlorophyll by pheophytin pheophorbide hydrolase (PPH) (Hörtensteiner and Kräutler, 2011; Schelbert *et al.,* 2009). However, the membrane-toxic phytol does not accumulate. Instead, phytol and free fatty acids, which are hydrolysis products of the thylakoid galactolipids, are converted to fatty acid phytyl esters (FAPE) and triacylglycerol (TAG) at PGs by phytyl ester synthases

1 and 2 (PES1 and PES2) (FIG 4) (Krauß and Vetter, 2018; Lippold *et al.,* 2012) . Gerontoplast PG transiently recruit LIPOXYGENASE 3 and 4 (LOX3 and LOX4) that peroxidate 16:3 and 18:3 fatty acids (Lundquist *et al.,* 2012). Together, allene oxide cyclase (AOC) and allene oxide synthase (AOS) convert oxidized 18:3 fatty acid into 12-oxo phytodienoic acid (OPDA) (FIG 4), a precursor for jasmonic acid synthesis in the peroxisome (Acosta and Farmer, 2010). The initial proteome studies found AOS in PG (Vidi *et al.,* 2006; Ytterberg *et al.,* 2006). A recent study demonstrated strongly increased levels of AOS in PG after high light treatment (Espinoza-Corral *et al.,* 2021). Senescence, nitrogen deprivation and high light treatment are useful conditions for studying dynamic behavior of PG morphology and metabolism (Gaude *et al.,* 2007; Zechmann, 2019).

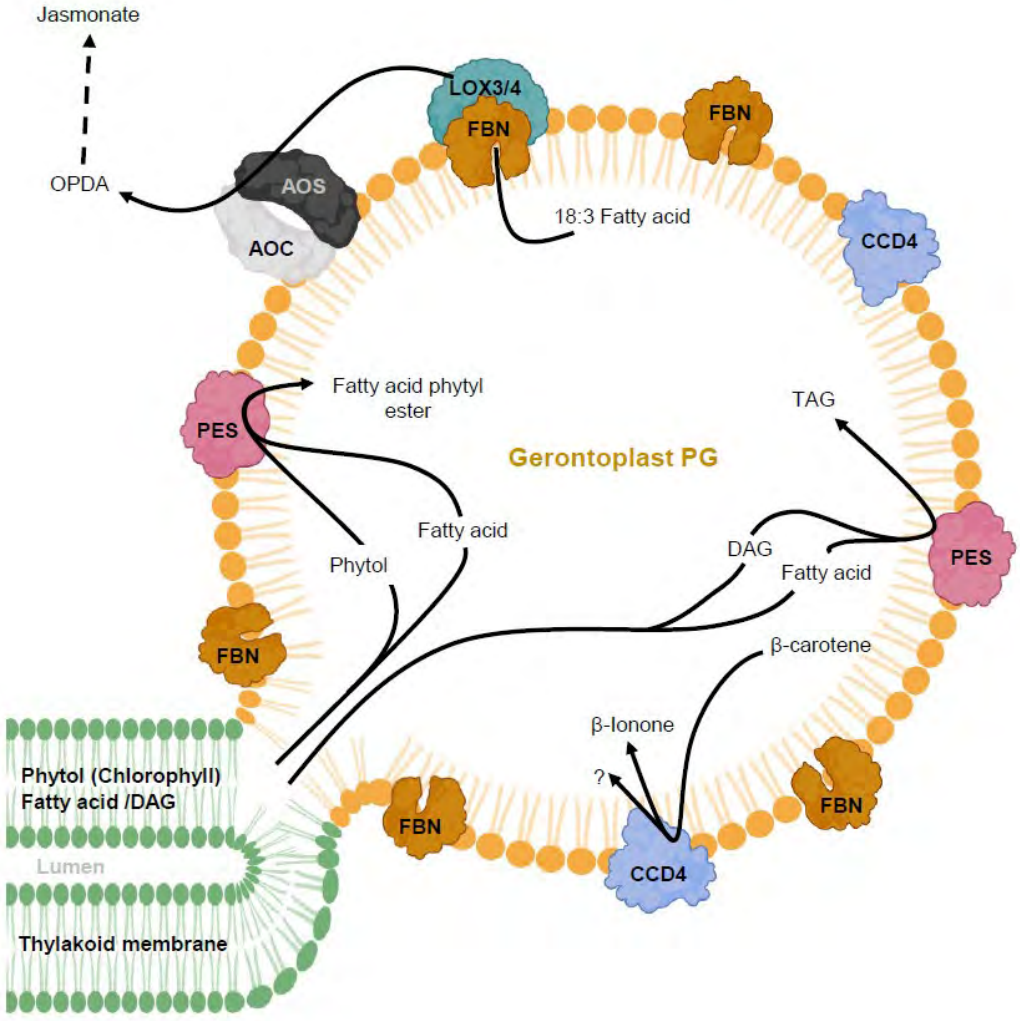

FIG 4| **Lipid metabolism in the gerontoplast plastoglobule.** The senescence process is characterized by the transformation of a chloroplast to a gerontoplast and the dismantling of the thylakoid membrane, which comprises galactolipid hydrolysis and chlorophyll breakdown. Phytyl ester synthases (PES) catalyze the synthesis of fatty acid phytyl esters from free fatty acids (from galactolipid hydrolysis) and phytol (from chlorophyll break down). In parallel, phytyl ester synthases contribute to triacylglycerol (TAG) synthesis from free fatty acids and diacylglycerol (DAG). The gerontoplast PG-localized LIPOXYGENASE (LOX) oxidizes unsaturated fatty acid and may be recruited by a fibrillin (FBN). In addition, allene oxide cyclase (AOC) and allene oxide synthase (AOS, also in PG) are essential enzymes to produce 12-oxo-phytodienoic acid (OPDA), a jasmonate precursor. The carotenoid cleavage dioxygenase 4 (CCD4) cleaves β-carotene to release β-ionone and other volatile compounds.

2.5.1 PES1 and PES2 are involved in phytol and fatty acid metabolism

PES1 and -2 belong to the esterase/lipase/thioesterase (ELT) acyl transferase family. PES1 and -2 are induced during leaf senescence and under nitrogen deprivation. Under nitrogen deprivation, the *pes1pes2* double mutant accumulated only residual levels of phytyl esters and far more free phytol than the wild type (Lippold *et al.,* 2012). The residual phytyl esters may be explained by the presence of additional ELT homologs. PES1 and PES2 converted phytol and fatty acids into FAPE in the heterologous yeast expression system thereby demonstrating phytyl ester synthase activity. Senescence and chlorophyll catabolism was slightly delayed in the *pes1pes2* double mutant emphasizing the physiological importance of the two enzymes in plant senescence (Lippold *et al.,* 2012).

PES1 and PES2 proteins have two distinct domains, a hydrolase domain at the N-terminus and an acyltransferase domain at the C-terminus of the protein. Thus, the PES1 and PES2 proteins potentially harbor two enzymatic functions, namely that of an esterase as well as that of an acyl transferase. In addition, PES1 and PES2 recruit a range of substrates including acyl-CoA species as well as the free fatty acids resulting from galactolipid breakdown. In addition, MGDG can directly serve as an acyl donor for PES1 and PES2 facilitating the release of fatty acids as well as TAG and FAPE biosynthesis (FIG 4). Acyltransferases typically synthesize triacylglycerol (TAG) from acyl-CoA and diacylglycerol. In a yeast mutant lacking acyltransferases gene and deficient in TAG, expression of Arabidopsis PES1 and PES2 genes rescued TAG accumulation. The results validated that PES1 and PES2 act as acyltransferases and may use DAG as a substrate. Also, the *pes1pes2* double mutant reduces TAG accumulation by about 30% in leaves under nitrogen deficiency (Lippold *et al.,* 2012). These results demonstrate that PES1 and PES2 are important DAG acyltransferases contributing to DAG to TAG conversion under stress. Overall, PES1 and PES2 at PGs play a central role in dismantling the photosynthetic membrane during senescence and abiotic stress.

2.6 PG act as the metabolic platform for carotenoid metabolism

The chromoplast is an organelle of the plastid family that develops from the chloroplast during fruit ripening (Camara *et al.,* 1995; Egea *et al.,* 2010). This begins with the dismantling of the photosynthetic thylakoid membrane that is accompanied by the tightly controlled degradation of chlorophyll as well as the yellow-colored carotenoids, processes visible as degreening (Egea *et al.,* 2010; Hörtensteiner and Kräutler, 2011). Simultaneously, the PG within chromoplasts enlarge and begin to accumulate large amounts of red-colored carotenoids and other prenyl lipids that may be synthesized *de novo* or stem from the mobilization of the thylakoid membranes (FIG 5). Chromoplast PGs may have tubular/fibrillar (example: red pepper) or globular structure (example: tomato) (Nogueira *et al.,* 2013; Pozueta-Romero *et al.,* 1997; Simkin *et al.,* 2007). *In vitro* reconstitution of fibrils was achieved from a mixture of membrane lipids, carotenoids and fibrillin (Deruère *et al.,* 1994). However, the PG of chromoplasts, as has already been seen for chloroplast PG, are more than just storage sites and play a central role in the biosynthesis and metabolism of carotenoids.

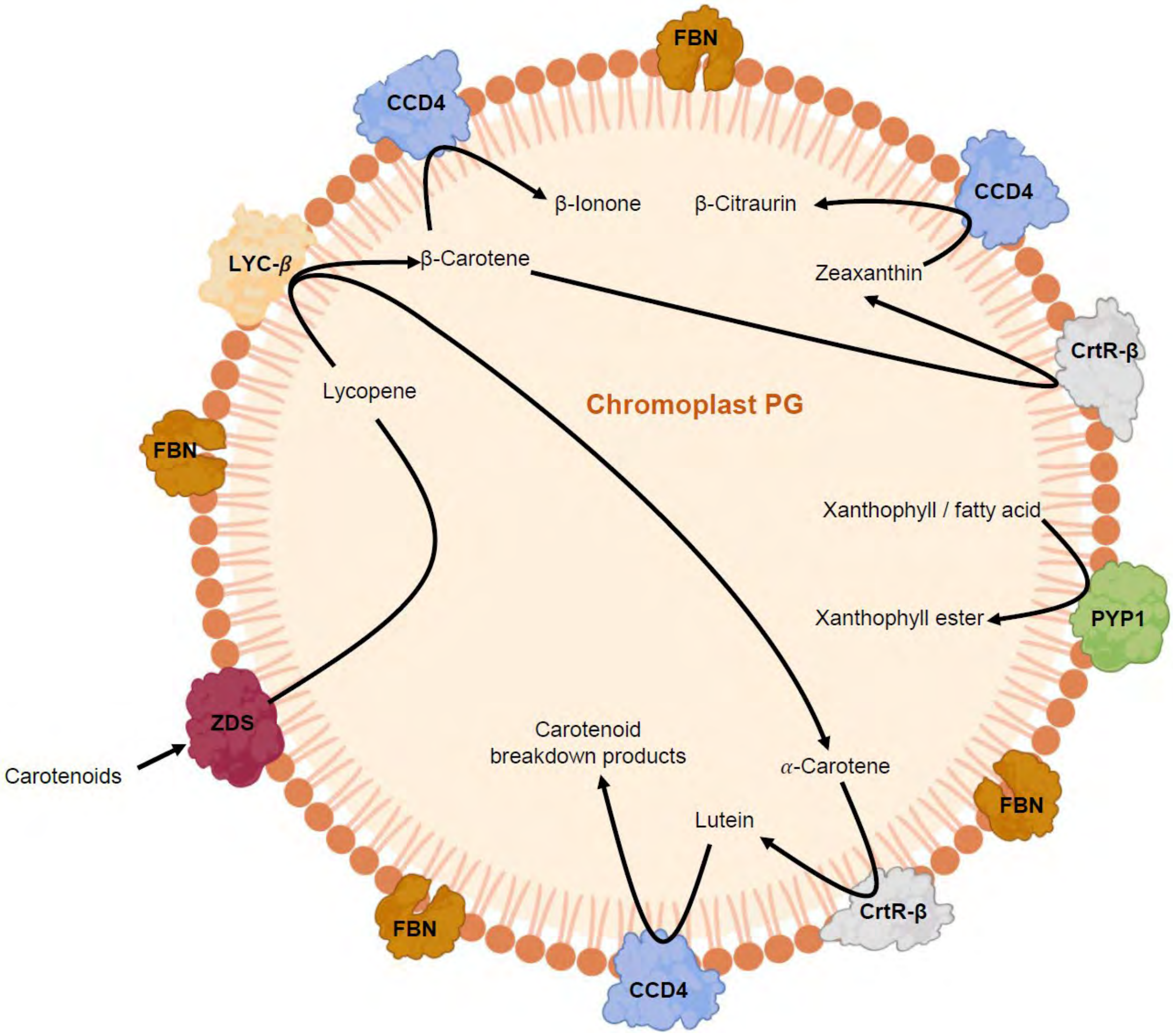

FIG 5| **Carotenoid metabolism in the chromoplast plastoglobule.** Chromoplast plastoglobules recruit specific enzymes such as lycopene β-cyclase (LYC-β), zeta-carotene desaturase (ZDS) and β-carotene β-hydroxylase (CrtR-β) to promote carotenoid biosynthesis. Fibrillins (FBNs) may contribute to carotenoid sequestration in PG. PALE YELLOW PETAL 1 (PYP1) catalyzes carotenoid ester synthesis in tomato petal chromoplasts. The carotenoid cleavage dioxygenase 4 (CCD4) cleaves carotenoids, releasing volatile compounds, contributing to aroma and fruit quality in tomatoes.

The proteome of pepper fruit PG has been determined and provided very interesting insight. Chromoplast PGs are highly enriched for several FBNs (FIG 5), particularly FBN1a and -1b, as well as several carotenoid biosynthetic enzymes; ZDS (ζ-carotene desaturase) involved in the synthesis of all-trans-lycopene a red pigment in tomato and LYC-β (lycopene beta cyclase) involved in the cyclization reactions that generate carotene (FIG 5). The β-carotene β-hydroxylases (CrtR-β) introduce hydroxyl groups to carotene resulting in lutein and zeaxanthin (FIG 5). These enzymes lack transmembrane domains and are therefore thought to associate with the chromoplast PG surface. The clustering of these enzymes at the PGs and associated membranes probably facilitates substrate channelling and accumulation of carotenoids inside PGs and fibrils (Lundquist *et al.,* 2012). PALE YELLOW PETAL 1 (PYP1) in tomato shares sequence homology with the PES enzymes and is responsible for the production of carotenoid esters, the most abundant form of carotenoids in chromoplasts (FIG 5) (Ariizumi *et al.,* 2014). Chloroplast and chromoplast PGs contain an additional carotenoid metabolic enzyme, carotenoid cleavage dioxygenase 4 (CCD4). In various plant species CCD4s are involved in carotenoid cleavage resulting in various apocarotenoids, especially the volatile β-ionone (FIG 5) (Varghese *et al.,* 2021). From the research on chromoplasts, it emerges that PG are key determinants of fruit pigmentation functioning as a site of carotenoid biosynthesis and sink for carotenoid accumulation. By the action of CCD4 PG may also contribute to the volatile bouquet of tomato fruit.

2.6.1 Role of CCD4 in chromoplasts and crop quality

CCD4 plays an important role in a surprising number of crops. In addition to its presence in the Arabidopsis PG proteome (Lundquist *et al.,* 2012; Rottet *et al.,* 2016), CCD4 was identified as a major negative regulator of seed carotenoid accumulation in a genome-wide association (GWAS) study. *ccd4* mutants had increased β-carotene content upon seed desiccation (Gonzalez-Jorge *et al.,* 2013). Petals of Chrysanthemum CCD4 knock down plant had yellow rather than white petals, demonstrating that CCD4 cleaves carotenoids in chromoplasts and contributes to the accumulation of colorless carotenoids (Ohmiya *et al.,* 2006). The red pigment β-citraurin in mandarin fruit is the CCD4 cleavage product of β-cryptoxanthin and zeaxanthin (FIG 5) (Rodrigo *et al.,* 2013). In *Brassica napus*, yellow petals contained higher carotenoid levels than white petals due to the disrupted expression of the CCD4 gene (Zhang *et al.,* 2015). Down-regulation of the CCD4 gene in potato tubers led to accumulation of 2- to 5-fold higher carotenoid content than in wild type tubers (Campbell *et al.,* 2010). In peaches, the expression of CCD4 is repressed in yellow flesh (Redhaven) cultivars as compared to white flesh (Redhaven Bianca) cultivars. Yellow flesh fruits accumulated approximately 10-fold more carotenoids than white flesh (Brandi *et al.,* 2011). CCD4, highly expressed in the stigmata of *Crocus sativus* (saffron), contributes to color, flavor and aroma of the desiccated stigmata by producing apocarotenoids such as safranal, picrocosin, crocetin and β-ionone (FIG 5). During *Crocus sativus* stigmata development PG size and number increase probably due to the accumulation of CCD4 cleavage products. Engineered CsCCD4 in bacteria preferentially cleaved β-carotene into β-ionone and β-cyclocitral (Frusciante *et al.,* 2014; Rubio-Moraga *et al.,* 2014).

Little is known whether and how CCD4 is regulated. PGM48, a plastoglobule-localized metalloprotease promotes senescence. PGM48 may do so in part by CCD4 degradation which is thought to accelerate senescence through the production of volatile, carotenoid-derived signals (Bhuiyan *et al.,* 2016).

2.7 Conclusions

In recent years plastoglobules have gone from poorly characterized osmiophile lipid-storing globules to important players in chloroplast lipid metabolism. Nevertheless, many mysteries remain. For one it is not known how metabolites are trafficked between PG and the associated thylakoid membrane network. Contact sites between the two systems exist and may permit lipid exchange (Austin *et al.,* 2006) but the implication of any proteins (fibrillins have been suggested) remains unknown. It is likely that the trafficking of different lipid species would be separate and highly regulated processes, as has been suggested for the allocation of PQ-9 to the thylakoid membrane (Pralon *et al.,* 2020; Pralon *et al.,* 2019). Early on, it had been hypothesized that plastoglobules contribute to thylakoid membrane formation during early plant development by the conversion of triacylglycerols to membrane lipids. The research tools currently available should allow to investigate this fascinating possibility. It will be of great interest in the future to address these and other open questions and their relevance for photosynthesis and metabolism.

A number of known PG core components have not been characterized so far. These include methyltransferases, reductases and others with various predicted functional domains and enzymatic activities (Lundquist *et al.,* 2012). This remaining wealth of uncharacterized components promises the discovery of further, currently unknown metabolic functions in PG. It will be exciting to see what these will be.

PG have potential biotechnological and agricultural applications. Vitamin E and K enhancement in various crops can easily be imagined. Modification of tomato pigmentation and volatile production can also be envisaged by modifying carotenoid biosynthetic and metabolic pathways that are present in PG. Targeting of recombinant proteins, such as vaccine antigens, has been suggested and attempted in the tobacco experimental system (Shanmugabalaji *et al.,* 2013). Of course, many other applications can also be imagined.

Clearly, research on PG has so far just scratched the surface and many exciting discoveries lie ahead of us.

2.8 Acknowledgements

This work was supported by grants from the Swiss National Science Foundation (31003A_156998 and 31003A_176191) and by the University of Neuchâtel.

2.9 References

1. Acosta, I.F., and Farmer, E.E. (2010). Jasmonates. Arabidopsis Book *8*, e0129-e0129. 10.1199/tab.0129.

2. Apel, K., and Hirt, H. (2004). Reactive oxygen species: metabolism, oxidative stress, and signal transduction. Annual review of plant biology *55*, 373-399. 10.1146/annurev.arplant.55.031903.141701.

3. Ariizumi, T., Kishimoto, S., Kakami, R., Maoka, T., Hirakawa, H., Suzuki, Y., Ozeki, Y., Shirasawa, K., Bernillon, S., Okabe, Y., et al. (2014). Identification of the carotenoid modifying gene PALE YELLOW PETAL 1 as an essential factor in xanthophyll esterification and yellow flower pigmentation in tomato (Solanum lycopersicum). The Plant journal : for cell and molecular biology *79*, 453-465. 10.1111/tpj.12570.

4. Austin, J.R., II, Frost, E., Vidi, P.-A., Kessler, F., and Staehelin, L.A. (2006). Plastoglobules Are Lipoprotein Subcompartments of the Chloroplast That Are Permanently Coupled to Thylakoid Membranes and Contain Biosynthetic Enzymes. The Plant Cell *18*, 1693-1703. 10.1105/tpc.105.039859 %J The Plant Cell.

5. Barton, R. (1966). Fine structure of mesophyll cells in senescing leaves of Phaseolus. Planta *71*, 314-325. 10.1007/bf00396319.

6. Berry, H.M., Rickett, D.V., Baxter, C.J., Enfissi, E.M.A., and Fraser, P.D. (2019). Carotenoid biosynthesis and sequestration in red chilli pepper fruit and its impact on colour intensity traits. Journal of Experimental Botany *70*, 2637-2650. 10.1093/jxb/erz086 %J Journal of Experimental Botany.

7. Besagni, C., and Kessler, F. (2013). A mechanism implicating plastoglobules in thylakoid disassembly during senescence and nitrogen starvation. Planta *237*, 463-470. 10.1007/s00425-012-1813-9.

8. Bhuiyan, N.H., Friso, G., Rowland, E., Majsec, K., and van Wijk, K.J. (2016). The Plastoglobule-Localized Metallopeptidase PGM48 Is a Positive Regulator of Senescence in Arabidopsis thaliana. Plant Cell *28*, 3020-3037. 10.1105/tpc.16.00745.

9. Boudière, L., Michaud, M., Petroutsos, D., Rébeillé, F., Falconet, D., Bastien, O., Roy, S., Finazzi, G., Rolland, N., Jouhet, J., et al. (2014). Glycerolipids in photosynthesis: Composition, synthesis and trafficking. Biochimica et Biophysica Acta (BBA) - Bioenergetics *1837*, 470-480. https://doi.org/10.1016/j.bbabio.2013.09.007.

10. Bousquet, I., Dujardin, G., and Slonimski, P.P. (1991). ABC1, a novel yeast nuclear gene has a dual function in mitochondria: it suppresses a cytochrome b mRNA translation defect and is essential

for the electron transfer in the bc 1 complex. *10*, 2023-2031. https://doi.org/10.1002/j.1460-2075.1991.tb07732.x.

11. Boyd, J.S., Mittelmeier, T.M., Lamb, M.R., and Dieckmann, C.L. (2011). Thioredoxin-family protein EYE2 and Ser/Thr kinase EYE3 play interdependent roles in eyespot assembly. Molecular biology of the cell *22*, 1421-1429. 10.1091/mbc.E10-11-0918.

12. Brandi, F., Bar, E., Mourgues, F., Horváth, G., Turcsi, E., Giuliano, G., Liverani, A., Tartarini, S., Lewinsohn, E., and Rosati, C. (2011). Study of 'Redhaven' peach and its white-fleshed mutant suggests a key role of CCD4 carotenoid dioxygenase in carotenoid and norisoprenoid volatile metabolism. BMC plant biology *11*, 24. 10.1186/1471-2229-11-24.

13. Brettel, K., Sétif, P., and Mathis, P. (1986). Flash-induced absorption changes in photosystem I at low temperature: evidence that the electron acceptor A1 is vitamin K1. FEBS Letters *203*, 220-224. https://doi.org/10.1016/0014-5793(86)80746-3.

14. Camara, B., Hugueney, P., Bouvier, F., Kuntz, M., and Monéger, R. (1995). Biochemistry and molecular biology of chromoplast development. International review of cytology *163*, 175-247. 10.1016/s0074-7696(08)62211-1.

15. Campbell, R., Ducreux, L.J., Morris, W.L., Morris, J.A., Suttle, J.C., Ramsay, G., Bryan, G.J., Hedley, P.E., and Taylor, M.A. (2010). The metabolic and developmental roles of carotenoid cleavage dioxygenase4 from potato. Plant Physiol *154*, 656-664. 10.1104/pp.110.158733.

16. Deruère, J., Römer, S., d'Harlingue, A., Backhaus, R.A., Kuntz, M., and Camara, B. (1994). Fibril assembly and carotenoid overaccumulation in chromoplasts: a model for supramolecular lipoprotein structures. The Plant Cell *6*, 119-133. 10.1105/tpc.6.1.119 %J The Plant Cell.

17. Desplats, C., Mus, F., Cuiné, S., Billon, E., Cournac, L., and Peltier, G. (2009). Characterization of Nda2, a plastoquinone-reducing type II NAD(P)H dehydrogenase in chlamydomonas chloroplasts. J Biol Chem *284*, 4148-4157. 10.1074/jbc.M804546200.

18. Do, T.Q., Hsu, A.Y., Jonassen, T., Lee, P.T., and Clarke, C.F. (2001). A Defect in Coenzyme Q Biosynthesis Is Responsible for the Respiratory Deficiency in Saccharomyces cerevisiae abc1Mutants*. Journal of Biological Chemistry *276*, 18161-18168. https://doi.org/10.1074/jbc.M100952200.

19. Domínguez, F., and Cejudo, F.J. (2021). Chloroplast dismantling in leaf senescence. J Exp Bot. 10.1093/jxb/erab200.

20. Egea, I., Barsan, C., Bian, W., Purgatto, E., Latché, A., Chervin, C., Bouzayen, M., and Pech, J.-C. (2010). Chromoplast Differentiation: Current Status and Perspectives. Plant and Cell Physiology *51*, 1601-1611. 10.1093/pcp/pcq136 %J Plant and Cell Physiology.

21. Espinoza-Corral, R., Schwenkert, S., and Lundquist, P.K.J.T.P.J. (2021). Molecular changes of Arabidopsis thaliana plastoglobules facilitate thylakoid membrane remodeling under high light stress.

22. Eugeni Piller, L., Abraham, M., Dörmann, P., Kessler, F., and Besagni, C. (2012). Plastid lipid droplets at the crossroads of prenylquinone metabolism. Journal of Experimental Botany *63*, 1609-1618. 10.1093/jxb/ers016 %J Journal of Experimental Botany.

23. Eugeni Piller, L., Besagni, C., Ksas, B., Rumeau, D., Bréhélin, C., Glauser, G., Kessler, F., and Havaux, M. (2011). Chloroplast lipid droplet type II NAD(P)H quinone oxidoreductase is essential for prenylquinone metabolism and vitamin K₁ accumulation. Proceedings of the National Academy of Sciences *108*, 14354-14359. 10.1073/pnas.1104790108.

24. Eugeni Piller, L., Glauser, G., Kessler, F., and Besagni, C. (2014). Role of plastoglobules in metabolite repair in the tocopherol redox cycle. Front Plant Sci *5*, 298. 10.3389/fpls.2014.00298.

25. Fatihi, A., Latimer, S., Schmollinger, S., Block, A., Dussault, P.H., Vermaas, W.F., Merchant, S.S., and Basset, G.J. (2015). A Dedicated Type II NADPH Dehydrogenase Performs the Penultimate Step in the Biosynthesis of Vitamin K1 in Synechocystis and Arabidopsis. The Plant cell *27*, 1730-1741. 10.1105/tpc.15.00103.

26. Flower, D.R., North, A.C., and Sansom, C.E. (2000). The lipocalin protein family: structural and sequence overview. Biochim Biophys Acta *1482*, 9-24. 10.1016/s0167-4838(00)00148-5.

27. Frusciante, S., Diretto, G., Bruno, M., Ferrante, P., Pietrella, M., Prado-Cabrero, A., Rubio-Moraga, A., Beyer, P., Gomez-Gomez, L., Al-Babili, S., and Giuliano, G. (2014). Novel carotenoid cleavage dioxygenase catalyzes the first dedicated step in saffron crocin biosynthesis. Proceedings of the National Academy of Sciences of the United States of America *111*, 12246-12251. 10.1073/pnas.1404629111.

28. Fryer, M. (1992). The antioxidant effects of thylakoid vitamin E (α-tocopherol). Plant, Cell & Environment *15*, 381-392.

29. Gámez-Arjona, F.M., de la Concepción, J.C., Raynaud, S., and Mérida, Á.J.F.l. (2014). Arabidopsis thaliana plastoglobule-associated fibrillin 1a interacts with fibrillin 1b in vivo. *588*, 2800-2804.

30. Gaude, N., Bréhélin, C., Tischendorf, G., Kessler, F., and Dörmann, P. (2007). Nitrogen deficiency in Arabidopsis affects galactolipid composition and gene expression and results in accumulation of fatty acid phytyl esters. *49*, 729-739. https://doi.org/10.1111/j.1365-313X.2006.02992.x.

31. Gerards, M., van den Bosch, B., Calis, C., Schoonderwoerd, K., van Engelen, K., Tijssen, M., de Coo, R., van der Kooi, A., and Smeets, H. (2010). Nonsense mutations in CABC1/ADCK3 cause progressive cerebellar ataxia and atrophy. Mitochondrion *10*, 510-515. 10.1016/j.mito.2010.05.008.

32. Gillet, B., Beyly, A., Peltier, G., and Rey, P. (1998). Molecular characterization of CDSP 34, a chloroplastic protein induced by water deficit in Solanum tuberosum L. plants, and regulation of CDSP 34 expression by ABA and high illumination. The Plant journal : for cell and molecular biology *16*, 257-262. 10.1046/j.1365-313x.1998.00292.x.

33. Gonzalez-Jorge, S., Ha, S.H., Magallanes-Lundback, M., Gilliland, L.U., Zhou, A., Lipka, A.E., Nguyen, Y.N., Angelovici, R., Lin, H., Cepela, J., et al. (2013). Carotenoid cleavage dioxygenase4 is a negative regulator of β-carotene content in Arabidopsis seeds. Plant Cell *25*, 4812-4826. 10.1105/tpc.113.119677.

34. Greenwood, A.D., Leech, R.M., and Williams, J.P. (1963). The osmiophilic globules of chloroplasts: I. Osmiophilic globules as a normal component of chloroplasts and their isolation and composition in Vicia faba L. Biochimica et Biophysica Acta *78*, 148-162. https://doi.org/10.1016/0006-3002(63)91620-2.

35. Gross, J., Cho, W.K., Lezhneva, L., Falk, J., Krupinska, K., Shinozaki, K., Seki, M., Herrmann, R.G., and Meurer, J. (2006). A plant locus essential for phylloquinone (vitamin K1) biosynthesis originated from a fusion of four eubacterial genes. J Biol Chem *281*, 17189-17196. 10.1074/jbc.M601754200.

36. Havaux, M. (2020). Plastoquinone In and Beyond Photosynthesis. Trends Plant Sci *25*, 1252-1265. 10.1016/j.tplants.2020.06.011.

37. Hörtensteiner, S., and Kräutler, B. (2011). Chlorophyll breakdown in higher plants. Biochim Biophys Acta *1807*, 977-988. 10.1016/j.bbabio.2010.12.007.

38. Huang, H., Yang, M., Su, Y.e., Qu, L., and Deng, X.W. (2015). Arabidopsis Atypical Kinases ABC1K1 and ABC1K3 Act Oppositely to Cope with Photodamage Under Red Light. Mol Plant *8*, 1122-1124. 10.1016/j.molp.2015.04.003.

39. Ischebeck, T., Zbierzak, A.M., Kanwischer, M., and Dormann, P. (2006). A salvage pathway for phytol metabolism in Arabidopsis. J Biol Chem *281*, 2470-2477. 10.1074/jbc.M509222200.

40. Kessler, F., Schnell, D., and Blobel, G. (1999). Identification of proteins associated with plastoglobules isolated from pea (Pisum sativum L.) chloroplasts. Planta *208*, 107-113. 10.1007/s004250050540.

41. Kim, E.-H., Lee, Y., and Kim, H.U. (2015). Fibrillin 5 Is Essential for Plastoquinone-9 Biosynthesis by Binding to Solanesyl Diphosphate Synthases in Arabidopsis. Plant Cell *27*, 2956-2971. 10.1105/tpc.15.00707.

42. Kim, E.H., Lee, D.W., Lee, K.R., Jung, S.J., Jeon, J.S., and Kim, H.U. (2017). Conserved Function of Fibrillin5 in the Plastoquinone-9 Biosynthetic Pathway in Arabidopsis and Rice. Front Plant Sci *8*, 1197. 10.3389/fpls.2017.01197.

43. Kirchhoff, H. (2019). Chloroplast ultrastructure in plants. The New phytologist *223*, 565-574. 10.1111/nph.15730.

44. Kobayashi, N., and DellaPenna, D. (2008). Tocopherol metabolism, oxidation and recycling under high light stress in Arabidopsis. The Plant journal : for cell and molecular biology *55*, 607-618. 10.1111/j.1365-313X.2008.03539.x.

45. Krauß, S., Vetter, W.J.E.J.o.L.S., and Technology (2018). Phytol and phytyl fatty acid esters: occurrence, concentrations, and relevance. *120*, 1700387.

46. Krieger-Liszkay, A., and Trebst, A. (2006). Tocopherol is the scavenger of singlet oxygen produced by the triplet states of chlorophyll in the PSII reaction centre. Journal of Experimental Botany *57*, 1677-1684. 10.1093/jxb/erl002 %J Journal of Experimental Botany.

47. Ksas, B., Légeret, B., Ferretti, U., Chevalier, A., Pospíšil, P., Alric, J., and Havaux, M. (2018). The plastoquinone pool outside the thylakoid membrane serves in plant photoprotection as a reservoir of singlet oxygen scavengers. *41*, 2277-2287. https://doi.org/10.1111/pce.13202.

48. Lagier-Tourenne, C., Tazir, M., López, L.C., Quinzii, C.M., Assoum, M., Drouot, N., Busso, C., Makri, S., Ali-Pacha, L., Benhassine, T., et al. (2008). ADCK3, an Ancestral Kinase, Is Mutated in a Form of Recessive Ataxia Associated with Coenzyme Q10 Deficiency. The American Journal of Human Genetics *82*, 661-672. https://doi.org/10.1016/j.ajhg.2007.12.024.

49. Laizet, Y., Pontier, D., Mache, R., and Kuntz, M. (2004). Subfamily organization and phylogenetic origin of genes encoding plastid lipid-associated proteins of the fibrillin type. Journal of Genome Science and Technology *3*, 19-28.

50. Langenkämper, G., Manac'h, N., Broin, M., Cuiné, S., Becuwe, N., Kuntz, M., and Rey, P. (2001). Accumulation of plastid lipid-associated proteins (fibrillin/CDSP34) upon oxidative stress, ageing and biotic stress in Solanaceae and in response to drought in other species. Journal of experimental botany *52*, 1545-1554. 10.1093/jexbot/52.360.1545.

51. Leggett Bailey, J., and Whyborn, A.G. (1963). The osmiophilic globules of chloroplasts II. Globules of the spinach-beet chloroplast. Biochimica et Biophysica Acta *78*, 163-174. https://doi.org/10.1016/0006-3002(63)91621-4.

52. Li, J., Yang, J., Zhu, B., and Xie, G. (2019). Overexpressing OsFBN1 enhances plastoglobule formation, reduces grain-filling percent and jasmonate levels under heat stress in rice. Plant science : an international journal of experimental plant biology *285*, 230-238. 10.1016/j.plantsci.2019.05.007.

53. Li, T., Jiang, J., Zhang, S., Shu, H., Wang, Y., Lai, J., Du, J., and Yang, C. (2015). OsAGSW1, an ABC1-like kinase gene, is involved in the regulation of grain size and weight in rice. J Exp Bot *66*, 5691-5701. 10.1093/jxb/erv160.

54. Lichtenthaler, H.J.E. (1968a). Plastoglobuli and fine structure of plastids. *27*, 144-+.

55. Lichtenthaler, H.K. (1968b). [Distribution and relative concentrations of lipophilic plastid quinones in green plants]. Planta *81*, 140-152. 10.1007/bf00417443.

56. Lichtenthaler, H.K., and Peveling, E. (1966). [Plastoglobuli in different types of plastids from Allium cepa L]. Planta *72*, 1-13. 10.1007/bf00388140.

57. Lichtenthaler, H.K., and Sprey, B.J.Z.f.N.B. (1966). Über die osmiophilen globulären Lipideinschlüsse der Chloroplasten. *21*, 690-697.

58. Lippold, F., vom Dorp, K., Abraham, M., Hölzl, G., Wewer, V., Yilmaz, J.L., Lager, I., Montandon, C., Besagni, C., Kessler, F., et al. (2012). Fatty Acid Phytyl Ester Synthesis in Chloroplasts of Arabidopsis The Plant Cell *24*, 2001-2014. 10.1105/tpc.112.095588 %J The Plant Cell.

59. Liu, X., Hua, X., Guo, J., Qi, D., Wang, L., Liu, Z., Jin, Z., Chen, S., and Liu, G. (2008). Enhanced tolerance to drought stress in transgenic tobacco plants overexpressing VTE1 for increased tocopherol production from Arabidopsis thaliana. Biotechnology letters *30*, 1275-1280.

60. Lohmann, A., Schöttler, M.A., Bréhélin, C., Kessler, F., Bock, R., Cahoon, E.B., and Dörmann, P. (2006). Deficiency in Phylloquinone (Vitamin K1) Methylation Affects Prenyl Quinone Distribution, Photosystem I Abundance, and Anthocyanin Accumulation in the Arabidopsis

AtmenG Mutant*. Journal of Biological Chemistry *281*, 40461-40472. https://doi.org/10.1074/jbc.M609412200.

61. Lohscheider, J.N., and Río Bártulos, C. (2016). Plastoglobules in algae: A comprehensive comparative study of the presence of major structural and functional components in complex plastids. Marine genomics *28*, 127-136. 10.1016/j.margen.2016.06.005.

62. Lundquist, P.K., Poliakov, A., Bhuiyan, N.H., Zybailov, B., Sun, Q., and van Wijk, K.J. (2012). The Functional Network of the Arabidopsis Plastoglobule Proteome Based on Quantitative Proteomics and Genome-Wide Coexpression Analysis Plant Physiology *158*, 1172-1192. 10.1104/pp.111.193144 %J Plant Physiology.

63. Lundquist, P.K., Poliakov, A., Giacomelli, L., Friso, G., Appel, M., McQuinn, R.P., Krasnoff, S.B., Rowland, E., Ponnala, L., Sun, Q., and van Wijk, K.J. (2013). Loss of Plastoglobule Kinases ABC1K1 and ABC1K3 Causes Conditional Degreening, Modified Prenyl-Lipids, and Recruitment of the Jasmonic Acid Pathway. The Plant Cell *25*, 1818-1839. 10.1105/tpc.113.111120.

64. Malkin, R. (1986). On the function of two vitamin K1 molecules in the PS I electron acceptor complex. *208*, 343-346. https://doi.org/10.1016/0014-5793(86)81046-8.

65. Manara, A., DalCorso, G., Guzzo, F., and Furini, A. (2015). Loss of the Atypical Kinases ABC1K7 and ABC1K8 Changes the Lipid Composition of the Chloroplast Membrane. Plant and Cell Physiology *56*, 1193-1204. 10.1093/pcp/pcv046.

66. Manara, A., DalCorso, G., Leister, D., Jahns, P., Baldan, B., and Furini, A. (2014). AtSIA1 AND AtOSA1: two Abc1 proteins involved in oxidative stress responses and iron distribution within chloroplasts. *201*, 452-465. https://doi.org/10.1111/nph.12533.

67. Martinis, J., Glauser, G., Valimareanu, S., and Kessler, F. (2013). A Chloroplast ABC1-like Kinase Regulates Vitamin E Metabolism in Arabidopsis Plant Physiology *162*, 652-662. 10.1104/pp.113.218644.

68. Martinis, J., Glauser, G., Valimareanu, S., Stettler, M., Zeeman, S.C., Yamamoto, H., Shikanai, T., and Kessler, F. (2014b). ABC1K1/PGR6 kinase: a regulatory link between photosynthetic activity and chloroplast metabolism. The Plant journal : for cell and molecular biology *77*, 269-283. 10.1111/tpj.12385.

69. Mène-Saffrané, L., Jones, A.D., and DellaPenna, D. (2010). Plastochromanol-8 and tocopherols are essential lipid-soluble antioxidants during seed desiccation and quiescence in Arabidopsis.

Proceedings of the National Academy of Sciences of the United States of America *107*, 17815-17820. 10.1073/pnas.1006971107.

70. Merchant, S.S., Prochnik, S.E., Vallon, O., Harris, E.H., Karpowicz, S.J., Witman, G.B., Terry, A., Salamov, A., Fritz-Laylin, L.K., Maréchal-Drouard, L., et al. (2007). The Chlamydomonas genome reveals the evolution of key animal and plant functions. Science (New York, N.Y.) *318*, 245-250. 10.1126/science.1143609.

71. Michalecka, A.M., Svensson, A.S., Johansson, F.I., Agius, S.C., Johanson, U., Brennicke, A., Binder, S., and Rasmusson, A.G. (2003). Arabidopsis genes encoding mitochondrial type II NAD(P)H dehydrogenases have different evolutionary origin and show distinct responses to light. Plant Physiol *133*, 642-652. 10.1104/pp.103.024208.

72. Mollet, J., Delahodde, A., Serre, V., Chretien, D., Schlemmer, D., Lombes, A., Boddaert, N., Desguerre, I., de Lonlay, P., Ogier de Baulny, H., et al. (2008). CABC1 Gene Mutations Cause Ubiquinone Deficiency with Cerebellar Ataxia and Seizures. The American Journal of Human Genetics *82*, 623-630. https://doi.org/10.1016/j.ajhg.2007.12.022.

73. Munné-Bosch, S. (2005). The role of α-tocopherol in plant stress tolerance. Journal of Plant Physiology *162*, 743-748. https://doi.org/10.1016/j.jplph.2005.04.022.

74. Munné-Bosch, S., and Alegre, L. (2002). The Function of Tocopherols and Tocotrienols in Plants. Critical Reviews in Plant Sciences *21*, 31-57. 10.1080/0735-260291044179.

75. Muñoz, P., and Munné-Bosch, S. (2019). Vitamin E in Plants: Biosynthesis, Transport, and Function. Trends Plant Sci *24*, 1040-1051. 10.1016/j.tplants.2019.08.006.

76. Neely, W.C., Martin, J.M., and Barker, S.A. (1988). Products and relative reaction rates of the oxidation of tocopherols with singlet molecular oxygen. Photochem Photobiol *48*, 423-428. 10.1111/j.1751-1097.1988.tb02840.x.

77. Nogueira, M., Mora, L., Enfissi, E.M., Bramley, P.M., and Fraser, P.D. (2013). Subchromoplast sequestration of carotenoids affects regulatory mechanisms in tomato lines expressing different carotenoid gene combinations. Plant Cell *25*, 4560-4579. 10.1105/tpc.113.116210.

78. Ohmiya, A., Kishimoto, S., Aida, R., Yoshioka, S., and Sumitomo, K. (2006). Carotenoid cleavage dioxygenase (CmCCD4a) contributes to white color formation in chrysanthemum petals. Plant Physiol *142*, 1193-1201. 10.1104/pp.106.087130.

79. Otsubo, M., Ikoma, C., Ueda, M., Ishii, Y., and Tamura, N. (2018). Functional Role of Fibrillin5 in Acclimation to Photooxidative Stress. Plant Cell Physiol *59*, 1670-1682. 10.1093/pcp/pcy093.

80. Poon, W.W., Davis, D.E., Ha, H.T., Jonassen, T., Rather, P.N., and Clarke, C.F. (2000). Identification of <i>Escherichia coli ubiB</i>, a Gene Required for the First Monooxygenase Step in Ubiquinone Biosynthesis. *182*, 5139-5146. doi:10.1128/JB.182.18.5139-5146.2000.

81. Pozueta-Romero, J., Rafia, F., Houlné, G., Cheniclet, C., Carde, J.P., Schantz, M.L., and Schantz, R. (1997). A ubiquitous plant housekeeping gene, PAP, encodes a major protein component of bell pepper chromoplasts. Plant Physiol *115*, 1185-1194. 10.1104/pp.115.3.1185.

82. Pralon, T., Collombat, J., Pipitone, R., Ksas, B., Shanmugabalaji, V., Havaux, M., Finazzi, G., Longoni, P., and Kessler, F. (2020). Mutation of the Atypical Kinase ABC1K3 Partially Rescues the PROTON GRADIENT REGULATION 6 Phenotype in Arabidopsis thaliana. *11*. 10.3389/fpls.2020.00337.

83. Pralon, T., Shanmugabalaji, V., Longoni, P., Glauser, G., Ksas, B., Collombat, J., Desmeules, S., Havaux, M., Finazzi, G., and Kessler, F. (2019). Plastoquinone homoeostasis by Arabidopsis proton gradient regulation 6 is essential for photosynthetic efficiency. Communications Biology *2*, 220. 10.1038/s42003-019-0477-4.

84. Rey, P., Gillet, B., Römer, S., Eymery, F., Massimino, J., Peltier, G., and Kuntz, M.J.T.P.J. (2000). Over-expression of a pepper plastid lipid-associated protein in tobacco leads to changes in plastid ultrastructure and plant development upon stress. *21*, 483-494.

85. Rodrigo, M.J., Alquézar, B., Alós, E., Medina, V., Carmona, L., Bruno, M., Al-Babili, S., and Zacarías, L. (2013). A novel carotenoid cleavage activity involved in the biosynthesis of Citrus fruit-specific apocarotenoid pigments. J Exp Bot *64*, 4461-4478. 10.1093/jxb/ert260.

86. Rottet, S., Devillers, J., Glauser, G., Douet, V., Besagni, C., and Kessler, F. (2016). Identification of Plastoglobules as a Site of Carotenoid Cleavage. Frontiers in plant science *7*, 1855. 10.3389/fpls.2016.01855.

87. Rubio-Moraga, A., Rambla, J.L., Fernández-de-Carmen, A., Trapero-Mozos, A., Ahrazem, O., Orzáez, D., Granell, A., and Gómez-Gómez, L. (2014). New target carotenoids for CCD4 enzymes are revealed with the characterization of a novel stress-induced carotenoid cleavage dioxygenase gene from Crocus sativus. Plant molecular biology *86*, 555-569. 10.1007/s11103-014-0250-5.

88. Santabarbara, S., and Casazza, A.P. (2019). Kinetics and Energetics of Phylloquinone Reduction in Photosystem I: Insight From Modeling of the Site Directed Mutants. *10*. 10.3389/fpls.2019.00852.

89. Schelbert, S., Aubry, S., Burla, B., Agne, B., Kessler, F., Krupinska, K., and Hörtensteiner, S. (2009). Pheophytin pheophorbide hydrolase (pheophytinase) is involved in chlorophyll breakdown during leaf senescence in Arabidopsis. Plant Cell *21*, 767-785. 10.1105/tpc.108.064089.

90. Schoeder, H.-U., and Lockau, W. (1986). Phylloquinone copurifies with the large subunit of photosystem I. *199*, 23-27. https://doi.org/10.1016/0014-5793(86)81216-9.

91. Shanmugabalaji, V., Besagni, C., Piller, L.E., Douet, V., Ruf, S., Bock, R., and Kessler, F. (2013). Dual targeting of a mature plastoglobulin/fibrillin fusion protein to chloroplast plastoglobules and thylakoids in transplastomic tobacco plants. Plant molecular biology *81*, 13-25. 10.1007/s11103-012-9977-z.

92. Shikanai, T., Munekage, Y., Shimizu, K., Endo, T., and Hashimoto, T. (1999). Identification and Characterization of Arabidopsis Mutants with Reduced Quenching of Chlorophyll Fluorescence. Plant and Cell Physiology *40*, 1134-1142. 10.1093/oxfordjournals.pcp.a029498 %J Plant and Cell Physiology.

93. Simkin, A.J., Gaffé, J., Alcaraz, J.P., Carde, J.P., Bramley, P.M., Fraser, P.D., and Kuntz, M. (2007). Fibrillin influence on plastid ultrastructure and pigment content in tomato fruit. Phytochemistry *68*, 1545-1556. 10.1016/j.phytochem.2007.03.014.

94. Singh, D.K., Laremore, T.N., Smith, P.B., Maximova, S.N., and McNellis, T.W. (2012). Knockdown of FIBRILLIN4 Gene Expression in Apple Decreases Plastoglobule Plastoquinone Content. PLOS ONE *7*, e47547. 10.1371/journal.pone.0047547.

95. Singh, D.K., Maximova, S.N., Jensen, P.J., Lehman, B.L., Ngugi, H.K., and McNellis, T.W. (2010). FIBRILLIN4 is required for plastoglobule development and stress resistance in apple and Arabidopsis. Plant Physiol *154*, 1281-1293. 10.1104/pp.110.164095.

96. Singh, D.K., and McNellis, T.W. (2011). Fibrillin protein function: the tip of the iceberg? Trends Plant Sci *16*, 432-441. 10.1016/j.tplants.2011.03.014.

97. Soll, J., Schultz, G., Joyard, J., Douce, R., and Block, M.A. (1985). Localization and synthesis of prenylquinones in isolated outer and inner envelope membranes from spinach chloroplasts. Archives of biochemistry and biophysics *238*, 290-299. 10.1016/0003-9861(85)90167-5.

98. Spicher, L., and Kessler, F. (2015). Unexpected roles of plastoglobules (plastid lipid droplets) in vitamin K1 and E metabolism. Current Opinion in Plant Biology *25*, 123-129. https://doi.org/10.1016/j.pbi.2015.05.005.

99. Spurr, A.R., and Harris, W.M. (1968). Ultrastructure of Chloroplasts and Chromoplasts in Capsicum Annuum I. Thylakoid Membrane Changes during Fruit Ripening. American Journal of Botany *55*, 1210-1224. 10.1002/j.1537-2197.1968.tb07487.x.

100. Steinmüller, D., and Tevini, M. (1985). Composition and function of plastoglobuli : I. Isolation and purification from chloroplasts and chromoplasts. Planta *163*, 201-207. 10.1007/bf00393507.

101. Tevini, M., and Steinmuller, D. (1985). Composition and function of plastoglobuli : II. Lipid composition of leaves and plastoglobuli during beech leaf senescence. Planta *163*, 91-96. 10.1007/BF00395902.

102. Thomson, W.W., and Platt, K. (1973). Plastid Ultrastructure in the Barrel Cactus, Echinocactus Acanthodes. New Phytologist *72*, 791-797. 10.1111/j.1469-8137.1973.tb02054.x.

103. Tikhonov, A.N. (2013). pH-Dependent regulation of electron transport and ATP synthesis in chloroplasts. Photosynthesis Research *116*, 511-534. 10.1007/s11120-013-9845-y.

104. Van Eerden, F.J., Melo, M.N., Frederix, P., Periole, X., and Marrink, S.J. (2017). Exchange pathways of plastoquinone and plastoquinol in the photosystem II complex. Nat Commun *8*, 15214. 10.1038/ncomms15214.

105. van Wijk, K.J., and Kessler, F. (2017). Plastoglobuli: Plastid Microcompartments with Integrated Functions in Metabolism, Plastid Developmental Transitions, and Environmental Adaptation. Annual review of plant biology *68*, 253-289. 10.1146/annurev-arplant-043015-111737.

106. Varghese, R., S, U.K., C, G.P.D., and Ramamoorthy, S. (2021). Unraveling the versatility of CCD4: Metabolic engineering, transcriptomic and computational approaches. Plant science : an international journal of experimental plant biology *310*, 110991. 10.1016/j.plantsci.2021.110991.

107. Vidi, P.A., Kanwischer, M., Baginsky, S., Austin, J.R., Csucs, G., Dormann, P., Kessler, F., and Brehelin, C. (2006). Tocopherol cyclase (VTE1) localization and vitamin E accumulation in chloroplast plastoglobule lipoprotein particles. J Biol Chem *281*, 11225-11234. 10.1074/jbc.M511939200.

108. Woggon, W.D. (1999). Improving the Yield of alpha-Tocopherol from Natural Sources-Chemistry versus Molecular Biology. Angewandte Chemie (International ed. in English) *38*, 2715-2716. 10.1002/(sici)1521-3773(19990917)38:18<2715::aid-anie2715>3.0.co;2-k.

109. Yang, M., Huang, H., Zhang, C., Wang, Z., Su, Y., Zhu, P., Guo, Y., and Deng, X.W. (2016). Arabidopsis atypical kinase ABC1K1 is involved in red light-mediated development. Plant Cell Rep *35*, 1213-1220. 10.1007/s00299-016-1953-7.

110. Youssef, A., Laizet, Y., Block, M.A., Maréchal, E., Alcaraz, J.P., Larson, T.R., Pontier, D., Gaffé, J., and Kuntz, M. (2010). Plant lipid-associated fibrillin proteins condition jasmonate production under photosynthetic stress. The Plant journal : for cell and molecular biology *61*, 436-445. 10.1111/j.1365-313X.2009.04067.x.

111. Ytterberg, A.J., Peltier, J.B., and van Wijk, K.J. (2006). Protein profiling of plastoglobules in chloroplasts and chromoplasts. A surprising site for differential accumulation of metabolic enzymes. Plant Physiol *140*, 984-997. 10.1104/pp.105.076083.

112. Zbierzak, A.M., Kanwischer, M., Wille, C., Vidi, P.A., Giavalisco, P., Lohmann, A., Briesen, I., Porfirova, S., Bréhélin, C., Kessler, F., and Dörmann, P. (2009). Intersection of the tocopherol and plastoquinol metabolic pathways at the plastoglobule. The Biochemical journal *425*, 389-399. 10.1042/bj20090704.

113. Zechmann, B. (2019). Ultrastructure of plastids serves as reliable abiotic and biotic stress marker. PloS one *14*, e0214811. 10.1371/journal.pone.0214811.

114. Zhang, B., Liu, C., Wang, Y., Yao, X., Wang, F., Wu, J., King, G.J., and Liu, K. (2015). Disruption of a CAROTENOID CLEAVAGE DIOXYGENASE 4 gene converts flower colour from white to yellow in Brassica species. The New phytologist *206*, 1513-1526. 10.1111/nph.13335.

3. Chromoplast plastoglobules recruit the carotenoid biosynthetic pathway and contribute to carotenoid accumulation during tomato fruit maturation

Wayne Zita[1], Ségolène Bressoud[1], Gaetan Glauser[2], Felix Kessler[1]*, Venkatasalam Shanmugabalaji[1]
1 Plant Physiology Laboratory, University of Neuchâtel, Neuchâtel, Switzerland,
2 Neuchâtel Platform of Analytical Chemistry, University of Neuchâtel, Neuchâtel, Switzerland
* felix.kessler@unine.ch (FK); shanmugabalaji.venkatasalam@unine.ch (VS)
https://doi.org/10.1371/journal.pone.0277774

3.1 Abstract

Tomato (*Solanum lycopersicum*) fruit maturation is associated with a developmental transition from chloroplasts (in mature green fruit) to chromoplasts (in red fruit). The hallmark red color of ripe tomatoes is due to carotenogenesis and accumulation of the red carotenoid lycopene inside chromoplasts. Plastoglobules (PG) are lipid droplets in plastids that are involved in diverse lipid metabolic pathways. In tomato, information on the possible role of PG in carotogenesis and the PG proteome is largely lacking. Here, we outline the role of PG in carotenogenesis giving particular attention to tomato fruit PG proteomes and metabolomes. The proteome analysis revealed the presence of PG-typical FBNs, ABC1K-like kinases, and metabolic enzymes, and those were decreased in the PG of tomato chromoplasts compared to chloroplasts. Notably, the complete β-carotene biosynthesis pathway was recruited to chromoplast PG, and the enzymes PHYTOENE SYNTHASE 1 (PSY-1), PHYTOENE DESATURASE (PDS), ZETA-CAROTENE DESATURASE (ZDS), and CAROTENOID ISOMERASE (CRTISO) were enriched up to twelvefold compared to chloroplast PG. We profiled the carotenoid and prenyl lipid changes in PG during the chloroplast to chromoplast transition and demonstrated large increases of lycopene and β-carotene in chromoplast PG. The PG proteome and metabolome are subject to extensive remodeling resulting in high accumulation of lycopene during the chloroplast-to-chromoplast transition. Overall, the results indicate that PGs contribute to carotenoid accumulation during tomato fruit maturation and suggest that they do so by functioning as a biosynthetic platform for carotenogenesis.

3.2 Introduction

Chloroplasts, specialized photosynthetic plastids are present in all green tissues of plants, and are characterized by the presence of an extensive membrane system called thylakoids [1]. Plastoglobules (PG) bud from the outer leaflet of the thylakoid membrane and remain associated with the thylakoid membranes [2]. These “osmophilic globuli” were discovered by Lichtenthaler in the early 1970s with the advances in transmission electron microscopy [3]. PG participate in thylakoid lipid metabolism in response to biotic and abiotic stresses (light stress and nitrogen deprivation) [4–6]. Metabolites stored in PG may be exchanged with the thylakoid membrane [7]. PG have dynamic properties changing in number and size and depending on developmental stage and environmental conditions to assure thylakoid homeostasis [8, 9]. Plastoglobules contain a small specialized proteome, consisting of approximately 30 proteins. The components of the Arabidopsis and Capsicum annuum (bell pepper) PG proteomes have been categorized into structural proteins, regulatory kinases, and enzymes. Structural proteins named plastid lipid-associated proteins, plastoglobulins or fibrillins (FBNs) have been identified in the proteomes of red bell pepper and Arabidopsis PG [10–12]. The presence of a lipocalin domain suggests that the FBNs may contribute to the transport of lipids or the channeling of metabolites contained in PG [13, 14]. The PG proteomes contain presumed regulatory proteins namely ABC1K-like kinases. ABC1K1 together with ABC1K3 may contribute to plastoquinone distribution within the chloroplast [15, 16]. Together with the FBNs, ABC1Ks are the most abundant components of the PG proteomes [12]. In addition, PGs contain several uncharacterized predicted enzymes but also some well-known ones such as TOCOPHEROL CYCLASE (VTE1) and NAD(P)H DEHYDROGENASE C1 (NDC1) [10, 17]. They are involved in α-tocopherol and phylloquinone biosynthesis, respectively, and implicate PG in these biosynthetic pathways. A considerable number of studies have identified PG as a storage compartment containing neutral and prenyl lipids, including phylloquinone (vitamin K), plastoquinone (PQ-9), plastochromanol 8 (PC-8), tocopherols, triacylglycerols, fatty acids, and carotenoids [18–21]. In tomato fruit, chromoplasts develop from chloroplasts, a process that involves the dismantling of thylakoid membranes and chlorophyll breakdown as well as the recycling of the breakdown products [22–24]. PG in chromoplasts contain carotenoids such as β-carotene and lycopene, a high level of which is responsible for the hallmark red color of tomato fruit [25]. Tomato chromoplast PG are globular, whereas those of red bell pepper are fibrillar [21, 26, 27]. Fibrillins were first discovered as a major protein component of fibrillar PG in bell pepper, hence their name [21]. Later, red bell pepper chromoplast PG were shown to contain several carotenoid biosynthetic pathway enzymes including LYCOPENE β-CYCLASE (LCYB) and z-CAROTENE DESATURASE (ZDS) [11]. To characterize and establish tomato plastoglobule proteomes, we isolated PG from lysed chloroplasts and chromoplasts by sucrose density gradient centrifugation followed by nano LC-MS/MS analysis (Nanoscale liquid chromatography coupled to tandem mass spectrometry) of the associated proteins. We identified multiple known as well as new candidate PG proteins. Notably, enzymes of the carotenoid biosynthetic pathway were recruited to PG and some of them were strongly enriched in chromoplast PG. This coincided with strongly increased accumulation of lycopene, supporting a possible role of PG in carotenogenesis during tomato fruit ripening and chloroplast to chromoplast differentiation.

3.3 Material and methods

3.3.1 Plant material and growth conditions

Tomato used was (*Solanum Lycopersicum*, cv. Micro-Tom). The plants were grown in soil under 200 µmol.m^{-2}.s^{-1} in a growth chamber, with a photoperiod of 16 h of day and 8 h of the dark at at 22˚ and 18˚C, respectively. The relative air humidity of the growth chamber was around 30%. The mature green fruits were harvested after 34–39 day after anthesis, and red fruits were harvested 10 days after the breaker stage and immediately put on ice for further experimentation.

3.3.2 Fractionation and isolation of tomato chloroplast and chromoplasts plastoglobules

Fruits were washed with distilled water. The peduncle, the gel, and the seeds were removed from the fruits, then the pericarp was cut into small pieces and stored at 4˚C overnight. 130 g of tomato pieces were put into a cold waring blender, 150 ml extraction buffer (0.4Msucrose, 50 mM Tris-HCl pH 7.8, 1 mM EDTA, 1 mM DTT) was added and followed by homogenization (twice for 3 seconds at low speed, then twice for 5 seconds at high speed). The homogenate was filtered through three to four layers of cheesecloth (gauze) and put in a 500 ml centrifuge tube on ice. Tubes were centrifuged at 5000x g for 10 min in a Sorvall RC-5B (SLA-1500 Super Lite rotor) at 4˚C. The supernatant was removed, and the pellet was resuspended in 5 ml of extraction buffer and transferred to a 50 ml centrifuge tube on ice. Tubes were centrifuged at 9000x g for 10 min in a Sorvall RC-5B (SM-24 rotor) at 4˚C. The supernatant was removed, and the pellet kept on ice. The pellet was resuspended in 5 ml of 45% sucrose (45% sucrose [w/v], 50 mM tricine pH7.9, 5 mM sodium bisulphite, 2 mM EDTA, 2mM DTT). Chloroplasts and chromoplasts were homogenized mechanically using a handheld Potter homogenizer. 3 ml of 45% sucrose were added to the potter homogenizer and 8 ml of the resulting homogenate were transferred to a 38.5 ml Ultra-Clear centrifuge tube. Layers of 38%, 20%, 15% and 5% sucrose were added, and the gradients centrifuged 20 h at 4˚C at 100 000x g. Western blot analysis indicated that PG were contained in the top sucrose layers.

3.3.3 Proteins precipitation and immunoblotting

Proteins contained in PG and other fractions were precipitated with acetone. Proteins were separated by SDS-PAGE and transferred to nitrocellulose membrane. The immunoblotting was performed using FBN1A [10], TOC75 [28], and LHCB2 (Agrisera) antibodies.

3.3.4 Protein identification by nano-LC-MS/MS

The dry pellet of the PG protein sample was resuspended in 45 µl of miST buffer (1% sodium deoxycholate, 100mM Tris pH 8.6 (-20˚C), 10 mM DTT, 0.2µM EDTA), vortexed and heated at 90˚C for 5 min. 160 mM chloroacetamide in 10 mM Tris pH 8.6 was added to the sample and incubated for 30 min at room temperature. Next, the tryptic digestion was performed with 0.3 ug LysC/Trypsin for 90 min at 37˚C. An OASIS plate was pre-equilibrated with acetonitrile (MeCN) and SCX buffer. 300 µl of 100% ethyl-acetate and 1% trifluoroacetic acid (TFA) were added to the samples, vortexed for 2 min, and centrifuged at 5000 rpm for 5 min. The bottom aqueous phase was transferred into prefilled SOLA SCX columns and spun through the column (not too fast, typically, 2000 rpm 1 min is sufficient). The column was washed with 300 ul ethyl acetate, 0.5% TFA and HPLC solvent A (2% MeCN, 0.1% formic acid). The sample was eluted with 200 ul elution buffer (80% MeCN, 19% water, 1% NH3). The eluted sample was dried in a speed vac and resuspended in HPLC solvent A for MS analysis (Fusion, IT mode). Scaffold viewer Scaffold (version Scaffold_5.1.2, Proteome Software Inc., Portland, OR) software was used to validate MS/MS based peptide and protein identifications. Peptide identifications were accepted if they could be established at greater than 90.0% probability by the Scaffold Local FDR algorithm. All MS/MS spectras were analyzed using Mascot (Matrix Science, London, UK; version 2.6.2) to find the known protein sequences with a fragment ion mass tolerance of 0.50 Da and a parent ion tolerance of 10.0 PPM.

3.3.5 Prenyl lipid and carotenoid analysis from whole tomato fruit and PG fractions

Prenyl lipids and carotenoids were extracted from whole tomato fruit and PG fractions using established methods [29, 30]. The prenyl quinones and carotenoids were separated and quantified by reverse-phase ultra-high-pressure liquid chromatography coupled to quadrupole-time-of-flight mass spectrometry (UHPLC-QTOFMS). Absolute concentrations of prenylquinones (PQ-9, PC-8, phylloquinone, α-T, γ-T, δ-T, PC-OH, PQH2-9 PQ-OH) and carotenoids (lycopene, lutein, β-carotene, phytoene) were calculated based on standard calibration curves. In addition, the carotenoids violaxanthin and neoxanthin were measured based on lutein standards.

3.4 Results

3.4.1 Isolation and quality assessment of chloroplast and chromoplast plastoglobules

To determine tomato fruit PG proteomes, tomato plants (*Solanum Lycopersicum*) were grown under standard light conditions (200 µmol.m^{-2}.s^{-1}) and mature green and red fruit were harvested [31]. PG from chloroplasts (in mature green fruit) and chromoplasts (in red fruit) were isolated by flotation centrifugation on a discontinuous sucrose gradient [26]. The low density of PG allowed separation from plastid membrane compartments by differential flotation. Visual inspection suggested that chloroplast plastoglobules (PG), EN (envelope) and TM (thylakoid membranes) from chloroplasts had been separated well (FIG 1A). The same held true for chromoplast plastoglobules (PG) that also appeared well separated from carotenoid membranous crystals (CR) and envelopes (EN) (FIG 1C). This was further assessed by western blotting analysis of the gradient fractions using specific antibodies against marker proteins for PG FBN1A, envelopes TOC75, and thylakoid membranes LHCB2 (FIG 1B and 1D).

The established PG marker FBN1A was detected in the first ten low-density fractions but also the last fractions, which has already been shown in previous studies and is likely due to the association of PG with plastid membranes [10, 12, 26] (FIG 1B and 1D). The absence of the thylakoid LHCB2 and the outer envelope membrane TOC75 markers in the low-density fractions indicated PG enrichment. Fractions one to five enriched in PG were selected for further analysis, pooled, and proteins were precipitated by acetone. The protein pellets were dried. Two independent biological replicates for both chloroplast and chromoplast PG were obtained.

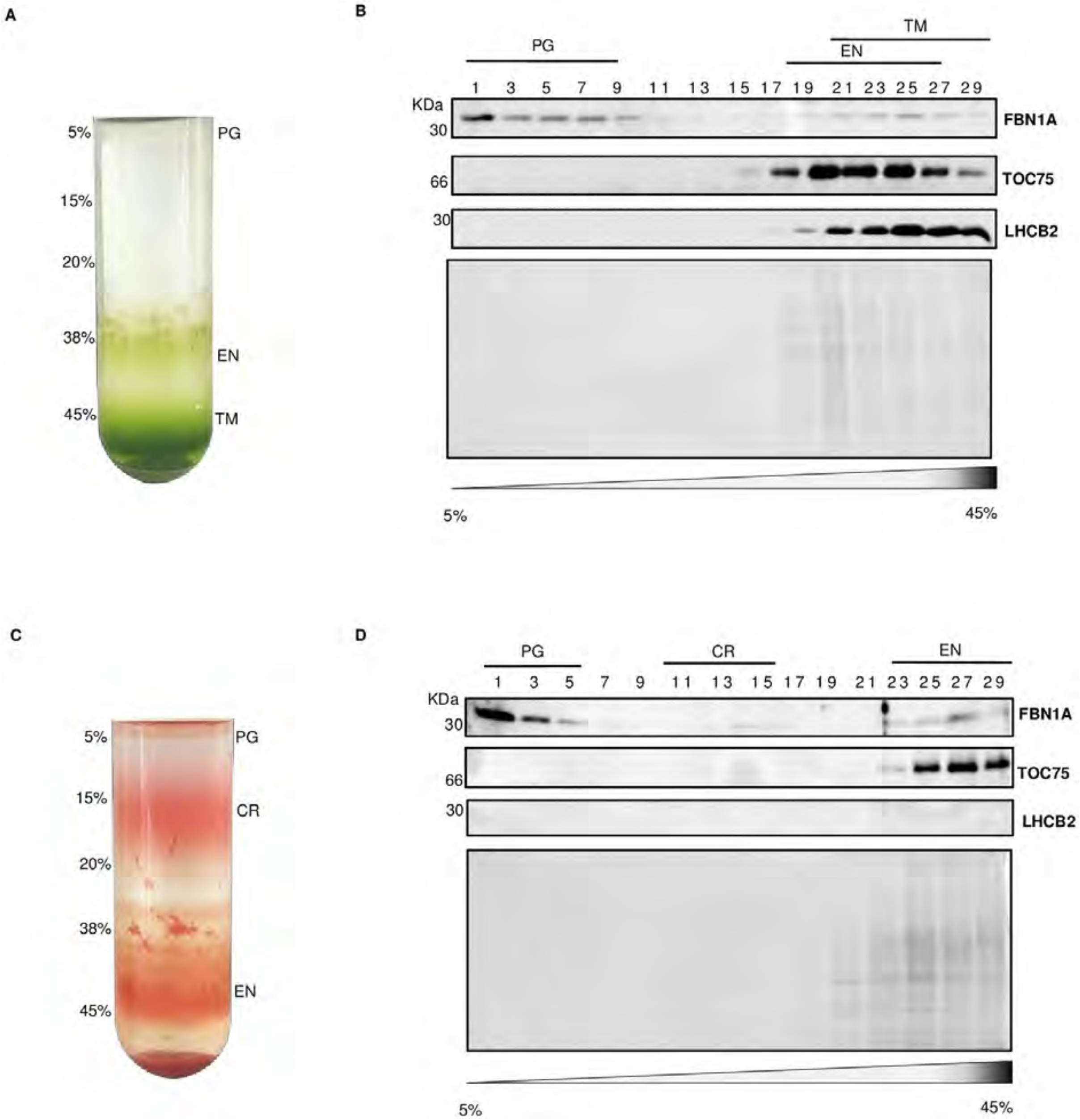

FIG 1| **Isolation of tomato fruit PG from chloroplast and chromoplast.** (A) Isolated chloroplasts were fractionated on a sucrose step gradient (5, 15, 20, 38, 45% sucrose). PG (plastoglobules); EN (envelope); TM (thylakoid membranes). (B) Uneven fractions from 1 to 29 were subjected to SDS-PAGE followed by immunoblotting using antibodies against FBN1A (PG marker), TOC75 (envelope marker), and LHCB2 (thylakoid marker). (C) Isolated chromoplasts from red tomato fruit were fractionated on a sucrose step gradient (5, 15, 20, 38, 45% sucrose). PG (plastoglobules); CR (carotenoid crystals); EN (envelope). (D) Uneven fractions 1 to 29 were subjected to SDS-PAGE followed by immunoblotting using antibodies FBN1A (PG marker), TOC75 (envelope marker), and LHCB2 (thylakoid marker).

3.4.2 Tomato plastoglobule proteome

Pooled and precipitated PG fractions were digested with trypsin. The tryptic peptides were analyzed by gel-enhanced liquid chromatography-mass spectrometry (GeLCMS). The data were analyzed using the MASCOT/MaxQuant and Scaffold algorithm to identify proteins corresponding to the peptides. The parameters were set to identify only those individual proteins that were common to both biological replicates of the experiment. A total of 1150 and 838 proteins were identified in chloroplast and chromoplast PG, respectively. These sets of proteins were further analyzed using the UniProt, TAIR and SUBA online resources as well as the TargetP algorithm. This analysis reduced the number to 271 and 147 candidate proteins for chloroplast and chromoplast PG. The established PG proteomes from *Arabidopsis thaliana* and red bell pepper [10–12] combined together were used as references to identify core components of the chloroplast and chromoplast PG proteomes. Thereby, 33 tomato chloroplast and 31 chromoplast proteins were found in common with Arabidopsis, and bell pepper and constituted the tomato fruit PG core proteomes. With the exception of the absence of CCD4 and NDC1 from chromoplast PG, the chloroplast and chromoplast PG core proteomes were identical. Abundant PG proteins including FBNs and predicted regulatory protein kinases ABC1Ks were identified [12]. Also present in both proteomes were prenyl lipid pathway enzymes (including VTE1, PHYTYL ESTER SYNTHASE (PES), ZDS and LCYB) and additional accepted PG proteins (including PGM48, PG18, and SOUL4) [10, 11, 24, 32–34]. In addition to the known PG proteins, we have identified 18 new candidates for the tomato chloroplast PG proteome and 17 for the chromoplast PG proteome of which 15 were common to both. They were identifed using PPDB and STRING databases as well as subcellular localization studies in the literature essentially by exclusion of curated stromal, thylakoid and envelope proteins. This allowed us to identify three additional candidates for carotenoid biosynthesis pathway (PSY1, PDS, CRTISO), for phylloquinone biosynthesis (MenG), for lipid metabolism (LOXC) and for isopentenyl diphosphate biosynthesis (1-deoxy-D-xylulose-5-phosphate synthase 1; DXS1) (FIG 2 and Table 1).

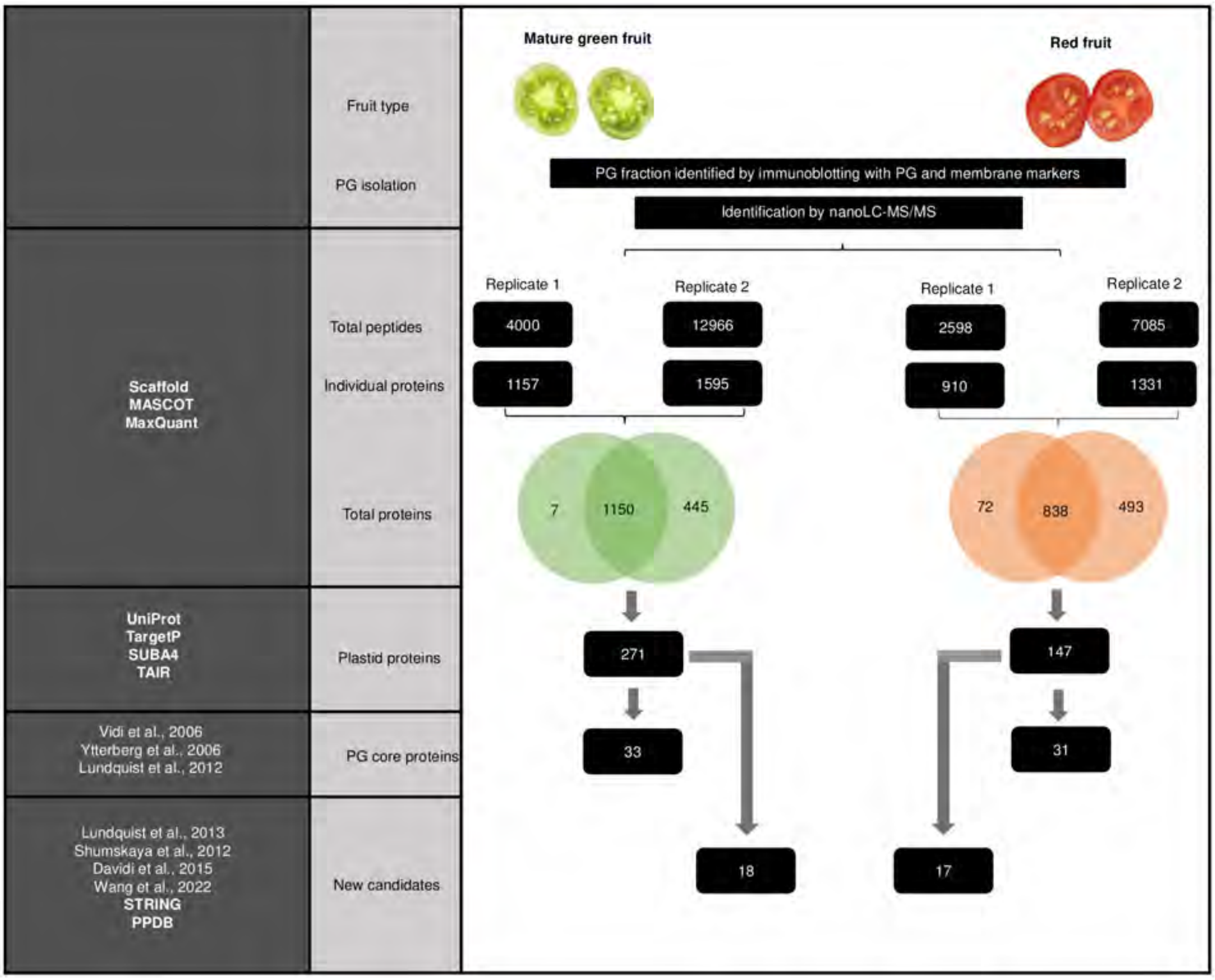

FIG 2| **Experimental design used for tomato fruit PG proteome analysis.** PGs from mature green and red fruit were isolated separately by sucrose gradient flotation. The two independent replicate PG fractions from mature green and red fruit were analyzed by nano-liquid chromatography (nanoLC)-electrospray ionization (ESI)-tandem mass spectrometry (MS / MS) for peptide identification. All identified peptides (Total Peptides) were further processed by Scaffold, MASCOT, and MaxQuant software to obtain corresponding individual proteins (Individual proteins). The number of individual proteins collected after merging two independent replicates (Total proteins). The Total proteins were filtered using the Uniport, TargetP, SUBA4, and TAIR databases to identify plastid protein (Plastid protein). Plastid proteins were filtered using known chloroplast and chromoplast proteome based on the existing literatures resulting in PG core proteins (PG core proteins). The new PG protein candidates (New candidates) were identified by exclusion of curated stromal, thylakoid and envelope proteins from plastid proteins (Plastid proteins) using PPDB and STRING databases as well as subcellular localization studies in the literature.

Table 1. Proteome of tomato fruit chloroplast and chromoplast plastoglobules.

Accession No	Protein Name	Peptide count		Homolog			
		PG chloroplast	PG chromoplast	*Arabidopsis thaliana*		*Capsicum annuum*	
Structural				Accession No	Lundquist et al., 2012	Accession No	Ytterberg et al.,2006
Solyc02g081170.2.1	FBN1a/b	153	99	AT4G04020	x	gi|1076575	x
Solyc08g076480.2.1	FBN2	162	53	AT2G35490	x	sgn|U197362	x
Solyc09g090330.2.1	FBN4	83	49	AT3G23400	x		x
Solyc10g080490.1.1	FBN7a	12	2	AT3G58010	x		-
Solyc03g062790.2.1	FBN7b	73	30	AT2G42130	x		-
Solyc08g068590.2.1	FBN8	41	40	AT2G46910	x		-
Regulatory							
Solyc08g074560.2.1	ABC1K1	62	31	AT4G31390	x		-
Solyc04g083010.2.1	ABC1K3	67	24	AT1G79600	x		-
Solyc04g072230.2.1	ABC1K5	39	11	AT1G71810	x		-
Solyc09g091580.2.1	ABC1K6	58	34	AT3G24190	x		-
Solyc07g045420.2.1	ABC1K7	39	26	AT3G07700	x		-
Solyc03g095620.2.1	ABC1K9	48	43	AT5G05200	x		x
Enzymes							
Solyc08g068570.2.1	VTE1	131	64	AT4G32770	x		x
Solyc08g075490.2.1	CCD4	15	0	AT4G19170	x		-
Solyc01g098110.2.1	PES1	56	68	AT1G54570	x		x
Solyc02g094430.2.1	PES2	65	57	AT3G26840	x		-
Solyc03g043750.2.1	NDC1	3	0	AT5G08740	x		-
Other							
Solyc01g056880.1.1	SOUL4	39	38	AT3G10130	x		-
Solyc07g007300.2.1	UbiE methyltransferase-related 1	7	14	AT2G41040	x		-
Solyc07g043570.2.1	Aldo/keto reductase	24	32	AT1G06690	x		x
Solyc09g061440.2.1	PG18	24	13	AT4G13200	x	sgn|U204835	x
Solyc03g096460.2.1	PLAT/LH2–1	9	4	AT4G39730	x		-
Solyc03g005000.2.1	PGM48	8	3	AT3G27110	x		-
Solyc08g076450.2.1	Flavin reductase-related 1	29	45	AT1G32220	x		x
Solyc02g070770.2.1	Flavin reductase-related 2	56	40	AT2G34460	x		-
Solyc08g075100.2.1	DUF1350	26	15	AT3G43540	x		-
Solyc03g118850.2.1	alpha/beta hydrolase family protein	16	10	AT1G73750	x		-
Solyc02g084440.2.1	Aldolase/ FBA8	59	23	AT3G52930	-		x
Solyc05g015390.2.1	Rubber elongation factor family	22	28	AT1G67360	-		x
Solyc04g039850.1.1	CF1b, atpB	62	57	ATCG00480	-		x
Solyc12g013810.1.1	Thioredoxin m4	11	13	AT3G15360	-	sgn|U201138	x
Carotenoid biosynthesis							
Solyc01g097810.2.1	ZDS	9	49	AT3G04870	-	gi|1583601	x
Solyc04g040190.1.1	LCYB	5	6	AT3G10230	-	gi|12643508	x
New candidates							
Carotenoid metabolism							
Solyc03g031860.2.1	PSY1 (Phytoene Synthase 1)	2	15	AT5G17230	-	-	-
Solyc03g123760.2.1	PDS (Phytoene desaturase)	5	36	AT4G14210	-	-	-
Solyc10g081650.1.1	CRTISO (Carotenoid isomerase)	3	36	AT1G06820	-	-	-
Other							
Solyc01g006540.2.1	LOXC	18	55	AT1G17420	-	-	-
Solyc05g056270.2.1	Phosphoenolpyruvate carboxylase family protein	62	39	AT2G43180	-	-	-
Solyc06g083770.2.1	Glutathione S-transferase family protein	22	12	AT5G44000	-	-	-
Solyc05g009390.2.1	Alpha/beta-Hydrolases superfamily protein	7	11	AT1G77420	-	-	-
Solyc08g083035.1.1	Uncharacterized protein	10	6	AT5G41960	-	-	-
Solyc01g068030.2.1	Polyketide cyclase domain protein	4	6	At1g02475	-	-	-
Solyc07g005550.2.1	Uncharacterized protein	2	11	AT2G44870	-	-	-
Solyc06g059720.2.1	Stearoyl-acyl carrier protein delta-9-desaturases	0	15	AT1G43800	-	-	-
Solyc06g073280.2.1	L-lysine alpha-aminotransferase	7	4	AT2G13810	-	-	-
Solyc12g019010.1.1	MenG	8	4	AT1G23360	-	-	-
Solyc09g092450.2.1	Acyl activating enzyme 16	2	5	AT3G23790	-	-	-
Solyc03g118130.2.1	Rubredoxin-like superfamily protein	4	0	AT5G51010	-	-	-
Solyc11g009080.2.1	DAHP synthetase 1 (DHS1)	5	2	AT4G39980	-	-	-
Solyc05g053100.2.1	Dihydrolipoamide dehydrogenase	6	0	AT4G16155	-	-	-
Solyc06g050590.3.1	Biotin/lipoyl attachment domain-containing protein	5	0	AT3G56130	-	-	-
Solyc01g005910.2.1	DUF1212	0	3	AT3G12685	-	-	-
Solyc01g067890.2.1	1-deoxy-D-xylulose-5-phosphate synthase 1	30	5	AT4G15560	-	-	-

Tomato PG proteome which is based on two biological replicates. One representative proteome was selected for the table. The Accession No is the ID identified for each protein on www.solgenomics.net; the common protein name is based on the literature. The accession numbers of homologs are also given based on TAIR for Arabidopsis and Solanaceae database (www.sgn.cornell.edu) for bell pepper. Peptide count represents the number of peptides detected in each sample. The known "core" PG proteome was categorized into five groups and the new candidate PG protein group into two categories.

3.4.3 Carotenoid biosynthetic enzymes are enriched in chromoplast PG

Five enzymes of the carotenoid biosynthesis pathway upto β-carotene were associated with chloroplast as well as chromoplast PG. The comparison of chloroplast with chromoplast PG revealed differences in their peptide counts. The heatmap based on peptide counts shows a clear increase in chromoplast PG of the first four enzymes required for lycopene biosynthesis namely PSY1, PDS, ZDS, and CRTISO. The higher numbers likely reflect higher enzyme levels that underpin lycopene biosynthetic activity in the chromoplast and during the chloroplast-tochromoplast transition (FIG 3). Peptide counts for LYCB were similar in both plastid types, suggesting a constant activity of this enzyme in PG during chloroplast to chromoplast conversion (FIG 3). Heatmaps also showed reduced presence of FBNs and ABC1Ks in the chromoplast PG compared with chloroplast PG (S1 FIG).

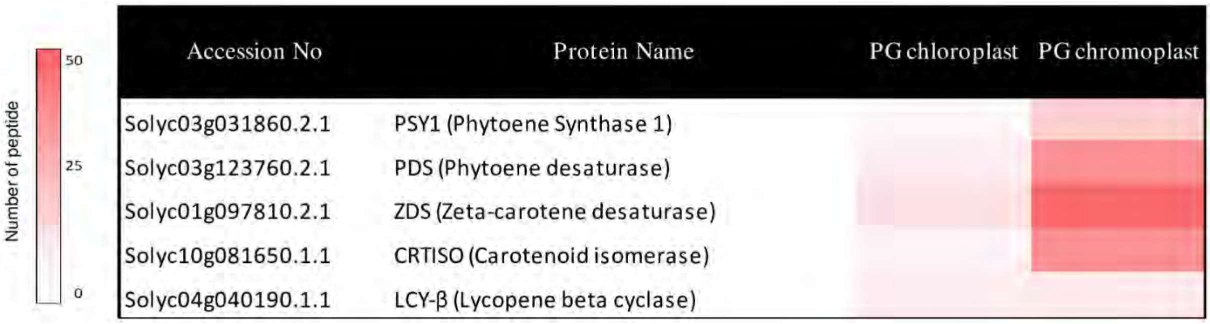

Accession No	Protein Name	PG chloroplast	PG chromoplast
Solyc03g031860.2.1	PSY1 (Phytoene Synthase 1)		
Solyc03g123760.2.1	PDS (Phytoene desaturase)		
Solyc01g097810.2.1	ZDS (Zeta-carotene desaturase)		
Solyc10g081650.1.1	CRTISO (Carotenoid isomerase)		
Solyc04g040190.1.1	LCY-β (Lycopene beta cyclase)		

FIG 3| **Carotenoid biosynthetic enzymes enriched in tomato PG chromoplasts.** The carotenoid biosynthetic enzymes heatmap was generated from peptide counts obtained from PG isolated from chloroplasts and chromoplasts, respectively.

3.4.4 Protein-protein interaction network of chromoplast PG protein

The chromoplast PG proteome contains various proteins annotated with a large range of functions. We carried out an analysis of the protein network of the chromoplast plastoglobule proteome using STRING (www.string-db.org). The classification and clusters of chromoplast PG proteins proposed by STRING are based on a curated database, experimental results, predicted gene neighborhood, annotated function, text mining, protein co-expression, and protein homology according to the recent literature [35, 36]. Application of STRING resulted in three distinct clusters and a number of non-associated proteins (FIG 4).

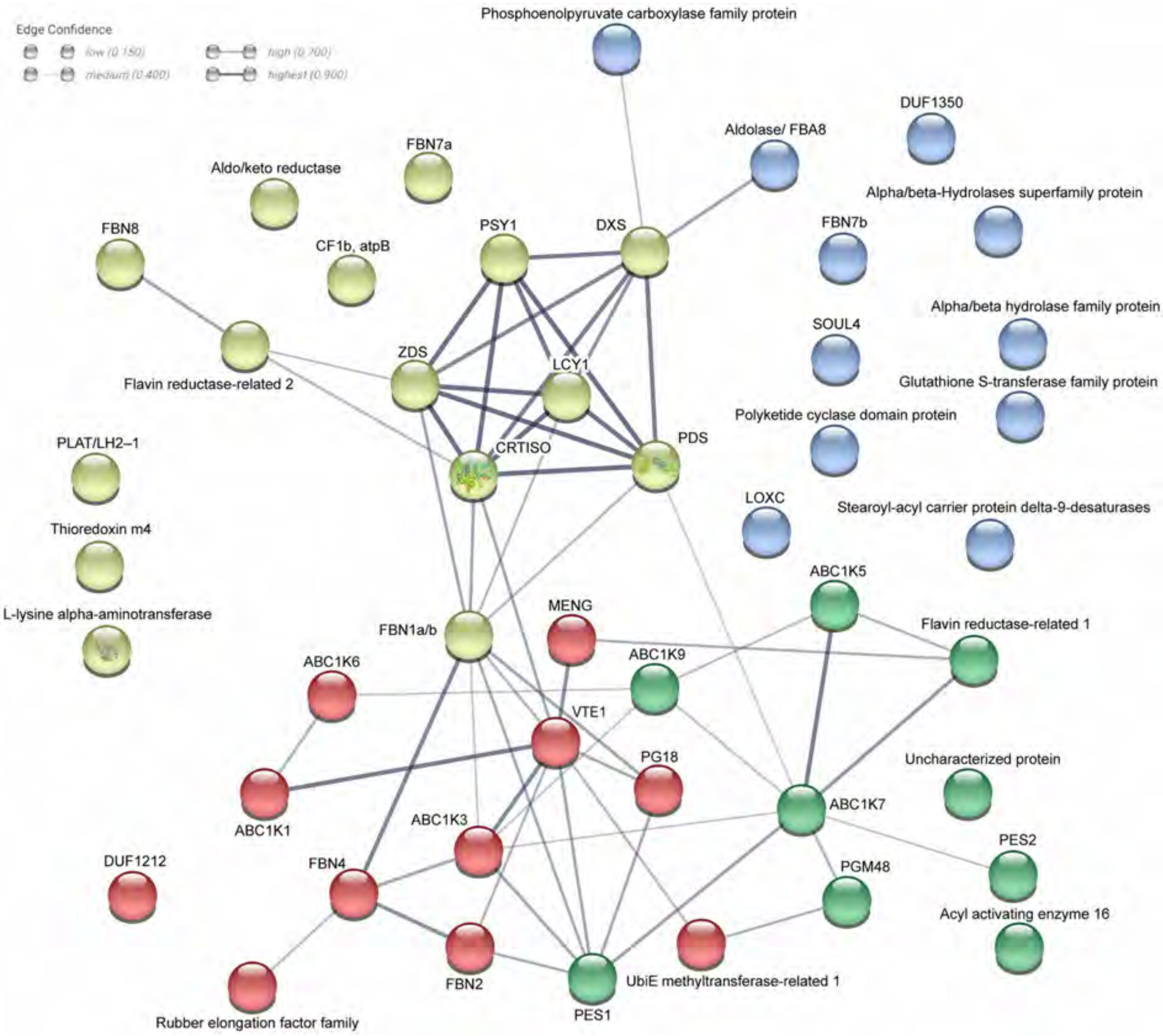

FIG 4| **Interaction network of chromoplast PG proteins.** The tomato chromoplast PG proteome analysis using the STRING software identified three clusters. Pear, (cluster 1) enriched in carotenoid biosynthetic enzymes; Red, (cluster 2) enriched in prenyl quinone metabolism and regulation; green, (cluster 3) enriched in chloroplast senescence and thylakoid membrane dismantling; blue, proteins not associated with the network.

Cluster 1 was mainly composed of carotenoid biosynthetic enzymes including PSY1, which condenses two geranylgeranyl diphosphates to phytoene. PDS and ZDS catalyse desaturation reactions, which are required for synthesis of 9,90-di-cis-z-carotene, and prolycopene, respectively. CRTISO (carotene isomerase) converts prolycopene into all-trans-lycopene. LYCB catalyses the cyclization of lycopene into β-carotene [25]. In addition, carotenoid biosynthesis key regulatory enzyme DXS1 [37] is part of cluster 1. Interestingly, FBN1 (CHRC) is part of cluster 1 and also closely associated with cluster 2. FBN1 (CHRC) is well known for its involvement in carotenoid accumulation and fibril formation but also carotenoid stabilization in chromoplasts [21]. Cluster 2 contain FBNs, VTE1, MenG, ABCK1 and ABC1K3. Functions of FBNs have been linked to tolerance to abiotic and biotic stress [4, 5]. Recent studies have shown that ABC1K1 and ABC1K3 are involved in the regulation of photosynthetic adaptation via plastoquinone pool homeostasis. [15, 16]. The tocopherol cyclase (VTE1) catalyzes the formation of the chromanol ring in α-tocopherol biosynthesis and may be regulated via phosphorylation by ABC1K1 [10, 38]. MenG catalyzes the final methylation step of 2-phytyl-1,4-naphthoquinone resulting in phylloquinone [39]. In conclusion, cluster 2 functions are mostly linked to prenyl quinone metabolism. Cluster 3 contains PES, PGM48 and ABC1Ks. PGM48, a PG-associated protease, which in Arabidopsis mainly interacts with other PG proteins and degrades them during senescence [32]. PES belongs to esterase/lipase/thioesterase and acyl transferase family and synthesizes phytol esters and triacyl glycerols during stress and senescence as well as carotenoid esters during the chloroplast-to-chromoplast transition [24]. ABC1K7 regulates the chloroplast membrane remodelling under stress and may act in the oxidative stress resistance pathway [40, 41]. Thus, cluster 3 functions are mostly linked to chloroplast senescence and thylakoid dismantling processes that also take place during fruit ripening and chloroplast-tochromoplast transition.

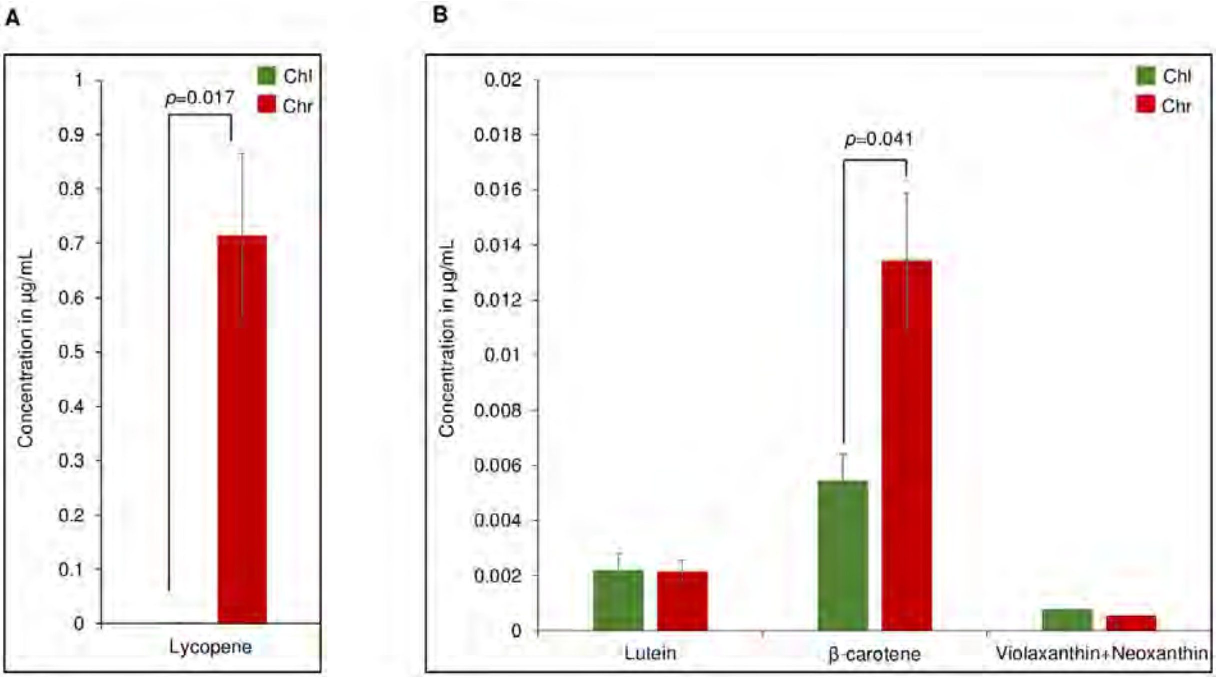

FIG 5| **Lycopene and β-Carotene accumulate high levels in chromoplast PG.** (A) Total carotenoids were extracted from equal volumes of gradient fractions containing chloroplast (Chl) or chromoplast (Chr) PG. Lycopene was quantified. (B) Quantification of lutein, β-carotene, and violaxanthin/neoxanthin. All values in the figures are the mean of 3 biological replicates (n = 3). Statistical differences were assessed with students' t test and p values are indicated.

3.4.5 Lycopene and β-carotene were enriched in the chromoplast PG

We analysed the total carotenoid content and composition in mature green fruit and red fruit as well as in PG purified from chloroplasts and chromoplasts using ultra-HPLC coupled with atmospheric pressure chemical ionization-quadrupole time-of-flight mass spectrometry (UHPLC-APCI-QTOF-MS). Lycopene and β-carotene accumulated to higher concentrations in red fruit than mature green fruit, lycopene being almost undetectable in mature green fruit (FIG S2A) while lutein and violaxanthin+neoxanthin accumulated to lower concentrations in red fruit than mature green fruit (FIG S2B). With regard to isolated PG, the relative concentration of lycopene was much higher in chromoplast PG than in chloroplast PG in equal volumes of the isolated fractions (FIG 5A) while the relative concentrations of lutein were the same and those of β-carotene higher and those of violaxanthin+neoxanthin lower (FIG 5B). In addition, we compared the relative distribution of lycopene, lutein, β-carotene and phytoene in equal volumes of the isolated fractions of PG, CR (carotenoid crystals) and EN (envelope) fractions. Lycopene and β-carotene levels were highest in CR but in addition to PG the envelopes also accumulated some lycopene and β-carotene (FIG S3).

3.4.6 Differential accumulation of prenyl lipids in PG upon chromoplast differentiation

We investigated the total prenyl lipid contents of mature green fruit and red fruit. We obtained prenyl lipid profiles by UHPLC-APCI-QTOF-MS. Red fruit accumulated higher concentrations of plastoquinone (PQ-9), plastochromanol (PC-8), α-tocopherol (α-T), γ-tocopherol (γ-T) and δ tocopherol (δ-T) while the phylloquinone concentration was lower in red than in mature green fruit (FIG S4). Interestingly, this was reversed in PG, the results using equal volumes of the isolated fractions revealed that the relative concentrations of PQ-9 and its derivatives (PC-8, PC-OH, PQH2-9 and PQ-OH), phylloquinone, α-T, γ-T were considerably lower in the chromoplast than in the chloroplast PG (FIG 6).

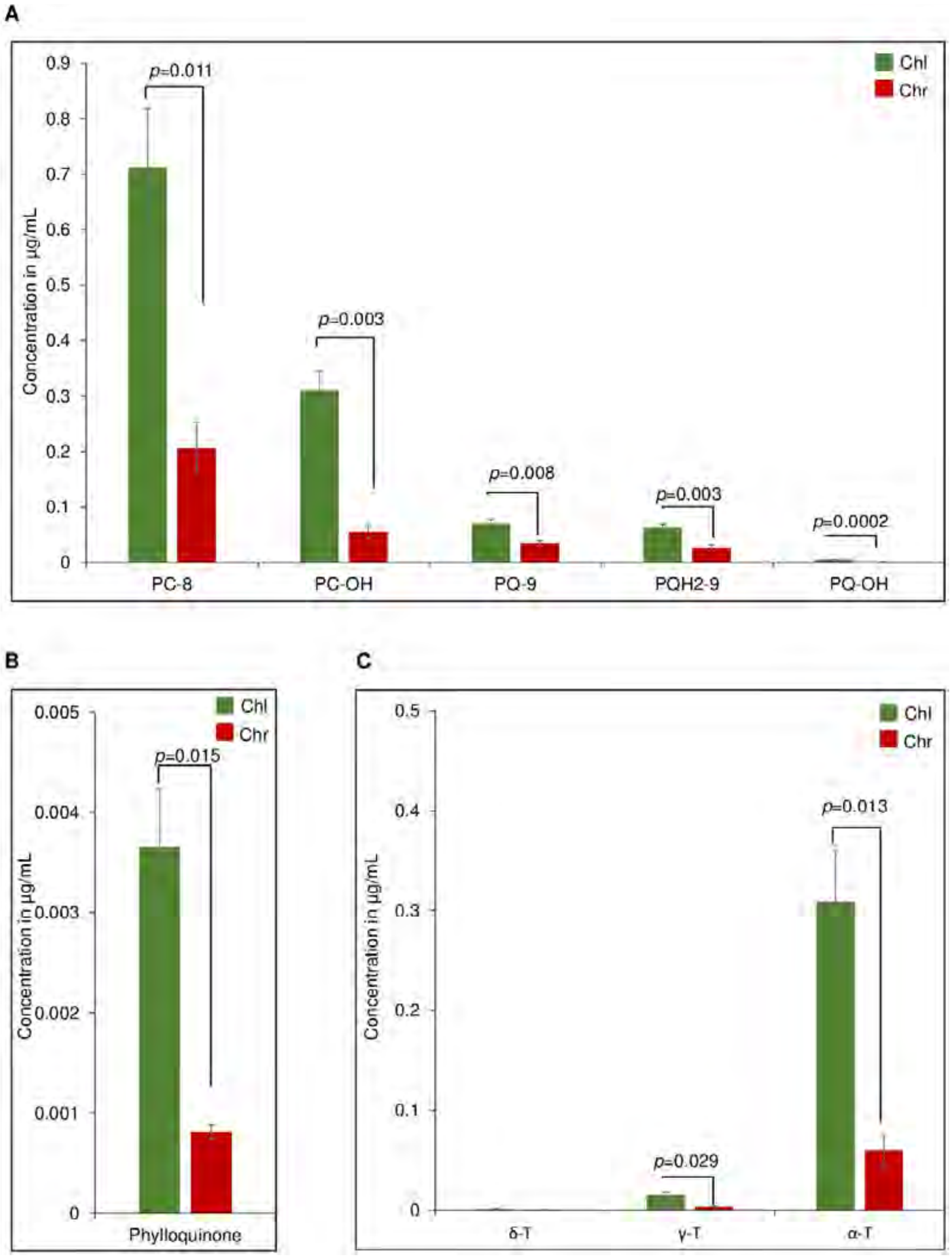

FIG 6| **Reduced levels of prenyl quinones in chromoplast PG.** (A) The total prenyl quinones were extracted from equal volumes of gradient fractions containing chloroplast (Chl) and chromoplast (Chr) PG, PC-8, plastochromanol; PC-OH, hydroxy-plastochromanol; PQ-9, plastoquinone; PQH2-9, plastoquinol and PQ-OH, hydroxy-plastoquinone were quantified (B) Quantification of phylloquinone. (C) Quantification of tocopherols. All values in the figures are the mean of 3 biological replicates (n = 3). Statistical differences were assessed with student's t test and *p* values are indicated.

3.5 Discussion

Purified PG were obtained from the chloroplasts and chromoplasts of mature green and red tomato fruit, respectively, and proteome analysis was carried out and thus resulted in a long list of proteins. UniProt, SUBA4, TAIR database and TargetP algorithm were used to filter the list and identify plastid proteins. Comparison of the resulting list with known PG proteomes indicated that tomato fruit chromoplasts and chloroplast PG together have a total of 33 proteins in common with Arabidopsis and red bell pepper (Table 1). This finding points to the overall functional conservation of PG in different species, tissues and plastid types. These "known" P proteins are considered core components of the chromoplast PG proteome based on previous reports i.e. CHRC (FBN1A) [21, 42–44]. Western blot analysis confirmed enrichment of CHRC (FBN1A) in PG fractions of chromoplasts and chloroplasts (FIG 1D). In addition to the core components, 17 new candidates that included carotenoid biosynthetic enzymes were identified based on the literature, STRING and PPDB annotation (Table 1) (FIG 2). The 17 new candidates of chromoplast PG were attributed to two categories, carotenoid biosynthetic enzymes and "others". In the "others" category was lipoxygenase C (LOXC), which is specifically expressed during tomato fruit ripening. LOXs participate in fatty acid catabolism during the disassembly of the thylakoid membranes during the chloroplast to chromoplast transition [45]. Moreover, previous studies propose a model in which the C-terminal PLAT (for polycystin-1, lipoxygenase and alpha toxin) domain may be responsible for LOX association with PG [46, 47]. Another intriguing candidate is MenG that is involved in phylloquinone biosynthesis [39]. MenG cooperates with the known PG protein NDC1 in the final methylation step of phylloquinone biosynthesis and assignment as PG candidate is therefore not surprising. Moreover, it has been shown previously that fluorescently-tagged MenG and multiprotein of phylloquinone biosynthesis (PHYLLO) resulted in patterns resembling those of PG [48]. Also, in this study, 1-deoxy-D-xylulose-5-phosphate synthase 1 (DXS1), key enzyme of the plastid isoprenoid pathway was present in the tomato PG. A recent report has indicated that both MenG and DXS1 are associated with PG via FBN and PDS in Chlamydomonas [49]. Chromoplast PG contained the carotenoid biosynthesis enzymes ZDS and LYCB as well as three other new candidates PSY1, PDS and CRTISO. Together these enzymes constitute the complete β-carotene biosynthesis pathway downstream of geranylgeranyl diphosphate. Based on the peptide count for PSY1, PDS, ZDS, and CRTISO, they are present at up to 12-fold higher levels in chromoplast PG than in chloroplast PG. However, the LYCB peptide count was almost the same in chromoplast PG and chloroplast PG (FIG 3; Table 1). The STRING analysis revealed that the enzymes of the carotenoid biosynthesis pathway form a distinct cluster 1 within the chromoplast PG proteome (FIG 4). Cluster 2 was enriched in enzymes involved in prenyl quinone metabolism and regulation and Cluster 3 in chloroplast senescence- and thylakoid dismantling-associated proteins.

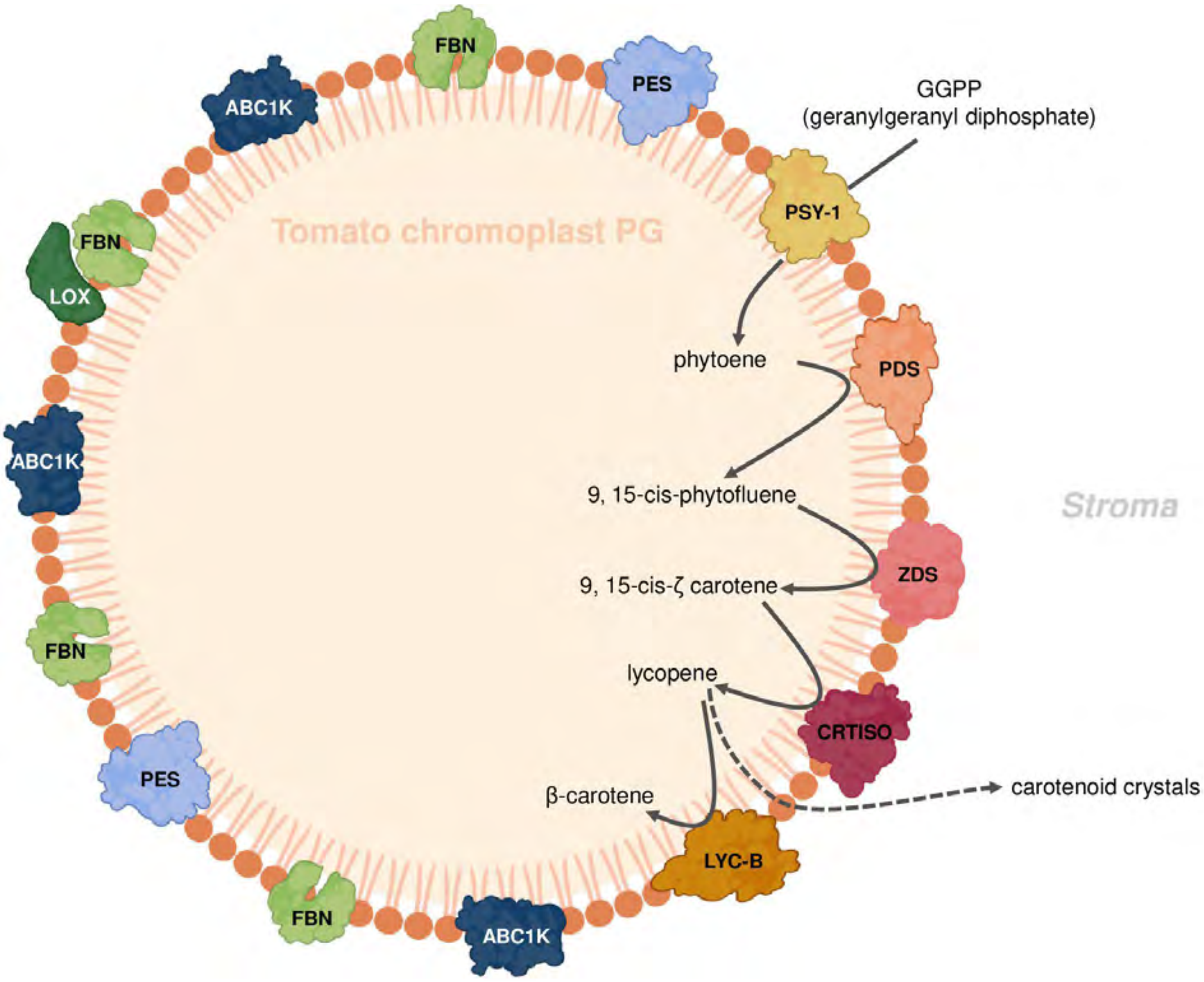

FIG 7| **Carotenoid biosynthetic pathway in tomato chromoplast PG.** Chromoplast plastoglobules recruit the carotenoid biosynthetic pathway enzymes: phytoene synthase 1 (PSY1), phytoene desaturase (PDS), z-carotene desaturase (ZDS), and carotenoid isomerase (CRTISO) and lycopene β-cyclase (LYC-β) to promote carotenoid biosynthesis. Lipoxygenase (LOX) may associate with PG, FBNs have structural functions and may contribute to carotenoid sequestration in PG. Phytyl ester synthase (PES) synthesizes phytyl esters and triacyl glycerol during thylakoid dismantling and Activity of BC1 complex kinase 1 (ABC1K1) is implicated in regulation of prenyl lipid metabolism.

Cluster 2 and 3 therefore identify two additional categories of functions that are critical during the chloroplast-to-chromoplast transition. The increased peptide counts of the first four β-carotene biosynthetic enzymes in chromoplast PG compared with chloroplast PG (FIG 3) indicates that PG recruit carotenoid biosynthetic enzymes and may turn them into a biosynthetic platform during carotenogenesis. Our lipidomic study reveals that lycopene and β-carotene become enriched in chromoplast PG during fruit ripening suggesting active contribution to biosynthesis (FIG 5). In agreement with an active role of PG in carotenoid metabolism in tomato, the chromoplast PG enzyme PALE YELLOW PETAL (PYP1) confers yellow flower pigmentation by carotenoid esterification [50]. With regard to PSY1, transient expression experiments provided evidence for PG localization in rice and Arabidopsis [51]. In addition, it was recently reported that bacterial phytoene synthase CrtB localised to PG and increased carotenoid levels when chloroplast-to-chromoplast transition was induced by CrtB expression [52]. Interestingly, a proteome study in the green algae *Dunaliella bardawil* revealed that β-carotene biosynthesis enzymes PDS, ZDS, and CRTISO were present in β-carotene-rich PG [53]. A recent study showed that PDS is one of the main protein components of Chlamydomonas PG [49]. Interestingly, carotenoid cleavage dehydrogenase 4 (CCD4) was identified only in chloroplast PG. PG protease PGM48, a chloroplast PG protease, interacts with CCD4 and degrades it during senescence [32]. Therefore, the presence of PGM48 in chloroplast and chromoplast PG might explain the disappearance of CCD4 during the chloroplast-to-chromoplast transition. We proposed a model for chromoplast PG hosting the carotenoid biosynthetic pathway. In the model, chromoplast PG function as a metabolic platform for carotenoid biosynthesis, especially for lycopene biosynthesis and accumulation (FIG 7). However, the data also indicate that carotenoid crystals accumulate a large proportion of lycopene and β-carotene (FIG S3). In summary, our data suggest that PG make an important contribution to fruit quality particularly to carotenoid accumulation.

3.6 References

1. Alba, R., Payton, P., Fei, Z., Mcquinn, R., Debbie, P., Martin, G.B., et al. (2005). Transcriptome and selected metabolite analyses reveal multiple points of ethylene control during tomato fruit development. *Plant Cell* 17**,** 2954-2965.

2. Bhuiyan, N.H., Friso, G., Rowland, E., Majsec, K., and Van Wijk, K.J. (2016). The Plastoglobule-Localized Metallopeptidase PGM48 Is a Positive Regulator of Senescence in Arabidopsis thaliana. *Plant Cell* 28**,** 3020-3037.

3. Bréhélin, C., Kessler, F., and Van Wijk, K.J. (2007). Plastoglobules: versatile lipoprotein particles in plastids. *Trends Plant Sci* 12**,** 260-266.

4. Camara, B., Hugueney, P., Bouvier, F., Kuntz, M., and Monéger, R. (1995). Biochemistry and molecular biology of chromoplast development. *Int Rev Cytol* 163**,** 175-247.

5. Davidi, L., Levin, Y., Ben-Dor, S., and Pick, U. (2015). Proteome analysis of cytoplasmatic and plastidic β-carotene lipid droplets in Dunaliella bardawil. *Plant Physiol* 167**,** 60-79.

6. Deruère, J., Römer, S., D'harlingue, A., Backhaus, R.A., Kuntz, M., and Camara, B. (1994). Fibril assembly and carotenoid overaccumulation in chromoplasts: a model for supramolecular lipoprotein structures. *Plant Cell* 6**,** 119-133.

7. Egea, I., Barsan, C., Bian, W., Purgatto, E., Latché, A., Chervin, C., et al. (2010). Chromoplast differentiation: current status and perspectives. *Plant Cell Physiol* 51**,** 1601-1611.

8. Espinoza-Corral, R., Heinz, S., Klingl, A., Jahns, P., Lehmann, M., Meurer, J., et al. (2019). Plastoglobular protein 18 is involved in chloroplast function and thylakoid formation. *J Exp Bot* 70**,** 3981-3993.

9. Espinoza-Corral, R., Herrera-Tequia, A., and Lundquist, P.K. (2021). Insights into topology and membrane interaction characteristics of plastoglobule-localized AtFBN1a and AtLOX2. *Plant Signal Behav* 16**,** 1945213.

10. Eugeni Piller, L., Besagni, C., Ksas, B., Rumeau, D., Bréhélin, C., Glauser, G., et al. (2011). Chloroplast lipid droplet type II NAD(P)H quinone oxidoreductase is essential for prenylquinone metabolism and vitamin K1 accumulation. *Proc Natl Acad Sci U S A* 108**,** 14354-14359.

11. Eugeni Piller, L., Glauser, G., Kessler, F., and Besagni, C. (2014). Role of plastoglobules in metabolite repair in the tocopherol redox cycle. *Front Plant Sci* 5**,** 298.

12. Gaude, N., Bréhélin, C., Tischendorf, G., Kessler, F., and Dörmann, P. (2007). Nitrogen deficiency in Arabidopsis affects galactolipid composition and gene expression and results in accumulation of fatty acid phytyl esters. *Plant J* 49**,** 729-739.

13. Gross, J., Cho, W.K., Lezhneva, L., Falk, J., Krupinska, K., Shinozaki, K., et al. (2006). A plant locus essential for phylloquinone (vitamin K1) biosynthesis originated from a fusion of four eubacterial genes. *J Biol Chem* 281**,** 17189-17196.

14. Hansmann, P., and Sitte, P. (1982). Composition and molecular structure of chromoplast globules of Viola tricolor. *Plant Cell Rep* 1**,** 111-114.

15. Heitz, T., Bergey, D.R., and Ryan, C.A. (1997). A gene encoding a chloroplast-targeted lipoxygenase in tomato leaves is transiently induced by wounding, systemin, and methyl jasmonate. *Plant Physiol* 114**,** 1085-1093.

16. Hiltbrunner, A., Bauer, J., Vidi, P.A., Infanger, S., Weibel, P., Hohwy, M., et al. (2001). Targeting of an abundant cytosolic form of the protein import receptor at Toc159 to the outer chloroplast membrane. *J Cell Biol* 154**,** 309-316.

17. Jarvis, P., and López-Juez, E. (2013). Biogenesis and homeostasis of chloroplasts and other plastids. *Nat Rev Mol Cell Biol* 14**,** 787-802.

18. Klinkenberg, J., Faist, H., Saupe, S., Lambertz, S., Krischke, M., Stingl, N., et al. (2014). Two fatty acid desaturases, STEAROYL-ACYL CARRIER PROTEIN Δ9-DESATURASE6 and FATTY ACID DESATURASE3, are involved in drought and hypoxia stress signaling in Arabidopsis crown galls. *Plant Physiol* 164**,** 570-583.

19. Lichtenthaler, H. (1968a). Plastoglobuli and fine structure of plastids. *Endeavour* 27**,** 144-+.

20. Lichtenthaler, H.K. (1968b). [Distribution and relative concentrations of lipophilic plastid quinones in green plants]. *Planta* 81**,** 140-152.

21. Lichtenthaler, H.K., and Sprey, B. (1966). Über die osmiophilen globulären Lipideinschlüsse der Chloroplasten. *Zeitschrift für Naturforschung B* 21**,** 690-697.

22. Lippold, F., Vom Dorp, K., Abraham, M., Hölzl, G., Wewer, V., Yilmaz, J.L., et al. (2012). Fatty acid phytyl ester synthesis in chloroplasts of Arabidopsis. *Plant Cell* 24**,** 2001-2014.

23. Liu, L., Shao, Z., Zhang, M., and Wang, Q. (2015). Regulation of carotenoid metabolism in tomato. *Mol Plant* 8**,** 28-39.

24. Lohmann, A., Schöttler, M.A., Bréhélin, C., Kessler, F., Bock, R., Cahoon, E.B., et al. (2006). Deficiency in phylloquinone (vitamin K1) methylation affects prenyl quinone distribution, photosystem I abundance, and anthocyanin accumulation in the Arabidopsis AtmenG mutant. *J Biol Chem* 281**,** 40461-40472.

25. Lois, L.M., Rodríguez-Concepción, M., Gallego, F., Campos, N., and Boronat, A. (2000). Carotenoid biosynthesis during tomato fruit development: regulatory role of 1-deoxy-D-xylulose 5-phosphate synthase. *Plant J* 22**,** 503-513.

26. Lundquist, P.K., Poliakov, A., Bhuiyan, N.H., Zybailov, B., Sun, Q., and Van Wijk, K.J. (2012). The functional network of the Arabidopsis plastoglobule proteome based on quantitative proteomics and genome-wide coexpression analysis. *Plant Physiol* 158**,** 1172-1192.

27. Lundquist, P.K., Poliakov, A., Giacomelli, L., Friso, G., Appel, M., Mcquinn, R.P., et al. (2013). Loss of plastoglobule kinases ABC1K1 and ABC1K3 causes conditional degreening, modified prenyl-lipids, and recruitment of the jasmonic acid pathway. *Plant Cell* 25**,** 1818-1839.

28. Manara, A., Dalcorso, G., Guzzo, F., and Furini, A. (2015). Loss of the Atypical Kinases ABC1K7 and ABC1K8 Changes the Lipid Composition of the Chloroplast Membrane. *Plant Cell Physiol* 56**,** 1193-1204.

29. Manara, A., Dalcorso, G., Leister, D., Jahns, P., Baldan, B., and Furini, A. (2014). AtSIA1 AND AtOSA1: two Abc1 proteins involved in oxidative stress responses and iron distribution within chloroplasts. *New Phytol* 201**,** 452-465.

30. Martinis, J., Glauser, G., Valimareanu, S., and Kessler, F. (2013). A chloroplast ABC1-like kinase regulates vitamin E metabolism in Arabidopsis. *Plant Physiol* 162**,** 652-662.

31. Martinis, J., Kessler, F., and Glauser, G. (2011). A novel method for prenylquinone profiling in plant tissues by ultra-high pressure liquid chromatography-mass spectrometry. *Plant Methods* 7**,** 23.

32. Nogueira, M., Mora, L., Enfissi, E.M., Bramley, P.M., and Fraser, P.D. (2013). Subchromoplast sequestration of carotenoids affects regulatory mechanisms in tomato lines expressing different carotenoid gene combinations. *Plant Cell* 25**,** 4560-4579.

33. Pozueta-Romero, J., Rafia, F., Houlné, G., Cheniclet, C., Carde, J.P., Schantz, M.L., et al. (1997). A ubiquitous plant housekeeping gene, PAP, encodes a major protein component of bell pepper chromoplasts. *Plant Physiol* 115**,** 1185-1194.

34. Pralon, T., Collombat, J., Pipitone, R., Ksas, B., Shanmugabalaji, V., Havaux, M., et al. (2020). Mutation of the Atypical Kinase ABC1K3 Partially Rescues the PROTON GRADIENT REGULATION 6 Phenotype in Arabidopsis thaliana. *Front Plant Sci* 11**,** 337.

35. Pralon, T., Shanmugabalaji, V., Longoni, P., Glauser, G., Ksas, B., Collombat, J., et al. (2019). Plastoquinone homoeostasis by Arabidopsis proton gradient regulation 6 is essential for photosynthetic efficiency. *Commun Biol* 2**,** 220.

36. Rottet, S., Devillers, J., Glauser, G., Douet, V., Besagni, C., and Kessler, F. (2016). Identification of Plastoglobules as a Site of Carotenoid Cleavage. *Front Plant Sci* 7**,** 1855.

37. Shanmugabalaji, V., Grimm, B., and Kessler, F. (2020). Characterization of a Plastoglobule-Localized SOUL4 Heme-Binding Protein in Arabidopsis thaliana. *Front Plant Sci* 11**,** 2.

38. Shumskaya, M., Bradbury, L.M., Monaco, R.R., and Wurtzel, E.T. (2012). Plastid localization of the key carotenoid enzyme phytoene synthase is altered by isozyme, allelic variation, and activity. *Plant Cell* 24**,** 3725-3741.

39. Singh, D.K., Maximova, S.N., Jensen, P.J., Lehman, B.L., Ngugi, H.K., and Mcnellis, T.W. (2010). FIBRILLIN4 is required for plastoglobule development and stress resistance in apple and Arabidopsis. *Plant Physiol* 154**,** 1281-1293.

40. Singh, D.K., and Mcnellis, T.W. (2011). Fibrillin protein function: the tip of the iceberg? *Trends Plant Sci* 16**,** 432-441.

41. Steinmüller, D., and Tevini, M. (1985). Composition and function of plastoglobuli : I. Isolation and purification from chloroplasts and chromoplasts. *Planta* 163**,** 201-207.

42. Szklarczyk, D., Franceschini, A., Wyder, S., Forslund, K., Heller, D., Huerta-Cepas, J., et al. (2015). STRING v10: protein-protein interaction networks, integrated over the tree of life. *Nucleic Acids Res* 43**,** D447-452.

43. Szklarczyk, D., Gable, A.L., Nastou, K.C., Lyon, D., Kirsch, R., Pyysalo, S., et al. (2021). The STRING database in 2021: customizable protein-protein networks, and functional characterization of user-uploaded gene/measurement sets. *Nucleic Acids Res* 49**,** D605-d612.

44. Van Wijk, K.J., and Kessler, F. (2017). Plastoglobuli: Plastid Microcompartments with Integrated Functions in Metabolism, Plastid Developmental Transitions, and Environmental Adaptation. *Annu Rev Plant Biol* 68**,** 253-289.

45. Vidi, P.A., Kanwischer, M., Baginsky, S., Austin, J.R., Csucs, G., Dörmann, P., et al. (2006). Tocopherol cyclase (VTE1) localization and vitamin E accumulation in chloroplast plastoglobule lipoprotein particles. *J Biol Chem* 281**,** 11225-11234.

46. Vishnevetsky, M., Ovadis, M., and Vainstein, A. (1999). Carotenoid sequestration in plants: the role of carotenoid-associated proteins. *Trends Plant Sci* 4**,** 232-235.

47. Wang, L., Patena, W., Van Baalen, K.A., Xie, Y., Singer, E.R., Gavrilenko, S., et al. (2022). A Chloroplast Protein Atlas Reveals Novel Structures and Spatial Organization of Biosynthetic Pathways. *bioRxiv***,** 2022.2005.2031.493820.

48. Youssef, A., Laizet, Y., Block, M.A., Maréchal, E., Alcaraz, J.P., Larson, T.R., et al. (2010). Plant lipid-associated fibrillin proteins condition jasmonate production under photosynthetic stress. *Plant J* 61**,** 436-445.

49. Ytterberg, A.J., Peltier, J.B., and Van Wijk, K.J. (2006). Protein profiling of plastoglobules in chloroplasts and chromoplasts. A surprising site for differential accumulation of metabolic enzymes. *Plant Physiol* 140**,** 984-997.

50. Zhang, R., Wise, R.R., Struck, K.R., and Sharkey, T.D. (2010). Moderate heat stress of Arabidopsis thaliana leaves causes chloroplast swelling and plastoglobule formation. *Photosynth Res* 105**,** 123-134.

4. A quantitative method to measure geranylgeranyl diphosphate (GGPP) and geranylgeranyl monophosphate (GGP) in tomato (Solanum lycopersicum) fruit

Wayne Zita[1], Venkatasalam Shanmugabalaji[1], Miguel Ezquerro[2], Manuel Rodriguez-Concepcion[2], Felix Kessler[1], Gaetan Glauser[3*]
Affiliations:
1 Plant Physiology Laboratory, University of Neuchâtel, 2000 Neuchâtel, Switzerland
2 Institute for Plant Molecular and Cell Biology (IBMCP), CSIC-Universitat Politècnica de València, 46022 Valencia, Spain
3 Neuchâtel Platform of Analytical Chemistry, University of Neuchâtel, 2000 Neuchâtel, Switzerland
*Corresponding author: gaetan.glauser@unine.ch

4.1 Abstract

Background

Isoprenoids are a very large class of metabolites playing a key role in plant physiological processes such as growth, stress resistance, fruit flavor, and color. In chloroplasts and chromoplasts, the diterpene compound geranylgeranyl diphosphate (GGPP) is the metabolic precursor required for the biosynthesis of tocopherols, plastoquinones, phylloquinone, chlorophylls, and carotenoids. Despite its key role for the plant metabolism, reports on GGPP physiological concentrations *in planta* have been extremely scarce.

Results

In this study, we developed a method to quantify GGPP and its hydrolysis product geranylgeranyl monophosphate (GGP) from tomato fruit, using ultra-high performance liquid chromatography coupled with tandem mass spectrometry (UHPLC-MS/MS). Quantification was done by external calibration and the method was validated in terms of specificity, precision, accuracy, and detection and quantitation limits. We further demonstrate the validity of our approach by analysing GGPP contents in the ripe fruits of wild-type tomatoes and mutants defective in GGPP production. Finally, we also show that the sample preparation is key to prevent GGPP hydrolysis and mitigate its conversion to GGP.

Conclusion

Our study provides an efficient tool to investigate the metabolic fluxes required for GGPP supply and consumption in tomato fruit.

4.2 Background

In plants, isoprenoids (terpenes or terpenoids) are a large family of primary and secondary metabolites essential for a multitude of physiological and biological functions [1, 2]. Geranylgeranyl diphosphate

(GGPP) is a C20 diterpene synthesized through the head-to-tail condensation of three isopentenyl diphosphate (IPP) groups and the head dimethylallyl diphosphate (DMAPP) by the geranylgeranyl diphosphate synthase (GGPPS) [3]. Plant cells synthesise IPP and DMAPP using the mevalonic acid (MVA) pathway in the cytosol or the methylerythritol 4-phosphate (MEP) pathway in plastids, where GGPP is most needed (FIG 1) [2, 3]. Plastidial GGPP is a key component in plants as it is required for the biosynthesis of many photosynthesis-related terpenoids such as carotenoids, chlorophylls, tocopherols, phylloquinone, and plastoquinones [2-4]. MEP-derived GGPP is also used for the production of gibberellins and diterpenes (FIG 1). In tomato (*Solanum lycopersicum*), five genes encode GGPPS-like enzymes. Among them, paralogs SlGGPPS1/SlG1 (Solyc11g011240), SlGGPPS2/SlG2 (Solyc04g079960) and SlGGPPS3/SlG3 (Solyc02g085700) have been localized in plastids and are required for GGPP biosynthesis [5, 6]. A recent study concluded that SlG2 and SlG3 are the main isoforms supplying GGPP in shoot tissues. Consistently, ripe fruit from *slg2* and *slg3* tomato knockouts showed decreased levels of lycopene, the red carotenoid that gives the characteristic colour to tomatoes [7].

Despite its central role in plants and other organisms, there is no commonly accepted method to measure GGPP at physiological levels. GGPP measurement represents a challenge due to its amphiphilic nature [8]. GGPP is not volatile, which makes its direct analysis by gas chromatography or gas chromatography-mass spectrometry impossible. In addition, the presence of phosphate groups complicates separation by conventional reversed-phase HPLC methods and may require ion-pairing chromatography or pre-column derivatization of the sample [9]. In addition, GGPP as an essential biosynthetic precursor in plant tissues is rapidly converted by enzymes to downstream secondary metabolites, complicating its detection. For these reasons, in most studies, instead of directly analysing GGPP, researchers have measured its downstream products such as carotenoids, quinones or other derived terpenoids [5, 6, 10, 11]. While some studies have proposed methods to detect GGPP in human plasma and cells using HPLC-MS or HPLC-fluorescence detection [13-15], we are not aware of any validated method able to measure GGPP physiological levels in plants. McCaskill et Croteau reported a complex and time-consuming procedure for the isolation and quantification of radiolabelled intermediates of the MVA pathway by ion-pairing chromatography coupled to radiodetection [12]. Recently, Ma et al. reported endogenous levels of GGPP in Arabidopsis leaves and inflorescences by UHPLC-MS/MS, however, information on the methodology employed was limited [16].

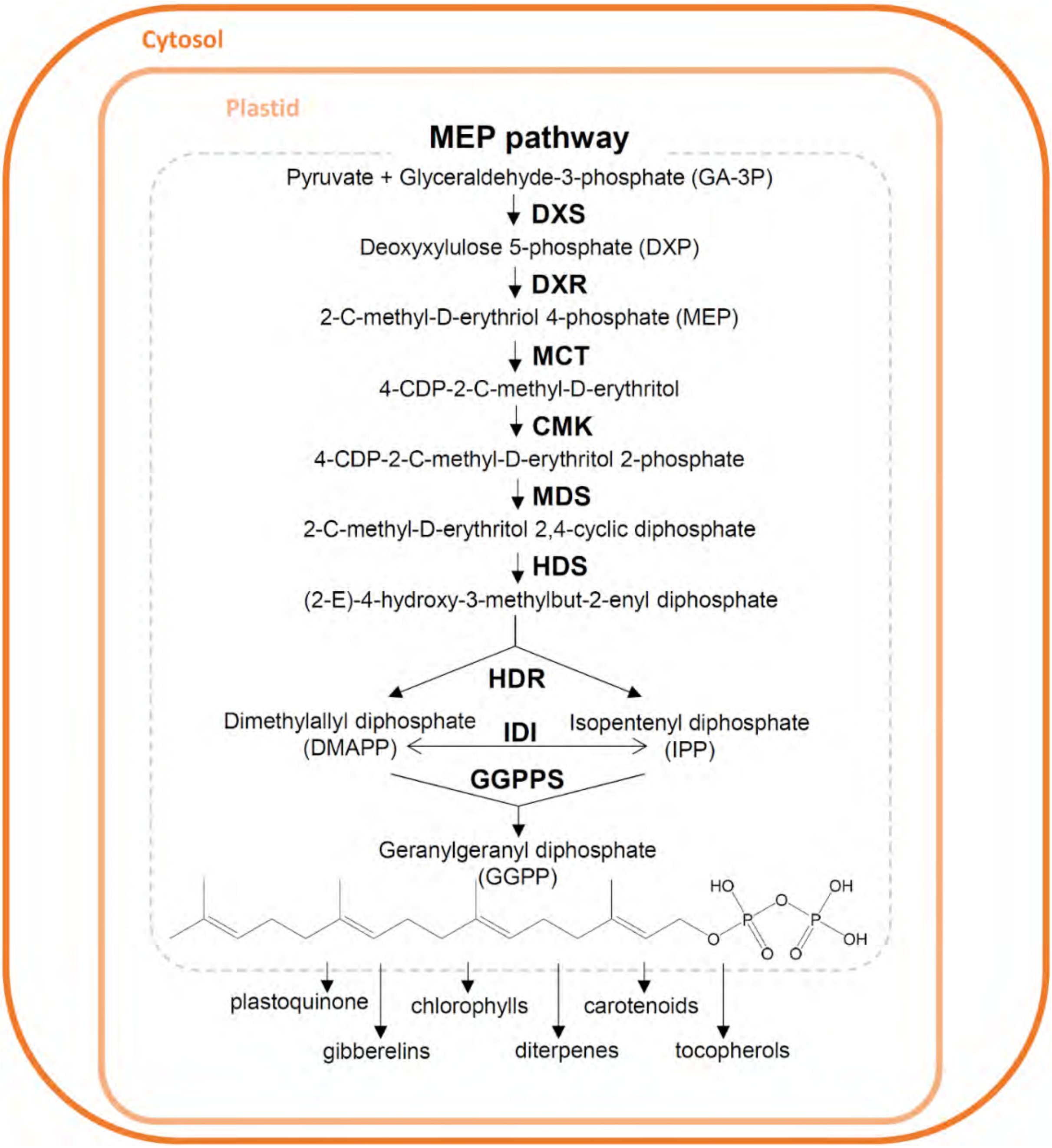

FIG 1| **Schematic representation of the MEP pathway**. Here, enzymes required for the biosynthesis of GGPP are represented. Enzymes: 1-deoxy-D-xylulose-5-phosphate synthase (DXS), 1-deoxy-D-xylulose-5-phosphate reductoisomerase (DXR), 4-(cytidine 5′-diphospho)-2-C-methyl-D-erythritol synthase (MCT), 4-(cytidine 5′-diphospho)-2-C-methyl-D-erythritol kinase (CMK), 2-C-methyl-D-erythritol 2,4-cyclodiphosphate synthase (MDS), 4-hydroxy-3-methylbut-2-enyl diphosphate synthase (HDS), 4-hydroxy-3-methylbut-2-enyl diphosphate reductase (HDR), isopentenyl diphosphate isomerase (IDI), geranylgeranyl diphosphate synthase (GGPPS).

In this work, we developed a simple but efficient method to measure GGPP and its hydrolysis product GGP in tomato fruit. The method is based on a single extraction step after quenching and lyophilisation of the fruits followed by reversed-phase UHPLC-MS/MS at alkaline pH. The method was validated according to standard guidelines and applied to the analysis of wild-type and GGPPS-defective *slg2* and *slg3* tomato fruits.

4.3 Results and Discussion

4.3.1 Optimisation of HPLC-MS/MS conditions

Due to the concomitant presence of a hydrophilic head (phosphate groups) and a lipophilic tail on their structures, there is no clearly defined scheme for the chromatographic separation of GGPP and GGP. Our aim was to find appropriate separation conditions without the need for ion-pairing or derivatization agents, which may reduce detection sensitivity and lengthen the extraction process. During our trials, we found that hydrophilic interaction chromatography (HILIC) was not conclusive and thus focused on reverse-phase chromatography. Using an ethylene-bridged C18 column with a wide pH range, we observed a very strong dependency on the pH: at pH 2.7, using 0.05% formic acid as an additive in the aqueous mobile phase, the peaks for GGPP and GGP were extremely wide and almost indistinguishable from the baseline (FIG 2A and 2D). By increasing the pH to 5.8 using a combination of 20 mM ammonium acetate and 0.01% acetic acid, the peak shapes improved but were still not acceptable to allow reliable quantitation (FIG 2B and 2E). At pH 10.0, using 0.05% NH_4OH as additive, the peaks became much thinner, although a slight fronting persisted (FIG 2C and 2F). Adding 0.05% NH_4OH to both aqueous and organic phases minimized peak fronting and enabled sharp and symmetrical peaks for both GGPP (RT 2.56 min, composition at elution 22.6%) and GGP (RT 3.20 min, composition at elution 28.4%) (FIG 3). Acetonitrile as an organic solvent gave narrower peaks and slightly higher signal-to-noise ratios than methanol and was therefore preferred. The effect of the injection volume was also investigated. Using an injection solvent composed of 50-80% ACN, we found that peak distortion started to occur above 2 µL injections. We thus selected an injection volume of 2 µL as the best compromise between peak shape and sensitivity. Noteworthily, these conditions are valid for an Acquity UPLC system with a fixed loop injector in the partial loop with needle overfill mode. Preliminary assays using identical injection parameters on a flow-through needle (FTN) autosampler indeed revealed some peak distortion and further optimisation would be required when using this type of autosampler.

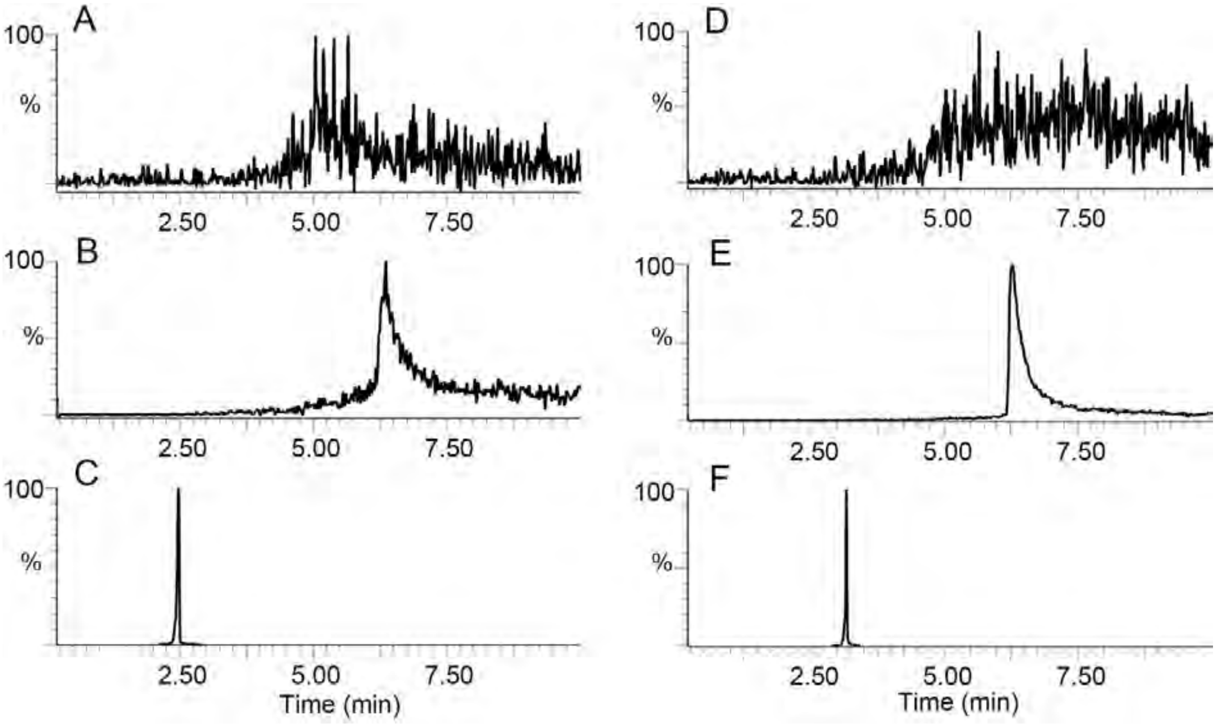

FIG 2| **Chromatograms for GGPP and GGP at different pHs using an ethylene-bridged C18 column**. A and D: Chromatograms for GGPP and GGP at pH 2.7 (formic acid 0.05%); B and E: chromatograms for GGPP and GGP at pH 5.8 (acetic acid 0.01% + 20 mM ammonium acetate); C and F: Chromatograms for GGPP and GGP at pH 10.0 (ammonia 0.05%). The organic mobile phase was acetonitrile in all cases.

Mass spectrometric detection was performed on a triple quadrupole instrument (TQ-XS) of the last generation. We tested electrospray (ESI) and atmospheric pressure chemical ionization (APCI) sources, both in positive and negative ionisation modes. Not surprisingly, ESI and APCI positive ionization gave no detectable peak. By contrast, the negative mode generated strong signals thanks to deprotonation of the phosphate group. Negative ESI was largely superior to APCI, with signals for GGPP and GGP approximately 10 and 15-fold higher, respectively. We tested different parameters of the ESI source, namely capillary voltage, source temperature, desolvation gas flow and temperature, nebulisation gas flow and cone gas flow. Only capillary voltage, desolvation gas temperature and cone gas flow had a significant impact on the signal-to-noise ratios, with optimal values at -2 kV, 500°C and 350 L/h, respectively. After having optimized source conditions, we determined MRM parameters. We found that GGPP readily lost a phosphate group in the MS source giving a prominent m/z 369.2 ion, corresponding to deprotonated GGP. The $(M-H)^-$ ion at m/z 449 was also present, albeit at a lower intensity. We thus selected m/z 369.2 > 79.0 as the quantitative transition for both GGPP and GGP, with no risk of interference between them since the two molecules were well separated in the chromatographic dimension (FIG 3). One and two additional qualitative transitions were found for GGP (m/z 369.2 > 97.0) and GGPP (m/z 369.2 > 97.0 and 449.2 > 97.0), respectively. Cone voltage and collision energies were tuned for maximal sensitivity and under optimized conditions, injections as low as 500 and 100 fg on column could be detected for GGPP and GGP, respectively.

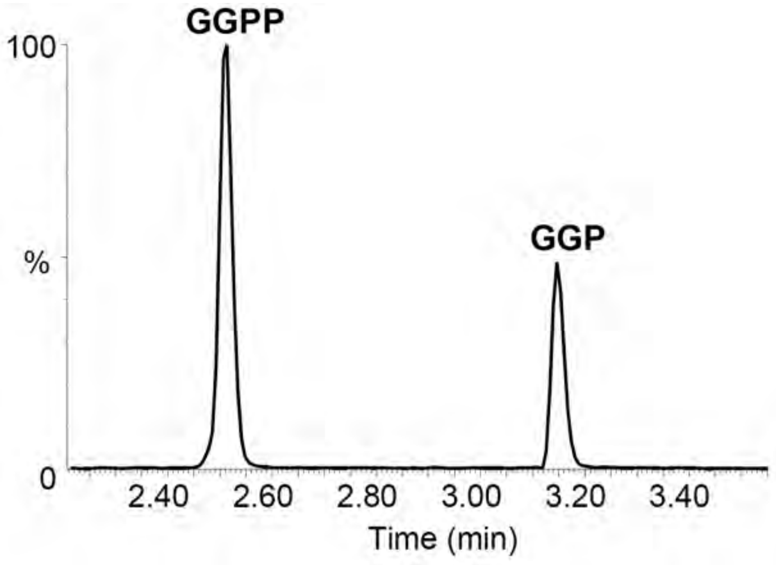

FIG 3| **Representative chromatograms for standard solutions of GGPP and GGP**. The concentrations of GGPP and GGP were 10 ng/mL and 1 ng/mL, respectively, both in acetonitrile:water (50:50, v/v). The MRM transition was 369.2 > 79.0 for both molecules. A gradient of H_2O + 0.05% NH_4OH and acetonitrile + 0.05% NH_4OH was applied.

4.3.2 Sample preparation

Once we had an analytical method which was able detect trace levels of GGPP and GGP, we attempted to optimize their extraction from plant tissues. We used wild-type tomato fruits and first tested different extraction solvents: acetonitrile:water (80:20, v/v), ethylacetate (in this particular case with evaporation and reconstitution in acetonitrile:water (80:20, v/v) since ethylacetate was incompatible as an injection solvent), methanol and 70% methanol:water:NH4OH (70:30:0.05, v/v/v) (FIG 4). Unanticipatedly, results were very different, with acetonitrile:water (80:20, v/v) being the solvent which seemed to best preserve GGPP and ethylacetate the one which led to highest conversion to GGP (possibly due to the evaporation step). Furthermore, acetonitrile:water (80:20, v/v) was the solvent which provided the best extraction yield, determined as the sum of GGPP and GGP peaks. Based on these considerations, we selected acetonitrile:water (80:20, v/v) as the solvent of choice for GGPP extraction.

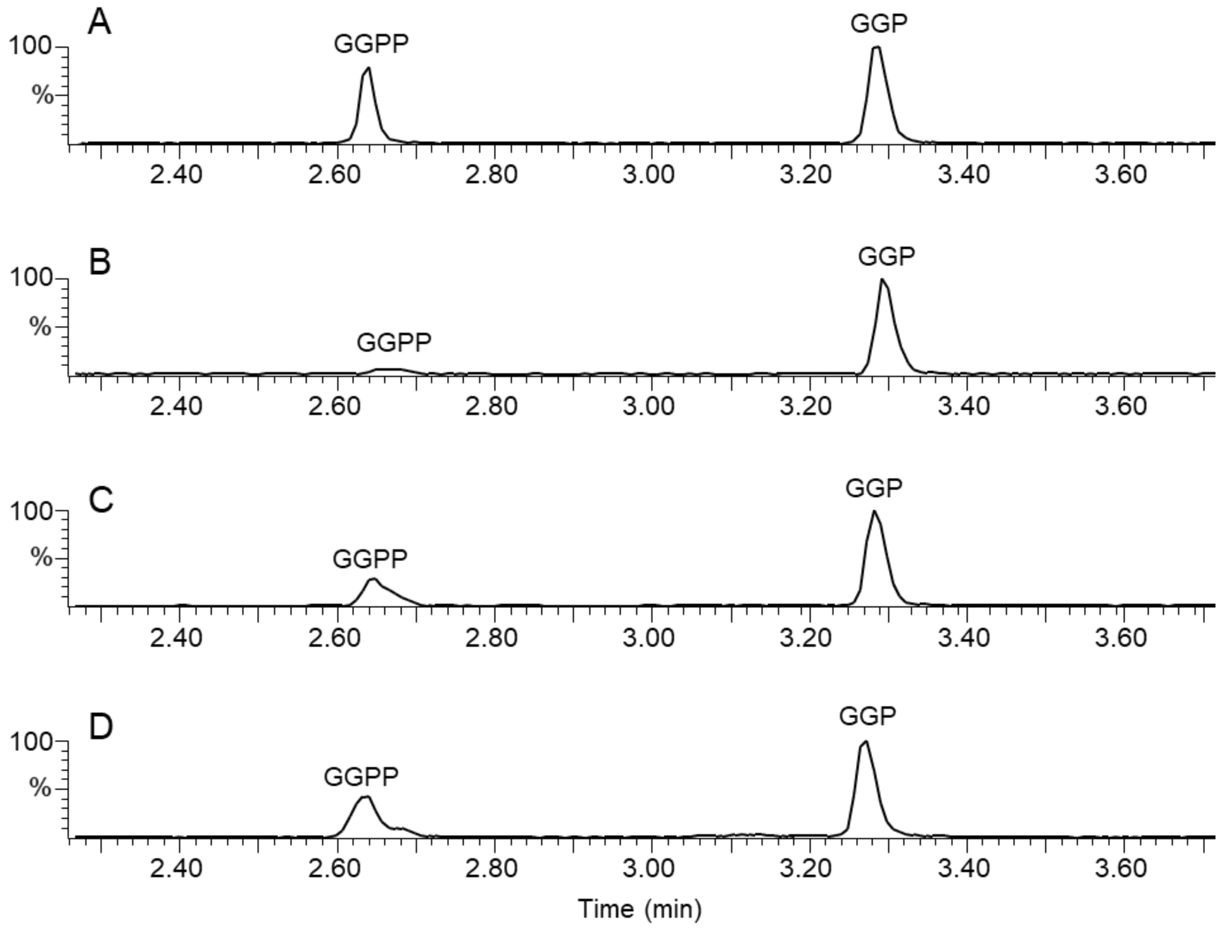

FIG 4| **Chromatograms for wild-type tomato fruits extracted with different solvents or solvent mixtures**. A: acetonitrile:water (80:20, v/v); B: ethylacetate; C: methanol; D: methanol:water:NH_4OH (70:30:0.05, v/v/v). For this experiment, fruits were not quenched in liquid N_2 prior to extraction.

The observation that different solvents may lead to different rates of conversion from GGPP to GGP during extraction prompted us to test whether the typical sample preparation steps of quenching, drying and solvent evaporation could also have an impact on the GGPP/GGP ratio. Using acetonitrile:water (80:20, v/v) as extraction solvent in all cases, we observed that quenching the fresh fruits in liquid nitrogen prior to grinding and extraction had a significant effect in preserving GGPP (FIG 5; t-test calculated on GGPP/GGP ratios, n= 3, p=0.002). By contrast, after quenching there was no difference if frozen or lyophilised tissues were used (t-test, n=3, p=0.12). It should however be noted that, from a practical viewpoint, we found it much easier to grind lyophilised than fresh tissues using stainless steel beads in a tissue lyser. In addition, since GGPP and GGP have phosphate groups which may bind to metal cations, we tested the use of metal versus glass beads and found no difference between them. Finally, evaporation at 40°C of the extraction solvent followed by reconstitution in the same solvent (80% acetonitrile) caused partial degradation of GGPP into GGP. Taken together, we thus recommend to quench the fruits as soon as they have been collected, lyophilise them as it makes subsequent steps easier, and avoid any evaporation during sample preparation to best preserve GGPP.

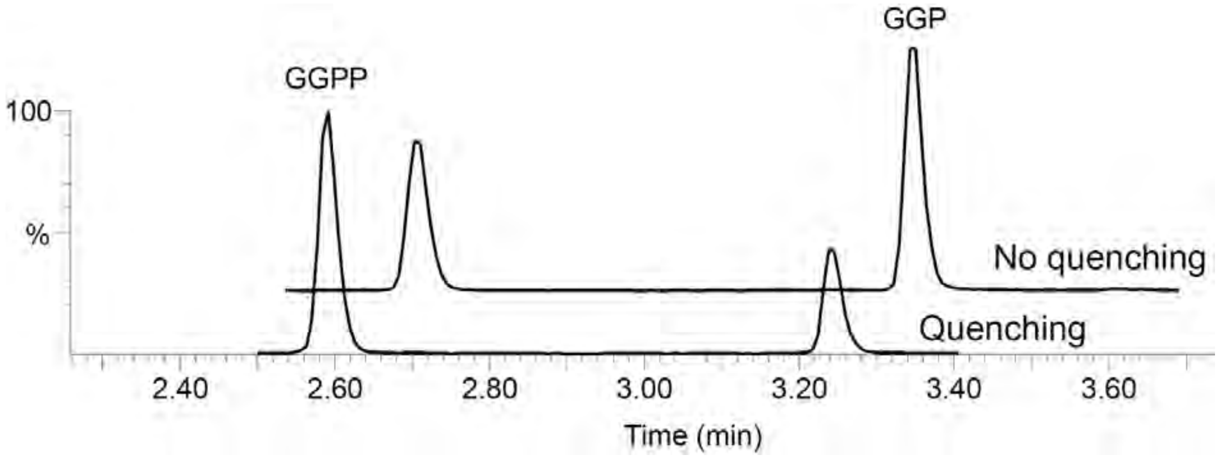

FIG 5| **Chromatograms for wild-type tomato fruits submitted to quenching in liquid N_2 immediately after sample collection or direct extraction in acetonitrile:water (80:20, v/v).**

4.3.3 Method calibration and validation

Spiking experiments with known concentrations of GGPP and GGP in plant extracts showed that matrix effects were negligible in tomato fruits. Therefore, the external calibration approach was selected and further evaluated during the method validation. Using linear calibration models, the r^2 were > 0.99 for both GGPP and GGP and back-calculated concentrations were always within +/- 10% of the true concentrations (Supplemental tables S1 and S2). Specificity was excellent in fruit samples (FIG 4 and 5). Precision and accuracy were determined at 4 different concentrations which were expected to cover the physiological concentrations in different mutants. RSD% (for precision) and deviations (for accuracy) always fell within 10% and 90-115%, respectively (Table 1). The fact that accuracy values were within acceptable ranges for both GGPP and GGP indicate that no significant conversion from GGPP to GGP occurred during the sample preparation process. The method's limits of quantitation were 1 ng/ml (or 50 ng/g DW) and 0.17 ng/mL (or 8.5 ng/g DW) for GGPP and GGP, respectively. The limits of detection were 0.2 ng/mL and 0.03 ng/mL for GGPP and GGP, respectively. Taken together, these results demonstrate that the developed method is reliable and can be applied to the analysis of tomato fruits from various backgrounds.

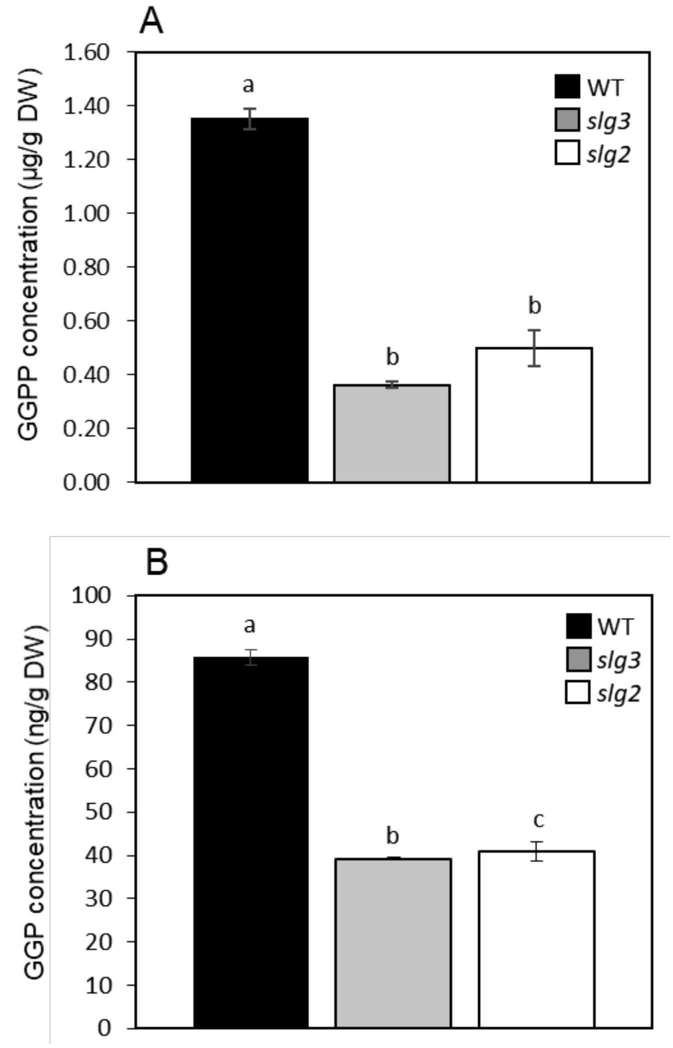

FIG 6| **GGPP and GGP levels in *slg2* and *slg3* compared to WT tomato fruit**. A: GGPP absolute concentrations in WT, *slg2*, *slg3* B+10 fruits; B: GGP absolute concentrations in WT, *slg2*, *slg3* B+10 fruits. Data are the means of three to four biological replicates (± SE). a-c: significant differences between genotypes as detected by one-way ANOVA followed by post-hoc tests ($p<0.05$).

Table 1: Precision and accuracy values obtained for GGPP and GGP in tomato fruits. See the methods section for details about the actual concentrations corresponding to C1-C4.

	Precision (RSD%, n=4)				Accuracy (%, n=4)			
	C1	C2	C3	C4	C1	C2	C3	C4
GGPP	9.8	6.6	7.6	4.7	105%	99%	90%	114%
GGP	8.9	6.9	3.3	2.1	95%	93%	92%	90%

4.3.4 Application to tomato fruits

To further validate our approach, we applied the developed method to the analysis of fruits from three "Micro-Tom" tomato genotypes: WT and two knockout mutants which lack one functional GGPPS (*slg2* and *slg3*). Fruits from these lines were tagged in the plant at the breaker (B) stage, i.e, when the first visual symptoms of colour change due to chlorophyll loss and carotenoid accumulation were visually detected. Ten days later, all fruits had acquired the characteristic red colour of ripe fruit. At this point (B+10), fruits were collected from the plant and pericarp samples were snap-frozen in liquid nitrogen for subsequent lyophilisation. Levels of GGPP and GGP were significantly reduced in lyophilised fruit samples from *slg2* and *slg3* samples as compared to the WT (FIG 6). Regarding GGPP levels specifically, WT, *slg2* and *slg3* contained 1.35, 0.50 and 0.36 µg/g DW, respectively. One-way ANOVA revealed significant differences between genotypes ($F_{2,7}$ = 181.77, p<0.001). Moreover, a Holm-Sidak post-hoc test showed that the levels of GGPP were significantly higher in *slg2* than in *slg3 (p = 0.037)*. This is consistent with the reported phenotype of carotenoid accumulation in these mutants, as described by Barja et al. 2021[7]. These findings are interesting as they shed light on the role of different GGPPS paralogs in tomato fruit ripening [7]. Our results hence confirm the predominant role of SlG3 for the synthesis of GGPP required for the burst of carotenoids that changes the fruit colour from green to red when ripe. GGP levels were much lower than those of GGPP, with 0.087, 0.041 and 0.039 µg/g DW in the WT, *slg2* and *slg3*, respectively. This represents less than 10% of the actual GGPP levels and confirms that our method is gentle enough to prevent GGPP hydrolysis to a large extent.

4.4 Conclusion

Our study establishes appropriate separation and detection conditions for GGPP and GGP without the need for ion-pairing or derivatization agents which may impact sensitivity and lengthen the extraction process. We show that reversed-phase chromatography at alkaline pH coupled to tandem mass spectrometry provides good peak shapes and sufficient sensitivity to enable the precise and accurate quantification of low levels of GGPP and GGP *in planta*. We applied our method to the analysis of ripe fruit from wild-type tomato and two knockout mutants of the main plastid-localised GGPPS isoforms. As expected, levels in the mutants were significantly lower than in the wild-type, thereby confirming the validity of our approach. Our method will be useful to identify new proteins and enzyme functions in a panoply of GGPP-dependent isoprenoid biosynthetic pathways with a view to improving tomato fruit quality and nutrition. In addition, the method may be extended to the detection of other prenyldiphosphates from the terpenoid pathway such as GPP and FPP to monitor new biotechnological approaches for plant and fruit fortification.

4.5 Methods

4.5.1 Chemicals

GGPP and GGP were purchased from Echelon Biosciences and Larodan respectively. For HPLC-MS analyses, milli-Q water, LC-MS grade acetonitrile from VWR, and LC-MS grade NH_4OH solution (25%) from Merck were used. For sample preparation, HPLC grade acetonitrile from Merck (Supelco) was employed.

4.5.2 Plants

Tomato used in this study was *Solanum lycopersicum*, cv. Micro-Tom. Three genetic backgrounds were used, the wild-type (WT), as well as the CRISPR mutant alleles *slg2-1* and *slg3-1* [7]. Plants were grown in a chamber under controlled conditions (14 h under white light - 150 µmol m^{-2} s^{-1} - at 25 ± 1 °C and 10 h in the dark at 22 ± 1 °C). Fruits were tagged at the breaker (B) stage, harvested at B+10 and quenched immediately in liquid nitrogen according to [17]. The samples were then stored at -80°C until lyophilisation in a Labconco benchtop freeze-dryer.

4.5.3 Sample preparation

GGPP and GGP were extracted from lyophilised tomato fruits pericarp. Twenty mg of dry tissues were ground with 3 stainless steel UFO-beads (3.5 mm diameter) in a 2.0 mL microcentrifuge tube. Then, fifty volumes of acetonitrile:water (80:20, v/v) were added and the mixture was shaken in a tissue lyser (TissueLyser LT, QIAGEN) with a frequency of 50 Hz for 5 min. The homogenate was sonicated at 60 Hz for 1 min and centrifuged at 16’000 x g for 10 min at room temperature. After centrifugation, 200 µL of supernatant was collected and transferred to glass vials for HPLC-MS/MS analysis.

4.5.4 HPLC-MS/MS conditions

GGPP and GGP analysis was performed on a binary pump Acquity UPLC connected to a TQ-XS triple quadrupole (Waters), both controlled by MassLynx 4.2 (Waters). An Acquity UPLC BEH C18 column (2.1x50 mm, 1.7 µm, Waters) was used for the separation. The flow rate was set to 0.4 mL/min. Mobile phases consisted of milli-Q water + 0.05% NH_4OH (phase A) and acetonitrile (ACN) + 0.05% NH_4OH (phase B). The gradient started at 5% phase B and increased linearly to 41% B in 4.0 min, then to 100%

B in 0.5 min. At the end of the run, a 2.0 min wash at 100% B for 2.0 min followed by re-equilibration at 5% B for 2.0 min was implemented. The column was maintained at 25°C. The injection volume was of 2 µL (fixed loop injector, partial loop with needle overfill mode) and the autosampler temperature was kept at 15°C. The strong needle wash was a mix of ACN:H_2O (90:10, v/v) and the weak needle wash a mix of ACN:H_2O (10:90, v/v).

The mass spectrometer was operated in electrospray negative ionisation using a capillary voltage of -2 kV, a source temperature of 150°C, a desolvation temperature of 500°C, a desolvation gas flow of 1000 L/h, a cone gas flow of 350 L/h, and a nebuliser gas flow of 7 bars. The StepWave was set to normal transmission values. The multiple reaction monitoring (MRM) mode was employed to maximize sensitivity. MRM transitions for both GGPP and GGP were 369.2 > 79.0 (quantitative, Q) and 369.2 > 97.0 (qualitative, q1). For GGPP, an additional qualitative transition (q2, 449.2 > 79.0, q2) was set. Cone and collision energy voltages for Q, q1 and q2 transitions were 15 and 21 V, 15 and 19 V, and 10 and 20 V, respectively. The dwell time was fixed to 136 ms. The HPLC flow was diverted to the waste from 0.0-2.25 min, and from 3.8 min to the end of the run.

4.5.5 Quantification and method validation

Quantification was done by external calibration using standard concentrations in acetonitrile:water (50:50, v/v) at 1, 2, 4, 8, 16 and 32 ng/mL for GGPP, and 0.125, 0.25, 0.5, 1, 2 and 4 ng/mL for GGP. A linear calibration with the origin excluded and weighted by 1/x was applied. The response function of the calibration curve was assessed by back-calculating the concentrations based on the linear model and accepting it if the deviation was within 15% for all calibration points. Selectivity was evaluated by analysing non-spiked samples and samples spiked with a mixture of GGPP and GGP at 15 and 3 ng/mL, respectively. Intra-day precision and accuracy were expressed as percentage of relative standard deviation (%RSD) and percentage of deviation from true values, respectively, and were determined from samples of the G3 mutant spiked at 1, 3, 6 and 12 ng/mL (respectively C1-C4) for GGPP and 0.17, 0.5, 1, and 2 ng/mL (respectively C1-C4) for GGP (n=4 for each concentration). Since GGPP and GGP are constitutively present in plants, including the G3 mutant, unspiked samples were also analyzed and their concentrations subtracted from those of the spiked samples. Limits of quantification (LOQ) were determined as the smallest spiked concentration which gave precision and accuracy values within 15% and 80-120%, respectively. The instrumental detection limit was evaluated on standard solutions which gave signal-to-noise ratios of 3. Data processing was performed in TargetLynx XS (Waters).

4.5.6 Statistics

All data in this study were the means of two independent experiments and the result of three to four technical or biological replicates, except the comparison of extraction solvents for which only two technical replicates were performed. No data were excluded from the analysis. The results were analyzed and compared for statistical differences by a two-sample, unequal variance (heteroscedastic) Student's t-test (Excel 2016), or by one-way ANOVA followed by Holm-Sidak post-hoc tests for pair-wise comparisons (SigmaPlot v.15).

4.6 Acknowledgments

The authors wish to thank Mrs. Sylvie Guinchard for her technical assistance.

4.7 Funding

This work was funded by the Swiss National Science Foundation (Project 310030_208000 to F.K.) and by the University of Neuchâtel.

4.8 Contributions

WZ and GG conceived the original research. WZ, ME and GG carried out the research and data analysis. WZ and GG wrote the original draft. All authors contributed to draft editing and approved the manuscript.

4.9 Declarations

Ethics approval and consent to participate

Not applicable.

Consent for publication

Not applicable.

Competing interests

The authors declare that they have no competing interests.

4.10 References

1. Gershenzon J, Dudareva N: The function of terpene natural products in the natural world. *Nat Chem Biol* 2007, 3(7):408-414.
2. Tholl D: Biosynthesis and biological functions of terpenoids in plants. *Adv Biochem Eng Biotechnol* 2015, 148:63-106.
3. Beck G, Coman D, Herren E, Ruiz-Sola MA, Rodríguez-Concepción M, Gruissem W, Vranová E: Characterization of the GGPP synthase gene family in Arabidopsis thaliana. *Plant Mol Biol* 2013, 82(4-5):393-416.

4. Ruiz-Sola M, Coman D, Beck G, Barja MV, Colinas M, Graf A, Welsch R, Rütimann P, Bühlmann P, Bigler L *et al*: Arabidopsis GERANYLGERANYL DIPHOSPHATE SYNTHASE 11 is a hub isozyme required for the production of most photosynthesis-related isoprenoids. *New Phytol* 2016, 209(1):252-264.

5. Zhou F, Pichersky E: The complete functional characterisation of the terpene synthase family in tomato. *New Phytol* 2020, 226(5):1341-1360.

6. Barja MV, Rodriguez-Concepcion M: Plant geranylgeranyl diphosphate synthases: every (gene) family has a story. *aBIOTECH* 2021, 2(3):289-298.

7. Barja MV, Ezquerro M, Beretta S, Diretto G, Florez-Sarasa I, Feixes E, Fiore A, Karlova R, Fernie AR, Beekwilder J *et al*: Several geranylgeranyl diphosphate synthase isoforms supply metabolic substrates for carotenoid biosynthesis in tomato. *New Phytol* 2021, 231(1):255-272.

8. Zhou F, Wang C-Y, Gutensohn M, Jiang L, Zhang P, Zhang D, Dudareva N, Lu S: A recruiting protein of geranylgeranyl diphosphate synthase controls metabolic flux toward chlorophyll biosynthesis in rice. *Proc Natl Acad Sci* 2017, 114(26):6866-6871.

9. Nürenberg G, Volmer DA: The analytical determination of isoprenoid intermediates from the mevalonate pathway. *Anal Bioanal Chem* 2012, 402(2):671-685.

10. Martinis J, Kessler F, Glauser G: A novel method for prenylquinone profiling in plant tissues by ultra-high pressure liquid chromatography-mass spectrometry. *Plant Methods* 2011, 7(1):23.

11. Zita W, Bressoud S, Glauser G, Kessler F, Shanmugabalaji V: Chromoplast plastoglobules recruit the carotenoid biosynthetic pathway and contribute to carotenoid accumulation during tomato fruit maturation. *PLOS ONE* 2022, 17(12):e0277774.

12. McCaskill D, Croteau R: Procedures for the isolation and quantification of the intermediates of the mevalonic acid pathway. *Anal Biochem* 1993, 215(1):142-149.

13. Henneman L, van Cruchten AG, Denis SW, Amolins MW, Placzek AT, Gibbs RA, Kulik W, Waterham HR: Detection of nonsterol isoprenoids by HPLC–MS/MS. *Anal Biochem* 2008, 383(1):18-24.

14. Sugimoto H, Iguchi M, Jinno F: Bioanalysis of farnesyl pyrophosphate in human plasma by high-performance liquid chromatography coupled to triple quadrupole tandem mass spectrometry and hybrid quadrupole Orbitrap high-resolution mass spectrometry. *Anal Bioanal Chem* 2017, 409(14):3551-3560.

15. Chhonker YS, Haney SL, Bala V, Holstein SA, Murry DJ: Simultaneous Quantitation of Isoprenoid Pyrophosphates in Plasma and Cancer Cells Using LC-MS/MS. *Molecules* 2018, 23(12).

16. Ma Y, Chen Q, Wang Y, Zhang F, Wang C, Wang G: Heteromerization of short-chain trans-prenyltransferase controls precursor allocation within a plastidial terpenoid network. J ournal of Integr ative Plant Biology 2023, 65(5):1170-1182.

17. Alba R, Payton P, Fei Z, McQuinn R, Debbie P, Martin GB, Tanksley SD, Giovannoni JJ: Transcriptome and selected metabolite analyses reveal multiple points of ethylene control during tomato fruit development. *Plant Cell* 2005, 17(11):2954-2965.

5. An atypical kinase ABC1K1 allocates geranylgeranyl diphosphate to the carotenoid biosynthesis pathway in plastoglobules of chromoplasts

Wayne Zita[1], Venkatasalam Shanmugabalaji[1]*, Gaetan Glauser[2], Saleh Alseekh[4], Gregory Roeder[3], Michaela Fischer-Stettler [5], Luca Morelli[6], Alisdair Fernie[4], Magdalena Rossi, Christophe Rothan[7], Samuel Zeeman [5], Ted Turlings[3], Manuel Rodriguez-Concepcion[6], Felix Kessler[1]*
1 Plant Physiology Laboratory, University of Neuchâtel, 2000 Neuchâtel, Switzerland,
2 Neuchâtel Platform of Analytical Chemistry, University of Neuchâtel, 2000 Neuchâtel, Switzerland,
3 Laboratory of Fundamental and Applied Research in Chemical Ecology, University of Neuchâtel, 2000 Neuchâtel, Switzerland,
4 Max-Planck-Institut für Molekulare Pflanzenphysiologie, 14476 Potsdam-Golm, Germany
5Institute of Molecular Plant Biology, ETH Zurich, 8092 Zürich, Switzerland,
6Institute for Plant Molecular and Cell Biology (IBMCP), CSIC-Universitat Politècnica de València, 46022 Valencia, Spain
Departamento de Botânica, Instituto de Biociências, Universidade de São Paulo, Rua do Matão, 277, São Paulo, 05508-090, Brazil
7Institut National de la Recherche Agronomique (INRAE), Université de Bordeaux, UMR 1332 Biologie du Fruit et Pathologie, F-33140 Villenave d'Ornon, France
*shanmugabalaji.venkatasalam@unine.ch (VS); felix.kessler@unine.ch (FK)

5.1 Abstract

Lycopene is the most abundant carotenoid in tomatoes (*Solanum lycopersicum*) and confers the hallmark red color to ripe fruit. During ripening, green chloroplasts differentiate into red chromoplasts. Within the chromoplast, lycopene as well as other carotenoids accumulate in plastoglobules (PG; plastid lipid droplets) and carotenoid crystals. What is more, the PG harbor the entire carotenoid biosynthesis pathway starting with phytoene synthase (PSY1). However, it is not known how the key precursor of PSY1 geranylgeranyl diphosphate (GGPP) is delivered to the PG. Our analysis demonstrates that knock-out (KO) of the atypical PG kinase SlABC1K1 results in an orange fruit phenotype lacking lycopene while the fruit ripening markers and carotenoid biosynthetic enzymes were expressed as in wildtype. Lipidomics and metabolomic experimentation pinpoints the biochemical defect immediately upstream of PSY-1 and shows increased accumulation of GGPP while that of phytoene was diminished. But the biosynthesis of other products in fruit that depend on GGPP (tocopherol, phylloquinone, plastoquinone) was not affected. Overall, the results indicate that SlABC1K1 is required for sufficient allocation of GGPP to PG and carotenoid biosynthetic pathway in PG. We thus identify a previously unknown contributor to lycopene accumulation in tomato fruit.

5.2 Introduction

Photosynthetic complexes are embedded in the thylakoid membrane of the chloroplast. Attached to the curved margins of thylakoid membranes are plastoglobules (PG) plastid lipid droplets) (Austin II et al. 2006). PG function as a reservoir for hydrophobic compounds including prenyl quinones, phytyl esters, DAG, and carotenoids. Proteomic studies of isolated chloroplast PG led to the discovery of a small proteome of around 30 proteins). The PG proteins belong to three characteristic groups: the fibrillins (**FBNs**), the **a**ctivity of **bc1** complex like-kinases (**ABC1Ks**), and metabolic enzymes such as tocopherol cyclase (**VTE1**), phytyl ester synthase (**PES**) and **N**AD(P)H **D**EHYDROGENASE **C1** (**NDC1**) (Vidi et al. 2006; Ytterberg et al. 2006; Lundquist et al. 2012). Numerous studies have demonstrated that the metabolic enzymes of PG actively contribute to the biosynthesis and metabolism of the above-mentioned lipid compounds (Eugeni-Piller L., *et al.,* 2011; Porfirova, S., *et al.,* 2002). ABC1Ks constitute a subfamily of the Protein Kinase-like superfamily (PKL). ABC1Ks are well conserved from bacteria (UbiB) to plants and animals. In yeast (COQ8) and humans (ADCKs), the ABC1Ks are found exclusively in mitochondria, while in plants they are also located in plastids (van Wijk, K.J., and Kessler, F., 2017; Shanmugabalaji, V., *et al.,* 2022). Seventeen ABC1Ks were identified in the plant model organism *Arabidopsis thaliana*. In *Arabidopsis thaliana*, six ABC1K/UbiB (ABC1K1, -K3, -K5, -K6-, -K7, and -K9) were associated to PG, ABC1K2, -K4 and -K8 elsewhere in the chloroplast, while ABC1K10a, -K10b, -K11, -K12a, -K12b, -K13, -K14 and -K15) were localized in mitochondria (Lundquist P.K, *et al.,* 2012).

The Arabidopsis Proton Gradient Regulation 6 (PGR6)/ABC1K1 mutant is deficient in **e**lectron **t**ransport **r**ate (**ETR**) and **n**on-**p**hotochemical **q**uenching (**NPQ**) under high light (Martinis *et al.,* 2014). More recently, studies have demonstrated that in *Arabidopsis thaliana abc1k1* mutant, the plants are impaired in plastoquinone (PQ) pool regulation and homeostasis under high light which may explain the photosynthetic phenotypes (Pralon *et al.,* 2019). A second family member, ABC1K3, also associated with PG, participates in PQ homeostasis (Pralon *et al.,* 2020). The work suggested that ABC1K1 and ABC1K3 work in tandem to distribute PQ between PG and thylakoids in a hypothetical "push-pull" mechanism: ABC1K1 provides of PQ from PG to thylakoids ("push"), while ABC1K3 retains PQ in PG ("pull"). (Pralon *et al.,* 2020). A related system appears to be at work in yeast: Cqd1 and Cqd2 (homologs of COQ8 and members of the ABC1K-family) in the mitochondrial envelope contribute to ubiquinone distribution whereby Cqd1 contributes to allocation of mitochondrial ubiquinone to the plasma membrane and Cqd2 to ubiquinone retention in mitochondria. The emerging theme is the implication of members of the ABC1K family in allocation of prenyl lipids to specific cellular and organellar compartments. The precise mechanisms of the atypical ABC1K kinases are currently not known but it appears likely that they function as ATPases rather than trans-phosphorylation kinases.

An ABC1K1 ortholog is also present in PG of tomato fruit chromoplasts but its function is unknown, given that chromoplasts do not carry out photosynthesis (Zita *et al.,* 2022). Chromoplasts differentiate into chloroplasts during fruit ripening. In the process, they lose their thylakoid membranes, develop super-sized PG and accumulate large amounts of carotenoids that confer the signature yellow to red colors to fruit.

Our recent study of the tomato fruit PG proteome revealed not only the presence of SlABC1K1 but that of the complete carotenoid biosynthetic pathway starting at PSY-1 (Zita *et al.,* 2022). The study included lipidomic analyses that confirmed concurrent accumulation of carotenoids in PG, lycopene being the most abundant in ripe red fruit (Zita *et al.,* 2022). We concluded that PG are transformed into a carotenoid biosynthetic platform and storage site during chloroplast to chromoplast conversion.

Carotenoids belong to the large family of isoprenoids. They are synthesized from the fundamental chain-building block isopentenyl diphosphate (IPP) and its isomer, dimethylallyl diphosphate (DMAPP) in a succession of enzymatic steps (T. Kuzuyama *et al.,* 2013; K. Zhou *et al.,* 2016) of the plastidial methylerythritol phosphate (MEP) pathway. The biosynthesis of carotenoids ("carotenogenesis") requires the key metabolite geranylgeranyl diphosphate (GGPP) a product of the MEP pathway in the chloroplast stroma that is also required for the biosynthesis of other essential plastidial isoprenoid components, including plastoquinone, phylloquinone (vitamin K_1), tocopherols (vitamin E), and chlorophylls (Pulido *et al.,* 2012; Rodriguez-Concepcion and Boronat 2015; Tholl 2015). But currently, it is unknown how GGPP reaches the carotenoid pathway in PG. The pathway is initiated by the condensation of two molecules of GGPP catalyzed by phytoene synthase (PSY-1) resulting in phytoene that is further converted to lycopene by sequential carotenoid biosynthetic enzymes. The expression of genes encoding carotenoid biosynthetic enzymes is under the control of transcription factors (TFs) including RIPENING INHIBITOR (RIN), COLORLESS NON-RIPENING (CNR), and NON-RIPENING (NOR) as well as phytohormones and environmental conditions (Lois *et al.,* 2000; Rodríguez-Concepción and Boronat, 2015; Wang *et al.,* 2020). RIN encodes a MADS-box transcription factor known as an essential regulator and inductor of ripening (Vrebalov *et al.,* 2002) and is frequently used as a ripening marker of tomato fruit (Quinet, M., *et al.,* 2019).

Given our earlier work, the presence of SlABC1K1 in the tomato chromoplasts prompted us to analyze its role in fruit chromoplasts.

Here, we report the phenotypes of a CRISPR-Cas9 engineered knockout mutant of tomato *slabc1k1*. The tomato mutant faithfully reproduced the PGR6 phenotype known from Arabidopsis. *abc1k1* fruit were orange rather than red and had low levels of lycopene while ripening markers and carotenoid biosynthetic enzymes were at least as highly expressed as in WT. Metabolomics analyses revealing GGPP accumulation indicated that the carotenoid biosynthetic pathway is disrupted immediately upstream of PG-localized phytoene synthase. We conclude that SlABC1K1 contributes to GGPP allocation to PG its mutation leading to a supply bottleneck limiting metabolite flux for large scale lycopene biosynthesis.

5.3 Results

5.3.1 Characterization of CRISPR/Cas-9-targeted mutagenesis of SlABC1K1

The CRISPR system was used to generate a knockout of tomato SlABC1K1 (Solyc08g074560, www.solgenomics.net)(Carroll, 2012). Two independent *slabc1k1* mutant lines (*abc1k1-1* and *abc1k1-5*) were obtained. In both *abc1k1-1* and *abc1k1-5* the mutations resulted in premature stop codons (FIG S1e). The fruits of the *abc1k1-5* mutant did not produce seeds, which did not allow us to go to T2 with this line. We segregated and selected CAS9-free lines of *abc1k1-1*. These lines were phenotyped in T2. The *abc1k1-1.1* and *-1.4* lines are representative and were used for the rest of this study (FIG 1a).

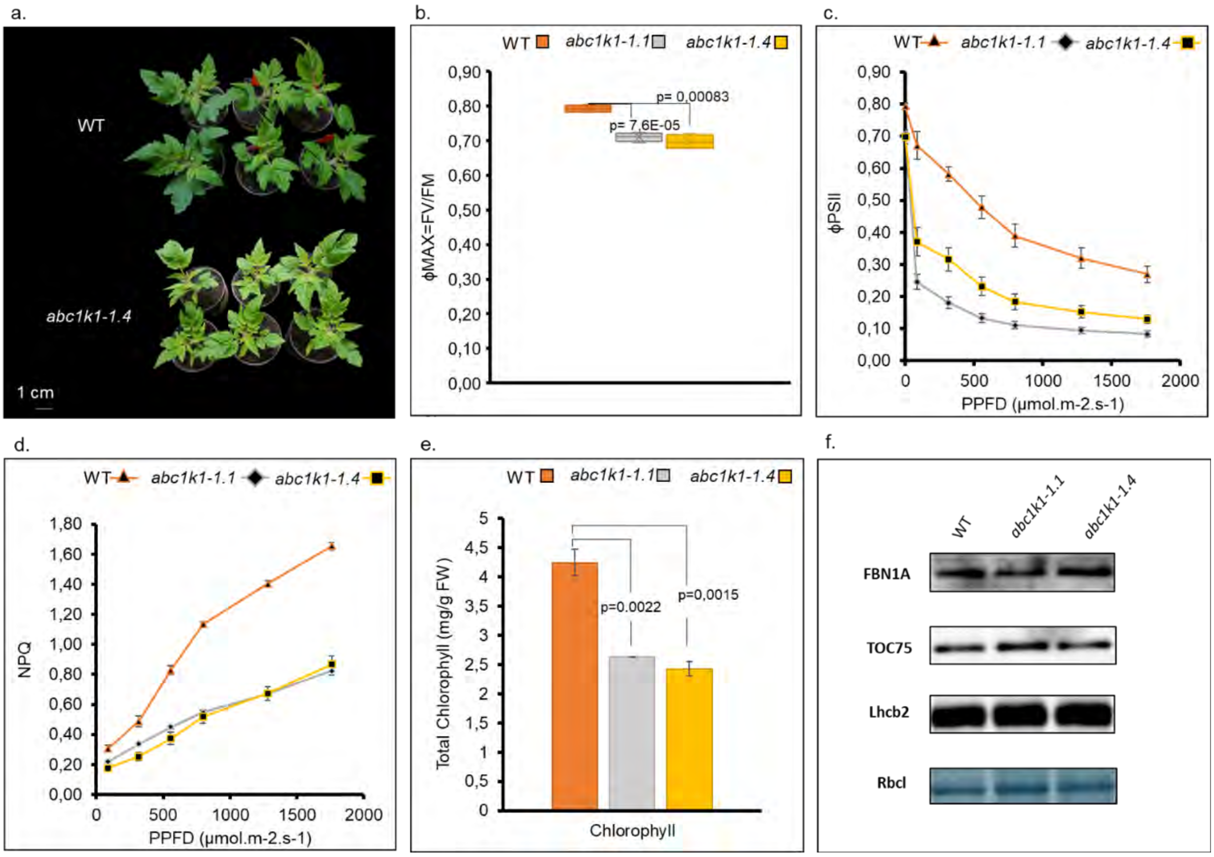

FIG 1| **Tomato *slabc1k1* mutants have the pgr6 photosynthetic defects.** a) Visible phenotype of WT and *abc1k1-1.4* plants; b) ΦMAX=FV/FM the PSII maximum quantum yield; c) ΦPSII=(FM' – FS)/FM') PSII quantum yield efficiency; d) NPQ=(FM – FM')/FM') is the non-photochemical quenching measured; e) The total chlorophylls (Chla/b) were measured by Arnon's method of 1949 with tomato grow under moderate light intensity (140 µmol m^{-2} s^{-1}) performed with a UV/Visible spectrophotometer; f) Protein expression analysis of tomato WT and *abc1k1-1* lines. Total protein extract from WT and *abc1k1-1.4* were separeted by SDS-PAGE followed by immunoblotting using antibodies against **Lhcb2**, a protein of photosystem II (PSII), **FBN1A** a plastoglobule marker, **TOC75** a protein channel of the outer envelope, **Rbcl** was used as a loading control. All calculation in the figures are based on a mean of 3 biological replicates (n=3) and 3 technical replicates (t=3). Statistical differences were assessed with students' t test and p values are indicated. The measurements were performed with Fluorcam (MF800 – PSI).

5.3.2 *slabc1k1* leaves have a PGR phenotype.

Arabidopsis *abc1k1/pgr6* is sensitive to high light and defective in photosynthetic efficiency (ΦPSII) and non-photochemical quenching (NPQ) (Shikanai, T *et al.,* 1999; Martinis, J *et al.,* 2014). Taking this into account, *slabc1k1* and WT tomato plants were grown under moderate light conditions (ML; 140 µmol.m^{-2}.s^{-1}) to minimize light stress. But even under moderate light tomato *slabc1k1* were visibly smaller and paler than WT (FIG 1a). Indeed, chlorophyll accumulation was reduced and maximal photosynthetic efficiency (ΦMAX=Fv/Fm) slightly diminished in *slabc1k1* when compared to WT (FIG 1b and c). The photosynthetic parameters ΦPSII and NPQ were strongly impaired in tomato *slabc1k1* (FIG 1d and e). Overall, the photosynthetic defects strongly resembled those reported in Arabidopsis. However, representative marker proteins including a major thylakoid-associated protein (Lhcb2), a PG marker (FBN1A), and plastid outer envelope marker (TOC75) were not significantly different when analyzed by western blot (FIG 1f).

5.3.3 SlABC1K1 contributes to carotenoid accumulation in tomato fruit.

slabc1k1 had an orange phenotype 10 days after breaker stage (BS+10) under ML conditions, while WT fruit were red (FIG 2a; S2) (Alba *et al.,* 2005). Transmission electron microscopy (TEM) of chromoplasts did not reveal recognizable ultrastructural differences between *slabc1k1* and WT at the level of envelope membranes, crystalline bodies and PG (FIG 2b).

To characterize the pigment composition, we profiled the prenyl lipid and carotenoid contents using ultra-high-performance liquid chromatography (UHPLC) (Martinis *et al.,* 2011). Total carotenoids present in orange *slabc1k1* fruit were around half of that in WT. The quantification showed approximately 3-fold lower accumulation of lycopene in *slabc1k1* than in WT fruit (FIG 2c). In comparison, lutein, β-carotene, and xanthophylls (violaxanthin and neoxanthin) concentrations (FIG 2d) as well as those of the prenyl quinones (tocopherol, plastoquinone, plastochromanol, and phylloquinone) were close to WT (FIG 2a, b, and c). In contrast to the aforementioned compounds, the UHPLC analysis revealed a 5-fold lower concentration of phytoene with in *slabc1k1* than in WT (FIG 2d).

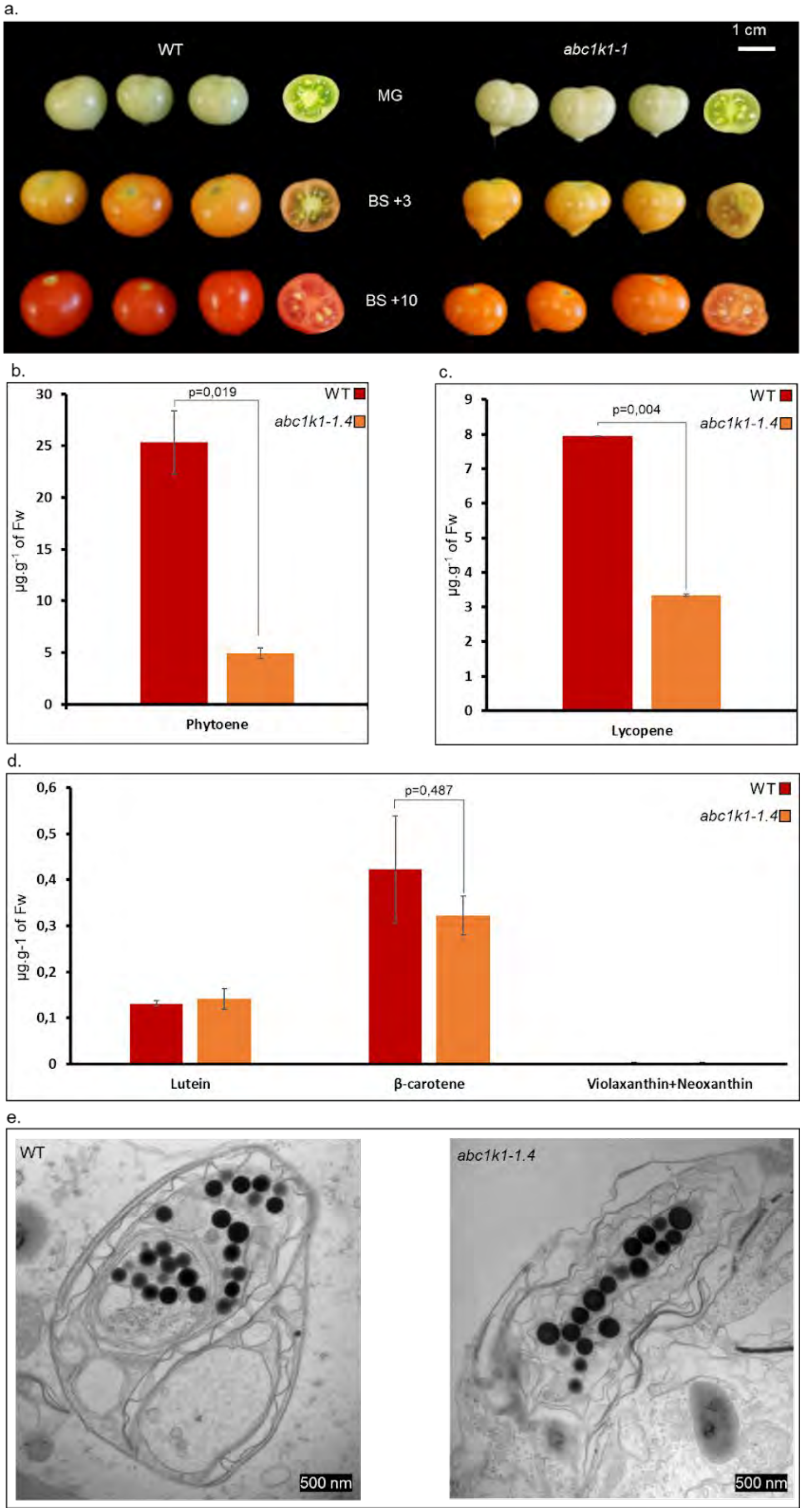

FIG 2| **Tomato *slabc1k1* mutant fruits are altered in carotenoid accumulation under moderate light.** a) Visible phenotype of total and slice WT and *abc1k1-1*.4 tomato fruits in the mature green stage (MG), breaker stage (BS+3), and ripe stage (BS+10) cultivated under ML condition (Bar=1 cm); b) Lycopene concentration; c) Phytoene concentration; d) Lutein, β-carotene, and violaxanthin + neoxanthin concentration; e) TEM pictures of WT and *abc1k1-1.4* chromoplasts of tomato fruit at BS+10 (Bar=500 nm). The carotenoid were extracted from WT and *abc1k1-1.4* and were analyzed by using UHPLC-APCI-

QTOF-MS. All value in the figure are the means of 3 biological and 3 technical replicates (n=3 and t=3). Statistical differences were assessed with students' t test and p values are indicated.

5.3.4 The tomato *slabc1k1* mutation does not diminish ripening markers and increases PSY-1 accumulation in fruit.

To exclude that the orange fruit phenotype was due to delayed ripening *in slabc1k1*, expression of ripening markers were analyzed (Bramley, 2002). To exclude a defect at the expression level, genes involved in carotenoid biosynthesis were also analyzed in *slabc1k1* and WT fruit (Bramley, 2002). qPCR was performed on cDNA derived from ripe *slabc1k1* and WT fruit at BS+10. The transcript levels of the ripening markers *RIN* and *NR* were 2- and 1.5-fold higher in *slabc1k1* than in the WT at BS + 10 (FIG 3a). The *PDS*, *CRTISO*, and *LCYB* genes involved in carotenoid biosynthesis did not show any differences in transcript levels whereas *PSY-1* was increased around 6-fold in *slabc1k1* over WT (FIG 3b). The protein level of PSY-1 was investigated by immunoblotting at BS+10 and was also higher in *slabc1k1* than in WT. In comparison, the FBN1A and ACTIN control proteins accumulated to the same levels (FIG 3c).

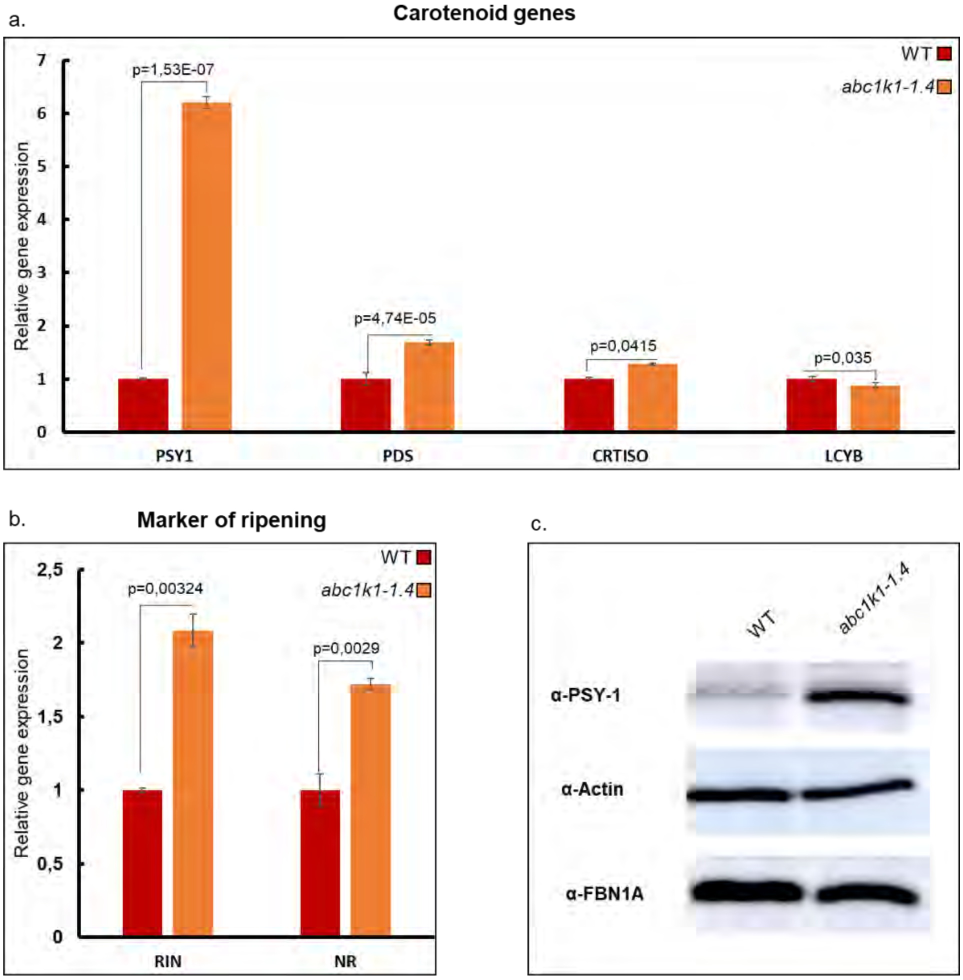

FIG 3| **Relative genes and proteins expression of *slabc1k1* and WT of tomato fruit at BS+10 grow under moderate light (ML)**. a) PSY1, phytoene synthase 1; PDS, phytoene desaturase; CRTISIO, carotenoid isomerase; LCYB, lycopene beta-cyclase. b) RIN, ripening inhibitor; NR, never ripe. c) Total protein extract from WT and *abc1k1-1.4* were separeted by SDS-PAGE followed by immunoblotting using antibodies against α-PSY-1, antibody of phytoene synthase enzyme; α-ACTIN, antibody of actin protein; α-FBN1A, antibody of fibrilin 1A (CHRC). All value in the figures are the means of 3 biological and 3 technical replicates (n=3 and t=3 independent samples). Statistical differences were assessed with students' t test and p values are indicated.

5.3.5 Primary metabolites accumulate differentially in *slabc1k1* tomato fruit.

In view of the preceding results, we were curious to know whether the low accumulation of lycopene in *slabc1k1* fruit at BS+10 is due to a reduced abundance of the carotenoid biosynthetic precursors upstream of phytoene. Primary metabolites including soluble sugars, amino acids, and lipids contained in extracts of *slabc1k1* and WT at BS+10 were analyzed by gas chromatography coupled with MS (GC-MS)(Carrari and Fernie, 2006; Beauvoit *et al.,* 2014; Biais *et al.,* 2014; Bauchet *et al.,* 2017). The results presented as a heatmap show significantly different profiles for *slabc1k1* and WT (FIG 4). Sucrose, glucose, and fructose accumulated to lower levels in *slabc1k1* fruit. In contrast, raffinose accumulated to higher levels in *slabc1k1* than in WT. Significant increases in aspartic acid, glutamic acid, serine, threonine, asparagine, and glutamine were observed in *slabc1k1*. γ-aminobutyric acid (GABA), an important primary metabolite involved in the metabolism of succinate and glutamate also accumulated to higher levels in the *slabc1k1* fruits. Interestingly, pyruvate and the glyceraldehyde 3 phosphate (3P-GA) which initiate the MEP pathway were more highly accumulated in *slabc1k1* than in WT. Volatiles released from fruit at BS+10 were analyzed by GC-MS and resulted in distinct profiles for *slabc1k1* and WT. Volatiles derived from amino acids, fatty acids, carotenoids, and isoprenoids were observed in both. Geranylacetone and 6-methyl-5-hepten-2-one derived from carotenoids were present to the same extent in *slabc1k1* than in the WT bouquet (Gao, H. *et al.,* 2008). The metabolomic analysis allowed the detection of primary metabolites required for the MEP pathway. However, the GC-MS method did not allow the detection of critical downstream components such as GGPP.

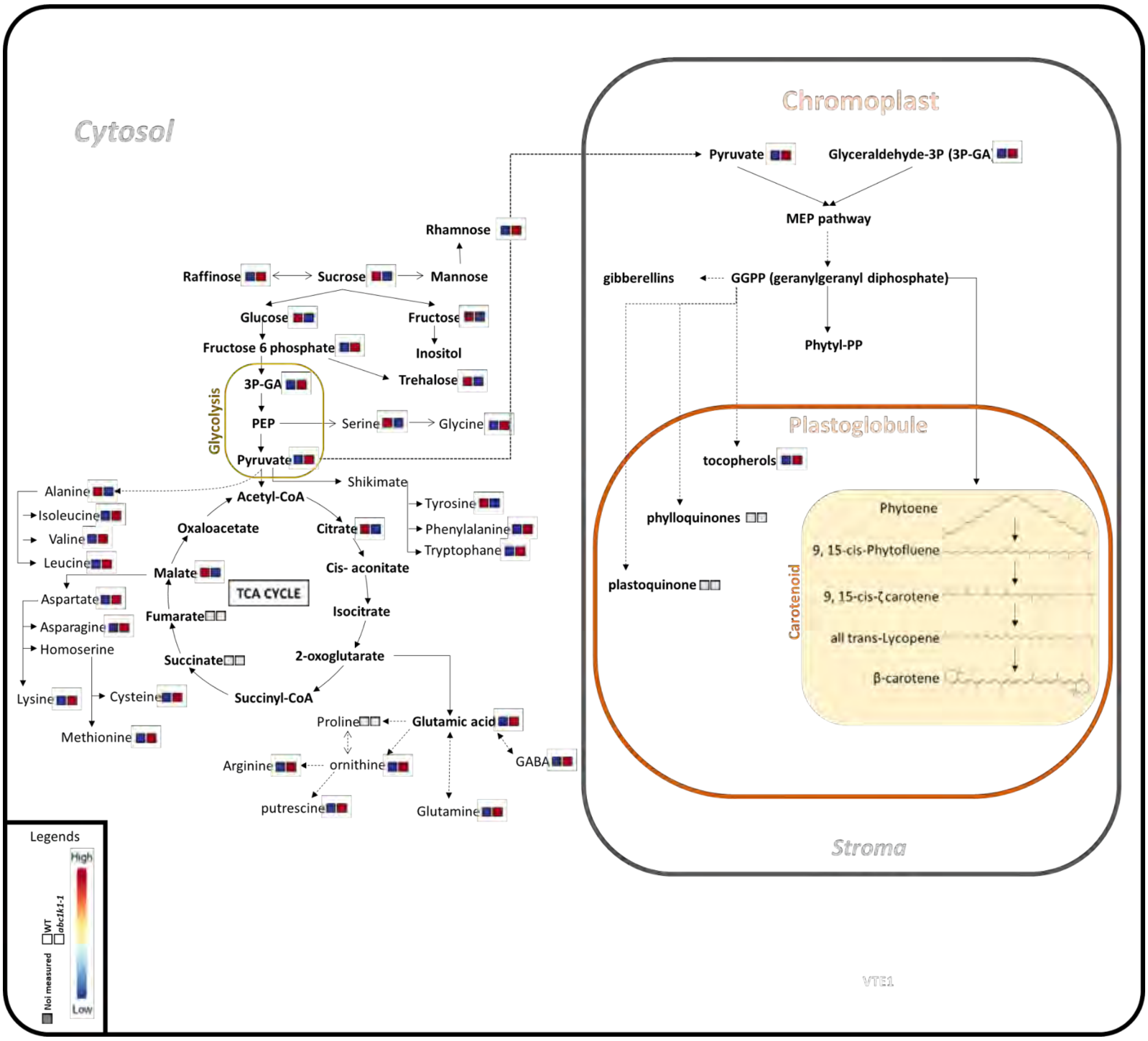

FIG 4| **Heatmap analysis of change in metabolite levels of fruits of tomato *slabc1k1* and WT**. Metabolites were quantified after normalizing on weight and compared with red and blue colors represent significant up- and down-regulation respectively as conducted by ANOVA.

5.3.6 GGPP accumulates to higher levels in *slabc1k1* tomato fruit than in WT.

We showed that phytoene is much lower in *slabc1k1* than in WT at BS+10 (FIG 2d). GGPP is the immediate precursor of phytoene and the substrate of phytoene synthase that is localized in PG. Potentially, GGPP biosynthesis presents a bottleneck in phytoene synthesis and consequently lycopene accumulation further downstream. What is more, GGPP is also required for biosynthesis of the prenyl side chains of tocopherols, plastoquinone and phylloquinone which were largely unchanged in *slabc1k1* compared to WT fruit at BS+10 (Fraser *et al.,* 2002; Coman *et al.,* 2014). However, the synthesis of these compounds largely takes place outside PG whereas carotenoid biosynthesis has been assigned to PG. It is therefore tempting to hypothesize that GGPP allocation to PG is perturbed in *slabc1k1*. As GGPP was not detectable by conventional GC+MS we developed a quantitative method using UHPLC and commercial GGPP as a standard. During this work, we noticed the presence of two peaks in the GGPP standard. The first peak detected was attributed to GGPP. The second peak was attributed to geranylgeranyl monophosphate (GGP) Analysis of the *slabc1k1* and WT BS+10 fruit extracts revealed the same profile as in the GGPP standard. We observed an approximately 3-fold higher accumulation of GGPP in *slabc1k1* than in WT (FIG 5a) while GGP accumulation was 1-5-fold higher in *slabc1k1* than in WT (FIG 5b). The concentrations measured were ~3-fold higher in *slabc1k1* than in the WT.

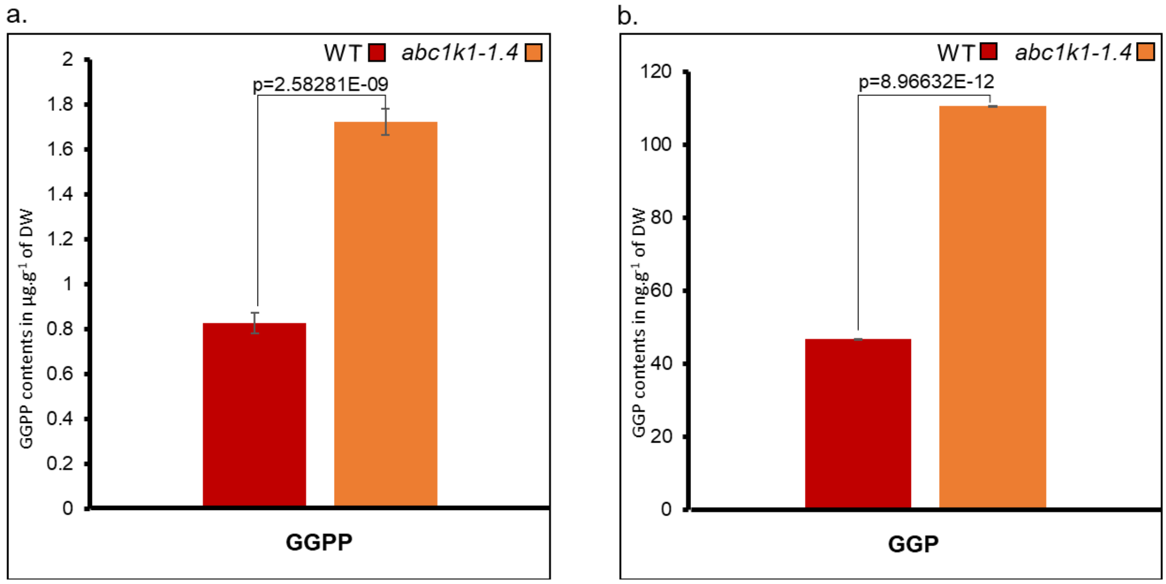

FIG 5| **Tomato *slabc1k1* mutant fruits accumulate high level of GGPP.** The absolute quantification of the GGPP and GGP were determined in WT and *abc1k1-1.4* by using UHPLC-APCI-QTOF-MS. GGPP and GGP standards were used for the absolute quantification. All value in the figures are the means of 3 biological and 3 technical replicates (n=3 and t=3). Statistical differences were assessed with students' t test and p values are indicated.

5.4 Discussion

ABC1K1/UbiB is a member of the PLK family. It is an atypical kinase characterized by an unconventional ATP-binding site. It has been suggested that ABC1K1 homologs in yeast and human may not possess trans kinase activity but may act as ATPases in intracellular lipid trafficking processes (Do, T.Q. *et al.,* 2001; Poon *et al.,* 2000). Our previous studies suggest that ABC1K1 is involved in PQ pool regulation and PQ trafficking between thylakoid and PG in Arabidopsis chloroplasts (Pralon, T., *et al.,* 2019). The role of ABC1K1 in other species and plastid types has not been characterized so far. This study aimed to identify the role of SlABC1K1 in tomato (*Solanum lycopersicum*). We demonstrate that *slabc1k1* in tomato leads to classical PGR6 defects, characterized by growth, ETR, and NPQ defects. The photosynthetic defects are caused by the limited electron transport rate due to decreased availability and improper distribution of PQ, which is regulated by PGR6 activity (Pralon, T., *et al.,* 2019; Pralon, T., *et al.,* 2020). These findings indicate that in tomato leaves SlABC1K1 has functions very similar to those in Arabidopsis (Martinis, J., *et al.,* 2014; Pralon, T., *et al.,* 2019). Our recent study revealed that carotenoid pathway enzymes are recruited to tomato chromoplast PG (Zita W. *et al.,* 2022). In addition, the high abundance of SlABC1K1 in tomato chromoplast PG provided a rationale to investigate tomato fruit phenotype.

Surprisingly, *slabc1k1* tomatoes were orange and not red like WT at BS + 10 (Alba, R., *et al.,* 2005). Expression of the fruit ripening markers RIN and NR was upregulated in *slabc1k1* compared to WT at BS+10 excluding that the orange fruit phenotype is due to a delay in ripening. Carotenoid quantification indicated that lycopene levels were much lower in *slabc1k1* than in WT while beta-carotene and lutein accumulated to the same level as in WT. This explains the orange fruit phenotype and also indicates that the carotenoid biosynthesis pathway is in principle functional in *slabc1k1*. This was corroborated by the expression levels of the carotenoid biosynthetic enzymes PSY-1, PDS, CRTISO, and LCYB that were the same or higher in *slabc1k1* than in WT. As in *slabc1k1* ripening progression was the same as in WT and the enzymes of the carotenoid biosynthesis pathway were normally expressed, we concluded that the SlABC1K1 protein contributes in a currently unknown way to tomato fruit carotenoid biosynthesis.

We had observed that *PSY-1* gene expression and protein accumulation were much higher in *slabc1k1* than in WT. However, overexpression of the PSY-1 gene has been shown to increase carotenoid contents in WT tomato fruit (Galpaz *et al.,* 2006) but it was reduced in *slabc1k1*. Moreover, phytoene levels in *slabc1k1* were also diminished when compared to WT. These results suggested a disruption of metabolic flow towards carotenoid biosynthesis. This may occur at different stages beginning with the MEP pathway.

For this reason, we investigated the primary metabolism to gain information on the availability of the pyruvate and glyceraldehyde 3 phosphate (3P-GA) building blocks of the MEP pathway. Both pyruvate and 3P-GA were increased in *slabc1k1* over WT indicating that the initial stages of carotenoid biosynthesis were not limited. As the phytoene levels in *slabc1k1* were diminished it appeared possible that the synthesis of the precursor GGPP was reduced. Using a newly developed method to measure GGPP we demonstrated that levels of GGPP were much higher in *slabc1k1* than in WT. GGPP is not only required as a substrate for the biosynthesis of carotenoids but also for that of the prenyl moieties of tocopherols, plastoquinone, and phylloquinone (Okada *et al.,* 2000). The lipidomic analysis of *slabc1k1* fruit pericarp showed no significant changes in tocopherols, plastoquinone, and phylloquinone compared to WT. Notably, the biosynthesis of these three compounds takes place outside PG while that of carotenoids takes place inside. We conclude that geranylgeranyl diphosphate allocation to PG was diminished in *slabc1k1* and resulted a metabolic bottleneck for the large-scale biosynthesis of lycopene.

The data indicate that *slabc1k1* is important for carotenoid accumulation but likely without participating in the enzymatic reactions. We have previously shown also that ABC1K1 together with K3 participate in PQ distribution between PG and the thylakoid membranes (Pralon, T., *et al.,* 2020). It has also been demonstrated that two mitochondrial members of the ABC1K/UbiB family in *S. cerevisiae*, Ypl109c (Cqd1) and Ylr253w (Cqd2), regulated CoQ distribution between mitochondria and extramitochondrial compartments in an ATP-dependent fashion (Kemmerer ZA *et al.,* 2021) (Bersuker, K. *et al.,* 2019; Doll, S. *et al.,* 2019). In view of the similarity of our findings with the known role of Arabidopsis and *S. cerevisiae* ABC1K/UbiB homologs in small molecule trafficking and allocation, a comparable role may also be proposed for the SlABC1K1 protein in tomato chromoplasts during fruit maturation.

In summary, our results support the hypothesis that SlABC1K1 protein is required for GGPP trafficking from the stroma to PG.

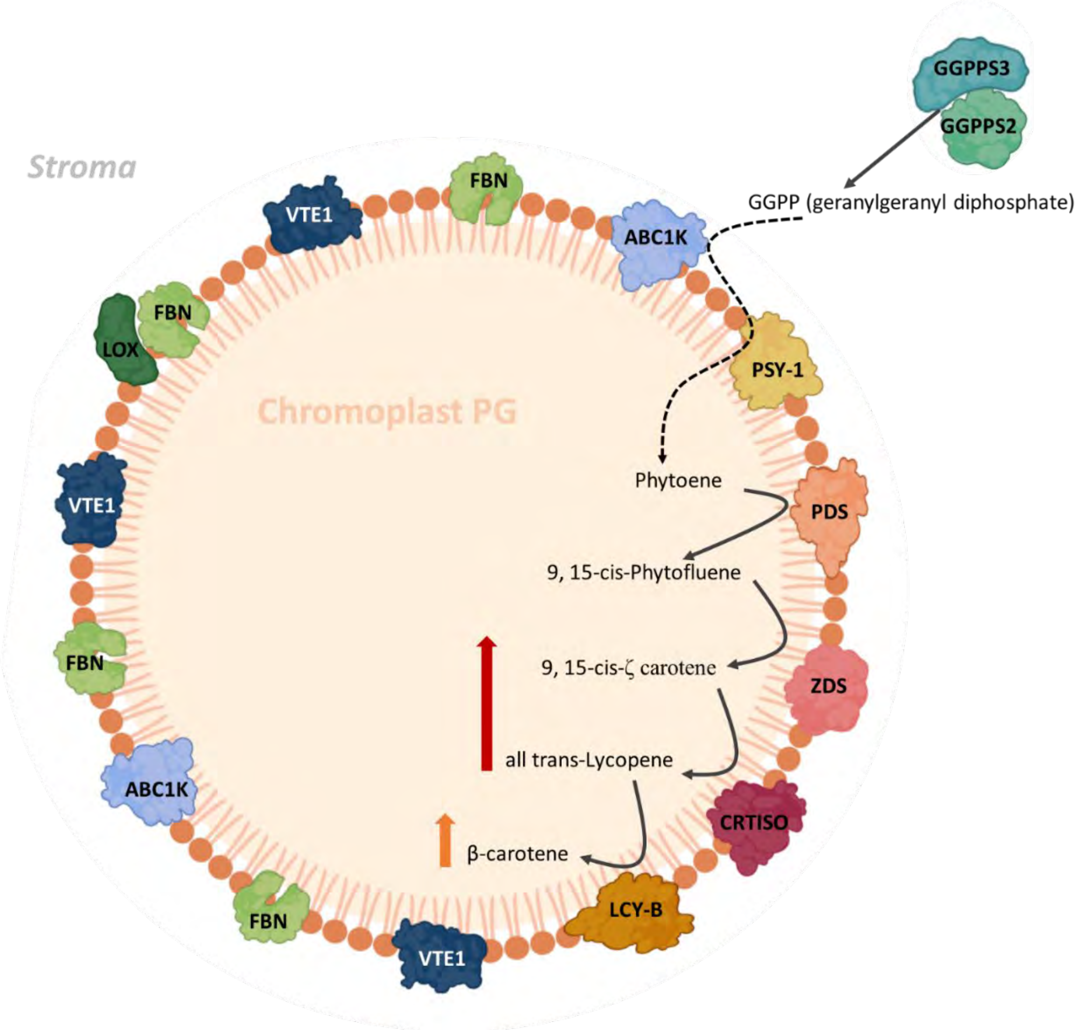

FIG 6| **Model of SlABC1K1 contributes to GGPP trafficking.** In this model, we proposed a hypothetical role of SlABC1K1 in GGPP supply to the carotenoid biosynthesis pathway to the plastoglobule platform. Arrows represent the direction of the biosynthetic pathway.

5.5 Materials and methods

5.5.1 Plant and Fruits Material

Wild type and mutant tomato seeds (*Solanum lycopersicum* cv. Micro-Tom) were kindly provided by our collaborator, Dr. Christophe Rothan (Group Leader at the French National Institute for Agriculture, Food, and Environment at INRAE Bordeaux, France). The tomato plants were grown in a greenhouse under moderate light conditions (140 µmol m−2 s−1). with a temperature and photoperiod adapted from (Rothan *et al.,* 2016). Manual pollination was performed on the day of flower opening to define the ripening stages of the fruits as days after pollination (DAP). Wild-type fruits were harvested at the breaker (BS +3), and red ripe fruit (RF or BS +10) stages, which occurred on an average at 40 (BS + 3) and 47 (BS + 10) DAP. Fruits of the *slabc1k1* mutants were harvested at the same ripening stages as WT. Upon harvesting, the fruit pericarp was collected, quenched immediately in liquid nitrogen, and stored at −80 °C until use or lyophilized.

5.5.2 Engineering of SlABC1K1 mutants using the CRISPR/ Cas9 system

Targeted CRISPR/Cas9 mutagenesis of the SlABC1K1(Solyc08g074560) gene was performed on WT tomato as described in (Xu, C. *et al.,* 2015). In short, constructs were engineered to produce deletions in the target gene coding sequence (CDS) by using two sgRNAs (sgRNA13 and sgRNA56; FIG S1a), followed by Cas9 endonuclease gene (Musseau, C., *et al.,* 2020). The process of Agrobacterium-mediated tomato transformation of Micro-Tom cotyledons was carried out following the method outlined in Cortina and Culiáñez-Macià's 2004 publication. A total of 2 independent transformation events were identified by Sanger sequencing, all of which exhibited the expected mutations in SlABC1K1 (the primer sequences used for sequencing can be found in TableS1). For this study, we utilized two CRISPR lines in the T2 generations (namely *abc1k1-5* and *abc1k1-1.1*and *-1.4*; FIG S1). When referring to the results that combined data from the different CRISPR lines, we referred to them as *slabc1k1*. We confirmed that there were no off-target effects in the homologous SlABC1K1 gene through Sanger sequencing.

5.5.3 Genotyping of the *slabc1k1*

A pair of forward (fw_prg6: 5' GTGCTAAGGCCGCAAATAGA 3') and reverse (rv_pgr6: 5' GAAGCTCGTAATATCGAAGAC 3') primers encompassing the sgRNA13 and the sgRNA56 was used to genotype the T1 *slabc1k1* mutants by PCR. PCR products were purified and sequenced. Homozygous *slabc1k1* plants were selected and phenotyped.

5.5.4 Chlorophyll measurement

Total chlorophyll was extracted from leaf tissue (10 mg fresh weight (FW)) in 80% (v/v) acetone, 20% (v/v) milliQ water (ddH2O). After centrifuging twice (2 min, 16'000 x g, 4 °C), the supernatant was analyzed by spectrometry (Arnon DI., 1949.). Chlorophyll pigments were identified by using four different wavelength absorption spectra which are 470nm, 646nm, 652nm, and 663nm. For quantification, the chlorophylls were normalized on Fw leaves used during the experiment.

5.5.5 Photosynthetic Parameters

To assess photosynthetic parameters, WT and *slabc1k1* tomato plants were dark acclimated inside the chamber for at least 15 min before saturation pulse (1760 µmolm−2 s−1 PPFD/PAR) was taken to measure photosynthetic parameters Fv/Fm. The measurements were performed with a Fluorcam (Photon System Instruments, Czech Republic) with an adapted light curve protocol (Pralon *et al.,* 2020). For measurement, the protocol of Arabidopsis was adapted for tomato. The plants were exposed to blue light (470nm) for 1min followed with increasing intensity (86, 316, 556, 797, 1281 and 1760 µmol m−2 s−1 PAR intensity). The fluorescence measured before the peak were used as Fs (steady-state chlorophyll fluorescence in the light). The maximal fluorescence (Fm) in light was measured with a saturation pulse after each increase in light intensity described above. The value obtained allows the calculation of three parameters which are the maximum efficiency of photosystem II (PSII) known as (ΦMAX= Fv/Fm), the PSII quantum yield efficiency (ΦPSII= ((FM' – FS)/FM')), and the non-photochemical quenching (NPQ= ((FM – FM')/FM')) (Shikanai, T *et al.,* 1999; Martinis, J *et al.,* 2014).

5.5.6 RNA extraction and qPCR

Lyophilized pericarps of fruits from three plants of WT and *slabc1k1* mutants were used for total RNA extraction using Trizol reagent following the instructions of the manufacturer. One microgram of total RNA (as measured by nanodrop) was used for first-strand cDNA synthesis with GoScriptTM Reverse Transcriptase|cDNA Synthesis (Promega kit). Primer sequences are listed in the supplementary table (tableS1). Quantitative real-time PCR was performed using the FastStart Essential DNA Green Master kit (Roche) and LightCycler® 96 (Roche Diagnostics). Gene expression levels were normalized with the housekeeping gene ACTIN (Solyc11g005330).

5.5.7 Protein extraction and western blotting

Total protein was extracted from lyophilized fruit pericarp and leaves of WT and *slabc1k1* plants using Rensink buffer (50 mM Tris-HCl, pH 7.5, 0.1M NaCl, 0.5% v/v Triton-X 100, 10 mM β-mercaptoethanol, and 1mM PMSF). The total extracted protein was precipitated with chloroform-methanol (75:25, v/v) (Pralon *et al.,* 2020). The total proteins were separated by SDS-PAGE and transferred into a nitrocellulose membrane. The immunoblotting was performed as described in Pralon et al, (2020). To probe the blots, anti-Actin (Sigma, A0480), anti-Lhcb2 (Agrisera, AS01003), anti-PSY-1 (Agrisera, AS163991), anti-FBN1A (Vidi P *et al.,* 2006) and anti-TOC75 (Hiltbrunner A *et al.,* 2001) were used. The secondary antibodies conjugated with HRP, anti-rabbit (Merck, AP132P) or anti-mouse (Sigma, A5278) were used to visualize the chemiluminescence with ECL by using a chemiluminescence imager (Amersham Imager 600, Amersham Biosciences, Inc.).

5.5.8 Transmission electron microscopy

Transmission electron microscopy was used to analyze and compare the chromoplast ultrastructure of WT and *slabc1k1* plants grown under moderate light. Tomato fruit sections were observed with a Philips CM-100 electron microscope operating at Sigma 60 kV as described (Spicher, L. *et al.,* 2017).

5.5.9 Prenyllipid extraction

The extraction and quantification methods were adapted from (Martinis *et al.,* 2011). leaves of 5 weeks-old WT and *slabc1k1* plants were ground in liquid nitrogen and 100mg of powder was resuspended in 500 µL of THF/MeOH (50:50, v/v) and centrifuged at 16’000 x g for 10 min at RT. The supernatant was transferred to a new Eppendorf tube then centrifuged at 16’000 x g for 5 min at RT to remove debris. 150 µL were transferred to an appropriate glass vial for immediate ultra-high-performance liquid chromatography-tandem mass spectrometry (UHPLC-MS/MS) analysis. Absolute concentrations of prenyl quinones (α-T, γ-T, δ-T, phylloquinone, PQ-9, PC-8, PC-OH and PQ-OH) were calculated based on standard calibration curves.

5.5.10 Carotenoid extraction from whole tomato fruit

Total carotenoids were extracted from lyophilized tomato fruit. Approximately 20 mg of powder was resuspended in 500 µL of THF/MeOH (50:50, v/v), vortexed and centrifuged at 16’000 x g for 10 min at RT. The supernatant was transferred to a new Eppendorf tube then centrifuge at 16’000 x g for 5 min at RT to remove debris. 150 ul were transferred to an appropriate glass vial for immediate determination of absolute concentrations of carotenoids (lycopene, lutein, phytoene) using standard calibration curves. β-carotene, violaxanthin, and neoxanthin were quantified based on lutein standards.

5.5.11 VOCs GC-MS analysis

In order to minimize any decomposition or delayed effects before chemical analyses, freshly harvested tomatoes (BS+10) from WT and *slabc1k1* were sliced, weighed to obtain around 1.5 g of fresh material, and placed in individual 20 mL glass vials closed with septum screw caps. For volatile organic compounds (VOCs) analyses, a gas chromatograph (GC, Agilent 7890a) coupled with a mass spectrometry detector (MSD, Agilent 5975c) was used. Chromatographic profiles were manually processed. Preliminary identifications were carried out by double spectral comparisons with both PBM search and NIST21 libraries. VOCs of interest were integrated in order to obtain relative abundances, which were corrected in function of respective sample’s weight.

GGPP and GGP extraction and quantification

GGPP and GGP levels were analysed by UHPLC-MS/MS. The UHPLC-MS/MS system used was an Acquity UPLC coupled to a TQ-XS triple quadrupole (Waters), both controlled by MassLynx 4.2. The column was an Acquity UPLC BEH C18 (50x2.1 mm, 1.7 µm, Waters) maintained at 25°C in an oven. Mobile phases consisted of A=H2O+NH4OH 0.05% and B=acetonitrile+NH4OH 0.05%. The flow rate was set to 0.4 mL/min. A gradient of 5% to 41% phase B in 4.0 min was applied, followed by increase to 100% B in 0.5 min, hold at 100% B for 2.0 min, and reequilibration at 5% B for 2.0 min. The injection volume was 3.5 µL. The mass spectrometer was operated in negative electrospray ionization using the following source parameters: capillary voltage -2 kV, cone voltage -25V, source temperature 150°C, desolvation gas temperature and flow 500°C and 1000 l/h, respectively, cone gas flow 350 l/h, nebulizer gas flow 7 bars. The multiple reaction monitoring (MRM) mode was used to detect both molecules with high sensitivity (MRM transitions for GGPP 449>79, 369>79 and 369>97; MRM transitions for GGP 369>79 and 369>97). GGPP eluted at a retention time of 2.56 min while GGP eluted at 3.19 min. For quantification, the standard addition method was used, with calibration standards at 5, 15, and 30 ng/mL and 1, 3, and 6 ng/mL for GGPP and GGP, respectively. Limits of quantifications for GGPP and GGP were 5 and 1 ng/g FW, respectively.

5.5.12 Primary metabolites analysis

Primary metabolites were extracted from lyophilized fruit pericarp of WT and *slabc1k1* (Giavalisco, P. *et al.,* 2011). The quantification and annotation as described previously (Alseekh, S. *et al.,* 2022).

5.5.13 Statistics

All data in this study were the means of two independent experiments and the result of four biological (n=3 or 4) and four technical (t=2 or 4) replicates. No data were excluded from the analysis. The results were analyzed and compared for the statistical difference by a two-sample, unequal variance (heteroscedastic) Student's t-test.

5.6 References

1. Alba, R., Payton, P., Fei, Z., McQuinn, R., Debbie, P., Martin, G.B., Tanksley, S.D., and Giovannoni, J.J. (2005). Transcriptome and selected metabolite analyses reveal multiple points of ethylene control during tomato fruit development. Plant Cell *17*, 2954-2965. 10.1105/tpc.105.036053.

2. Ampomah-Dwamena, C., Tomes, S., Thrimawithana, A.H., Elborough, C., Bhargava, N., Rebstock, R., Sutherland, P., Ireland, H., Allan, A.C., and Espley, R.V. (2022). Overexpression of PSY1 increases fruit carotenoid content and reveals associated transcription factors in apple (Malus x domestica Borkh). Front Plant Sci, 2986.

3. Austin, J.R., 2nd, Frost, E., Vidi, P.A., Kessler, F., and Staehelin, L.A. (2006). Plastoglobules are lipoprotein subcompartments of the chloroplast that are permanently coupled to thylakoid membranes and contain biosynthetic enzymes. Plant Cell *18*, 1693-1703. 10.1105/tpc.105.039859.

4. Balibrea, M.E., Martínez-Andújar, C., Cuartero, J., Bolarín, M.C., and Pérez-Alfocea, F. (2006). The high fruit soluble sugar content in wild Lycopersicon species and their hybrids with cultivars depends on sucrose import during ripening rather than on sucrose metabolism. Funct Plant Biol *33*, 279-288. 10.1071/fp05134.

5. Bauchet, G., Grenier, S., Samson, N., Segura, V., Kende, A., Beekwilder, J., Cankar, K., Gallois, J.-L., Gricourt, J., Bonnet, J., et al. (2017). Identification of major loci and genomic regions controlling acid and volatile content in tomato fruit: implications for flavor improvement. New Phytologist *215*, 624-641. https://doi.org/10.1111/nph.14615.

6. Beauvoit, B.P., Colombié, S., Monier, A., Andrieu, M.H., Biais, B., Bénard, C., Chéniclet, C., Dieuaide-Noubhani, M., Nazaret, C., Mazat, J.P., and Gibon, Y. (2014). Model-assisted analysis of sugar metabolism throughout tomato fruit development reveals enzyme and carrier properties in relation to vacuole expansion. Plant Cell *26*, 3224-3242. 10.1105/tpc.114.127761.

7. Berman, J., Zorrilla-López, U., Sandmann, G., Capell, T., Christou, P., and Zhu, C. (2017). The silencing of carotenoid β-hydroxylases by RNA interference in different maize genetic backgrounds increases the β-carotene content of the endosperm. International journal of molecular sciences *18*, 2515.

8. Bersuker, K., Hendricks, J.M., Li, Z., Magtanong, L., Ford, B., Tang, P.H., Roberts, M.A., Tong, B., Maimone, T.J., and Zoncu, R. (2019). The CoQ oxidoreductase FSP1 acts parallel to GPX4 to inhibit ferroptosis. Nature *575*, 688-692.

9. Bramley, P.M. (2002). Regulation of carotenoid formation during tomato fruit ripening and development. Journal of Experimental Botany *53*, 2107-2113. 10.1093/jxb/erf059.

10. Carrari, F., and Fernie, A.R. (2006). Metabolic regulation underlying tomato fruit development. Journal of Experimental Botany *57*, 1883-1897. 10.1093/jxb/erj020.

11. Carroll, D. (2012). A CRISPR approach to gene targeting. Molecular Therapy *20*, 1658-1660.

12. Chayut, N., Yuan, H., Ohali, S., Meir, A., Sa'ar, U., Tzuri, G., Zheng, Y., Mazourek, M., Gepstein, S., and Zhou, X. (2017). Distinct mechanisms of the ORANGE protein in controlling carotenoid flux. Plant Physiology *173*, 376-389.

13. Coman, D., Altenhoff, A., Zoller, S., Gruissem, W., and Vranová, E. (2014). Distinct evolutionary strategies in the GGPPS family from plants. Front Plant Sci *5*, 230. 10.3389/fpls.2014.00230.

14. Degenhardt, J., Köllner, T.G., and Gershenzon, J. (2009). Monoterpene and sesquiterpene synthases and the origin of terpene skeletal diversity in plants. Phytochemistry *70*, 1621-1637.

15. Do, T.Q., Hsu, A.Y., Jonassen, T., Lee, P.T., and Clarke, C.F. (2001). A Defect in Coenzyme Q Biosynthesis Is Responsible for the Respiratory Deficiency in Saccharomyces cerevisiae abc1Mutants*. Journal of Biological Chemistry *276*, 18161-18168. https://doi.org/10.1074/jbc.M100952200.

16. Doll, S., Freitas, F.P., Shah, R., Aldrovandi, M., da Silva, M.C., Ingold, I., Goya Grocin, A., Xavier da Silva, T.N., Panzilius, E., and Scheel, C.H. (2019). FSP1 is a glutathione-independent ferroptosis suppressor. Nature *575*, 693-698.

17. Espinoza-Corral, R., and Lundquist, P.K. (2022). The plastoglobule-localized protein AtABC1K6 is a Mn2+-dependent kinase necessary for timely transition to reproductive growth. Journal of Biological Chemistry *298*, 101762. https://doi.org/10.1016/j.jbc.2022.101762.

18. Farcuh, M., Li, B., Rivero, R.M., Shlizerman, L., Sadka, A., and Blumwald, E. (2017). Sugar metabolism reprogramming in a non-climacteric bud mutant of a climacteric plum fruit during development on the tree. J Exp Bot *68*, 5813-5828. 10.1093/jxb/erx391.

19. Feder, A., Chayut, N., Gur, A., Freiman, Z., Tzuri, G., Meir, A., Saar, U., Ohali, S., Baumkoler, F., and Gal-On, A. (2019). The role of carotenogenic metabolic flux in carotenoid accumulation and chromoplast differentiation: lessons from the melon fruit. Front Plant Sci *10*, 1250.

20. Feng, Z., Zhang, B., Ding, W., Liu, X., Yang, D.-L., Wei, P., Cao, F., Zhu, S., Zhang, F., and Mao, Y. (2013). Efficient genome editing in plants using a CRISPR/Cas system. Cell research *23*, 1229-1232.

21. Fraser, P.D., Kiano, J.W., Truesdale, M.R., Schuch, W., and Bramley, P.M. (1999). Phytoene synthase-2 enzyme activity in tomato does not contribute to carotenoid synthesis in ripening fruit. Plant molecular biology *40*, 687-698.

22. Fraser, P.D., Romer, S., Shipton, C.A., Mills, P.B., Kiano, J.W., Misawa, N., Drake, R.G., Schuch, W., and Bramley, P.M. (2002). Evaluation of transgenic tomato plants expressing an additional phytoene synthase in a fruit-specific manner. Proceedings of the National Academy of sciences *99*, 1092-1097.

23. Gady, A.L., Vriezen, W.H., Van de Wal, M.H., Huang, P., Bovy, A.G., Visser, R.G., and Bachem, C.W. (2012). Induced point mutations in the phytoene synthase 1 gene cause differences in carotenoid content during tomato fruit ripening. Mol Breed *29*, 801-812. 10.1007/s11032-011-9591-9.

24. Galpaz, N., Ronen, G., Khalfa, Z., Zamir, D., and Hirschberg, J. (2006). A chromoplast-specific carotenoid biosynthesis pathway is revealed by cloning of the tomato white-flower locus. The Plant Cell *18*, 1947-1960.

25. Gao, H., Zhu, H., Shao, Y., Chen, A., Lu, C., Zhu, B., and Luo, Y. (2008). Lycopene Accumulation Affects the Biosynthesis of Some Carotenoid-related Volatiles Independent of Ethylene in Tomato. Journal of Integrative Plant Biology *50*, 991-996. https://doi.org/10.1111/j.1744-7909.2008.00685.x.

26. Heath, J.J., Cipollini, D.F., and Stireman Iii, J.O. (2013). The role of carotenoids and their derivatives in mediating interactions between insects and their environment. Arthropod-Plant Interactions *7*, 1-20. 10.1007/s11829-012-9239-7.

27. Kang, B., Gu, Q., Tian, P., Xiao, L., Cao, H., and Yang, W. (2014). A chimeric transcript containing Psy1 and a potential mRNA is associated with yellow flesh color in tomato accession PI 114490. Planta *240*, 1011-1021. 10.1007/s00425-014-2052-z.

28. Kannan, N., Taylor, S.S., Zhai, Y., Venter, J.C., and Manning, G. (2007). Structural and functional diversity of the microbial kinome. PLoS biology *5*, e17.

29. Kemmerer, Z.A., Robinson, K.P., Schmitz, J.M., Manicki, M., Paulson, B.R., Jochem, A., Hutchins, P.D., Coon, J.J., and Pagliarini, D.J. (2021). UbiB proteins regulate cellular CoQ distribution in Saccharomyces cerevisiae. Nature Communications *12*, 4769. 10.1038/s41467-021-25084-7.

30. Leonard, C.J., Aravind, L., and Koonin, E.V. (1998). Novel families of putative protein kinases in bacteria and archaea: evolution of the “eukaryotic” protein kinase superfamily. Genome research *8*, 1038-1047.

31. Li, X., Wang, Y., Chen, S., Tian, H., Fu, D., Zhu, B., Luo, Y., and Zhu, H. (2018). Lycopene Is Enriched in Tomato Fruit by CRISPR/Cas9-Mediated Multiplex Genome Editing. Front Plant Sci *9*. 10.3389/fpls.2018.00559.

32. Liu, L. (2016). Ultramicroscopy reveals that senescence induces in-situ and vacuolar degradation of plastoglobules in aging watermelon leaves. Micron *80*, 135-144.

33. Liu, L., and Fan, X.-D. (2014). CRISPR–Cas system: a powerful tool for genome engineering. Plant molecular biology *85*, 209-218.

34. Lois, L.M., Rodríguez-Concepción, M., Gallego, F., Campos, N., and Boronat, A. (2000). Carotenoid biosynthesis during tomato fruit development: regulatory role of 1-deoxy-D-xylulose 5-phosphate synthase. Plant J *22*, 503-513. 10.1046/j.1365-313x.2000.00764.x.

35. Lopez, A.B., Van Eck, J., Conlin, B.J., Paolillo, D.J., O'Neill, J., and Li, L. (2008). Effect of the cauliflower Or transgene on carotenoid accumulation and chromoplast formation in transgenic potato tubers. Journal of experimental botany *59*, 213-223.

36. Lundquist, P.K., Davis, J.I., and van Wijk, K.J. (2012a). ABC1K atypical kinases in plants: filling the organellar kinase void. Trends Plant Sci *17*, 546-555. 10.1016/j.tplants.2012.05.010.

37. Lundquist, P.K., Poliakov, A., Bhuiyan, N.H., Zybailov, B., Sun, Q., and van Wijk, K.J. (2012b). The functional network of the Arabidopsis plastoglobule proteome based on quantitative proteomics and genome-wide coexpression analysis. Plant physiology *158*, 1172-1192. 10.1104/pp.111.193144.

38. Lundquist, P.K., Poliakov, A., Giacomelli, L., Friso, G., Appel, M., McQuinn, R.P., Krasnoff, S.B., Rowland, E., Ponnala, L., Sun, Q., and van Wijk, K.J. (2013). Loss of Plastoglobule Kinases ABC1K1 and ABC1K3 Causes Conditional Degreening, Modified Prenyl-Lipids, and Recruitment of the Jasmonic Acid Pathway. The Plant Cell *25*, 1818-1839. 10.1105/tpc.113.111120.

39. Martinis, J., Glauser, G., Valimareanu, S., and Kessler, F. (2013). A Chloroplast ABC1-like Kinase Regulates Vitamin E Metabolism in Arabidopsis Plant Physiology *162*, 652-662. 10.1104/pp.113.218644.

40. Martinis, J., Glauser, G., Valimareanu, S., Stettler, M., Zeeman, S.C., Yamamoto, H., Shikanai, T., and Kessler, F. (2014). ABC1K1/PGR6 kinase: a regulatory link between photosynthetic activity and chloroplast metabolism. The Plant Journal *77*, 269-283. https://doi.org/10.1111/tpj.12385.

41. Okada, K., Saito, T., Nakagawa, T., Kawamukai, M., and Kamiya, Y. (2000). Five geranylgeranyl diphosphate synthases expressed in different organs are localized into three subcellular compartments in Arabidopsis. Plant physiology *122*, 1045-1056.

42. Pagliarini, D.J., Calvo, S.E., Chang, B., Sheth, S.A., Vafai, S.B., Ong, S.-E., Walford, G.A., Sugiana, C., Boneh, A., and Chen, W.K. (2008). A mitochondrial protein compendium elucidates complex I disease biology. Cell *134*, 112-123.

43. Poon, W.W., Davis, D.E., Ha, H.T., Jonassen, T., Rather, P.N., and Clarke, C.F. (2000). Identification of Escherichia coli ubiB, a gene required for the first monooxygenase step in ubiquinone biosynthesis. J Bacteriol *182*, 5139-5146. 10.1128/jb.182.18.5139-5146.2000.

44. Pralon, T., Collombat, J., Pipitone, R., Ksas, B., Shanmugabalaji, V., Havaux, M., Finazzi, G., Longoni, P., and Kessler, F. (2020). Mutation of the Atypical Kinase ABC1K3 Partially Rescues the PROTON GRADIENT REGULATION 6 Phenotype in Arabidopsis thaliana. Front Plant Sci *11*. 10.3389/fpls.2020.00337.

45. Pralon, T., Shanmugabalaji, V., Longoni, P., Glauser, G., Ksas, B., Collombat, J., Desmeules, S., Havaux, M., Finazzi, G., and Kessler, F. (2019). Plastoquinone homoeostasis by Arabidopsis proton gradient regulation 6 is essential for photosynthetic efficiency. Communications Biology *2*, 220. 10.1038/s42003-019-0477-4.

46. Pulido, P., Perello, C., and Rodriguez-Concepcion, M. (2012). New insights into plant isoprenoid metabolism. Molecular plant *5*, 964-967.

47. Quinet, M., Angosto, T., Yuste-Lisbona, F.J., Blanchard-Gros, R., Bigot, S., Martinez, J.-P., and Lutts, S. (2019). Tomato Fruit Development and Metabolism. Front Plant Sci *10*.

48. Reidenbach, A.G., Kemmerer, Z.A., Aydin, D., Jochem, A., McDevitt, M.T., Hutchins, P.D., Stark, J.L., Stefely, J.A., Reddy, T., Hebert, A.S., et al. (2018). Conserved Lipid and Small-Molecule Modulation of COQ8 Reveals Regulation of the Ancient Kinase-like UbiB Family. Cell Chem Biol *25*, 154-165.e111. 10.1016/j.chembiol.2017.11.001.

49. Rodríguez-Concepción, M., and Boronat, A. (2015). Breaking new ground in the regulation of the early steps of plant isoprenoid biosynthesis. Current Opinion in Plant Biology *25*, 17-22. https://doi.org/10.1016/j.pbi.2015.04.001.

50. Schaffer, A.A., and Petreikov, M. (1997). Sucrose-to-Starch Metabolism in Tomato Fruit Undergoing Transient Starch Accumulation. Plant Physiology *113*, 739-746. 10.1104/pp.113.3.739.

51. Schauer, N., Zamir, D., and Fernie, A.R. (2005). Metabolic profiling of leaves and fruit of wild species tomato: a survey of the Solanum lycopersicum complex. Journal of experimental botany *56*, 297-307.

52. Shikanai, T., Munekage, Y., Shimizu, K., Endo, T., and Hashimoto, T. (1999). Identification and characterization of Arabidopsis mutants with reduced quenching of chlorophyll fluorescence. Plant Cell Physiol *40*, 1134-1142. 10.1093/oxfordjournals.pcp.a029498.

53. Sorrequieta, A., Ferraro, G., Boggio, S.B., and Valle, E.M. (2010). Free amino acid production during tomato fruit ripening: a focus on l-glutamate. Amino Acids *38*, 1523-1532. 10.1007/s00726-009-0373-1.

54. Stefely, J.A., Reidenbach, A.G., Ulbrich, A., Oruganty, K., Floyd, B.J., Jochem, A., Saunders, J.M., Johnson, I.E., Minogue, C.E., Wrobel, R.L., et al. (2015). Mitochondrial ADCK3 employs an atypical protein kinase-like fold to enable coenzyme Q biosynthesis. Mol Cell *57*, 83-94. 10.1016/j.molcel.2014.11.002.

55. Sun, L., Wang, J., Lian, L., Song, J., Du, X., Liu, W., Zhao, W., Yang, L., Li, C., Qin, Y., and Yang, R. (2022). Systematic analysis of the sugar accumulation mechanism in sucrose- and hexose-accumulating cherry tomato fruits. BMC Plant Biol *22*, 303. 10.1186/s12870-022-03685-8.

56. Tan, T., Özbalci, C., Brügger, B., Rapaport, D., and Dimmer, K.S. (2013). Mcp1 and Mcp2, two novel proteins involved in mitochondrial lipid homeostasis. Journal of cell science *126*, 3563-3574.

57. Tholl, D. (2015). Biosynthesis and biological functions of terpenoids in plants. Biotechnology of isoprenoids, 63-106.

58. Tuquet, C., and Newman, D.W. (1980). Aging and regreening in soybean cotyledons. 1 Ultrastructural changes in plastids and plastoglobuli. Cytobios *29*, 43-59.

59. Vidi, P.-A., Kanwischer, M., Baginsky, S., Austin, J.R., Csucs, G., Dörmann, P., Kessler, F., and Bréhélin, C. (2006). Tocopherol Cyclase (VTE1) Localization and Vitamin E Accumulation in Chloroplast Plastoglobule Lipoprotein Particles. *281*, 11225-11234. 10.1074/jbc.M511939200.

60. Vranová, E., Coman, D., and Gruissem, W. (2013). Network analysis of the MVA and MEP pathways for isoprenoid synthesis. Annu Rev Plant Biol *64*, 665-700.

61. Vrebalov, J., Ruezinsky, D., Padmanabhan, V., White, R., Medrano, D., Drake, R., Schuch, W., and Giovannoni, J. (2002). A MADS-Box Gene Necessary for Fruit Ripening at the Tomato <i>Ripening-Inhibitor </i>(<i>Rin</i>) Locus. Science *296*, 343-346. doi:10.1126/science.1068181.

62. Walter, M.H., Floss, D.S., and Strack, D. (2010). Apocarotenoids: hormones, mycorrhizal metabolites and aroma volatiles. Planta *232*, 1-17. 10.1007/s00425-010-1156-3.

63. Wang, R., Lammers, M., Tikunov, Y., Bovy, A.G., Angenent, G.C., and de Maagd, R.A. (2020). The rin, nor and Cnr spontaneous mutations inhibit tomato fruit ripening in additive and epistatic manners. Plant Science *294*, 110436. https://doi.org/10.1016/j.plantsci.2020.110436.

64. Xie, K., Minkenberg, B., and Yang, Y. (2015). Boosting CRISPR/Cas9 multiplex editing capability with the endogenous tRNA-processing system. Proceedings of the National Academy of Sciences *112*, 3570-3575.

65. Ytterberg, A.J., Peltier, J.B., and van Wijk, K.J. (2006). Protein profiling of plastoglobules in chloroplasts and chromoplasts. A surprising site for differential accumulation of metabolic enzymes. Plant Physiol *140*, 984-997. 10.1104/pp.105.076083.

66. Zanor, M.I., Rambla, J.L., Chaïb, J., Steppa, A., Medina, A., Granell, A., Fernie, A.R., and Causse, M. (2009). Metabolic characterization of loci affecting sensory attributes in tomato allows an assessment of the influence of the levels of primary metabolites and volatile organic contents. J Exp Bot *60*, 2139-2154. 10.1093/jxb/erp086.

67. Zita, W., Bressoud, S., Glauser, G., Kessler, F., and Shanmugabalaji, V. (2022). Chromoplast plastoglobules recruit the carotenoid biosynthetic pathway and contribute to carotenoid accumulation during tomato fruit maturation. PLOS ONE *17*, e0277774. 10.1371/journal.pone.0277774.

5.7 Supplementary

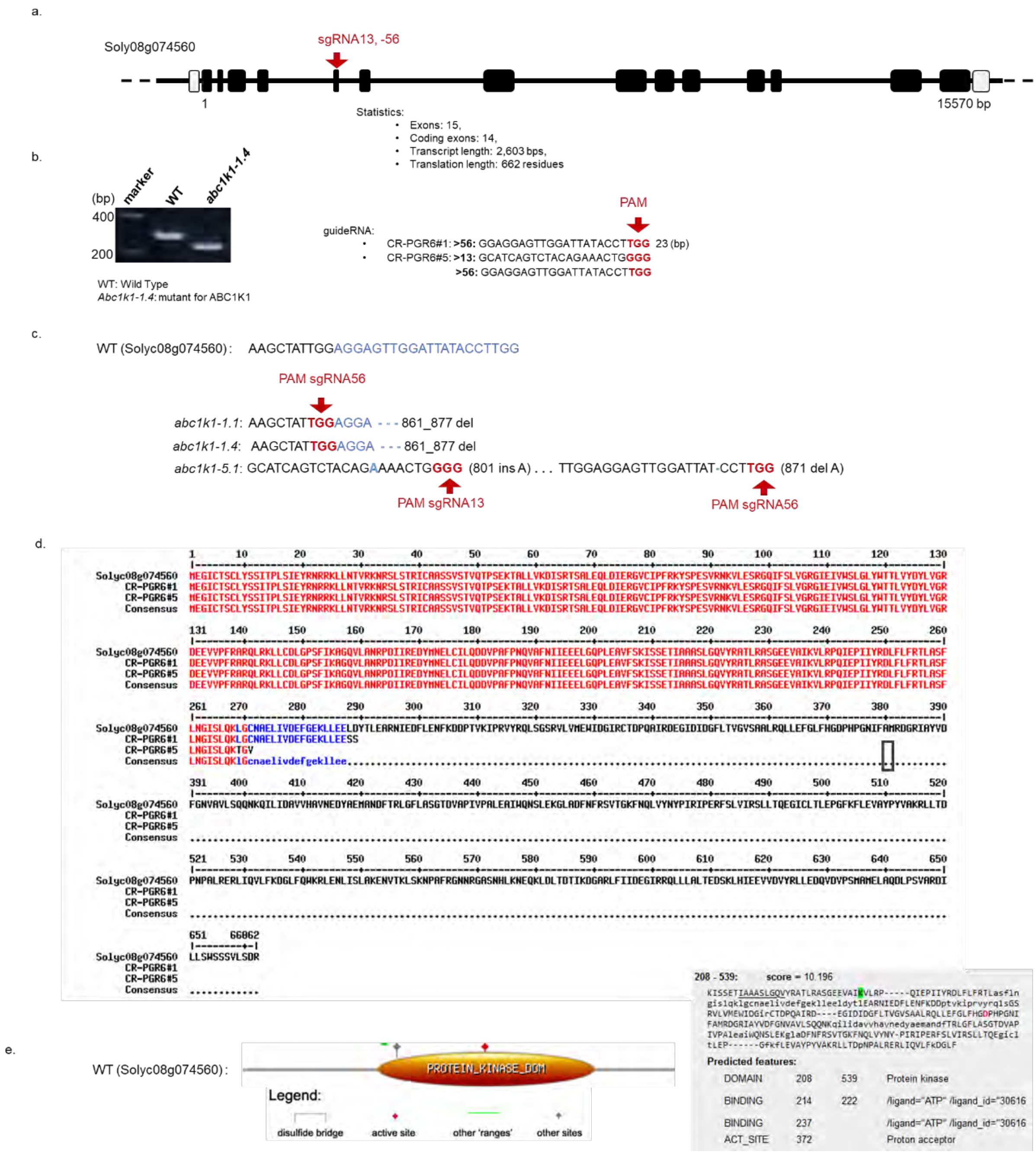

208 - 539: score = 10.196

```
KISSETIAAASLGQVYRATLRASGEEVAIKVLRP-----QIEPIIYRDLFLFRTLasfln
gislqklgcnaelivdefgeklleeldytlEARNIEDFLENFKDDptvkiprvyrqlsGS
RVLVMEWIDGirCTDPQAIRD----EGIDIDGFLTVGVSAALRQLLEFGLFHGDPHPGNI
FAMRDGRIAYVDFGNVAVLSQQNKqilidavvhavnedyaemandfTRLGFLASGTDVAP
IVPAleaiWQNSLEKglaDFNFRSVTGKFNQLVYNY-PIRIPERFSLVIRSLLTQEgicl
tLEP------GfkfLEVAYPYVAKRLLTDpNPALRERLIQVLFkDGLF
```

Predicted features:

DOMAIN	208	539	Protein kinase
BINDING	214	222	/ligand="ATP" /ligand_id="30616
BINDING	237		/ligand="ATP" /ligand_id="30616
ACT_SITE	372		Proton acceptor

FIG.S1| **Tomato *abc1k1* genotyping.** a) Graphic view of Solyc08g074560. black rectangles show exons, red arrow indicates the position of the mutations. b) PCR amplicon encompass the sgRNAs targeted the exon 5. c) Sequence of the *abc1k1-1.1 and -.4/pgr6#1* and *abc1k1-5/pgr6#5* mutants. d) Amino acids sequence alignment of WT (Solyc08g074560) and *abc1k1-1/pgr6#1(cr-PGR6#1)* and *abc1k1-5/pgr6#5(cr-PGR6#5)* CRISPR mutants using Multalin (v5.4.1). The gray rectangle shows the predicted active site of protein kinase domain. e) Representation of WT protein with predicted kinase domain annotate generated by PROSITE (Expasy) (Hulo N *et al.,* 2008). The red diamond shows the amino acid required to kinase activity.

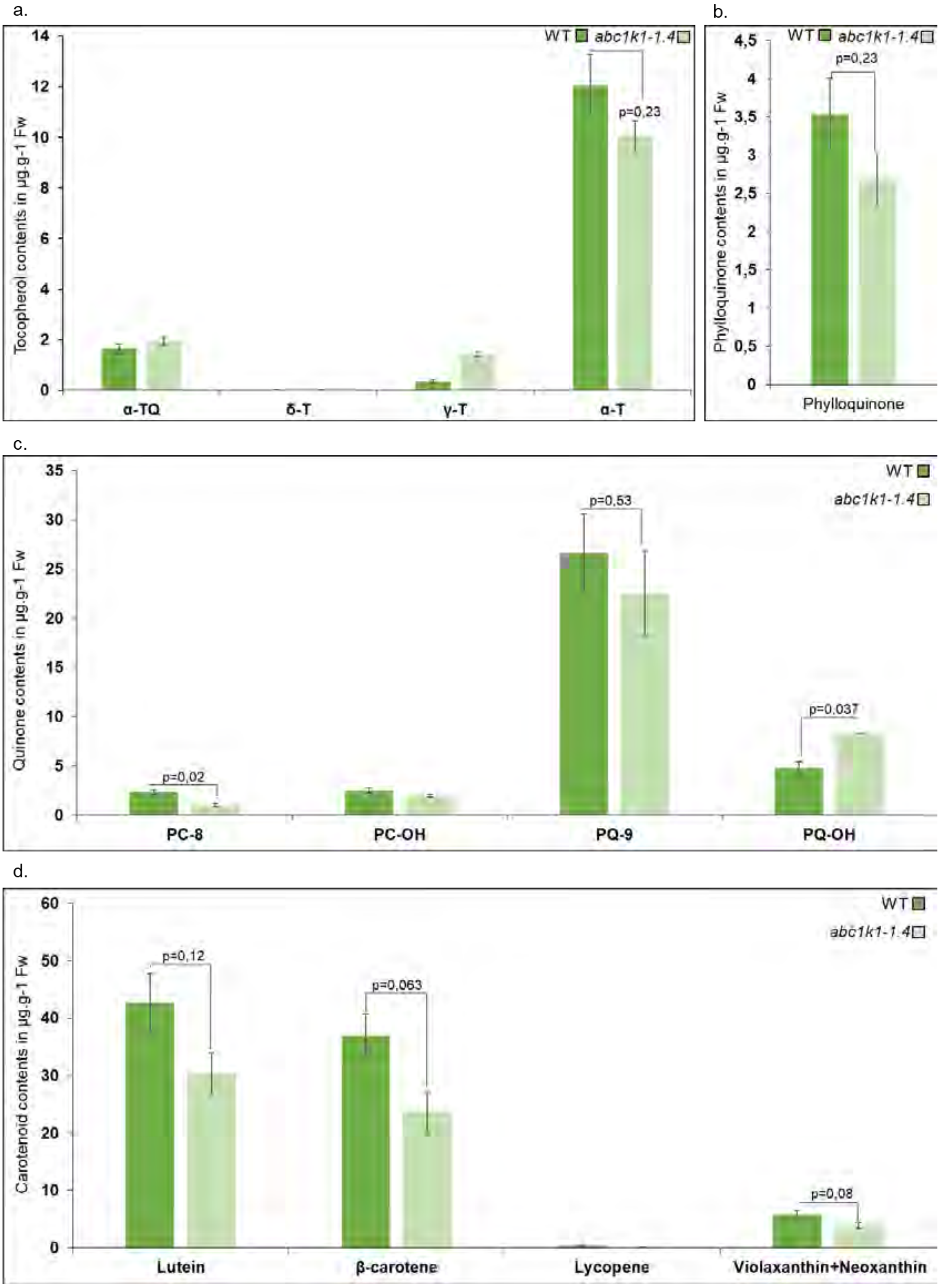

FIG.S2| **Prenyllipid concentration of mature tomato leaves of WT and *abc1k1* mutant lines analyzed by UHPLC.** The total prenyl-lipids were extract of leaves from WT and *abc1k1-1.4* adult plants grown under moderate light (140 µmol m^{-2} s^{-1}). a) α-TQ, alpha tocoquinone; δ-T, delta tocopherol; γ-T, gamma tocopherol and α-T, alpha tocopherol. b)Phylloquinone (vitamin K_1). c) PC-8, plastochromanol; PC-OH, hydroxy-plastochromanol; PQ-9, plastoquinone; and PQ-OH, hydroxy-plastoquinone. The prenyl-lipids were extracted from WT and *abc1k1-1.4* and were analyzed by using UHPLC-APCI-QTOF-MS. All values in the figures are the mean of 3 biological replicates (n = 3). Statistical differences were assessed with student's t test and ***p*** values are indicated

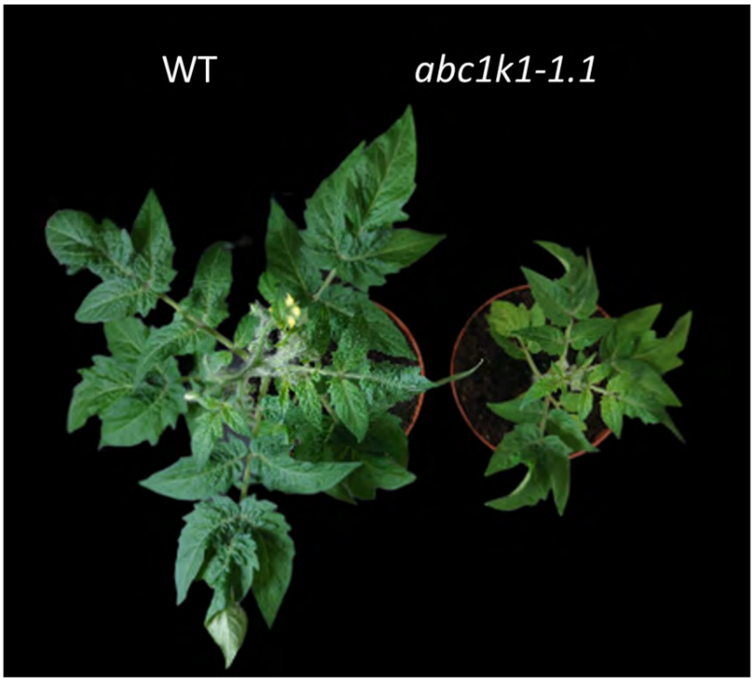

FIG.S3| ***abc1k1-1.1* and WT plants grown under ML conditions**.

Visible phenotype of WT and *abc1k1-1.4* plants

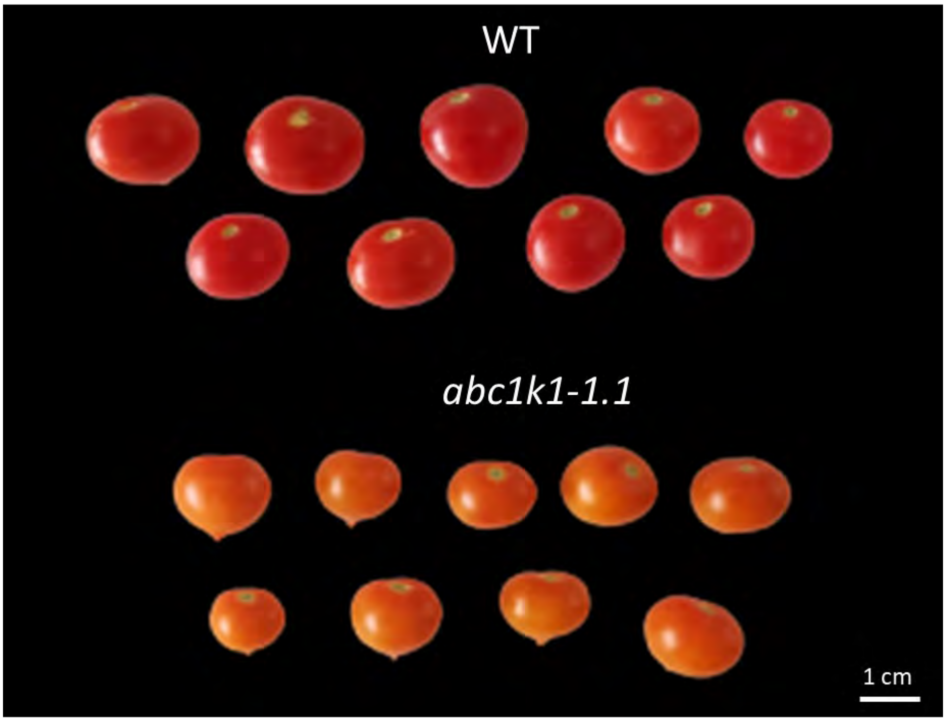

FIG.S3|**Visible observation of *abc1k1-1.1* and WT.**

Visible phenotype of WT and *abc1k1-1.4* tomato fruits.

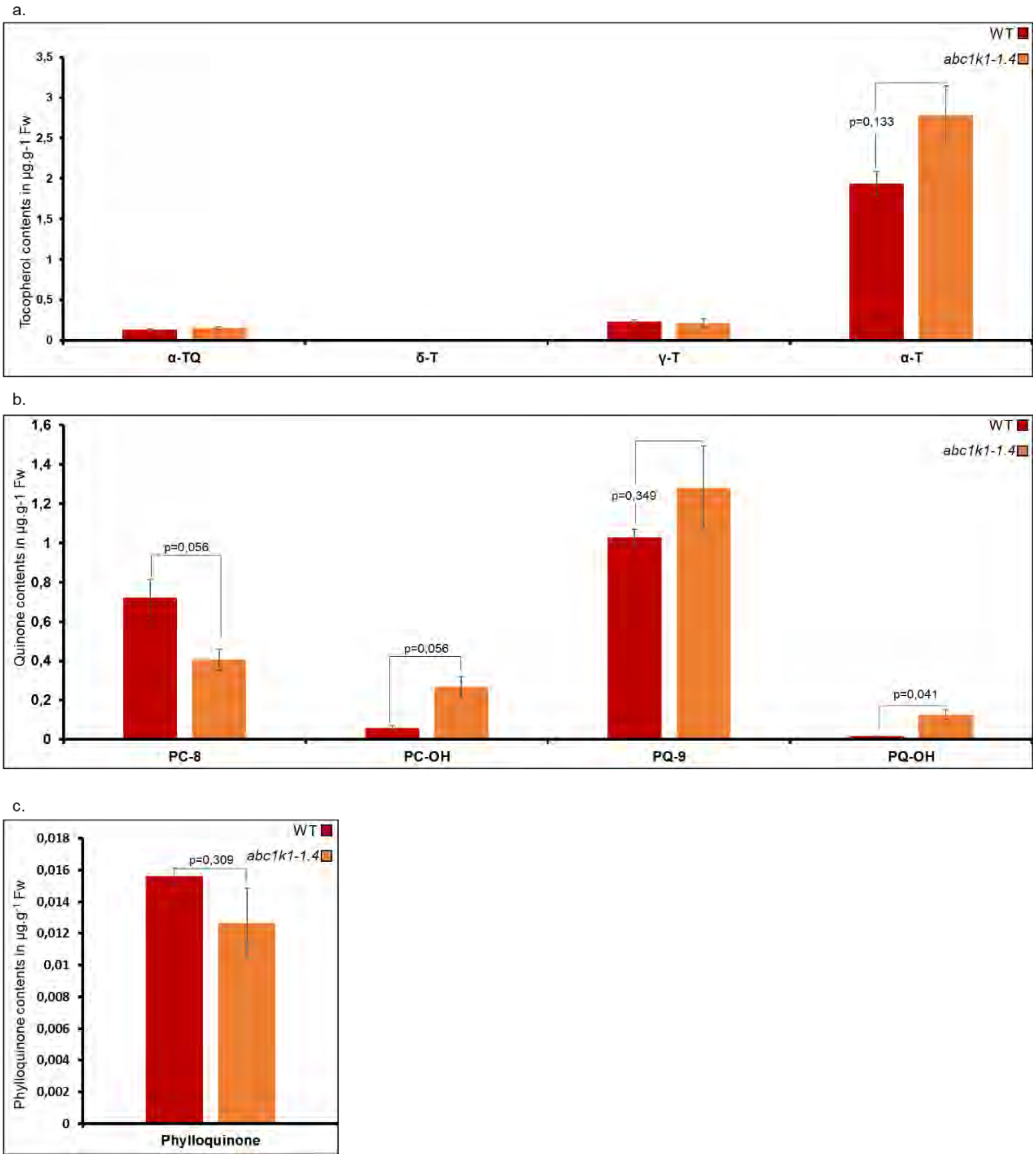

FIG.S4| ***abc1k1* and WT tomato fruits prenyl-lipid analysis by UHPLC**. a) The total prenyl-lipids were extracted from fruits extract WT and *abc1k1-1.4* grown under moderate light (140 µmol m^{-2} s^{-1}). a) α-TQ, alpha tocoquinone; δ-T, delta tocopherol; γ-T, gamma tocopherol and α-T, alpha tocopherol. b)Phylloquinone (vitamin K$_1$). c) PC-8, plastochromanol; PC-OH, hydroxy-plastochromanol; PQ-9, plastoquinone; and PQ-OH, hydroxy-plastoquinone. The prenyl-lipids were extracted from WT and *abc1k1-1.4* and were analyzed by using UHPLC-APCI-QTOF-MS. All values in the figures are the mean of 3 biological replicates (n = 3). Statistical differences were assessed with student's t test and ***p*** values are indicated

Table S1| **List of primers**

Primers name	primer sequence 5'-3'	Tm °C	gene name and id	references:
PSY1-Fw	AGAGGTGGTGGAAAGCAA	55	phytoene synthase (PSY)|Solyc03g031860	(D'Andrea, L. et al., 2018)
PSY1-Rv	TCTCGGGAGTCATTAGCAT			
PDS-F	GCTTTACCCGCTCCTTTA	54	phytoene desaturase (PDS)| Solyc03g123760	
PDS-R	ACCTTGCTTTCTCATCCA			
CRTISO-F	GATCGCCAAATCCTTAGCAA	55.5	carotenoid isomerase (CRTISO)| Solyc10g081650	(Suzuki, M. et al., 2015)
CRTISO-R	GCCCTGGGAAGAGTGTTTTT			
LCYB-Fw	TTGACTTAGAACCTCGTTATTGG	54.9	lycopene β–cyclase (LCYB)|Solyc10g079480	(D'Andrea, L. et al., 2018)
LCYB-Rv	AACAGTTCCCTTTGTCATTATCTC			
RIN-Fw	CATCATGGCATTGTGGTGAGC	59	ripening inhibitor (RIN)|Solyc05g012020	
RIN-Rv	AATTCAAAGCATCCATCCAGGTAC			
NR-Fw	CTCCCAGAGGCAGATTGAAC	57	never ripe (NR)|Solyc09g075440	(Yazdani, M. et al., 2019) (D'Andrea, L. et al., 2018)
NR-Rv	TTCACAGACATCCCACCATC			
ACT-Fw	CCTTCCACATGCCATTCTCC	57.9	ACTIN|Solyc04g011500	
ACT-Rv	CCACGCTCGGTCAGGATCT			

References:

Expósito-Rodríguez M, Borges AA, Borges-Pérez A, Pérez JA. 2008. Selection of internal control genes for quantitative real-time RT-PCR studies during tomato development process. BMC Plant Biology 8, 131.

González-Aguilera KL, Saad CF, Chávez Montes RA, Alves-Ferreira M, de Folter S. 2016. Selection of Reference Genes for Quantitative Real-Time RT-PCR Studies in Tomato Fruit of the Genotype MT-Rg1. Frontiers in Plant Science 7, 1386.

Rodríguez-Concepción M, Forés O, Martínez-García JF, González V, Phillips MA, Ferrer A, Boronat A. 2004. Distinct Light-Mediated Pathways Regulate the Biosynthesis and Exchange of Isoprenoid Precursors during Arabidopsis Seedling Development. Plant Cell 16, 144-156.

6. General conclusion

We have discussed of all data provided in this thesis in each chapter nested upstream. I will now give an overall view and general conclusion of my thesis.

Tomato (*Solanum lycopersicum*) is a powerful crop model system used to investigate the maturation and ripening processes in fleshy fruits. The studies on tomato as a model organism represent a real interest in agriculture applications, for its health benefits, and as an important nutrient sink.

The results highlighted in my thesis provide new insights into the tomato plastoglobule proteome and carotenoid biosynthesis during the fruit ripening process.

Chapter I reviewed the plastoglobule proteome in Arabidopsis and bell pepper to highlight the structural and regulatory proteins,enzymes functions which are the fibrillin (**FBNs**) family, the **a**ctivity of **bc1** complex like-kinases (**ABC1Ks**), metabolic enzymes such as tocopherol cyclase (**VTE1**), phytyl ester synthase (**PES**) and **N**AD(P)H **D**EHYDROGENASE **C1** (**NDC1**) (Lundquist *et al.,* 2012; Vidi *et al.,* 2006; Ytterberg *et al.,* 2006; Eugeni Piller *et al.,* 2011).

In this context, Chapter II profiled the plastoglobule proteome during the chloroplast-to-chromoplast transition in tomato fruits. The most abundant regulatory proteins and enzymes known as plastoglobule markers were identified as FBNs, ABC1Ks, VTE1, and NDC1. The complete carotenoid pathway (PSY1, PDS, ZDS, and CRTISO) required for lycopene synthesis is recruited by plastoglobule during the chloroplast to chromoplast transition. The strong presence of the ABC1Ks protein family protein in the PG chromoplast has raised a central question for chapter IV of my thesis.

On the other hand, a method was developed in Chapter III, to quantify GGPP content in tomato fruit by using conventional ultra-high performance liquid chromatography coupled with tandem mass spectrometry (UHPLC-MS/MS). This method was able to detect ng level in tomato *slg2 and slg3* mutants defective in GGPP production, which demonstrates the sensibility of our method. In addition, µg level of GGPP was quantified in WT tomato fruit. In next chapter, we apply this method to investigate the role SlABC1K1 protein in tomato fruit.

In the next chapter (Chapter IV), the role of the ABC1K1/PGR6 protein in tomato plants and fruit development was investigated. ABC1K1 is implicated in photosynthesis as a proton gradient regulation 6 (PGR6) (Shikanai *et al.,* 1999; Martinis *et al.,* 2014). Recent studies revealed the role of ABC1K1 in the regulation of plastoquinone pool homeostasis (Pralon *et al.,* 2019).

To reveal the SlABC1K1 functions on fruit crop, we have engineered the knockout lines of the *SlABC1K1* gene (Solyc08g074560) in tomato (*Solanum lycopersicum cv* Micro-Tom). The SlABC1K1 mutant confirmed *prg6* phenotype consisting of the deficiency of ETR and NPQ. Surprisingly an orange fruit phenotype was observed in *abc1k1*mutant tomato. This observation was never reported before, highlighting the role of SlABC1K1 protein in fruit pigment accumulation. The low phytoene and lycopene levels measured in the fruit pericarps confirmed the orange color. In addition, plastoquinone, tocopherol, beta-carotene and lutein levels were constant in fruit pericarps reveals that SlABC1K1 is necessary for a carotenoid biosynthetic pathway at fruit chromoplast.

The analysis performed on carotenoid gene expression and the ripening markers revealed that *PSY1* was highly upregulated in *slabc1k1* mutant. PDS, ZDS, and CRTISO (carotenoid enzymes) and RN, RIN (ripening markers) did not show a significant difference. In addition, the PSY1 protein level a significantly increased in *slabc1k1*. In addition, analysis of primary metabolites shown that pyruvate and glyceraldehyde three phosphate which are required to initiate the MEP were accumulated in a sufficient extent in *slabc1k1*. We decided to investigate the geranylgeranyl diphosphate (**GGPP**), the primary build block required for fruit carotenoid biosynthesis as well as plastoquinone, phylloquinone, tocopherols, and gibberellin (M. Victoria Barja & Manuel Rodriguez-Concepcion, 2021).

Measurement of GGPP and its hydrolysis product GGP have been realized and revealed a high accumulation in *slabc1k1*than in the WT. Thus, the difference observed was approximately 3-fold higher in *slabc1k1* compared to WT. This result suggested that in absence of SlABC1K1 protein, the GGPP cannot be supplied to the carotenoid biosynthetic platform properly to produce lycopene to a good extent.

Finally, this work allowed us to identify a possible function of ABC1K1 protein during the fruit ripening process. It has been demonstrated by that PQ is retained in plastoglobule in the *abc1k1/pgr6* mutant lines (Pralon *et al.,* 2019). In addition, ABC1K1 and ABC1K3 (homolog of ABC1K1) are involved in the mobility and exchange of plastoquinone pool between plastoglobule and photosystems II and I (Pralon *et al.,* 2020). The recent studies led by (Kemmerer *et al.,* 2021) on protein homologs members of the ABC1K/UbiB family namely Cqd1 and Cqd2, demonstrated that these proteins influence the cellular distribution of mitochondria-derived CoQ. to the extramitochondrial membrane from the inner mitochondrial membrane (Kemmerer *et al.,* 2021).

These results have supported our findings on the role of SlABC1K1 protein in tomato and crop species more broadly. We have proposed that SlABC1K1 could be involved in metabolites distribution in chloroplast and chromoplast, via their conserved atypical kinase/ATPase domains activity.

In conclusion, to our knowledge, SlABC1K1 protein has been never reported as being involved in geranylgeranyl diphosphate trafficking or distribution. We are confident that this work provides new insight into carotenoid biosynthesis in tomato fruit and crop species. Our work provides a new approach to engineering carotenoid biosynthesis in crop species and improved fruit resistance, fortifications, and nutrients.

Future research needs to understand: How does ABC1K1 protein regulate metabolite fluxes in plastoglobules? The molecular mechanism between GGPP and ABC1K1 protein (docking assay with recombinant protein of ABC1K1 and the GGPP as being a ligand). What would be the profile of an ABC1K1 overexpressor? If the double mutants *slabc1k1* and *slabc1k3* could allow the recovery of the red fruit phenotype? These questions could be addressed in the future in a doctoral thesis.

7. Acknowledgments

First of all, I would like to thank Prof. Dr. Felix Kessler for giving me the opportunity to perform my Ph.D. thesis in his laboratory at University of Neuchâtel. He gave me very good advice and gave me the freedom to experiment.

I would also like to thank my supervisor Balaji for the supervision of my projects throughout my thesis, as well as for his numerous advices. I am so grateful for his support, following the cyber-attack, his encouragement, its good idea, reviews and positivity.

I also want to acknowledge Dr. Gaëtan Glauser of the NPAC platform, University of Neuchâtel, for his devotion in the development of the method for the geranylgeranyl diphosphate profiling by UHPLC-MS and for performing the lipidomics measurements.

I would like to thank Fiamma Longoni for nice discussion about photosynthetic parameters.

I am also grateful to Gregory Roeder and Marine Mamin for their precious collaboration for biological analysis in GC-MS and volatile profiling.

I do not want to forget to thank my colleagues and friends Hamed SATTARI VAYGHAN and Thibaut Pralon for his criticism and advice, but also our long and very constructive discussions.

I would like also to thanks Professor. Dr. Christophe Rothan from French National Institute for Agriculture, Food, and Environment (INRAE) Bordeaux (FRANCE) and Professor. Dr. Theodor Turlings for accepting to be members of my thesis committee.

I would like to thank the University of Neuchâtel Faculty Science and the Swiss National Funding (SNF) for providing funding, materials and space to work in order to complete my thesis.

I also thank my colleagues: Hamed SATTARI VAYGHAN, Thibaut Pralon, Ségolène Bressoud, Morgane Bouverot, Delphine Gaillard, Delphine Conges, Sonia ACCOSSATO, Rosa PIPITONE, Joy COLLOMBAT, Véronique DOUET, Bruno CABETE, Gautier PIZZOLON.

Finally, the last but not least thanks are for my lovely family particularly my wife, my mother and all my friends.

Thank you all.

9. Published manuscripts

Plastoglobules: A hub of lipid metabolism in the chloroplast

Venkatasalam Shanmugabalaji*, Wayne Zita, Joy Collombat, and Felix Kessler
Laboratoire de Physiologie Végétale, Université de Neuchâtel, Neuchâtel, Switzerland
*Corresponding author: e-mail address: shanmugabalaji.venkatasalam@unine.ch

Contents

Abstract

Chloroplasts in plant and algae are the home of photosynthesis and many essential metabolic pathways. The photosynthetic light reactions occur at an extensive membrane system, the thylakoids. The main constituents of thylakoid membranes are the galactolipids, in particular monogalactosyldiacylglycerol (MGDG) and digalactosyldiacylglycerol (DGDG). Apart from these, thylakoid membranes contain a number of other lipid molecules that function as electron transporters (plastoquinone) or as lipid antioxidants (tocopherols) and that are free to diffuse in the membrane system. Others such as phylloquinone, carotenoids and chlorophylls are mostly associated with protein components of the photosystems that reside in the thylakoids. The thylakoids are extremely dynamic and rapidly respond to environmental stresses. Plastoglobules (PG), lipoprotein

Advances in Botanical Research
ISSN 0065-2296
https://doi.org/10.1016/bs.abr.2021.09.002

particles or lipid droplets associated with thylakoids, play a central role in these responses. PG are thought to allocate stored electron carriers as well as lipid antioxidants to the membranes. PG also contribute to the enzymatic capacity for antioxidant and electron carrier synthesis and metabolism. During senescence and under nitrogen deprivation PG actively participate in membrane catabolism. PG become supersized while absorbing triacylglycerols and fatty acid phytol esters resulting from galactolipid and chlorophyll degradation. This chapter aims at giving a broad overview of the role of PG in chloroplast lipid metabolism.

1. Introduction

1.1 Discovery and history

The advent of electron microscopy as a tool in cellular biology in the late 1950s and 1960s allowed a first glimpse inside the plant cell and its subcellular structures. Among other features within the chloroplast the electron micrographs revealed the presence of globular structures. Osmium tetroxide stained these structures intensely which hence were called osmiophile globules. Due to their presence in many plastid types the name was later changed to plastoglobules (abbreviated PG) (Greenwood, Leech, & Williams, 1963; Lichtenthaler, 1968a; Spurr & Harris, 1968). These early studies carried out on multiple species revealed a diversity of osmiophile globules which varied in size (30 nm to several μm) and number under various environmental (for instance drought) or developmental conditions (for instance in older and younger leaves or fruit) (Lichtenthaler, 1968a; Thomson & Platt, 1973). Supersized PG, several μm in diameter, were readily observed in old and senescent leaves (Gaude, Bréhélin, Tischendorf, Kessler, & Dörmann, 2007; Tevini & Steinmuller, 1985). It was also observed that numerous PG were contained in the prolamellar body of etiolated, dark grown seedlings. When exposed to light the thylakoid system rapidly emerged and the number of PG diminished during the greening process. The authors noted this correlation and suggested that PG may contribute to the lipids of the developing photosynthetic membrane system (Lichtenthaler & Sprey, 1966).

It was quickly recognized that the globules were lipidic in nature and of low density, a property which allowed their isolation by flotation centrifugation. Isolated globules were subjected to biochemical analyses that revealed the presence of relatively large quantities of neutral lipids (mostly triacylglycerol (TAG), plastoquinone/plastoquinol (PQ/PQH$_2$)

Table 1 Lipids in PG from different plastid types.

Plastids	Enriched lipids	References
Chloroplast	Galactolipids DAG (diacylglycerol) TAG (triacylglycerol) α-Tocopherol (Vitamin E) Phylloquinone (Vitamin K1) Plastoquinone/ol (PQ/PQH2) Fatty acid phytyl esters	Steinmüller and Tevini (1985) Leggett Bailey and Whyborn (1963) Lichtenthaler (1968b) Lichtenthaler and Peveling (1966) Lippold et al. (2012)
Chromoplast	Triacylglycerol (TAG) Carotenoids Carotenoid esters Phytol α-Tocopherol (Vitamin E) Galactolipids	Hansmann and Sitte (1982) Deruère et al. (1994) Arango and Heise (1997)
Gerontoplast	Fatty acid phytyl esters Triacylglycerol (TAG)	Gaude et al. (2007) Steinmüller and Tevini (1985) Lippold et al. (2012)

and tocopherol) as well as smaller quantities of polar galactolipids and traces of protein (Table 1) (Gaude et al., 2007; Greenwood et al., 1963; Leggett Bailey & Whyborn, 1963; Lichtenthaler & Peveling, 1966; Tevini & Steinmuller, 1985). A model emerged in which a monolayer of polar galactolipids surrounded a lipophilic core (Fig. 1). The trace amounts of protein were not accounted for as individual proteins could not be identified at the time. The variations in size and number of PG in chloroplast and their correlation with the state of thylakoid membrane system suggested a dynamic relation between the two systems. The increase in PG size correlated with the disassembly of the thylakoid system during chloroplast senescence suggesting that PG function as a storage site for thylakoid membrane catabolites. In the absence of further evidence, PG were thought to function as passive lipid storage sites.

This model started to evolve only recently with the discovery of the PG protein components (Table 2) (Deruère et al., 1994; Kessler et al., 1999; Vidi et al., 2006; Ytterberg et al., 2006). Ensuing studies revealed that PG contained a set of enzymatic activities and participated in a multitude of lipid metabolic pathways associated with PG and thylakoids. It has now been

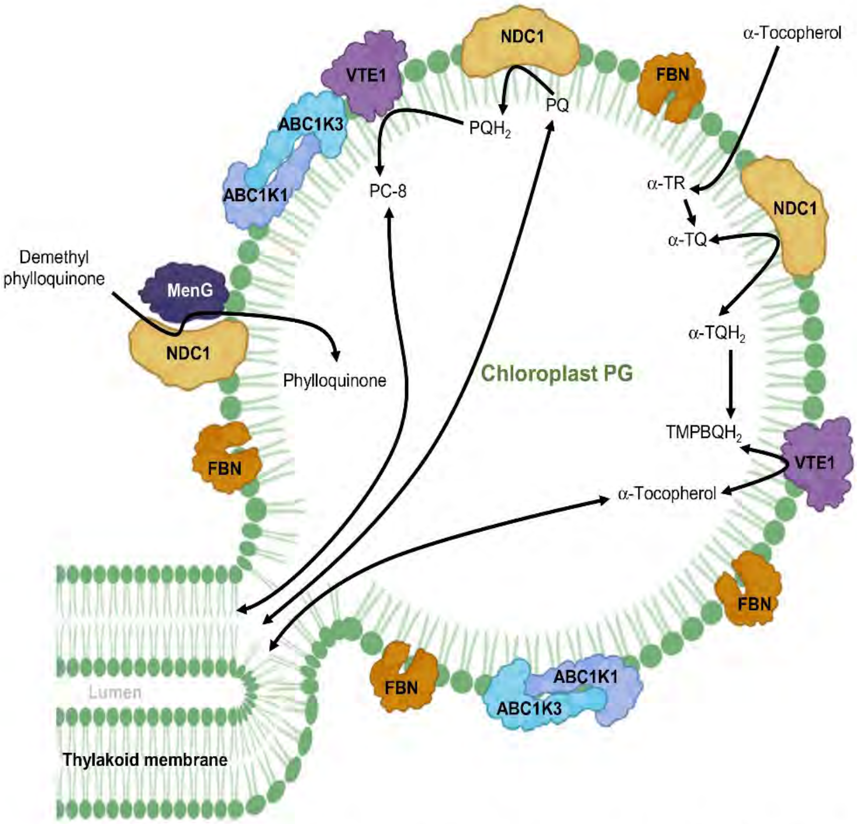

Fig. 1 Prenyl lipid metabolism in the chloroplast plastoglobule. Tocopherol cyclase (VTE1) catalyzes the biosynthesis of plastochromanol (PC8) from plastoquinol (PQH2) resulting from the prior reduction of PQ by type II NAD(P)H dehydrogenase C1 (NDC1). In addition, NDC1 derived trimethylbenzoquinol ($TMPBQH_2$) is converted to α-tocopherol by VTE1. ACTIVITY OF BC1-LIKE 1/3 KINASE (ABC1K1/ABC1K3) have been implicated in the regulation of VTE1 activity and may do so by directly phosphorylating VTE1. NDC1 reduces demethylphylloquinone promoting methylation by MenG resulting in phylloquinone synthesis. Abundant fibrillins (FBNs) are thought to have mainly structural roles. The tocopherol repair and recycling involve NDC1 and VTE1, specifically to convert α-tocopherolquinone (α-TQ) to α-tocopherol (α-T) in PG. Abbreviations: α-TQH2, α-tocopherolquinol; α-TR, α-tocopheroxyl radical

shown that PG even harbor regulatory functions (van Wijk & Kessler, 2017; Vidi et al., 2006; Ytterberg et al., 2006). To present these concepts, the present chapter will give an overview of the current state of knowledge on PG and their protein components. While most of the known functions pertain to prenyl lipids, attention will also be given to the role of PG in galactolipid metabolism.

Table 2 PG core proteins based on proteome studies in *Arabidopsis thaliana* and *Capsicum annuum*.

Protein name	**Accession**	**Functions**
Fibrillins		
Fibrillin 1a (FBN1a)	AT4G04020	Structural protein
Fibrillin 1b (FBN1b)	AT4G22240	
Fibrillin 2 (FBN2)	AT2G35490	
Fibrillin 4 (FBN4)	AT3G23400	
Fibrillin 7a (FBN7a)	AT3G58010	
Fibrillin 7b (FBN7b)	AT2G42130	
Fibrillin 8 (FBN8)	AT2G46910	
Enzymes		
Tocopherol cyclase VTE1	AT4G32770	Tocopherol metabolism
NAD(P)H dehydrogenase C1 NDC1	AT5G08740	Phylloquinone and PQ metabolism
Phytyl ester synthase PES1	AT1G54570	TAG and FAPEs biosynthesis
Phytyl ester synthase PES2	AT3G26840	
Regulatory kinases		
Activity of bc1-like kinase ABC1K1	AT4G31390	Metabolic regulation and PQ homeostasis
Activity of bc1-like kinase ABC1K3	AT1G79600	Metabolic regulation and PQ homeostasis
Activity of bc1-like kinase ABC1K5	AT1G71810	
Activity of bc1-like kinaseABC1K6	AT3G24190	
Activity of bc1-like kinase ABC1K7	AT3G07700	Metabolic regulation
Activity of bc1-like kinase ABC1K9	AT5G05200	
Other proteins		
SOUL heme binding protein 4 (SOUL 4)	AT3G10130	Heme metabolism

Continued

Table 2 PG core proteins based on proteome studies in *Arabidopsis thaliana* and *Capsicum annuum*.—cont'd

Protein name	Accession	Functions
UbiE methyltransferase-related	AT1G78140	
UbiE methyltransferase-related	AT2G41040	
Aldo/keto reductase	AT1G06690	
Plastoglobular protein 18 PG18	AT4G13200	Thylakoid biogenesis
PLAT/LH2-1	AT4G39730	
PGM48	AT3G27110	Protein homeostasis
Flavin reductase-related 1	AT1G32220	
Flavin reductase-related 2	AT2G34460	
DUF1350	AT3G43540	
alpha/beta hydrolase family protein	AT1G73750	
Esterase 1	AT5G41120	
Chromoplast PG carotenoid enzymes		
Carotenoid cleavage dioxygenase 4 CCD4	AT4G19170	Carotenoid metabolism
ζ-Carotene desaturase ZDS	gi|12643508 (Capsicum annuum)	Carotenoid biosynthesis
Lycopene β-cyclase LCY-β	gi|12643508 (Capsicum annuum)	
β-Carotene β-hydroxylase CrtR-β	gi|12643508 (Capsicum annuum)	

2. Metabolites and proteins

2.1 The role of plastoglobules in thylakoid (prenyl) lipid metabolism

After their discovery by electron microscopy it quickly became clear that PG contain large and variable quantities of lipids that were in one way or the other linked to thylakoid function (Greenwood et al., 1963; Tevini &

Steinmuller, 1985). PG being lipid droplets, they contain neutral, hydrophobic lipids while the surface consists of a membrane lipid monolayer. Indeed, plastoquinone (large quantities) together with the tocopherols and phylloquinone (both in moderate quantities) were identified as major components (Leggett Bailey & Whyborn, 1963; Lichtenthaler, 1968b; Lichtenthaler & Peveling, 1966; Steinmüller & Tevini, 1985) (Table 1). All three belong to the prenyl quinone family and in part share biosynthetic pathways that are integrated at the PG (Figs. 1–3). It is important to note that all three fulfill important functions at the thylakoid membrane and do not appear to carry out any specifically within PG. Plastoquinone is a membrane mobile electron carrier transferring electrons from Photosystem II to the cytochrome b6f complex (Tikhonov, 2013; Van Eerden et al., 2017). It also "moonlights" as an anti-oxidant, the unsaturated prenyl tail able to react with and quench ROS whereby it is consumed (Apel & Hirt, 2004; Ksas et al., 2018). Tocopherol is considered a membrane anti-oxidant quenching ROS via chromanol ring opening (Krieger-Liszkay & Trebst, 2006; Munné-Bosch, 2005; Neely et al., 1988). The tocopherol oxidation product tocopherol quinone is known to be recycled to tocopherol (Kobayashi & DellaPenna, 2008), the process taking place at least in part at the PG level (Eugeni Piller et al., 2014) (Fig. 1). Phylloquinone is an electron carrier functioning within Photosystem I (Malkin, 1986; Santabarbara & Casazza, 2019; Schoeder & Lockau, 1986). Functions of free phylloquinone within the thylakoid membrane have to our knowledge not been described.

Other neutral lipids in PG are triacylglycerols that are present in large quantities and mostly derived from thylakoid galactolipid hydrolysis (Table 1). Free fatty acids were also detected and likely to be galactolipid hydrolysis products as well (Gaude et al., 2007; Tevini & Steinmuller, 1985). In addition, PG of senescent chloroplasts accumulate large quantities of fatty acid phytyl esters (Fig. 4) (Gaude et al., 2007). Phytol is a product of chlorophyll breakdown and thought to be membrane toxic due to detergent-like properties (Krauß & Vetter, 2018). Esterification with free fatty acid detoxifies phytol and results in very hydrophobic fatty acid phytol esters that can be sequestered from the thylakoid membrane and deposited in PG (Hörtensteiner & Kräutler, 2011; Ischebeck et al., 2006; Krauß & Vetter, 2018) (Table 1). Membrane lipids are present in minor quantities as they only constitute the membrane lipid monolayer at surface of the PG. They include monogalactosyl- and digalactosyldiacylglycerol (MGDG and DGDG) as well sulfoquinovosyldiacylglycerol which are the major membrane lipid components of the thylakoid membrane (Boudière et al., 2014). Phospholipids have also been detected at trace levels.

Electron microscopic images indicate that the membrane lipid monolayer surrounding the PG is contiguous with the outer membrane lipid layer of the thylakoid membrane (Austin et al., 2006; Kessler et al., 1999). This arrangement would allow for a lipid conduit from the PG interior to the thylakoid membrane. Such a conduit has been postulated to explain the lipid exchange processes that must occur between the thylakoid membrane and PG (Havaux, 2020; Kirchhoff, 2019). However, such conduits have not been functionally demonstrated so far.

Interestingly, PG composition may vary with plastid type. Senescent chloroplasts, also known as gerontoplasts, accumulate very large amounts of TAG and fatty acid phytyl esters that result from thylakoid membrane catabolism and chlorophyll breakdown (Fig. 4; Table 1) (Gaude et al., 2007; Tevini & Steinmuller, 1985). This accumulation is directly linked to PG supersizing that can easily be observed by electron microscopy (Barton, 1966). During chloroplast-to-chromoplast transition, thylakoid membranes are dismantled and large PG appear (Egea et al., 2010; Spurr & Harris, 1968). In red pepper large PG transiently appear and are progressively replaced by carotenoid fibrils that are structurally related to PG (Deruère et al., 1994). The PG and fibrils contain large quantities of carotenoids such as the linear lycopene in tomato and/or carotenoid esters that may constitute up to 90% of carotenoids in red pepper (Berry et al., 2019; Deruère et al., 1994) (Table 1). It is interesting to note here that the PG in chromoplasts recruit enzymes of the carotenoid biosynthesis pathway. Presumably, this enhances sequestration of these hydrophobic molecules within a hydrophobic metabolic sink (i.e., PG and/or fibrils).

2.2 The plastoglobule proteome

The first PG protein to be identified was called fibrillin due to its association with carotenoid fibrils (as well as PG) in red pepper fruit (Deruère et al., 1994). Since then, a series of analyses have determined a proteome of around 30 *bona fide* PG proteins (Table 2) that may vary between plastid types and environmental conditions. Rather surprisingly, around a third of the proteins turned out be enzymes with known or predicted roles in lipid metabolism (Eugeni Piller et al., 2011; Vidi et al., 2006). Several members of the family of atypical ABC1K kinases were also present in the proteome suggesting that PG also had regulatory functions (Fig. 1) (Lundquist et al., 2013; Martinis et al., 2014; Pralon et al., 2019, 2020). Finally, members of the fibrillin (FBN) family constituted the largest portion of the mass of the PG proteome and have been attributed roles in PG structure and maintenance (Fig. 1) (Kessler et al., 1999; Pozueta-Romero et al., 1997; Rey et al., 2000; Simkin et al., 2007; Singh et al., 2012). Interestingly, the PG proteins partitioned to various degrees between thylakoid membranes, stroma and PG, but there are few physical explanations for this. But, the distribution of the fibrillin proteins between the compartments correlated with their isoelectric points and hydrophobicity. Fibrillins that associated with PG tended to have a lower isoelectric point and be more hydrophobic (Lundquist et al., 2012). While the precise functions of many PG components remain unknown, a genome-wide coexpression network of PG genes attributed PG proteins to four distinct "modules" (1–4) that were particularly enriched for senescence, carotenoid metabolism, redox regulation/"photoacclimation" and plastid biogenesis (Lundquist et al., 2012). In the following paragraphs, we will discuss notable PG proteins and their functions.

2.2.1 The versatile but elusive fibrillin family

Quantitatively, the largest portion of the PG proteome is made up of members of the fibrillin/FBN family, sometimes also called plastoglobulins (PG) (Kessler et al., 1999; Lundquist et al., 2012). FBNs originated from a cyanobacterial chloroplast progenitor and are part of the green cut (Lohscheider & Río Bártulos, 2016; Merchant et al., 2007). The first fibrillin was discovered in red pepper (*Capsicum annuum*) through its association with carotenoid-sequestering fibrils (Deruère et al., 1994). Red pepper fibrillin protein allowed to reconstitute carotenoid fibrils from the fibril lipid components. This finding was taken as indication for a structural function of fibrillin (Deruère et al., 1994). Additional support for this notion comes from the ability of FBN1a and -1b to dimerize *in vivo*. This may allow formation of a stabilizing FBN network around PG (Gámez-Arjona et al., 2014). Overexpression of FBN in tobacco led to increased numbers and clustering of PG suggesting that FBN may form an interface at the surface of PG and prevent their coalescence (Rey et al., 2000). FBNs share limited sequence homology with lipocalins, small proteins involved in the binding and transport of small hydrophobic compounds. The presence of a lipocalin signature suggested that some fibrillins may directly participate in lipid trafficking between PG and membrane compartments (Flower et al., 2000; Singh & McNellis, 2011).

The Arabidopsis genome encodes 14 FBNs, 7 of which (FBN1a, -1b, -2, -4, -7a, -7b, and -8) are considered PG core proteins (Vidi et al., 2006; Ytterberg et al., 2006). The other FBNs are associated with thylakoid membranes (FBN3a, -3b, -6, and -9 and FBN-like) or present in the chloroplast stroma (FBN5) (Kim et al., 2015). The loss-of-function mutants for FBN1a, -1b, -2, and -4 in Arabidopsis as well as other species suggested the (direct or indirect) involvement of these FBNs in responses to biotic stresses, heat stress, and excess light (Gillet et al., 1998; Langenkämper et al., 2001; Li et al., 2015; Singh et al., 2012; Youssef et al., 2010). Arabidopsis FBN5 is not a PG component but a soluble stromal protein. FBN5 is required for the synthesis of solanesyl diphosphate, an essential step in the PQ-9 biosynthetic pathway (Kim et al., 2017, 2015; Otsubo et al., 2018). FBN5 interacts directly with SPS1 and -2 (solanesyl diphosphate synthase 1 and -2) to stimulate the elongation of the prenyl chain resulting in the essential solanesyl moiety of PQ-9 (Kim et al., 2015) (Fig. 2). FBN4 has also been linked to PQ-9 metabolism. The PG of an apple FBN4

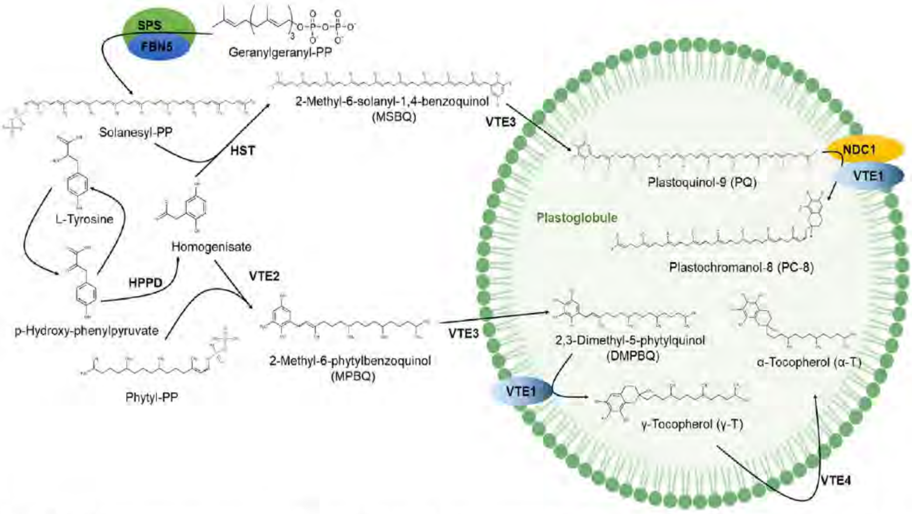

Fig. 2 Plastochromanol and tocopherol biosynthetic pathways in chloroplasts. The tyrosine aminotransferase (TAT) converts the precursor L-tyrosine derived from the shikimate pathway into p-hydroxy-phenylpyruvate. The p-hydroxyphenyl-pyruvate dioxygenase (HPPD) converts p-hydroxy-phenylpyruvate into homogentisate. Homogentisate phytyltransferase (VTE2) adds the phytyl-pp tail to homogentisate resulting in 2,3-dimethyl-6-phytyl-1,4-benzoquinone (MPBQ). Alternatively, homogentisate solanesyltransferase (HST) adds a solanesyl-tail to homogentisate resulting in 2-methylmethyl-6-solanyl-1,4-benzoquinol (MSBQ). Solanesyl-PP is derived from geranylgeranyl-PP elongation catalyzed by solanesyl diphosphate synthases 1 and 2 (SPS1 and 2) in conjunction with fibrillin 5 (FBN5). MPBQ methyltransferase (VTE3) methylates MPBQ resulting in DMPBQ as well as MSBQ resulting in plastoquinol-9 (PQ-9). Tocopherol cyclase (VTE1), localized at the surface of the plastoglobule (PG; shown as green lipid droplet) catalyzes the cyclization of DMPBQ generating γ-Tocopherol (γ-T). Also, at the PG, NDC1 reduces PQ-9 to PQH_2-9 prior to conversion into plastochromanol-8 (PC-8) by VTE1. Tocopherol O-methyltransferase (VTE4) methylates γ-Tocopherol (γ-T) resulting in α-Tocopherol (α-T).

knockdown mutant had strongly reduced levels of PQ-9 while overall concentrations were comparable to WT suggesting that FBN4 participates in partitioning and/or trafficking of PQ-9 between PG and thylakoid membrane (Singh et al., 2012). The current knowledge suggests that FBNs are highly versatile proteins contributing to PG structure as well as several metabolic pathways and metabolite trafficking. However, the functional mechanisms of the fibrillins remain elusive.

2.2.2 Members of the ABC1K family contribute to control the prenyl lipid metabolism and photosynthetic electron flow

Members of ABC1 (Activity of BC1 complex)-like kinase family (ABC1K) constitute the second most abundant family of proteins in PG (Lundquist et al., 2012). The founding member of the ABC1K family [also called UbiB or ABC1 domain–containing kinases (ADCKs)] is UbiB from *E. coli*, which is required for the aerobic biosynthesis of ubiquinone (Poon et al., 2000). The yeast (*Saccharomyces cerevisiae*) mitochondrial ABC1K, also known as coenzyme Q biosynthesis 8 (ScCOQ8), and the mammalian homologs ADCK3 and -4 are required for ubiquinone synthesis in the mitochondria of their respective organisms, possibly through phosphorylation-dependent assembly of a large biosynthetic multi-enzyme complex (Bousquet et al., 1991; Do et al., 2001; Lagier-Tourenne et al., 2008; Mollet et al., 2008). Due to the lack of ubiquinone, the *coq8* mutation compromises the mitochondrial bc1 complex and aerobic metabolic activity. Defects of the kind are linked to hereditary disease in humans (Gerards et al., 2010).

Arabidopsis has 17 ABC1Ks, 8 of which are likely localized in mitochondria and 9 in plastids. Six of nine of the plastid ABC1Ks are localized in PG (ABC1K1, -3, -5, -6, -7,-9) (Lundquist et al., 2012). Notably, the ABC1K family represents the majority of known kinases in plastids and mitochondria; however, relatively little is known about this family in plants. Functional studies of PG-localized ABC1K1, -3 and -7, have been initiated in Arabidopsis, and the role of ABC1K3 has been addressed in rice (Li et al., 2015). PG-localized ABC1K7 is involved in cadmium tolerance, oxidative stress response, iron distribution, lipid metabolism and in crosstalk between abscisic acid and ROS signaling (Manara et al., 2014; Manara et al., 2015). The Chlamydomonas homolog of ABC1K6 (EYE3) located in the eyespot, is involved in the biogenesis of pigment granules (Boyd et al., 2011). Still, the modes of action of the ABC1K family members, for instance phosphorylation of proteins or metabolites, are quite unclear.

Apart from its association with PG, ABC1K1 was identified in at least two genetic screens. In a genetic screen to identify mutants defective in seedling growth under continuous red light, ABC1K1 was identified as BDR1 (bleaching and dwarf under red light 1) (Yang et al., 2016). Under continuous red light *abc1k1/bdr1* exhibited an albino and dwarf phenotype and, while most photosynthetic proteins accumulated normally, the Photosystem II core protein D1 was diminished. To identify additional components required for ABC1K1/BDR1 function, a genetic screen to find suppressors of *abc1k1-2* was carried out and resulted in the isolation of *rbd1* (repressor of *bdr1-2*) that turned out to be identical with ABC1K3 (Huang et al., 2015). It is thought that ABC1K3 in the *abc1k1* background interferes with red light signaling acting downstream of PhyB and HY5 and affects expression of PIF genes. This is supported by the observation that ABC1K3 overexpression produced a phenotype similar to that of the *abc1k1* mutant (Huang et al., 2015).

In a second screen for mutants with reduced non-photochemical quenching (NPQ) of chlorophyll fluorescence (Shikanai et al., 1999), PGR6 (Proton Gradient Regulation 6) was identified and found to be identical with ABC1K1. *abc1k1* has a photosynthetic phenotype characterized by strong photoinhibition and reduced NPQ after high light exposure (Martinis et al., 2014; Pralon et al., 2019). Prenyl lipid metabolism was affected in *abc1k1*: Tocopherol concentrations did not increase under high light stress and carotenoid concentrations were diminished even under moderate light conditions (Martinis et al., 2014; Martinis et al., 2013). After high light treatment, sugar metabolism was perturbed and carbon-allocation shifted from starch to soluble sugars. In addition to the genetic interaction between ABC1K1 and its closest homolog, ABC1K3, the two atypical kinases interact physically (Fig. 1). (Lundquist et al., 2013). Moreover, additional reports demonstrated that ABC1K1 and -3 together are involved in PQ-9 homeostasis (maintenance of sufficient PQ-9 in the photoactive thylakoid membrane pool) (Pralon et al., 2019; Pralon et al., 2020). In the *abc1k1* mutant, the photoactive PQ-9 pool in the thylakoid membranes was selectively depleted under moderate high light stress. The depleted photoactive PQ-9 pool phenotype of *abc1k1*is rescued in the *abc1k1/abc1k3* double mutant. Thus, ABC1K1 and ABC1K3 appear to regulate the distribution of PQ-9 between the plastoglobule and thylakoid membrane pools.

The perturbed plastoquinone homeostasis in the *abc1k1* mutant may explain the "proton gradient regulation"/PGR phenotype that is characterized by decreased NPQ: concomitantly with its role as an electron carrier, plastoquinone transports protons from the stromal side of the thylakoid membrane to the lumenal side generating a ΔpH. An increasing ΔpH serves as a proxy for excess light and induces NPQ, to protect the photosynthetic apparatus. In *abc1k1*, plastoquinone levels in the electron chain are diminished under high light. These insufficient amounts of plastoquinone in *abc1k1* would limit not only electron transport but also the ΔpH across the thylakoid membrane. Therefore, induction of non-photochemical quenching, would be decreased, resulting in the observed PGR phenotype. Thus, ABC1K1 may be a very direct regulator of the proton gradient (Pralon et al., 2019).

It remains unclear how the photosynthetic PGR phenotype relates to the cellular signaling phenotype also observed for ABC1K1 and -K3. It will be important to reconcile the two phenomena in the future. One possibility is that these two atypical kinases transmit signals emanating from the photosynthetic electron transport chain to the nucleus thereby affecting gene expression.

3. Role of PG proteins in the context of thylakoid lipid metabolism

3.1 NDC1 a new enzyme in phylloquinone biosynthesis

Phylloquinone mainly acts as an electron carrier in Photosystem I in the thylakoid membrane (Brettel et al., 1986). But it has been demonstrated that about one-third of phylloquinone is present in PG (Lohmann et al., 2006; Spicher & Kessler, 2015). This suggests phylloquinone trafficking between PG and the thylakoid membrane. The MenG enzyme, a predicted methylase, catalyzes the final methylation step of the biosynthetic pathway from 2-phytyl-1,4-naphthoquinone (demethylphylloquinone) to phylloquinone (Fig. 3). The AtmenG knockout mutant lacks phylloquinone but accumulates the precursor demethylphylloquinone instead. The lack of phylloquinone in *atmenG* has rather minor consequences resulting in reduced levels of Photosystem I and consequently a slight decrease of photosynthetic efficiency upon high light (HL) treatment (Eugeni Piller et al., 2011; Lohmann et al., 2006). Thus, it appears that the precursor of phylloquinone can functionally replace phylloquinone, at least under standard conditions. Surprisingly, the *ndc1* mutant in Arabidopsis mimics the *atmenG* phenotype and has identical phylloquinone and demethylphylloquinone profiles (Eugeni Piller et al., 2011).

In Arabidopsis, NDC1 is one of seven NDH-2 (Type II NAD(P)H-dependent dehydrogenases). NDC1 appears to be localized mostly in chloroplast PG (Fig. 3) whereas the remaining homologs have been localized in mitochondria. However, NDC1 was initially also found in mitochondria

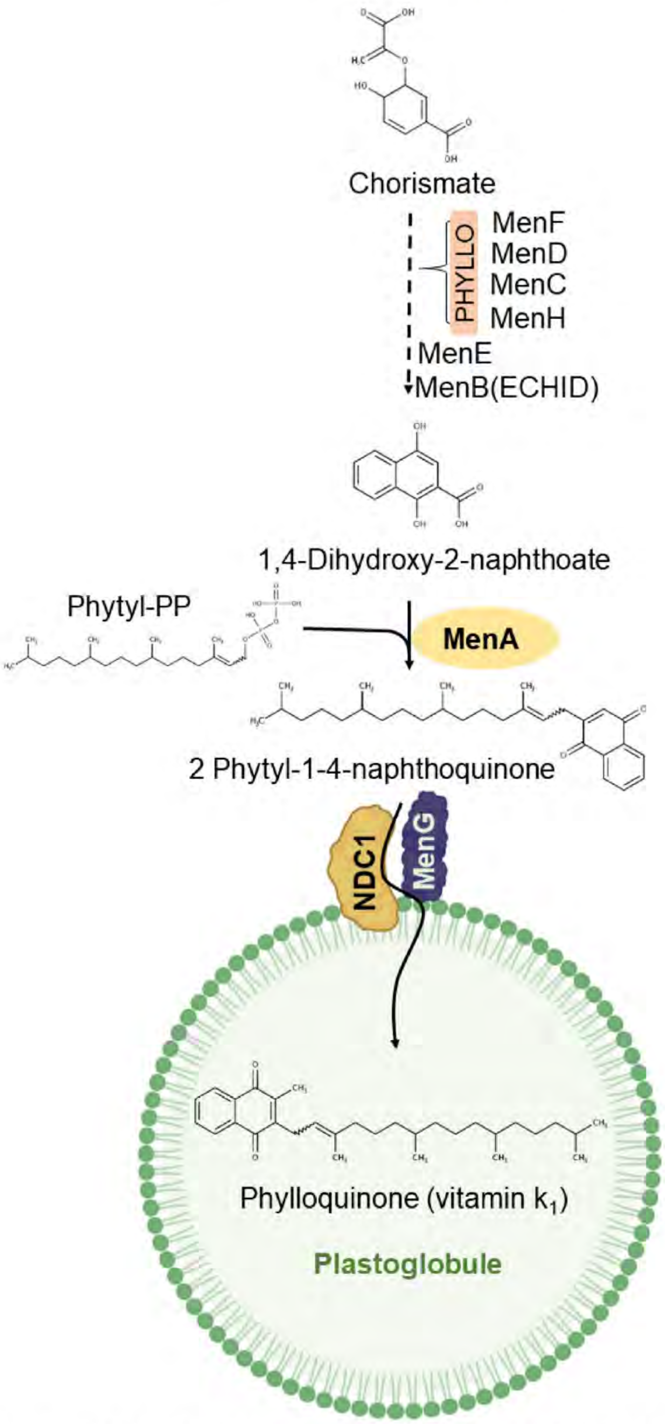

Fig. 3 Phylloquinone biosynthetic pathway in plants. PHYLLO, a fusion protein of menaquinone synthesis enzymes (MenF, D, H, C) followed by MenE and MenB convert chorismate into 1,4-dihydroxydihydroxy-2-naphthoate (DHNA). DHNA phytyltransferase (MenA) converts DHNA to 2-phytyl-1,4-naphthoquinone (demethylphylloquinone). Next, the demethylphylloquinone is reduced by type II NAD(P)H dehydrogenase C1 (NDC1) resulting in demethylphylloquinol. Depending on the prior reduction of demethylphylloquinone by NDC1, MenG methylates demethylphylloquinol to complete the synthesis of phylloquinone.

(Michalecka et al., 2003), and dual localization in mitochondria and chloroplasts cannot be excluded. NDC1 is evolutionarily conserved from cyanobacteria. In Chlamydomonas NDA2 NAD(P)H:quinone oxidoreductase, the homolog of NDC1, is involved in cyclic electron flow and chlororespiration directly transferring electrons from NAD(P)H to plastoquinone (Desplats et al., 2009). NDC1 in cyanobacteria is part of the MEN operon and its deletion also leads to loss of phylloquinone (Fatihi et al., 2015). The mechanism of NDC1 in the methylation step of phylloquinone synthesis has been solved: The NDC1-dependent reduction of demethylphylloquinone intermediate is essential for the subsequent methylation by MenG. NDC1 is therefore considered a *bona fide* enzyme of the phylloquinone biosynthesis pathway (Fig. 3). (Eugeni Piller et al., 2011; Fatihi et al., 2015). Interestingly, Gross et al. (2006) also demonstrated that the PHYLLO metabolon (genetic fusion of MenF, MenD, MenC, and MenH) fused to a fluorescent marker resulted in a plastoglobuli-like fluorescence pattern inside chloroplasts (Gross et al., 2006). The fluorescence pattern suggests that the PHYLLO metabolon may also be recruited to PG coupling the upstream portion of pathway with NDC1 and AtMenG activity (Gross et al., 2006).

3.2 NDC1 regulates the PQ-9 redox state and contributes to plastochromanol biosynthesis and tocopherol recycling

It has been demonstrated that recombinant NDC1 reduces decyl plastoquinone (a PQ-9 analog) in a NAD(P)H dependent fashion (Eugeni Piller et al., 2011). However, NDC1 in Arabidopsis is not directly implicated in either linear or cyclic electron flow in Arabidopsis. In chloroplasts, plastoquinone is distributed between the thylakoids and PG, constituting photoactive and non-photoactive pools, respectively. The non-photoactive pool may communicate with the photoactive plastoquinone pool to maintain adequate PQ-9 levels in the photoactive pool ("plastoquinone homeostasis") as seen in the earlier paragraphs on the ABC1K1 and -3 kinases. Total PQ-9 in *ndc1* was significantly more oxidized than in the wild-type while electron transport rates and other photosynthetic parameters were not affected. This suggested that NDC1 selectively reduces the photoinactive PQ-9 pool inside PG (Eugeni Piller et al., 2011).

In an interesting twist, the *ndc1* mutant accumulates less plastochromanol-8 (PC-8) than WT (Eugeni Piller et al., 2011). PC-8 is the product of tocopherol cyclase/VTE1 activity on reduced PQ-9 (PQH_2-9). VTE1 preferentially cyclizes reduced substrates, in this case PQH_2-9 contained in PG (Fig. 2)

(Woggon, 1999). In the absence of *ndc1* PQ-9 in PG is more oxidized impeding the action of VTE1 (Fig. 2) and hence the biosynthesis of PC-8.

Under stress conditions, Photosystem II generates reactive oxygen species to which the thylakoid membranes are exposed. Tocopherols are one of the primary antioxidants able to quench ROS and protect the membrane lipids from oxidation (Munné-Bosch & Alegre, 2002). Scavenging of lipid peroxy radicals leads to chromanol ring opening in α-tocopherol and α-tocoquinone production (Muñoz & Munné-Bosch, 2019). α-tocoquinone can be "repaired" by a sequence of enzymatic steps culminating in chromanol ring formation by VTE1. This step occurs preferentially in the reduced substrate α-tocopherol quinol (α-TQH2) (Eugeni Piller et al., 2014; Kobayashi & DellaPenna, 2008). In the *ndc1* mutant, α-tocopherol quinol is produced less efficiently leading to diminished α-tocopherol repair and increased concentrations of α-tocoquinone (Eugeni Piller et al., 2014).

3.3 The tocopherol cyclase VTE1 (VITAMIN E DEFICIENT 1), the key enzyme in tocochromanol biosynthesis and metabolism

α-tocopherol is the primary tocochromanol protecting thylakoid membranes from lipid peroxidation under stress (Fryer, 1992; Liu et al., 2008; Munné-Bosch & Alegre, 2002). Most of the enzymes of the tocopherol biosynthesis pathway, including tocopherol cyclase (VTE1), were originally localized at the inner envelope membrane of the chloroplast by activity measurements in isolated membrane fractions (Soll et al., 1985). Tocopherol cyclase introduces the chromanol ring in DMPBQ, converting it to γ-tocopherol (Fig. 2). Subsequently, VTE4 methylates γ-tocopherol resulting in α-tocopherol. Surprisingly, given the earlier results, VTE1 was discovered in the PG proteome (Vidi et al., 2006; Ytterberg et al., 2006). The majority of tocopherol cyclase VTE1 has been localized at PG using a variety of independent techniques: VTE1-fluorescence tagging, immunoelectron microscopy, immunoelectron tomography and Western blotting of isolated chloroplast membrane fractions. Moreover, DMPBQ, the substrate of VTE1, accumulated in the PG of the *vte1* mutant, providing supporting evidence for the localization of VTE1 at PG (Austin et al., 2006; Vidi et al., 2006; Ytterberg et al., 2006). The *vte1* mutant largely resembled the wild type suggesting that DMPBQ or other tocochromanols such as PC-8 can substitute for tocopherol as a functional antioxidant.

Together with plastochromanol-8 (PC-8), tocopherol protects seeds from oxidation and is required for seed longevity (Mène-Saffrané et al., 2010). PC-8 is derived from plastoquinol (PQH_2-9) by tocopherol cyclase/VTE1 activity (Fig. 2). PC-8 has the longest solanesyl side chain of plastoquinones but the chromanol-containing headgroup is identical to that of γ-tocopherol. The VTE1 overexpression lines resulted in a large increase of PC-8 that mainly accumulated in PG. It therefore appeared likely that VTE1 localized at PG converted PQH_2-9 to PC-8 (Zbierzak et al., 2009). Notably, the *ndc1* mutant accumulated less PC-8 likely due to the preference of VTE1 for reduced PQH_2-9 over PQ-9 (Eugeni Piller et al., 2012).

4. Role of PG in thylakoid membrane remodeling under stress

Various abiotic environmental stresses (oxidative stress, high light intensity, nitrate starvation, drought) and plastid developmental transitions (chloroplast-to-chromoplast, chloroplast-to-gerontoplast) are associated with remodeling or even wholesale dismantling of thylakoid membranes and with increased accumulation of lipid antioxidants to cope with such conditions. Typically, PG number and size increase due to lipid deposition in PG resulting from thylakoid membrane dismantling during chloroplast-to-gerontoplast transition or under nitrogen deprivation (Besagni & Kessler, 2013; Domínguez & Cejudo, 2021; Gaude et al., 2007; Hörtensteiner & Kräutler, 2011). This process may result in supersized PG of several micrometers in diameter due to triacylglycerol and fatty acid phytyl ester accumulation. These products result from the combined simultaneous breakdown of galactolipids and chlorophyll in the presence of PG-localized enzymes (Fig. 4) (Zechmann, 2019).

Phytol is released from chlorophyll by pheophytin pheophorbide hydrolase (PPH) (Hörtensteiner & Kräutler, 2011; Schelbert et al., 2009). However, the membrane-toxic phytol does not accumulate. Instead, phytol and free fatty acids, which are hydrolysis products of the thylakoid galactolipids, are converted to fatty acid phytyl esters (FAPE) and triacylglycerol (TAG) in PG by phytyl ester synthases 1 and 2 (PES1 and PES2) (Fig. 4) (Krauß & Vetter, 2018; Lippold et al., 2012). Gerontoplast PG transiently recruit LIPOXYGENASE 3 and 4 (LOX3 and LOX4) that peroxidate 16:3 and 18:3 fatty acids (Lundquist et al., 2012). Together, allene oxide cyclase (AOC) and allene oxide synthase (AOS) convert oxidized 18:3 fatty acid into 12-oxo phytodienoic acid (OPDA) (Fig. 4), a precursor for jasmonic acid synthesis in the peroxisome (Acosta & Farmer, 2010). The initial proteome studies found AOS in PG (Vidi et al., 2006; Ytterberg et al., 2006). A recent study demonstrated strongly increased levels of AOS in PG

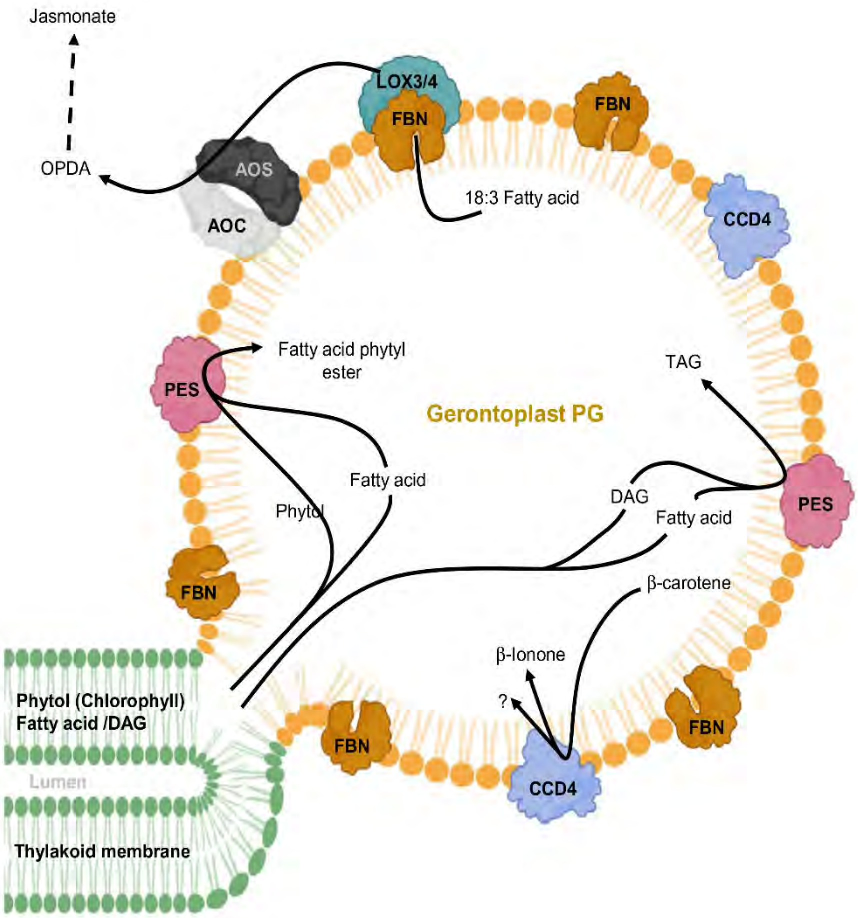

Fig. 4 Lipid metabolism in the gerontoplast plastoglobule. The senescence process is characterized by the transformation of a chloroplast to a gerontoplast and the dismantling of the thylakoid membrane, which comprises galactolipid hydrolysis and chlorophyll breakdown. Phytyl ester synthases (PES) catalyze the synthesis of fatty acid phytyl esters from free fatty acids (from galactolipid hydrolysis) and phytol (from chlorophyll break down). In parallel, phytyl ester synthases contribute to triacylglycerol (TAG) synthesis from free fatty acids and diacylglycerol (DAG). The gerontoplast PG-localized LIPOXYGENASE (LOX) oxidizes unsaturated fatty acid and may be recruited by a fibrillin (FBN). In addition, allene oxide cyclase (AOC) and allene oxide synthase (AOS, also in PG) are essential enzymes to produce 12-oxo-phytodienoic acid (OPDA), a jasmonate precursor. The carotenoid cleavage dioxygenase 4 (CCD4) cleaves β-carotene to release β-ionone and other volatile compounds.

after high light treatment (Espinoza-Corral et al., 2021). Senescence, nitrogen deprivation and high light treatment are useful conditions for studying dynamic behavior of PG morphology and metabolism (Gaude et al., 2007; Zechmann, 2019).

4.1 PES1 and PES2 are involved in phytol and fatty acid metabolism

PES1 and -2 belong to the esterase/lipase/thioesterase (ELT) acyl transferase family. PES1 and -2 are induced during leaf senescence and under nitrogen deprivation. Under nitrogen deprivation, the *pes1pes2* double mutant accumulated only residual levels of phytyl esters and far more free phytol than the wild type (Lippold et al., 2012). The residual phytyl esters may be explained by the presence of additional ELT homologs. PES1 and PES2 converted phytol and fatty acids into FAPE in the heterologous yeast expression system thereby demonstrating phytyl ester synthase activity. Senescence and chlorophyll catabolism was slightly delayed in the *pes1pes2* double mutant emphasizing the physiological importance of the two enzymes in plant senescence (Lippold et al., 2012).

PES1 and PES2 proteins have two distinct domains, a hydrolase domain at the N-terminus and an acyltransferase domain at the C-terminus of the protein. Thus, the PES1 and PES2 proteins potentially harbor two enzymatic functions, namely that of an esterase as well as that of an acyl transferase. In addition, PES1 and PES2 recruit a range of substrates including acyl-CoA species as well as the free fatty acids resulting from galactolipid breakdown. In addition, MGDG can directly serve as an acyl donor for PES1 and PES2 facilitating the release of fatty acids as well as TAG and FAPE biosynthesis (Fig. 4). Acyltransferases typically synthesize triacylglycerol (TAG) from acyl-CoA and diacylglycerol. In a yeast mutant lacking acyltransferase genes and deficient in TAG, expression of Arabidopsis PES1 and PES2 genes rescued TAG accumulation. The results validated that PES1 and PES2 act as acyltransferases and may use DAG as a substrate. Also, the *pes1pes2* double mutant reduces TAG accumulation by about 30% in leaves under nitrogen deficiency (Lippold et al., 2012). These results demonstrate that PES1 and PES2 are important DAG acyltransferases contributing to DAG to TAG conversion under stress. Overall, PES1 and PES2 in PG play a central role in dismantling the photosynthetic membrane during senescence and abiotic stresses.

5. PG act as the metabolic platform for carotenoid metabolism

The chromoplast is an organelle of the plastid family that develops from the chloroplast during fruit ripening (Camara et al., 1995; Egea et al., 2010). This begins with the dismantling of the photosynthetic thylakoid membrane that is accompanied by the tightly controlled degradation of chlorophyll as well as yellow-colored carotenoids, processes visible as degreening (Egea et al., 2010; Hörtensteiner & Kräutler, 2011). Simultaneously, the PG within chromoplasts enlarge and begin to accumulate large amounts of red-colored carotenoids and other prenyl lipids that may be synthesized *de novo* or stem from the mobilization of the thylakoid membranes (Fig. 5). Chromoplast PG may have tubular/fibrillar (example: red pepper) or globular structure (example: tomato) (Nogueira et al., 2013; Pozueta-Romero et al., 1997; Simkin et al., 2007). *In vitro* reconstitution of fibrils was achieved from a mixture of membrane lipids, carotenoids and fibrillin (Deruère et al., 1994). However, the PG of chromoplasts, as already

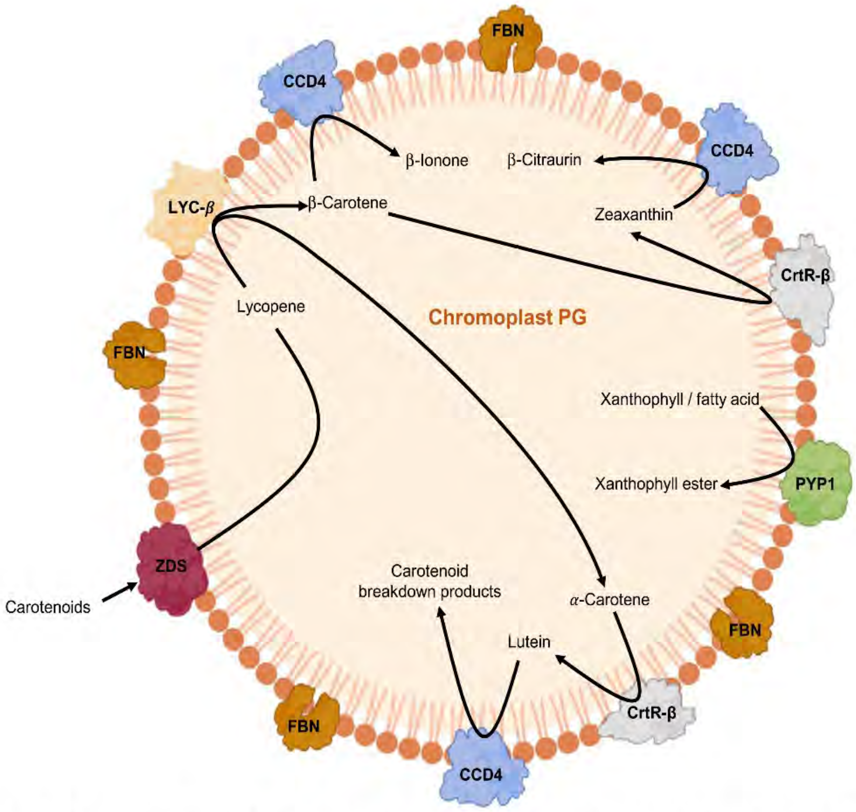

Fig. 5 Carotenoid metabolism in the chromoplast plastoglobule. Chromoplast plastoglobules recruit specific enzymes such as lycopene β-cyclase (LYC-β), zeta-carotene desaturase (ZDS) and β-carotene β-hydroxylase (CrtR-β) to promote carotenoid biosynthesis. Fibrillins (FBNs) may contribute to carotenoid sequestration in PG. PALE YELLOW PETAL 1 (PYP1) catalyzes carotenoid ester synthesis in tomato petal chromoplasts. The carotenoid cleavage dioxygenase 4 (CCD4) cleaves carotenoids, releasing volatile compounds, contributing to aroma and fruit quality in tomatoes.

seen for chloroplast PG, are more than just storage sites and play a central role in the biosynthesis and metabolism of carotenoids.

The proteome of pepper fruit PG has been determined and provided very interesting insight. Chromoplast PG are highly enriched in several FBNs (Fig. 5), particularly FBN1a and -1b, as well as several carotenoid biosynthetic enzymes: ZDS (ζ-carotene desaturase) involved in the synthesis of all-trans-lycopene, a red pigment in tomato, and LYC-β (lycopene beta cyclase) involved in the cyclization reactions that generate carotene (Fig. 5). The β-carotene β-hydroxylases (CrtR-β) introduce hydroxyl groups to carotene, resulting in lutein and zeaxanthin (Fig. 5). These enzymes lack transmembrane domains and are therefore thought to associate with the chromoplast PG surface. The clustering of these enzymes at PG and associated membranes probably facilitates substrate channeling and accumulation of carotenoids inside PG and fibrils (Lundquist et al., 2012). PALE YELLOW PETAL 1 (PYP1) in tomato shares sequence homology with the PES enzymes and is responsible for the production of carotenoid esters, the most abundant form of carotenoids in chromoplasts (Fig. 5) (Ariizumi et al., 2014). Chloroplast and chromoplast PG contain an additional carotenoid metabolic enzyme, carotenoid cleavage dioxygenase 4 (CCD4). In various plant species CCD4s are involved in carotenoid cleavage resulting in various apocarotenoids, especially the volatile β-ionone (Fig. 5) (Varghese et al., 2021). From researches on chromoplasts, it emerges that PG are key determinants of fruit pigmentation, functioning as a site of carotenoid biosynthesis and a sink for carotenoid accumulation. By the action of CCD4, PG may also contribute to the volatile bouquet of tomato fruit.

5.1 Role of CCD4 in chromoplasts and crop quality

CCD4 plays an important role in a surprising number of crops. In addition to its presence in the Arabidopsis PG proteome (Lundquist et al., 2012; Rottet et al., 2016), CCD4 was identified as a major negative regulator of seed carotenoid accumulation in a genome-wide association (GWAS) study. *ccd4* mutants had increased β-carotene content upon seed desiccation (Gonzalez-Jorge et al., 2013). Petals of Chrysanthemum CCD4 knock down plant had yellow rather than white petals, demonstrating that CCD4 cleaves carotenoids in chromoplasts and contributes to the accumulation of colorless carotenoids (Ohmiya et al., 2006). The red pigment β-citraurin in mandarin fruit is the CCD4 cleavage product of β-cryptoxanthin and zeaxanthin (Fig. 5) (Rodrigo et al., 2013). In *Brassica napus*, yellow petals contained higher carotenoid levels than white petals due to the disrupted expression of the CCD4 gene (Zhang et al., 2015). Down-regulation of the CCD4 gene in potato tubers led to accumulation of two- to fivefold higher carotenoid content than in wild type tubers (Campbell et al., 2010). In peaches, the expression of CCD4 is repressed in yellow flesh (Redhaven) cultivars as compared to white flesh (Redhaven Bianca) cultivars. Yellow flesh fruits accumulated approximately 10-fold more carotenoids than white flesh (Brandi et al., 2011). CCD4, highly expressed in the stigmata of *Crocus sativus* (saffron), contributes to color, flavor and aroma of the desiccated stigmata by producing apocarotenoids such as safranal, picrocosin, crocetin and β-ionone (Fig. 5). During *Crocus sativus* stigmata development PG size and number increase probably due to the accumulation of CCD4 cleavage products. Engineered CsCCD4 in bacteria preferentially cleaved β-carotene into β-ionone and β-cyclocitral (Frusciante et al., 2014; Rubio-Moraga et al., 2014).

Little is known whether and how CCD4 is regulated. PGM48, a plastoglobule-localized metalloprotease promotes senescence. PGM48 may do so in part by CCD4 degradation which is thought to accelerate senescence through the plant hormone abscisic acid and reduction of apocarotenoid signals (Bhuiyan et al., 2016).

6. Conclusions

In recent years plastoglobules have gone from poorly characterized osmiophile lipid-storing globules to important players in chloroplast lipid metabolism. Nevertheless, many mysteries remain. For one, it is not known how metabolites are trafficked between PG and the associated thylakoid membrane network. Contact sites between the two systems exist and may permit lipid exchange (Austin et al., 2006) but the implication of any proteins (fibrillins have been suggested) remains unknown. It is likely that the trafficking of different lipid species would be separate and highly regulated processes, as has been suggested for the allocation of PQ-9 to the thylakoid membrane (Pralon et al., 2019; Pralon et al., 2020). Early on, it had been hypothesized that plastoglobules contribute to thylakoid membrane formation during early plant development by the conversion of triacylglycerols to membrane lipids. The research tools currently available should allow to investigate this fascinating possibility. It will be of great interest in the future to address these and other open questions and their relevance for photosynthesis and metabolism.

A number of known PG core components have not been characterized so far. These include methyltransferases, reductases and others with various predicted functional domains and enzymatic activities (Lundquist et al., 2012). This remaining wealth of uncharacterized components promises the discovery of further, currently unknown metabolic functions in PG. It will be exciting to see what these will be.

PG have potential biotechnological and agricultural applications. Vitamin E and K enhancement in various crops can easily be imagined. Modification of tomato pigmentation and volatile production can also be envisaged by modifying carotenoid biosynthetic and metabolic pathways that are present in PG. Targeting of recombinant proteins, such as vaccine antigens, has been suggested and attempted in the tobacco experimental system (Shanmugabalaji et al., 2013). Of course, many other applications can also be imagined.

Clearly, research on PG has so far just scratched the surface and many exciting discoveries lie ahead of us.

Acknowledgments

This work was supported by grants from the Swiss National Science Foundation (31003A_156998 and 31003A _176191) and by the University of Neuchâtel.

References

Acosta, I. F., & Farmer, E. E. (2010). Jasmonates. *Arabidopsis Book*, *8*, e0129.

Apel, K., & Hirt, H. (2004). Reactive oxygen species: Metabolism, oxidative stress, and signal transduction. *Annual Review of Plant Biology*, *55*, 373–399.

Arango, Y., & Heise, K. P. (1997). Tocopherol synthesis from homogentisate in Capsicum anuum L. (yellow pepper) chromoplast membranes: Evidence for tocopherol cyclase. *The Biochemical Journal*, *3*, 531–533.

Ariizumi, T., Kishimoto, S., Kakami, R., Maoka, T., Hirakawa, H., Suzuki, Y., et al. (2014). Identification of the carotenoid modifying gene PALE YELLOW PETAL 1 as an essential factor in xanthophyll esterification and yellow flower pigmentation in tomato (Solanum lycopersicum). *The Plant Journal: For Cell and Molecular Biology*, *79*, 453–465.

Austin, J. R., II, Frost, E., Vidi, P.-A., Kessler, F., & Staehelin, L. A. (2006). Plastoglobules are lipoprotein subcompartments of the chloroplast that are permanently coupled to thylakoid membranes and contain biosynthetic enzymes. *The Plant Cell*, *18*, 1693–1703.

Barton, R. (1966). Fine structure of mesophyll cells in senescing leaves of Phaseolus. *Planta*, *71*, 314–325.

Berry, H. M., Rickett, D. V., Baxter, C. J., Enfissi, E. M. A., & Fraser, P. D. (2019). Carotenoid biosynthesis and sequestration in red chilli pepper fruit and its impact on colour intensity traits. *Journal of Experimental Botany*, *70*, 2637–2650.

Besagni, C., & Kessler, F. (2013). A mechanism implicating plastoglobules in thylakoid disassembly during senescence and nitrogen starvation. *Planta*, *237*, 463–470.

Bhuiyan, N. H., Friso, G., Rowland, E., Majsec, K., & van Wijk, K. J. (2016). The plastoglobule-localized metallopeptidase PGM48 is a positive regulator of senescence in *Arabidopsis thaliana*. *Plant Cell*, *28*, 3020–3037.

Boudière, L., Michaud, M., Petroutsos, D., Rébeillé, F., Falconet, D., Bastien, O., et al. (2014). Glycerolipids in photosynthesis: Composition, synthesis and trafficking. *Biochimica et Biophysica Acta (BBA)—Bioenergetics*, *1837*, 470–480.

Bousquet, I., Dujardin, G., & Slonimski, P. P. (1991). ABC1, a novel yeast nuclear gene has a dual function in mitochondria: It suppresses a cytochrome b mRNA translation defect and is essential for the electron transfer in the bc 1 complex. *The EMBO Journal*, *10*, 2023–2031.

Boyd, J. S., Mittelmeier, T. M., Lamb, M. R., & Dieckmann, C. L. (2011). Thioredoxin-family protein EYE2 and Ser/Thr kinase EYE3 play interdependent roles in eyespot assembly. *Molecular Biology of the Cell*, *22*, 1421–1429.

Brandi, F., Bar, E., Mourgues, F., Horváth, G., Turcsi, E., Giuliano, G., et al. (2011). Study of 'Redhaven' peach and its white-fleshed mutant suggests a key role of CCD4 carotenoid dioxygenase in carotenoid and norisoprenoid volatile metabolism. *BMC Plant Biology*, *11*, 24.

Brettel, K., Sétif, P., & Mathis, P. (1986). Flash-induced absorption changes in photosystem I at low temperature: Evidence that the electron acceptor A1 is vitamin K1. *FEBS Letters*, *203*, 220–224.

Camara, B., Hugueney, P., Bouvier, F., Kuntz, M., & Monéger, R. (1995). Biochemistry and molecular biology of chromoplast development. *International Review of Cytology*, *163*, 175–247.

Campbell, R., Ducreux, L. J., Morris, W. L., Morris, J. A., Suttle, J. C., Ramsay, G., et al. (2010). The metabolic and developmental roles of carotenoid cleavage dioxygenase4 from potato. *Plant Physiology*, *154*, 656–664.

Deruère, J., Römer, S., d'Harlingue, A., Backhaus, R. A., Kuntz, M., & Camara, B. (1994). Fibril assembly and carotenoid overaccumulation in chromoplasts: A model for supramolecular lipoprotein structures. *The Plant Cell*, *6*, 119–133.

Desplats, C., Mus, F., Cuiné, S., Billon, E., Cournac, L., & Peltier, G. (2009). Characterization of Nda2, a plastoquinone-reducing type II NAD(P)H dehydrogenase in chlamydomonas chloroplasts. *Journal of Biological Chemistry*, *284*, 4148–4157.

Do, T. Q., Hsu, A. Y., Jonassen, T., Lee, P. T., & Clarke, C. F. (2001). A defect in coenzyme Q biosynthesis is responsible for the respiratory deficiency in saccharomyces cerevisiae abc1 mutants. *Journal of Biological Chemistry*, *276*, 18161–18168.

Domínguez, F., & Cejudo, F. J. (2021). Chloroplast dismantling in leaf senescence. *The Journal of Experimental Botany*.

Egea, I., Barsan, C., Bian, W., Purgatto, E., Latché, A., Chervin, C., et al. (2010). Chromoplast differentiation: Current status and perspectives. *Plant and Cell Physiology*, *51*, 1601–1611.

Espinoza-Corral, R., Schwenkert, S., & Lundquist, P. K. J. T. P. J. (2021). Molecular changes of *Arabidopsis thaliana* plastoglobules facilitate thylakoid membrane remodeling under high light stress. *The Plant Journal*.

Eugeni Piller, L., Abraham, M., Dörmann, P., Kessler, F., & Besagni, C. (2012). Plastid lipid droplets at the crossroads of prenylquinone metabolism. *Journal of Experimental Botany*, *63*, 1609–1618.

Eugeni Piller, L., Besagni, C., Ksas, B., Rumeau, D., Bréhélin, C., Glauser, G., et al. (2011). Chloroplast lipid droplet type II NAD(P)H quinone oxidoreductase is essential for prenylquinone metabolism and vitamin K_1 accumulation. *Proceedings of the National Academy of Sciences*, *108*, 14354–14359.

Eugeni Piller, L., Glauser, G., Kessler, F., & Besagni, C. (2014). Role of plastoglobules in metabolite repair in the tocopherol redox cycle. *Frontiers in Plant Science*, *5*, 298.

Fatihi, A., Latimer, S., Schmollinger, S., Block, A., Dussault, P. H., Vermaas, W. F., et al. (2015). A dedicated type II NADPH dehydrogenase performs the penultimate step in the biosynthesis of vitamin K1 in synechocystis and arabidopsis. *The Plant cell*, *27*, 1730–1741.

Flower, D. R., North, A. C., & Sansom, C. E. (2000). The lipocalin protein family: Structural and sequence overview. *Biochim Biophys Acta*, *1482*, 9–24.

Frusciante, S., Diretto, G., Bruno, M., Ferrante, P., Pietrella, M., Prado-Cabrero, A., et al. (2014). Novel carotenoid cleavage dioxygenase catalyzes the first dedicated step in saffron crocin biosynthesis. *Proceedings of the National Academy of Sciences of the United States of America*, *111*, 12246–12251.

Fryer, M. (1992). The antioxidant effects of thylakoid vitamin E (α-tocopherol). *Plant, Cell & Environment*, *15*, 381–392.

Gámez-Arjona, F. M., de la Concepción, J. C., Raynaud, S., & Mérida, Á. (2014). Arabidopsis thaliana plastoglobule-associated fibrillin 1a interacts with fibrillin 1b in vivo. *FEBS Letters*, *588*, 2800–2804.

Gaude, N., Bréhélin, C., Tischendorf, G., Kessler, F., & Dörmann, P. (2007). Nitrogen deficiency in Arabidopsis affects galactolipid composition and gene expression and results in accumulation of fatty acid phytyl esters. *The Plant Journal*, *49*, 729–739.

Gerards, M., van den Bosch, B., Calis, C., Schoonderwoerd, K., van Engelen, K., Tijssen, M., et al. (2010). Nonsense mutations in CABC1/ADCK3 cause progressive cerebellar ataxia and atrophy. *Mitochondrion*, *10*, 510–515.

Gillet, B., Beyly, A., Peltier, G., & Rey, P. (1998). Molecular characterization of CDSP 34, a chloroplastic protein induced by water deficit in Solanum tuberosum L. plants, and regulation of CDSP 34 expression by ABA and high illumination. *The Plant Journal*, *16*, 257–262.

Gonzalez-Jorge, S., Ha, S. H., Magallanes-Lundback, M., Gilliland, L. U., Zhou, A., Lipka, A. E., et al. (2013). Carotenoid cleavage dioxygenase4 is a negative regulator of β-carotene content in Arabidopsis seeds. *Plant Cell*, *25*, 4812–4826.

Greenwood, A. D., Leech, R. M., & Williams, J. P. (1963). The osmiophilic globules of chloroplasts: I. Osmiophilic globules as a normal component of chloroplasts and their isolation and composition in Vicia faba L. *Biochimica et Biophysica Acta*, *78*, 148–162.

Gross, J., Cho, W. K., Lezhneva, L., Falk, J., Krupinska, K., Shinozaki, K., et al. (2006). A plant locus essential for phylloquinone (vitamin K1) biosynthesis originated from a fusion of four eubacterial genes. *Journal of Biological Chemistry*, *281*, 17189–17196.

Hansmann, P., & Sitte, P. (1982). Composition and molecular structure of chromoplast globules of Viola tricolor. *Plant Cell Reports*, *1*, 111–114.

Havaux, M. (2020). Plastoquinone in and beyond photosynthesis. *Trends in Plant Science*, *25*, 1252–1265.

Hörtensteiner, S., & Kräutler, B. (2011). Chlorophyll breakdown in higher plants. *Biochimica et Biophysica Acta (BBA)—Bioenergetics*, *1807*, 977–988.

Huang, H., Yang, M., Su, Y.e., Qu, L., & Deng, X. W. (2015). Arabidopsis atypical kinases ABC1K1 and ABC1K3 act oppositely to cope with photodamage under red light. *Molecular Plant*, *8*, 1122–1124.

Ischebeck, T., Zbierzak, A. M., Kanwischer, M., & Dormann, P. (2006). A salvage pathway for phytol metabolism in Arabidopsis. *Journal of Biological Chemistry*, *281*, 2470–2477.

Kessler, F., Schnell, D., & Blobel, G. (1999). Identification of proteins associated with plastoglobules isolated from pea (Pisum sativum L.) chloroplasts. *Planta*, *208*, 107–113.

Kim, E. H., Lee, Y., & Kim, H. U. (2015). Fibrillin 5 is essential for plastoquinone-9 biosynthesis by binding to solanesyl diphosphate synthases in arabidopsis. *Plant Cell*, *27*, 2956–2971.

Kim, E. H., Lee, D. W., Lee, K. R., Jung, S. J., Jeon, J. S., & Kim, H. U. (2017). Conserved function of fibrillin5 in the plastoquinone-9 biosynthetic pathway in arabidopsis and rice. *Frontiers in Plant Science*, *8*, 1197.

Kirchhoff, H. (2019). Chloroplast ultrastructure in plants. *The New Phytologist*, *223*, 565–574.

Kobayashi, N., & DellaPenna, D. (2008). Tocopherol metabolism, oxidation and recycling under high light stress in Arabidopsis. *The Plant Journal*, *55*, 607–618.

Krauß, S., & Vetter, W. (2018). Phytol and phytyl fatty acid esters: Occurrence, concentrations, and relevance. *European Journal of Lipid Science and Technology*, *120*, 1700387.

Krieger-Liszkay, A., & Trebst, A. (2006). Tocopherol is the scavenger of singlet oxygen produced by the triplet states of chlorophyll in the PSII reaction centre. *Journal of Experimental Botany*, *57*, 1677–1684.

Ksas, B., Légeret, B., Ferretti, U., Chevalier, A., Pospíšil, P., Alric, J., et al. (2018). The plastoquinone pool outside the thylakoid membrane serves in plant photoprotection as a reservoir of singlet oxygen scavengers. *Plant, Cell & Environment*, *41*, 2277–2287.

Lagier-Tourenne, C., Tazir, M., López, L. C., Quinzii, C. M., Assoum, M., Drouot, N., et al. (2008). ADCK3, an ancestral kinase, is mutated in a form of recessive ataxia associated with coenzyme Q10 deficiency. *The American Journal of Human Genetics*, *82*, 661–672.

Langenkämper, G., Manac'h, N., Broin, M., Cuiné, S., Becuwe, N., Kuntz, M., et al. (2001). Accumulation of plastid lipid-associated proteins (fibrillin/CDSP34) upon oxidative stress, ageing and biotic stress in Solanaceae and in response to drought in other species. *Journal of Experimental Botany*, *52*, 1545–1554.

Leggett Bailey, J., & Whyborn, A. G. (1963). The osmiophilic globules of chloroplasts II. Globules of the spinach-beet chloroplast. *Biochimica et Biophysica Acta*, *78*, 163–174.

Li, T., Jiang, J., Zhang, S., Shu, H., Wang, Y., Lai, J., et al. (2015). OsAGSW1, an ABC1-like kinase gene, is involved in the regulation of grain size and weight in rice. *The Journal of Experimental Botany*, *66*, 5691–5701.

Lichtenthaler, H. J. E. (1968a). Plastoglobuli and fine structure of plastids. *Endeavor*, *27*, 144.

Lichtenthaler, H. K. (1968b). Distribution and relative concentrations of lipophilic plastid quinones in green plants. *Planta*, *81*, 140–152.

Lichtenthaler, H. K., & Peveling, E. (1966). Plastoglobuli in different types of plastids from Allium cepa L. *Planta*, *72*, 1–13.

Lichtenthaler, H. K., & Sprey, B. (1966). Über die osmiophilen globulären Lipideinschlüsse der Chloroplasten. *Zeitschrift für Naturforschung B*, *21*, 690–697.

Lippold, F., vom Dorp, K., Abraham, M., Hölzl, G., Wewer, V., Yilmaz, J. L., et al. (2012). Fatty acid phytyl ester synthesis in chloroplasts of arabidopsis. *The Plant Cell*, *24*, 2001–2014.

Liu, X., Hua, X., Guo, J., Qi, D., Wang, L., Liu, Z., et al. (2008). Enhanced tolerance to drought stress in transgenic tobacco plants overexpressing VTE1 for increased tocopherol production from *Arabidopsis thaliana*. *Biotechnology Letters*, *30*, 1275–1280.

Lohmann, A., Schöttler, M. A., Bréhélin, C., Kessler, F., Bock, R., Cahoon, E. B., et al. (2006). Deficiency in phylloquinone (vitamin K1) methylation affects prenyl quinone distribution, photosystem I abundance, and anthocyanin accumulation in the arabidopsis atmenG mutant. *Journal of Biological Chemistry*, *281*, 40461–40472.

Lohscheider, J. N., & Río Bártulos, C. (2016). Plastoglobules in algae: A comprehensive comparative study of the presence of major structural and functional components in complex plastids. *Marine Genomics*, *28*, 127–136.

Lundquist, P. K., Poliakov, A., Bhuiyan, N. H., Zybailov, B., Sun, Q., & van Wijk, K. J. (2012). The functional network of the arabidopsis plastoglobule proteome based on quantitative proteomics and genome-wide coexpression analysis. *Plant Physiology*, *158*, 1172–1192.

Lundquist, P. K., Poliakov, A., Giacomelli, L., Friso, G., Appel, M., McQuinn, R. P., et al. (2013). Loss of plastoglobule kinases ABC1K1 and ABC1K3 causes conditional degreening, modified prenyl-lipids, and recruitment of the jasmonic acid pathway. *The Plant Cell*, *25*, 1818–1839.

Malkin, R. (1986). On the function of two vitamin K1 molecules in the PS I electron acceptor complex. *FEBS Letters*, *208*, 343–346.

Manara, A., DalCorso, G., Guzzo, F., & Furini, A. (2015). Loss of the atypical kinases ABC1K7 and ABC1K8 changes the lipid composition of the chloroplast membrane. *Plant and Cell Physiology*, *56*, 1193–1204.

Manara, A., DalCorso, G., Leister, D., Jahns, P., Baldan, B., & Furini, A. (2014). AtSIA1 AND AtOSA1: Two Abc1 proteins involved in oxidative stress responses and iron distribution within chloroplasts. *The New phytologist*, *201*, 452–465.

Martinis, J., Glauser, G., Valimareanu, S., & Kessler, F. (2013). A chloroplast ABC1-like kinase regulates vitamin E metabolism in arabidopsis. *Plant Physiology*, *162*, 652–662.

Martinis, J., Glauser, G., Valimareanu, S., Stettler, M., Zeeman, S. C., Yamamoto, H., et al. (2014). ABC1K1/PGR6 kinase: A regulatory link between photosynthetic activity and chloroplast metabolism. *The Plant Journal*, *77*, 269–283.

Mène-Saffrané, L., Jones, A. D., & DellaPenna, D. (2010). Plastochromanol-8 and tocopherols are essential lipid-soluble antioxidants during seed desiccation and quiescence in Arabidopsis. *Proceedings of the National Academy of Sciences of the United States of America*, *107*, 17815–17820.

Merchant, S. S., Prochnik, S. E., Vallon, O., Harris, E. H., Karpowicz, S. J., Witman, G. B., et al. (2007). The Chlamydomonas genome reveals the evolution of key animal and plant functions. *Science (New York, NY)*, *318*, 245–250.

Michalecka, A. M., Svensson, A. S., Johansson, F. I., Agius, S. C., Johanson, U., Brennicke, A., et al. (2003). Arabidopsis genes encoding mitochondrial type II NAD(P)H dehydrogenases have different evolutionary origin and show distinct responses to light. *Plant Physiology*, *133*, 642–652.

Mollet, J., Delahodde, A., Serre, V., Chretien, D., Schlemmer, D., Lombes, A., et al. (2008). CABC1 gene mutations cause ubiquinone deficiency with cerebellar ataxia and seizures. *The American Journal of Human Genetics*, *82*, 623–630.

Munné-Bosch, S. (2005). The role of α-tocopherol in plant stress tolerance. *Journal of Plant Physiology*, *162*, 743–748.

Munné-Bosch, S., & Alegre, L. (2002). The function of tocopherols and tocotrienols in plants. *Critical Reviews in Plant Sciences*, *21*, 31–57.

Muñoz, P., & Munné-Bosch, S. (2019). Vitamin E in plants: Biosynthesis, transport, and function. *Trends in Plant Science*, *24*, 1040–1051.

Neely, W. C., Martin, J. M., & Barker, S. A. (1988). Products and relative reaction rates of the oxidation of tocopherols with singlet molecular oxygen. *Photochemistry and Photobiology*, *48*, 423–428.

Nogueira, M., Mora, L., Enfissi, E. M., Bramley, P. M., & Fraser, P. D. (2013). Subchromoplast sequestration of carotenoids affects regulatory mechanisms in tomato lines expressing different carotenoid gene combinations. *Plant Cell*, *25*, 4560–4579.

Ohmiya, A., Kishimoto, S., Aida, R., Yoshioka, S., & Sumitomo, K. (2006). Carotenoid cleavage dioxygenase (CmCCD4a) contributes to white color formation in chrysanthemum petals. *Plant Physiology*, *142*, 1193–1201.

Otsubo, M., Ikoma, C., Ueda, M., Ishii, Y., & Tamura, N. (2018). Functional role of fibrillin 5 in acclimation to photooxidative stress. *Plant & Cell Physiology*, *59*, 1670–1682.

Poon, W. W., Davis, D. E., Ha, H. T., Jonassen, T., Rather, P. N., & Clarke, C. F. (2000). Identification of *Escherichia coli*, a gene required for the first monooxygenase step in ubiquinone biosynthesis. *Journal of Bacteriology*, *182*, 5139–5146.

Pozueta-Romero, J., Rafia, F., Houlné, G., Cheniclet, C., Carde, J. P., Schantz, M. L., et al. (1997). A ubiquitous plant housekeeping gene, PAP, encodes a major protein component of bell pepper chromoplasts. *Plant Physiology*, *115*, 1185–1194.

Pralon, T., Collombat, J., Pipitone, R., Ksas, B., Shanmugabalaji, V., Havaux, M., et al. (2020). Mutation of the atypical kinase ABC1K3 partially rescues the PROTON GRADIENT REGULATION 6 phenotype in *Arabidopsis thaliana*. *Frontiers in Plant Science*, *11*.

Pralon, T., Shanmugabalaji, V., Longoni, P., Glauser, G., Ksas, B., Collombat, J., et al. (2019). Plastoquinone homoeostasis by Arabidopsis proton gradient regulation 6 is essential for photosynthetic efficiency. *Communications Biology*, *2*, 220.

Rey, P., Gillet, B., Römer, S., Eymery, F., Massimino, J., Peltier, G., et al. (2000). Over-expression of a pepper plastid lipid-associated protein in tobacco leads to changes in plastid ultrastructure and plant development upon stress. *The Plant Journal*, *21*, 483–494.

Rodrigo, M. J., Alquézar, B., Alós, E., Medina, V., Carmona, L., Bruno, M., et al. (2013). A novel carotenoid cleavage activity involved in the biosynthesis of Citrus fruit-specific apocarotenoid pigments. *The Journal of Experimental Botany*, *64*, 4461–4478.

Rottet, S., Devillers, J., Glauser, G., Douet, V., Besagni, C., & Kessler, F. (2016). Identification of plastoglobules as a site of carotenoid cleavage. *Frontiers in Plant Science*, *7*, 1855.

Rubio-Moraga, A., Rambla, J. L., Fernández-de-Carmen, A., Trapero-Mozos, A., Ahrazem, O., Orzáez, D., et al. (2014). New target carotenoids for CCD4 enzymes are revealed with the characterization of a novel stress-induced carotenoid cleavage dioxygenase gene from Crocus sativus. *Plant Molecular Biology*, *86*, 555–569.

Santabarbara, S., & Casazza, A. P. (2019). Kinetics and energetics of phylloquinone reduction in photosystem i: insight from modeling of the site directed mutants. *Frontiers in Plant Science*, *10*.

Schelbert, S., Aubry, S., Burla, B., Agne, B., Kessler, F., Krupinska, K., et al. (2009). Pheophytin pheophorbide hydrolase (pheophytinase) is involved in chlorophyll breakdown during leaf senescence in Arabidopsis. *Plant Cell*, *21*, 767–785.

Schoeder, H.-U., & Lockau, W. (1986). Phylloquinone copurifies with the large subunit of photosystem I. *FEBS Letters*, *199*, 23–27.

Shanmugabalaji, V., Besagni, C., Piller, L. E., Douet, V., Ruf, S., Bock, R., et al. (2013). Dual targeting of a mature plastoglobulin/fibrillin fusion protein to chloroplast plastoglobules and thylakoids in transplastomic tobacco plants. *Plant Molecular Biology*, *81*, 13–25.

Shikanai, T., Munekage, Y., Shimizu, K., Endo, T., & Hashimoto, T. (1999). Identification and characterization of arabidopsis mutants with reduced quenching of chlorophyll fluorescence. *Plant and Cell Physiology*, *40*, 1134–1142.

Simkin, A. J., Gaffé, J., Alcaraz, J. P., Carde, J. P., Bramley, P. M., Fraser, P. D., et al. (2007). Fibrillin influence on plastid ultrastructure and pigment content in tomato fruit. *Phytochemistry*, *68*, 1545–1556.

Singh, D. K., Laremore, T. N., Smith, P. B., Maximova, S. N., & McNellis, T. W. (2012). Knockdown of FIBRILLIN4 gene expression in apple decreases plastoglobule plastoquinone content. *PLos One*, *7*, e47547.

Singh, D. K., & McNellis, T. W. (2011). Fibrillin protein function: The tip of the iceberg? *Trends in Plant Science*, *16*, 432–441.

Soll, J., Schultz, G., Joyard, J., Douce, R., & Block, M. A. (1985). Localization and synthesis of prenylquinones in isolated outer and inner envelope membranes from spinach chloroplasts. *Archives of Biochemistry and Biophysics*, *238*, 290–299.

Spicher, L., & Kessler, F. (2015). Unexpected roles of plastoglobules (plastid lipid droplets) in vitamin K1 and E metabolism. *Current Opinion in Plant Biology*, *25*, 123–129.

Spurr, A. R., & Harris, W. M. (1968). Ultrastructure of chloroplasts and chromoplasts in capsicum annuum I. Thylakoid membrane changes during fruit ripening. *American Journal of Botany*, *55*, 1210–1224.

Steinmüller, D., & Tevini, M. (1985). Composition and function of plastoglobuli: I. Isolation and purification from chloroplasts and chromoplasts. *Planta*, *163*, 201–207.

Tevini, M., & Steinmuller, D. (1985). Composition and function of plastoglobuli: II. Lipid composition of leaves and plastoglobuli during beech leaf senescence. *Planta*, *163*, 91–96.

Thomson, W. W., & Platt, K. (1973). Plastid ultrastructure in the barrel cactus, echinocactus acanthodes. *New Phytologist*, *72*, 791–797.

Tikhonov, A. N. (2013). pH-Dependent regulation of electron transport and ATP synthesis in chloroplasts. *Photosynthesis Research*, *116*, 511–534.

Van Eerden, F. J., Melo, M. N., Frederix, P., Periole, X., & Marrink, S. J. (2017). Exchange pathways of plastoquinone and plastoquinol in the photosystem II complex. *Nature Communications*, *8*, 15214.

van Wijk, K. J., & Kessler, F. (2017). Plastoglobuli: Plastid microcompartments with integrated functions in metabolism, plastid developmental transitions, and environmental adaptation. *Annual Review of Plant Biology*, *68*, 253–289.

Varghese, R., Udhaya Kumar, S., Doss, C. G. P., & Ramamoorthy, S. (2021). Unraveling the versatility of CCD4: Metabolic engineering, transcriptomic and computational approaches. *Plant Science: an International Journal of Experimental Plant Biology*, *310*, 110991.

Vidi, P. A., Kanwischer, M., Baginsky, S., Austin, J. R., Csucs, G., Dormann, P., et al. (2006). Tocopherol cyclase (VTE1) localization and vitamin E accumulation in chloroplast plastoglobule lipoprotein particles. *Journal of Biological Chemistry*, *281*, 11225–11234.

Woggon, W. D. (1999). Improving the yield of alpha-tocopherol from natural sources-chemistry versus molecular biology. *Angewandte Chemie (International ed in English)*, *38*, 2715–2716.

Yang, M., Huang, H., Zhang, C., Wang, Z., Su, Y., Zhu, P., et al. (2016). Arabidopsis atypical kinase ABC1K1 is involved in red light-mediated development. *Plant Cell Reports*, *35*, 1213–1220.

Youssef, A., Laizet, Y., Block, M. A., Maréchal, E., Alcaraz, J. P., Larson, T. R., et al. (2010). Plant lipid-associated fibrillin proteins condition jasmonate production under photosynthetic stress. *The Plant Journal*, *61*, 436–445.

Ytterberg, A. J., Peltier, J. B., & van Wijk, K. J. (2006). Protein profiling of plastoglobules in chloroplasts and chromoplasts. A surprising site for differential accumulation of metabolic enzymes. *Plant Physiology*, *140*, 984–997.

Zbierzak, A. M., Kanwischer, M., Wille, C., Vidi, P. A., Giavalisco, P., Lohmann, A., et al. (2009). Intersection of the tocopherol and plastoquinol metabolic pathways at the plastoglobule. *The Biochemical Journal*, *425*, 389–399.

Zechmann, B. (2019). Ultrastructure of plastids serves as reliable abiotic and biotic stress marker. *PLoS One*, *14*, e0214811.

Zhang, B., Liu, C., Wang, Y., Yao, X., Wang, F., Wu, J., et al. (2015). Disruption of a CAROTENOID CLEAVAGE DIOXYGENASE 4 gene converts flower colour from white to yellow in Brassica species. *The New Phytologist*, *206*, 1513–1526.

PLOS ONE

RESEARCH ARTICLE

Chromoplast plastoglobules recruit the carotenoid biosynthetic pathway and contribute to carotenoid accumulation during tomato fruit maturation

Wayne Zita[1], **Ségolène Bressoud**[1], **Gaetan Glauser**[2], **Felix Kessler**[1]*, **Venkatasalam Shanmugabalaji**[1]*

1 Plant Physiology Laboratory, University of Neuchâtel, Neuchâtel, Switzerland, 2 Neuchâtel Platform of Analytical Chemistry, University of Neuchâtel, Neuchâtel, Switzerland

* felix.kessler@unine.ch (FK); shanmugabalaji.venkatasalam@unine.ch (VS)

Citation: Zita W, Bressoud S, Glauser G, Kessler F, Shanmugabalaji V (2022) Chromoplast plastoglobules recruit the carotenoid biosynthetic pathway and contribute to carotenoid accumulation during tomato fruit maturation. PLoS ONE 17(12): e0277774. https://doi.org/10.1371/journal.pone.0277774

Editor: Hiroshi Ezura, University of Tsukuba, JAPAN

Received: September 15, 2022

Accepted: November 2, 2022

Published: December 6, 2022

Data Availability Statement: The mass spectrometry proteomics data have been deposited to the ProteomeXchange Consortium via the PRIDE partner repository with the dataset identifier PXD035763 and 10.6019/PXD035763.

Funding: This work was supported by the Swiss National Science Foundation (SNSF) grant 31003A_176191 to FK. The Role of Funder statment: Felix Kessler obtained funding and

Abstract

Tomato (*Solanum lycopersicum*) fruit maturation is associated with a developmental transition from chloroplasts (in mature green fruit) to chromoplasts (in red fruit). The hallmark red color of ripe tomatoes is due to carotenogenesis and accumulation of the red carotenoid lycopene inside chromoplasts. Plastoglobules (PG) are lipid droplets in plastids that are involved in diverse lipid metabolic pathways. In tomato, information on the possible role of PG in carotogenesis and the PG proteome is largely lacking. Here, we outline the role of PG in carotenogenesis giving particular attention to tomato fruit PG proteomes and metabolomes. The proteome analysis revealed the presence of PG-typical FBNs, ABC1K-like kinases, and metabolic enzymes, and those were decreased in the PG of tomato chromoplasts compared to chloroplasts. Notably, the complete β-carotene biosynthesis pathway was recruited to chromoplast PG, and the enzymes PHYTOENE SYNTHASE 1 (PSY-1), PHYTOENE DESATURASE (PDS), ZETA-CAROTENE DESATURASE (ZDS), and CAROTENOID ISOMERASE (CRTISO) were enriched up to twelvefold compared to chloroplast PG. We profiled the carotenoid and prenyl lipid changes in PG during the chloroplast to chromoplast transition and demonstrated large increases of lycopene and β-carotene in chromoplast PG. The PG proteome and metabolome are subject to extensive remodeling resulting in high accumulation of lycopene during the chloroplast-to-chromoplast transition. Overall, the results indicate that PGs contribute to carotenoid accumulation during tomato fruit maturation and suggest that they do so by functioning as a biosynthetic platform for carotenogenesis.

Introduction

Chloroplasts, specialized photosynthetic plastids are present in all green tissues of plants, and are characterized by the presence of an extensive membrane system called thylakoids [1]. Plastoglobules (PG) bud from the outer leaflet of the thylakoid membrane and remain associated

contributed to the experi-mental design and the manuscript preparation.

Competing interests: The authors have declared that no competing interests exist.

with the thylakoid membranes [2]. These "osmophilic globuli" were discovered by Lichtenthaler in the early 1970s with the advances in transmission electron microscopy [3]. PG participate in thylakoid lipid metabolism in response to biotic and abiotic stresses (light stress and nitrogen deprivation) [4–6]. Metabolites stored in PG may be exchanged with the thylakoid membrane [7]. PG have dynamic properties changing in number and size and depending on developmental stage and environmental conditions to assure thylakoid homeostasis [8, 9].

Plastoglobules contain a small specialized proteome, consisting of approximately 30 proteins. The components of the Arabidopsis and *Capsicum annuum* (bell pepper) PG proteomes have been categorized into structural proteins, regulatory kinases, and enzymes. Structural proteins named plastid lipid-associated proteins, plastoglobulins or fibrillins (FBNs) have been identified in the proteomes of red bell pepper and Arabidopsis PG [10–12]. The presence of a lipocalin domain suggests that the FBNs may contribute to the transport of lipids or the channeling of metabolites contained in PG [13, 14]. The PG proteomes contain presumed regulatory proteins namely ABC1K-like kinases. ABC1K1 together with ABC1K3 may contribute to plastoquinone distribution within the chloroplast [15, 16]. Together with the FBNs, ABC1Ks are the most abundant components of the PG proteomes [12]. In addition, PGs contain several uncharacterized predicted enzymes but also some well-known ones such as TOCOPHEROL CYCLASE (VTE1) and NAD(P)H DEHYDROGENASE C1 (NDC1) [10, 17]. They are involved in α-tocopherol and phylloquinone biosynthesis, respectively, and implicate PG in these biosynthetic pathways. A considerable number of studies have identified PG as a storage compartment containing neutral and prenyl lipids, including phylloquinone (vitamin K), plastoquinone (PQ-9), plastochromanol 8 (PC-8), tocopherols, triacylglycerols, fatty acids, and carotenoids [18–21].

In tomato fruit, chromoplasts develop from chloroplasts, a process that involves the dismantling of thylakoid membranes and chlorophyll breakdown as well as the recycling of the breakdown products [22–24]. PG in chromoplasts contain carotenoids such as β-carotene and lycopene, a high level of which is responsible for the hallmark red color of tomato fruit [25]. Tomato chromoplast PG are globular, whereas those of red bell pepper are fibrillar [21, 26, 27]. Fibrillins were first discovered as a major protein component of fibrillar PG in bell pepper, hence their name [21]. Later, red bell pepper chromoplast PG were shown to contain several carotenoid biosynthetic pathway enzymes including LYCOPENE β-CYCLASE (LCYB) and ζ-CAROTENE DESATURASE (ZDS) [11]. To characterize and establish tomato plastoglobule proteomes, we isolated PG from lysed chloroplasts and chromoplasts by sucrose density gradient centrifugation followed by nano LC-MS/MS analysis (Nanoscale liquid chromatography coupled to tandem mass spectrometry) of the associated proteins. We identified multiple known as well as new candidate PG proteins. Notably, enzymes of the carotenoid biosynthetic pathway were recruited to PG and some of them were strongly enriched in chromoplast PG. This coincided with strongly increased accumulation of lycopene, supporting a possible role of PG in carotenogenesis during tomato fruit ripening and chloroplast to chromoplast differentiation.

Material & methods

Plant material and growth conditions

Tomato used was (*Solanum Lycopersicum*, cv. Micro-Tom). The plants were grown in soil under 200 μmol.m^{-2}.s^{-1} in a growth chamber, with a photoperiod of 16 h of day and 8 h of the dark at at 22° and 18°C, respectively. The relative air humidity of the growth chamber was around 30%. The mature green fruits were harvested after 34–39 day after anthesis, and red fruits were harvested 10 days after the breaker stage and immediately put on ice for further experimentation.

Fractionation and isolation of tomato chloroplast and chromoplasts plastoglobules

Fruits were washed with distilled water. The peduncle, the gel, and the seeds were removed from the fruits, then the pericarp was cut into small pieces and stored at 4˚C overnight. 130 g of tomato pieces were put into a cold waring blender, 150 ml extraction buffer (0.4 M sucrose, 50 mM Tris-HCl pH 7.8, 1 mM EDTA, 1 mM DTT) was added and followed by homogenization (twice for 3 seconds at low speed, then twice for 5 seconds at high speed). The homogenate was filtered through three to four layers of cheesecloth (gauze) and put in a 500 ml centrifuge tube on ice. Tubes were centrifuged at 5000x g for 10 min in a Sorvall RC-5B (SLA-1500 Super Lite rotor) at 4˚C. The supernatant was removed, and the pellet was resuspended in 5 ml of extraction buffer and transferred to a 50 ml centrifuge tube on ice. Tubes were centrifuged at 9000x g for 10 min in a Sorvall RC-5B (SM-24 rotor) at 4˚C. The supernatant was removed, and the pellet kept on ice. The pellet was resuspended in 5 ml of 45% sucrose (45% sucrose [w/v], 50 mM tricine pH7.9, 5 mM sodium bisulphite, 2 mM EDTA, 2mM DTT). Chloroplasts and chromoplasts were homogenized mechanically using a hand-held Potter homogenizer. 3 ml of 45% sucrose were added to the potter homogenizer and 8 ml of the resulting homogenate were transferred to a 38.5 ml Ultra-Clear centrifuge tube. Layers of 38%, 20%, 15% and 5% sucrose were added, and the gradients centrifuged 20 h at 4˚C at 100 000x g. Western blot analysis indicated that PG were contained in the top sucrose layers.

Proteins precipitation and immunoblotting

Proteins contained in PG and other fractions were precipitated with acetone. Proteins were separated by SDS-PAGE and transferred to nitrocellulose membrane. The immunoblotting was performed using FBN1A [10], TOC75 [28], and LHCB2 (Agrisera) antibodies.

Protein identification by nano-LC-MS/MS

The dry pellet of the PG protein sample was resuspended in 45 μl of miST buffer (1% sodium deoxycholate, 100mM Tris pH 8.6 (-20˚C), 10 mM DTT, 0.2μM EDTA), vortexed and heated at 90˚C for 5 min. 160 mM chloroacetamide in 10 mM Tris pH 8.6 was added to the sample and incubated for 30 min at room temperature. Next, the tryptic digestion was performed with 0.3 ug LysC/Trypsin for 90 min at 37˚C. An OASIS plate was pre-equilibrated with acetonitrile (MeCN) and SCX buffer. 300 μl of 100% ethyl-acetate and 1% trifluoroacetic acid (TFA) were added to the samples, vortexed for 2 min, and centrifuged at 5000 rpm for 5 min. The bottom aqueous phase was transferred into prefilled SOLA SCX columns and spun through the column (not too fast, typically, 2000 rpm 1 min is sufficient). The column was washed with 300 ul ethyl acetate, 0.5% TFA and HPLC solvent A (2% MeCN, 0.1% formic acid). The sample was eluted with 200 ul elution buffer (80% MeCN, 19% water, 1% NH3). The eluted sample was dried in a speed vac and resuspended in HPLC solvent A for MS analysis (Fusion, IT mode). Scaffold viewer Scaffold (version Scaffold_5.1.2, Proteome Software Inc., Portland, OR) software was used to validate MS/MS based peptide and protein identifications. Peptide identifications were accepted if they could be established at greater than 90.0% probability by the Scaffold Local FDR algorithm. All MS/MS spectras were analyzed using Mascot (Matrix Science, London, UK; version 2.6.2) to find the known protein sequences with a fragment ion mass tolerance of 0.50 Da and a parent ion tolerance of 10.0 PPM.

Prenyl lipid and carotenoid analysis from whole tomato fruit and PG fractions

Prenyl lipids and carotenoids were extracted from whole tomato fruit and PG fractions using established methods [29, 30]. The prenyl quinones and carotenoids were separated and quantified by reverse-phase ultra-high-pressure liquid chromatography coupled to quadrupole-time-of-flight mass spectrometry (UHPLC-QTOFMS). Absolute concentrations of prenylquinones (PQ-9, PC-8, phylloquinone, α-T, γ-T, δ-T, PC-OH, PQH2-9 PQ-OH) and carotenoids (lycopene, lutein, β-carotene, phytoene) were calculated based on standard calibration curves. In addition, the carotenoids violaxanthin and neoxanthin were measured based on lutein standards.

Results

Isolation and quality assessment of chloroplast and chromoplast plastoglobules

To determine tomato fruit PG proteomes, tomato plants (*Solanum Lycopersicum*) were grown under standard light conditions (200 $\mu mol.m^{-2}.s^{-1}$) and mature green and red fruit were harvested [31]. PG from chloroplasts (in mature green fruit) and chromoplasts (in red fruit) were isolated by flotation centrifugation on a discontinuous sucrose gradient [26]. The low density of PG allowed separation from plastid membrane compartments by differential flotation. Visual inspection suggested that chloroplast plastoglobules (PG), EN (envelope) and TM (thylakoid membranes) from chloroplasts had been separated well (Fig 1A). The same held true for chromoplast plastoglobules (PG) that also appeared well separated from carotenoid membranous crystals (CR) and envelopes (EN) (Fig 1C). This was further assessed by western blotting analysis of the gradient fractions using specific antibodies against marker proteins for PG FBN1A, envelopes TOC75, and thylakoid membranes LHCB2 (Fig 1B and 1D). The established PG marker FBN1A was detected in the first ten low-density fractions but also the last fractions, which has already been shown in previous studies and is likely due to the association of PG with plastid membranes [10, 12, 26] (Fig 1B and 1D). The absence of the thylakoid LHCB2 and the outer envelope membrane TOC75 markers in the low-density fractions indicated PG enrichment. Fractions one to five enriched in PG were selected for further analysis, pooled, and proteins were precipitated by acetone. The protein pellets were dried. Two independent biological replicates for both chloroplast and chromoplast PG were obtained.

Tomato plastoglobule proteome

Pooled and precipitated PG fractions were digested with trypsin. The tryptic peptides were analyzed by gel-enhanced liquid chromatography-mass spectrometry (GeLCMS). The data were analyzed using the MASCOT/MaxQuant and Scaffold algorithm to identify proteins corresponding to the peptides. The parameters were set to identify only those individual proteins that were common to both biological replicates of the experiment. A total of 1150 and 838 proteins were identified in chloroplast and chromoplast PG, respectively. These sets of proteins were further analyzed using the UniProt, TAIR and SUBA online resources as well as the TargetP algorithm. This analysis reduced the number to 271 and 147 candidate proteins for chloroplast and chromoplast PG. The established PG proteomes from *Arabidopsis thaliana* and red bell pepper [10–12] combined together were used as references to identify core components of the chloroplast and chromoplast PG proteomes. Thereby, 33 tomato chloroplast and 31 chromoplast proteins were found in common with Arabidopsis, and bell pepper and constituted the tomato fruit PG core proteomes. With the exception of the absence of CCD4 and

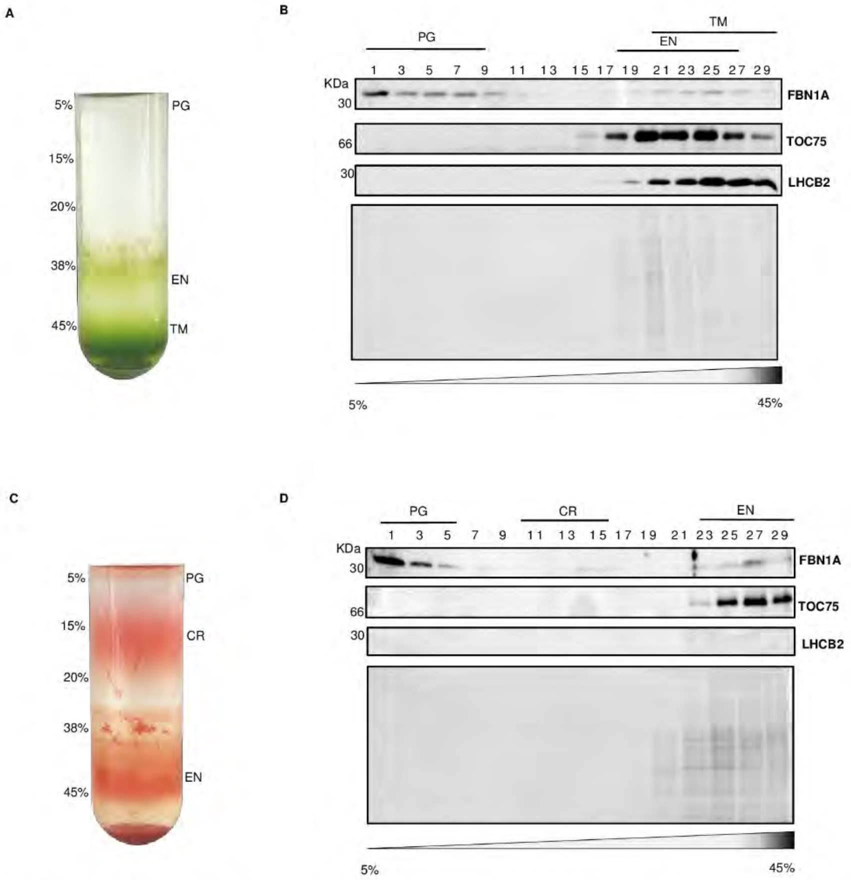

Fig 1. Isolation of tomato fruit PG from chloroplast and chromoplast. (A) Isolated chloroplasts were fractionated on a sucrose step gradient (5, 15, 20, 38, 45% sucrose). PG (plastoglobules); EN (envelope); TM (thylakoid membranes). (B) Uneven fractions from 1 to 29 were subjected to SDS-PAGE followed by immunoblotting using antibodies against FBN1A (PG marker), TOC75 (envelope marker), and LHCB2 (thylakoid marker). (C) Isolated chromoplasts from red tomato fruit were fractionated on a sucrose step gradient (5, 15, 20, 38, 45% sucrose). PG (plastoglobules); CR (carotenoid crystals); EN (envelope). (D) Uneven fractions 1 to 29 were subjected to SDS-PAGE followed by immunoblotting using antibodies FBN1A (PG marker), TOC75 (envelope marker), and LHCB2 (thylakoid marker).

https://doi.org/10.1371/journal.pone.0277774.g001

NDC1 from chromoplast PG, the chloroplast and chromoplast PG core proteomes were identical. Abundant PG proteins including FBNs and predicted regulatory protein kinases ABC1Ks were identified [12]. Also present in both proteomes were prenyl lipid pathway enzymes (including VTE1, PHYTYL ESTER SYNTHASE (PES), ZDS and LCYB) and additional accepted PG proteins (including PGM48, PG18, and SOUL4) [10, 11, 24, 32–34]. In addition to the known PG proteins, we have identified 18 new candidates for the tomato chloroplast PG proteome and 17 for the chromoplast PG proteome of which 15 were common to both. They were identifed using PPDB and STRING databases as well as subcellular localization studies in the literature essentially by exclusion of curated stromal, thylakoid and envelope proteins. This allowed us to identify three additional candidates for carotenoid biosynthesis

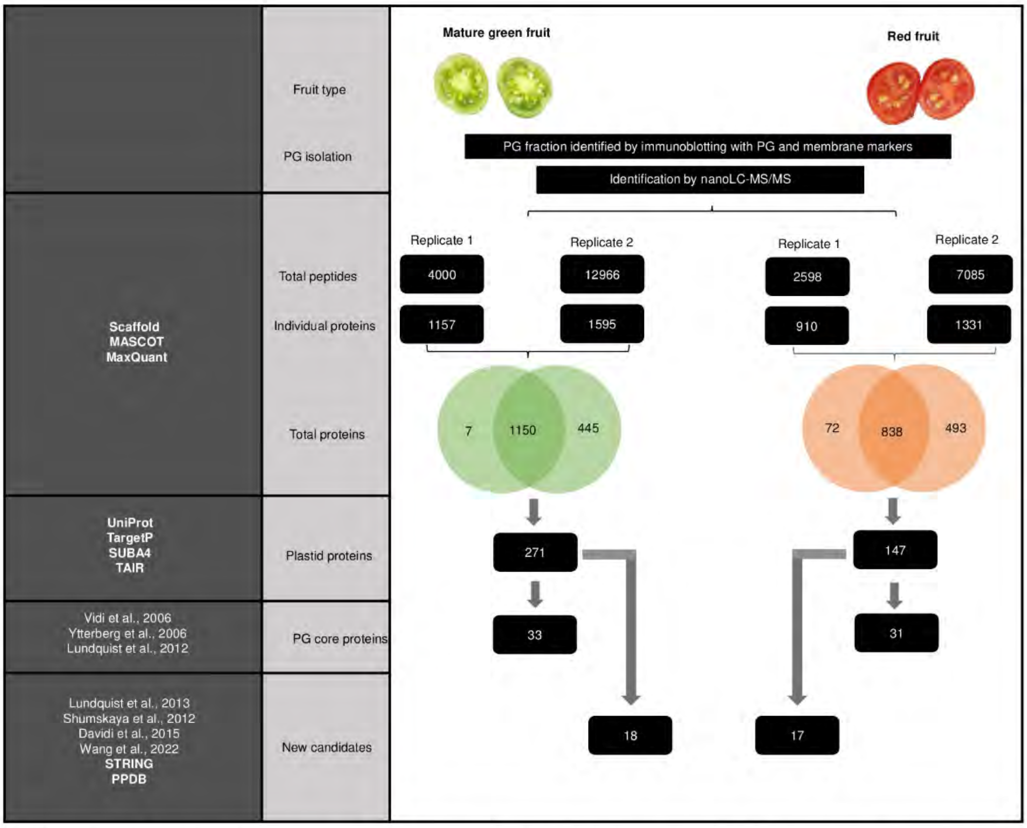

Fig 2. Experimental design used for tomato fruit PG proteome analysis. PGs from mature green and red fruit were isolated separately by sucrose gradient flotation. The two independent replicate PG fractions from mature green and red fruit were analyzed by nano-liquid chromatography (nanoLC)-electrospray ionization (ESI)-tandem mass spectrometry (MS / MS) for peptide identification. All identified peptides (Total Peptides) were further processed by Scaffold, MASCOT, and MaxQuant software to obtain corresponding individual proteins (Individual proteins). The number of individual proteins collected after merging two independent replicates (Total proteins). The Total proteins were filtered using the Uniport, TargetP, SUBA4, and TAIR databases to identify plastid protein (Plastid protein). Plastid proteins were filtered using known chloroplast and chromoplast proteome based on the existing literatures resulting in PG core proteins (PG core proteins). The new PG protein candidates (New candidates) were identified by exclusion of curated stromal, thylakoid and envelope proteins from plastid proteins (Plastid proteins) using PPDB and STRING databases as well as subcellular localization studies in the literature.

https://doi.org/10.1371/journal.pone.0277774.g002

pathway (PSY1, PDS, CRTISO), for phylloquinone biosynthesis (MenG), for lipid metabolism (LOXC) and for isopentenyl diphosphate biosynthesis (1-deoxy-D-xylulose-5-phosphate synthase 1; DXS1) (Fig 2 and Table 1).

Carotenoid biosynthetic enzymes are enriched in chromoplast PG

Five enzymes of the carotenoid biosynthesis pathway upto β-carotene were associated with chloroplast as well as chromoplast PG. The comparison of chloroplast with chromoplast PG revealed differences in their peptide counts. The heatmap based on peptide counts shows a clear increase in chromoplast PG of the first four enzymes required for lycopene biosynthesis namely PSY1, PDS, ZDS, and CRTISO. The higher numbers likely reflect higher enzyme levels

Table 1. Proteome of tomato fruit chloroplast and chromoplast plastoglobules.

Accession No	Protein Name	Peptide count		Homolog			
		PG chloroplast	PG chromoplast	*Arabidopsis thaliana*		*Capsicum annuum*	
Structural				Accession No	Lundquist et al., 2012	Accession No	Ytterberg et al.,2006
Solyc02g081170.2.1	FBN1a/b	153	99	AT4G04020	x	gi|1076575	x
Solyc08g076480.2.1	FBN2	162	53	AT2G35490	x	sgn| U197362	x
Solyc09g090330.2.1	FBN4	83	49	AT3G23400	x		x
Solyc10g080490.1.1	FBN7a	12	2	AT3G58010	x		-
Solyc03g062790.2.1	FBN7b	73	30	AT2G42130	x		-
Solyc08g068590.2.1	FBN8	41	40	AT2G46910	x		-
Regulatory							
Solyc08g074560.2.1	ABC1K1	62	31	AT4G31390	x		-
Solyc04g083010.2.1	ABC1K3	67	24	AT1G79600	x		-
Solyc04g072230.2.1	ABC1K5	39	11	AT1G71810	x		-
Solyc09g091580.2.1	ABC1K6	58	34	AT3G24190	x		-
Solyc07g045420.2.1	ABC1K7	39	26	AT3G07700	x		-
Solyc03g095620.2.1	ABC1K9	48	43	AT5G05200	x		x
Enzymes							
Solyc08g068570.2.1	VTE1	131	64	AT4G32770	x		x
Solyc08g075490.2.1	CCD4	15	0	AT4G19170	x		-
Solyc01g098110.2.1	PES1	56	68	AT1G54570	x		x
Solyc02g094430.2.1	PES2	65	57	AT3G26840	x		-
Solyc03g043750.2.1	NDC1	3	0	AT5G08740	x		-
Other							
Solyc01g056880.1.1	SOUL4	39	38	AT3G10130	x		-
Solyc07g007300.2.1	UbiE methyltransferase-related 1	7	14	AT2G41040	x		-
Solyc07g043570.2.1	Aldo/keto reductase	24	32	AT1G06690	x		x
Solyc09g061440.2.1	PG18	24	13	AT4G13200	x	sgn| U204835	x
Solyc03g096460.2.1	PLAT/LH2-1	9	4	AT4G39730	x		-
Solyc03g005000.2.1	PGM48	8	3	AT3G27110	x		-
Solyc08g076450.2.1	Flavin reductase-related 1	29	45	AT1G32220	x		x
Solyc02g070770.2.1	Flavin reductase-related 2	56	40	AT2G34460	x		-
Solyc08g075100.2.1	DUF1350	26	15	AT3G43540	x		-
Solyc03g118850.2.1	alpha/beta hydrolase family protein	16	10	AT1G73750	x		-
Solyc02g084440.2.1	Aldolase/ FBA8	59	23	AT3G52930	-		x
Solyc05g015390.2.1	Rubber elongation factor family	22	28	AT1G67360	-		x
Solyc04g039850.1.1	CF1b, atpB	62	57	ATCG00480	-		x
Solyc12g013810.1.1	Thioredoxin m4	11	13	AT3G15360	-	sgn| U201138	x
Carotenoid biosynthesis							
Solyc01g097810.2.1	ZDS	9	49	AT3G04870	-	gi|1583601	x
Solyc04g040190.1.1	LCYB	5	6	AT3G10230	-	gi|12643508	x
New candidates							
Carotenoid metabolism							
Solyc03g031860.2.1	PSY1 (Phytoene Synthase 1)	2	15	AT5G17230	-	-	-
Solyc03g123760.2.1	PDS (Phytoene desaturase)	5	36	AT4G14210	-	-	-

(Continued)

Table 1. (Continued)

Accession No	Protein Name	Peptide count		Homolog			
		PG chloroplast	PG chromoplast	*Arabidopsis thaliana*		*Capsicum annuum*	
Solyc10g081650.1.1	CRTISO (Carotenoid isomerase)	3	36	AT1G06820	-	-	-
Other							
Solyc01g006540.2.1	LOXC	18	55	AT1G17420	-	-	-
Solyc05g056270.2.1	Phosphoenolpyruvate carboxylase family protein	62	39	AT2G43180	-	-	-
Solyc06g083770.2.1	Glutathione S-transferase family protein	22	12	AT5G44000	-	-	-
Solyc05g009390.2.1	Alpha/beta-Hydrolases superfamily protein	7	11	AT1G77420	-	-	-
Solyc08g083035.1.1	Uncharacterized protein	10	6	AT5G41960	-	-	-
Solyc01g068030.2.1	Polyketide cyclase domain protein	4	6	At1g02475	-	-	-
Solyc07g005550.2.1	Uncharacterized protein	2	11	AT2G44870	-	-	-
Solyc06g059720.2.1	Stearoyl-acyl carrier protein delta-9-desaturases	0	15	AT1G43800	-	-	-
Solyc06g073280.2.1	L-lysine alpha-aminotransferase	7	4	AT2G13810	-	-	-
Solyc12g019010.1.1	MenG	8	4	AT1G23360	-	-	-
Solyc09g092450.2.1	Acyl activating enzyme 16	2	5	AT3G23790	-	-	-
Solyc03g118130.2.1	Rubredoxin-like superfamily protein	4	0	AT5G51010	-	-	-
Solyc11g009080.2.1	DAHP synthetase 1 (DHS1)	5	2	AT4G39980	-	-	-
Solyc05g053100.2.1	Dihydrolipoamide dehydrogenase	6	0	AT4G16155	-	-	-
Solyc06g050590.3.1	Biotin/lipoyl attachment domain-containing protein	5	0	AT3G56130	-	-	-
Solyc01g005910.2.1	DUF1212	0	3	AT3G12685	-	-	-
Solyc01g067890.2.1	1-deoxy-D-xylulose-5-phosphate synthase 1	30	5	AT4G15560	-	-	-

Tomato PG proteome which is based on two biological replicates. One representative proteome was selected for the table. The Accession No is the ID identified for each protein on www.solgenomics.net; the common protein name is based on the literature. The accession numbers of homologs are also given based on TAIR for Arabidopsis and Solanaceae database (www.sgn.cornell.edu) for bell pepper. Peptide count represents the number of peptides detected in each sample. The known "core" PG proteome was categorized into five groups and the new candidate PG protein group into two categories.

https://doi.org/10.1371/journal.pone.0277774.t001

that underpin lycopene biosynthetic activity in the chromoplast and during the chloroplast-to-chromoplast transition (Fig 3). Peptide counts for LYCB were similar in both plastid types, suggesting a constant activity of this enzyme in PG during chloroplast to chromoplast conversion (Fig 3). Heatmaps also showed reduced presence of FBNs and ABC1Ks in the chromoplast PG compared with chloroplast PG (S1 Fig).

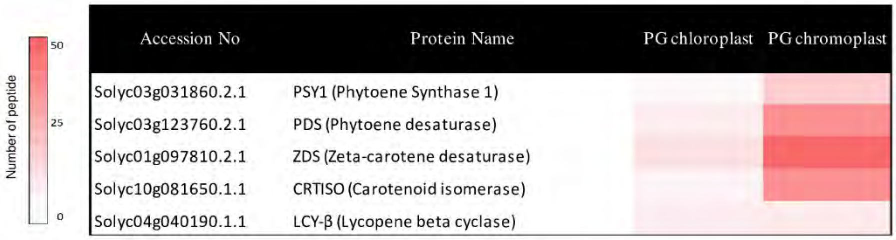

Accession No	Protein Name	PG chloroplast	PG chromoplast
Solyc03g031860.2.1	PSY1 (Phytoene Synthase 1)		
Solyc03g123760.2.1	PDS (Phytoene desaturase)		
Solyc01g097810.2.1	ZDS (Zeta-carotene desaturase)		
Solyc10g081650.1.1	CRTISO (Carotenoid isomerase)		
Solyc04g040190.1.1	LCY-β (Lycopene beta cyclase)		

Fig 3. Carotenoid biosynthetic enzymes enriched in tomato PG chromoplasts. The carotenoid biosynthetic enzymes heatmap was generated from peptide counts obtained from PG isolated from chloroplasts and chromoplasts, respectively.

https://doi.org/10.1371/journal.pone.0277774.g003

Protein-protein interaction network of chromoplast PG protein

The chromoplast PG proteome contains various proteins annotated with a large range of functions. We carried out an analysis of the protein network of the chromoplast plastoglobule proteome using STRING (www.string-db.org). The classification and clusters of chromoplast PG proteins proposed by STRING are based on a curated database, experimental results, predicted gene neighborhood, annotated function, text mining, protein co-expression, and protein homology according to the recent literature [35, 36]. Application of STRING resulted in three distinct clusters and a number of non-associated proteins (Fig 4). Cluster 1 was mainly composed of carotenoid biosynthetic enzymes including PSY1, which condenses two geranylgeranyl diphosphates to phytoene. PDS and ZDS catalyse desaturation reactions, which are required for synthesis of 9,9′-di-*cis*-ζ-carotene, and prolycopene, respectively. CRTISO

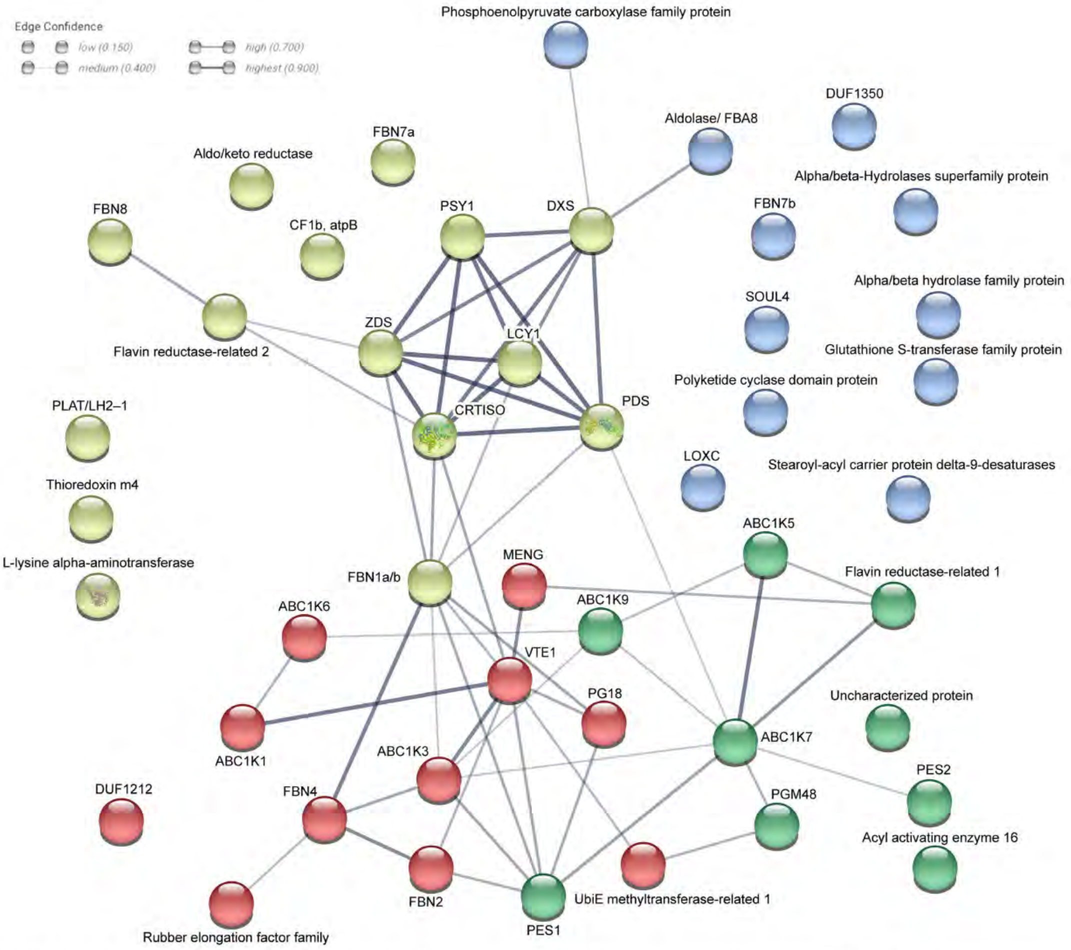

Fig 4. Interaction network of chromoplast PG proteins. The tomato chromoplast PG proteome analysis using the STRING software identified three clusters. Pear, (cluster 1) enriched in carotenoid biosynthetic enzymes; Red, (cluster 2) enriched in prenyl quinone metabolism and regulation; green, (cluster 3) enriched in chloroplast senescence and thylakoid membrane dismantling; blue, proteins not associated with the network.

https://doi.org/10.1371/journal.pone.0277774.g004

(carotene isomerase) converts prolycopene into all-trans-lycopene. LYCB catalyses the cyclization of lycopene into β-carotene [25]. In addition, carotenoid biosynthesis key regulatory enzyme DXS1 [37] is part of cluster 1. Interestingly, FBN1 (CHRC) is part of cluster 1 and also closely associated with cluster 2. FBN1 (CHRC) is well known for its involvement in carotenoid accumulation and fibril formation but also carotenoid stabilization in chromoplasts [21]. Cluster 2 contain FBNs, VTE1, MenG, ABCK1 and ABC1K3. Functions of FBNs have been linked to tolerance to abiotic and biotic stress [4, 5]. Recent studies have shown that ABC1K1 and ABC1K3 are involved in the regulation of photosynthetic adaptation via plastoquinone pool homeostasis. [15, 16]. The tocopherol cyclase (VTE1) catalyzes the formation of the chromanol ring in α-tocopherol biosynthesis and may be regulated via phosphorylation by ABC1K1 [10, 38]. MenG catalyzes the final methylation step of 2-phytyl-1,4-naphthoquinone resulting in phylloquinone [39]. In conclusion, cluster 2 functions are mostly linked to prenyl quinone metabolism. Cluster 3 contains PES, PGM48 and ABC1Ks. PGM48, a PG-associated protease, which in Arabidopsis mainly interacts with other PG proteins and degrades them during senescence [32]. PES belongs to esterase/lipase/thioesterase and acyl transferase family and synthesizes phytol esters and triacyl glycerols during stress and senescence as well as carotenoid esters during the chloroplast-to-chromoplast transition [24]. ABC1K7 regulates the chloroplast membrane remodelling under stress and may act in the oxidative stress resistance pathway [40, 41]. Thus, cluster 3 functions are mostly linked to chloroplast senescence and thylakoid dismantling processes that also take place during fruit ripening and chloroplast-to-chromoplast transition.

Lycopene and β-carotene were enriched in the chromoplast PG

We analysed the total carotenoid content and composition in mature green fruit and red fruit as well as in PG purified from chloroplasts and chromoplasts using ultra-HPLC coupled with atmospheric pressure chemical ionization-quadrupole time-of-flight mass spectrometry (UHPLC-APCI-QTOF-MS). Lycopene and β-carotene accumulated to higher concentrations in red fruit than mature green fruit, lycopene being almost undetectable in mature green fruit (S2A Fig) while lutein and violaxanthin+neoxanthin accumulated to lower concentrations in red fruit than mature green fruit (S2B Fig). With regard to isolated PG, the relative concentration of lycopene was much higher in chromoplast PG than in chloroplast PG in equal volumes of the isolated fractions (Fig 5A) while the relative concentrations of lutein were the same and those of β-carotene higher and those of violaxanthin+neoxanthin lower (Fig 5B). In addition, we compared the relative distribution of lycopene, lutein, β-carotene and phytoene in equal volumes of the isolated fractions of PG, CR (carotenoid crystals) and EN (envelope) fractions. Lycopene and β-carotene levels were highest in CR but in addition to PG the envelopes also accumulated some lycopene and β-carotene (S3 Fig).

Differential accumulation of prenyl lipids in PG upon chromoplast differentiation

We investigated the total prenyl lipid contents of mature green fruit and red fruit. We obtained prenyl lipid profiles by UHPLC-APCI-QTOF-MS. Red fruit accumulated higher concentrations of plastoquinone (PQ-9), plastochromanol (PC-8), α-tocopherol (α-T), γ-tocopherol (γ-T) and δ-tocopherol (δ-T) while the phylloquinone concentration was lower in red than in mature green fruit (S4 Fig). Interestingly, this was reversed in PG, the results using equal volumes of the isolated fractions revealed that the relative concentrations of PQ-9 and its derivatives (PC-8, PC-OH, PQH2-9 and PQ-OH), phylloquinone, α-T, γ-T were considerably lower in the chromoplast than in the chloroplast PG (Fig 6).

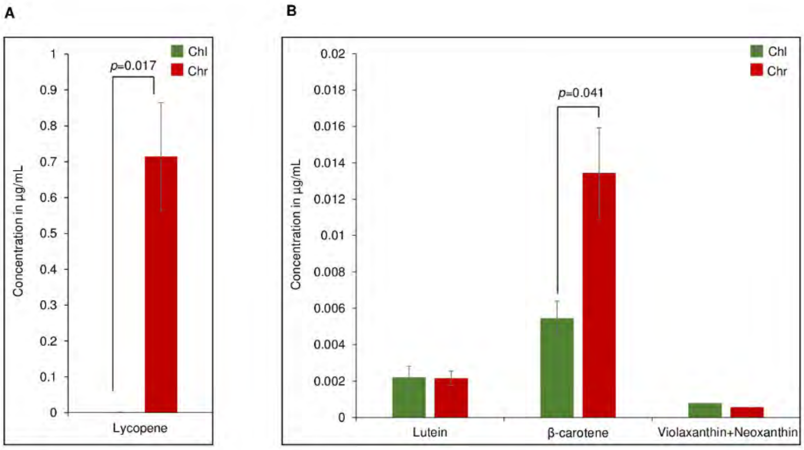

Fig 5. Lycopene and β-Carotene accumulate high levels in chromoplast PG. (A) Total carotenoids were extracted from equal volumes of gradient fractions containing chloroplast (Chl) or chromoplast (Chr) PG. Lycopene was quantified. (B) Quantification of lutein, β-carotene, and violaxanthin/neoxanthin. All values in the Fig are the mean of 3 biological replicates (n = 3). Statistical differences were assessed with students' t test and p values are indicated.

https://doi.org/10.1371/journal.pone.0277774.g005

Discussion

Purified PG were obtained from the chloroplasts and chromoplasts of mature green and red tomato fruit, respectively, and proteome analysis was carried out and thus resulted in a long list of proteins. UniProt, SUBA4, TAIR database and TargetP algorithm were used to filter the list and identify plastid proteins. Comparison of the resulting list with known PG proteomes indicated that tomato fruit chromoplasts and chloroplast PG together have a total of 33 proteins in common with Arabidopsis and red bell pepper (Table 1). This finding points to the overall functional conservation of PG in different species, tissues and plastid types. These "known" PG proteins are considered core components of the chromoplast PG proteome based on previous reports i.e. CHRC (FBN1A) [21, 42–44]. Western blot analysis confirmed enrichment of CHRC (FBN1A) in PG fractions of chromoplasts and chloroplasts (Fig 1D). In addition to the core components, 17 new candidates that included carotenoid biosynthetic enzymes were identified based on the literature, STRING and PPDB annotation (Table 1) (Fig 2).

The 17 new candidates of chromoplast PG were attributed to two categories, carotenoid biosynthetic enzymes and "others". In the "others" category was lipoxygenase C (LOXC), which is specifically expressed during tomato fruit ripening. LOXs participate in fatty acid catabolism during the disassembly of the thylakoid membranes during the chloroplast to chromoplast transition [45]. Moreover, previous studies propose a model in which the C-terminal PLAT (for polycystin-1, lipoxygenase and alpha toxin) domain may be responsible for LOX association with PG [46, 47]. Another intriguing candidate is MenG that is involved in phylloquinone biosynthesis [39]. MenG cooperates with the known PG protein NDC1 in the final methylation step of phylloquinone biosynthesis and assignment as PG candidate is therefore not surprising. Moreover, it has been shown previously that fluorescently-tagged MenG and multiprotein of phylloquinone biosynthesis (PHYLLO) resulted in patterns resembling those of PG [48]. Also, in this study, 1-deoxy-D-xylulose-5-phosphate synthase 1 (DXS1), key enzyme of the plastid isoprenoid pathway was present in the tomato PG. A recent report has indicated that both MenG and DXS1 are associated with PG via FBN and PDS in Chlamydomonas [49].

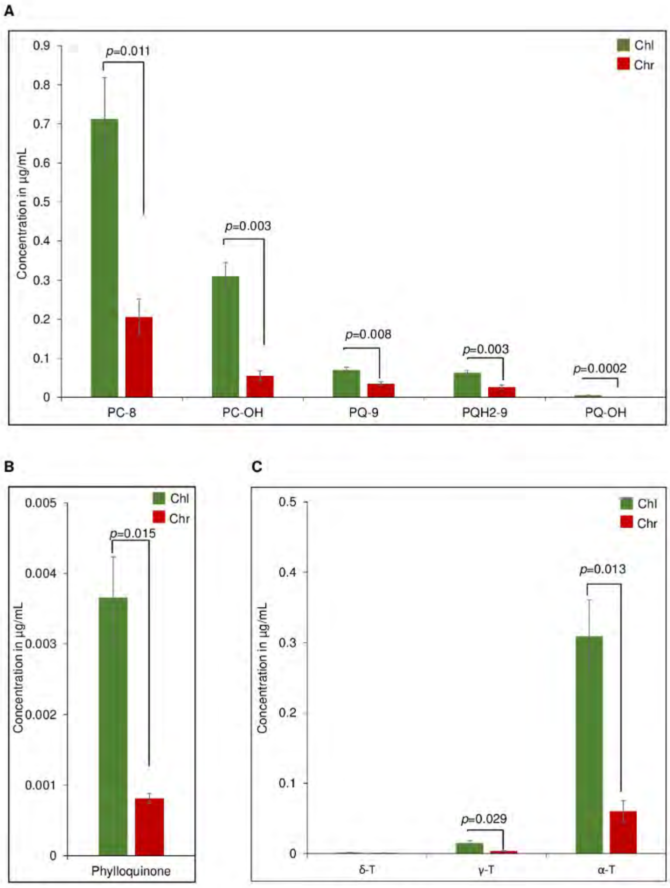

Fig 6. Reduced levels of prenyl quinones in chromoplast PG. (A) The total prenyl quinones were extracted from equal volumes of gradient fractions containing chloroplast (Chl) and chromoplast (Chr) PG, PC-8, plastochromanol; PC-OH, hydroxy-plastochromanol; PQ-9, plastoquinone; PQH_2-9, plastoquinol and PQ-OH, hydroxy-plastoquinone were quantified (B) Quantification of phylloquinone. (C) Quantification of tocopherols. All values in the Fig are the mean of 3 biological replicates (n = 3). Statistical differences were assessed with student's t test and *p* values are indicated.

https://doi.org/10.1371/journal.pone.0277774.g006

Chromoplast PG contained the carotenoid biosynthesis enzymes ZDS and LYCB as well as three other new candidates PSY1, PDS and CRTISO. Together these enzymes constitute the complete β-carotene biosynthesis pathway downstream of geranylgeranyl diphosphate. Based on the peptide count for PSY1, PDS, ZDS, and CRTISO, they are present at up to 12-fold higher levels in chromoplast PG than in chloroplast PG. However, the LYCB peptide count was almost the same in chromoplast PG and chloroplast PG (Fig 3; Table 1). The STRING analysis revealed that the enzymes of the carotenoid biosynthesis pathway form a distinct cluster 1 within the chromoplast PG proteome (Fig 4). Cluster 2 was enriched in enzymes involved in prenyl quinone metabolism and regulation and Cluster 3 in chloroplast senescence- and thylakoid dismantling-associated proteins. Cluster 2 and 3 therefore identify two additional categories of functions that are critical during the chloroplast-to-chromoplast transition. The

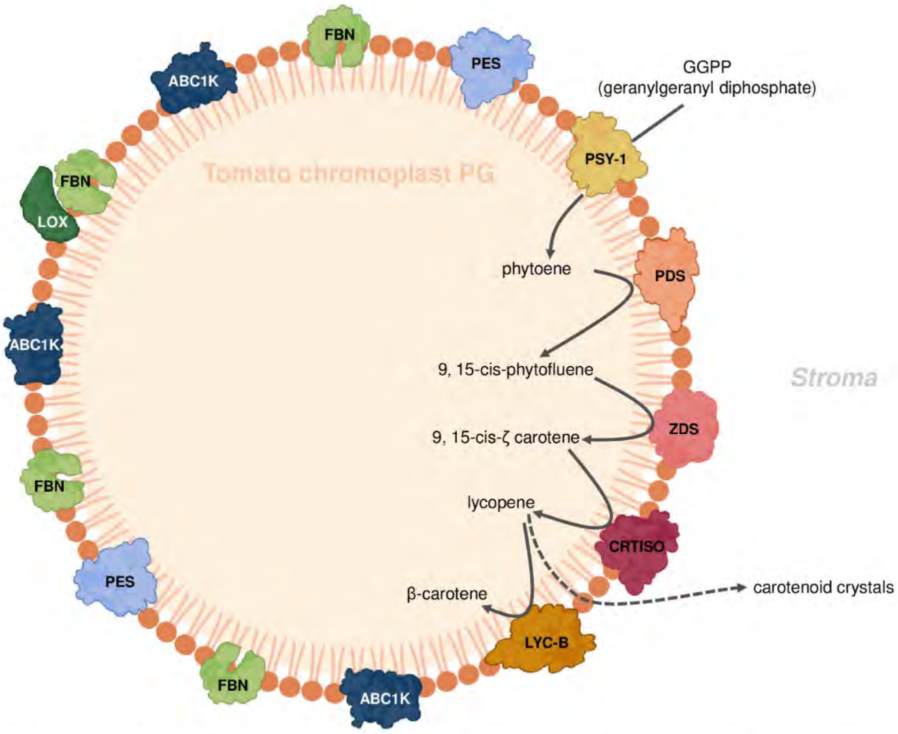

Fig 7. Carotenoid biosynthetic pathway in tomato chromoplast PG. Chromoplast plastoglobules recruit the carotenoid biosynthetic pathway enzymes: phytoene synthase 1 (PSY1), phytoene desaturase (PDS), z-carotene desaturase (ZDS), and carotenoid isomerase (CRTISO) and lycopene β-cyclase (LYC-β) to promote carotenoid biosynthesis. Lipoxygenase (LOX) may associate with PG, FBNs have structural functions and may contribute to carotenoid sequestration in PG. Phytyl ester synthase (PES) synthesizes phytyl esters and triacyl glycerol during thylakoid dismantling and Activity of BC1 complex kinase 1 (ABC1K1) is implicated in regulation of prenyl lipid metabolism.

https://doi.org/10.1371/journal.pone.0277774.g007

increased peptide counts of the first four β-carotene biosynthetic enzymes in chromoplast PG compared with chloroplast PG (Fig 3) indicates that PG recruit carotenoid biosynthetic enzymes and may turn them into a biosynthetic platform during carotenogenesis. Our lipidomic study reveals that lycopene and β-carotene become enriched in chromoplast PG during fruit ripening suggesting active contribution to biosynthesis (Fig 5). In agreement with an active role of PG in carotenoid metabolism in tomato, the chromoplast PG enzyme PALE YELLOW PETAL (PYP1) confers yellow flower pigmentation by carotenoid esterification [50]. With regard to PSY1, transient expression experiments provided evidence for PG localization in rice and Arabidopsis [51]. In addition, it was recently reported that bacterial phytoene synthase CrtB localised to PG and increased carotenoid levels when chloroplast-to-chromoplast transition was induced by CrtB expression [52]. Interestingly, a proteome study in the green algae *Dunaliella bardawil* revealed that β-carotene biosynthesis enzymes PDS, ZDS, and CRTISO were present in β-carotene-rich PG [53]. A recent study showed that PDS is one of the main protein components of Chlamydomonas PG [49]. Interestingly, carotenoid cleavage dehydrogenase 4 (CCD4) was identified only in chloroplast PG. PG protease PGM48, a chloroplast PG protease, interacts with CCD4 and degrades it during senescence [32]. Therefore, the presence of PGM48 in chloroplast and chromoplast PG might explain the disappearance of CCD4 during the chloroplast-to-chromoplast transition. We proposed a model for chromoplast PG hosting the carotenoid biosynthetic pathway. In the model, chromoplast PG function as a metabolic platform for carotenoid biosynthesis, especially for lycopene biosynthesis and accumulation (Fig 7). However, the data also indicate that carotenoid crystals accumulate a large proportion of lycopene and β-carotene (S3 Fig). In summary, our data suggest that PG make an important contribution to fruit quality particularly to carotenoid accumulation.

Supporting information

S1 Fig. FBNs and ABC1K- kinases were reduced in tomato chromoplast PG. (A) FBN heatmap and (B) ABC1K-like kinase heatmap were generated from peptide counts obtained from PG isolated from chloroplast and chromoplast, respectively.
(PDF)

S2 Fig. Lycopene was highly accumulated in the red tomato fruit. (A) Total carotenoids were extracted from mature green (MG) and red (R) tomato fruit and lycopene was quantified. (B) Quantification of lutein, β-carotene, and violaxanthin/neoxanthin. All values in the figure are the mean of 3 biological replicates (n = 3). Statistical differences were assessed with student's t test and p values are indicated.
(PDF)

S3 Fig. Carotenoids were differentially accumulated in the chromoplast sub-compartments. The total carotenoids were extracted from equal volumes of mature red (R) tomato fruit PG (plastoglobules); CR (carotenoid crystals) fractions; EN (envelope). The isolated lycopene, phytoene, β-carotene, and lutein were quantified. Values are the mean of 3 biological replicates (n = 3).
(PDF)

S4 Fig. Tocopherols and plastoquinone were highly accumulated in the red tomato fruit. (A) The total prenyl quinones were extracted from mature green (MG) and red (R) tomato fruit, PC-8, plastochromanol; PC-OH, hydroxy-plastochromanol; PQ-9, plastoquinone; and PQH_2-9, plastoquinol were quantified (B) Quantification of phylloquinone. (C) Quantification of tocopherols. All values in the figure are the mean of 3 biological replicates (n = 3). Statistical differences were assessed with student's t test and p values are indicated.
(PDF)

S1 File.
(DOCX)

S1 Raw images.
(PDF)

Acknowledgments

We thank the Protein Analysis Facility (PAF), University of Lausanne for supporting mass spectrometry acquisition and analysis.

Author Contributions

Conceptualization: Venkatasalam Shanmugabalaji.

Data curation: Wayne Zita, Venkatasalam Shanmugabalaji.

Formal analysis: Wayne Zita, Venkatasalam Shanmugabalaji.

Funding acquisition: Felix Kessler.

Investigation: Wayne Zita, Ségolène Bressoud, Gaetan Glauser.

Methodology: Wayne Zita, Ségolène Bressoud, Gaetan Glauser, Venkatasalam Shanmugabalaji.

Project administration: Felix Kessler, Venkatasalam Shanmugabalaji.

Resources: Wayne Zita, Felix Kessler.

Software: Wayne Zita.

Supervision: Felix Kessler, Venkatasalam Shanmugabalaji.

Validation: Venkatasalam Shanmugabalaji.

Visualization: Venkatasalam Shanmugabalaji.

Writing – original draft: Wayne Zita, Venkatasalam Shanmugabalaji.

Writing – review & editing: Felix Kessler, Venkatasalam Shanmugabalaji.

References

1. Jarvis P, López-Juez E. Biogenesis and homeostasis of chloroplasts and other plastids. Nat Rev Mol Cell Biol. 2013; 14(12):787–802. Epub 2013/11/23. https://doi.org/10.1038/nrm3702 PMID: 24263360.
2. Bréhélin C, Kessler F, van Wijk KJ. Plastoglobules: versatile lipoprotein particles in plastids. Trends Plant Sci. 2007; 12(6):260–6. Epub 2007/05/15. https://doi.org/10.1016/j.tplants.2007.04.003 PMID: 17499005.
3. Lichtenthaler H. Plastoglobuli and fine structure of plastids. Endeavour. 1968; 27(102):144-+.
4. Youssef A, Laizet Y, Block MA, Maréchal E, Alcaraz JP, Larson TR, et al. Plant lipid-associated fibrillin proteins condition jasmonate production under photosynthetic stress. Plant J. 2010; 61(3):436–45. Epub 2009/11/13. https://doi.org/10.1111/j.1365-313X.2009.04067.x PMID: 19906042.
5. Singh DK, Maximova SN, Jensen PJ, Lehman BL, Ngugi HK, McNellis TW. FIBRILLIN4 is required for plastoglobule development and stress resistance in apple and Arabidopsis. Plant Physiol. 2010; 154 (3):1281–93. Epub 2010/09/04. https://doi.org/10.1104/pp.110.164095 PMID: 20813909.
6. Gaude N, Bréhélin C, Tischendorf G, Kessler F, Dörmann P. Nitrogen deficiency in Arabidopsis affects galactolipid composition and gene expression and results in accumulation of fatty acid phytyl esters. Plant J. 2007; 49(4):729–39. Epub 2007/02/03. https://doi.org/10.1111/j.1365-313X.2006.02992.x PMID: 17270009.
7. Lichtenthaler HK, Sprey B. Über die osmiophilen globulären Lipideinschlüsse der Chloroplasten. Zeitschrift für Naturforschung B. 1966; 21(7):690–7. https://doi.org/10.1515/znb-1966-0716
8. Zhang R, Wise RR, Struck KR, Sharkey TD. Moderate heat stress of Arabidopsis thaliana leaves causes chloroplast swelling and plastoglobule formation. Photosynth Res. 2010; 105(2):123–34. Epub 2010/06/22. https://doi.org/10.1007/s11120-010-9572-6 PMID: 20563644.
9. van Wijk KJ, Kessler F. Plastoglobuli: Plastid Microcompartments with Integrated Functions in Metabolism, Plastid Developmental Transitions, and Environmental Adaptation. Annu Rev Plant Biol. 2017; 68:253–89. Epub 2017/01/27. https://doi.org/10.1146/annurev-arplant-043015-111737 PMID: 28125283.
10. Vidi PA, Kanwischer M, Baginsky S, Austin JR, Csucs G, Dörmann P, et al. Tocopherol cyclase (VTE1) localization and vitamin E accumulation in chloroplast plastoglobule lipoprotein particles. J Biol Chem. 2006; 281(16):11225–34. Epub 2006/01/18. https://doi.org/10.1074/jbc.M511939200 PMID: 16414959.
11. Ytterberg AJ, Peltier JB, van Wijk KJ. Protein profiling of plastoglobules in chloroplasts and chromoplasts. A surprising site for differential accumulation of metabolic enzymes. Plant Physiol. 2006; 140 (3):984–97. Epub 2006/02/08. https://doi.org/10.1104/pp.105.076083 PMID: 16461379.
12. Lundquist PK, Poliakov A, Bhuiyan NH, Zybailov B, Sun Q, van Wijk KJ. The functional network of the Arabidopsis plastoglobule proteome based on quantitative proteomics and genome-wide coexpression analysis. Plant Physiol. 2012; 158(3):1172–92. Epub 2012/01/26. https://doi.org/10.1104/pp.111.193144 PMID: 22274653.

13. Vishnevetsky M, Ovadis M, Vainstein A. Carotenoid sequestration in plants: the role of carotenoid-associated proteins. Trends Plant Sci. 1999; 4(6):232–5. Epub 1999/06/15. https://doi.org/10.1016/s1360-1385(99)01414-4 PMID: 10366880.
14. Singh DK, McNellis TW. Fibrillin protein function: the tip of the iceberg? Trends Plant Sci. 2011; 16 (8):432–41. Epub 2011/05/17. https://doi.org/10.1016/j.tplants.2011.03.014 PMID: 21571574.
15. Pralon T, Shanmugabalaji V, Longoni P, Glauser G, Ksas B, Collombat J, et al. Plastoquinone homoeostasis by Arabidopsis proton gradient regulation 6 is essential for photosynthetic efficiency. Commun Biol. 2019; 2:220. Epub 2019/06/27. https://doi.org/10.1038/s42003-019-0477-4 PMID: 31240258.
16. Pralon T, Collombat J, Pipitone R, Ksas B, Shanmugabalaji V, Havaux M, et al. Mutation of the Atypical Kinase ABC1K3 Partially Rescues the PROTON GRADIENT REGULATION 6 Phenotype in Arabidopsis thaliana. Front Plant Sci. 2020; 11:337. Epub 2020/04/10. https://doi.org/10.3389/fpls.2020.00337 PMID: 32269582.
17. Eugeni Piller L, Besagni C, Ksas B, Rumeau D, Bréhélin C, Glauser G, et al. Chloroplast lipid droplet type II NAD(P)H quinone oxidoreductase is essential for prenylquinone metabolism and vitamin K1 accumulation. Proc Natl Acad Sci U S A. 2011; 108(34):14354–9. Epub 2011/08/17. https://doi.org/10.1073/pnas.1104790108 PMID: 21844348.
18. Lichtenthaler HK. [Distribution and relative concentrations of lipophilic plastid quinones in green plants]. Planta. 1968; 81(2):140–52. Epub 1968/06/01. https://doi.org/10.1007/bf00417443 PMID: 24519649.
19. Steinmüller D, Tevini M. Composition and function of plastoglobuli: I. Isolation and purification from chloroplasts and chromoplasts. Planta. 1985; 163(2):201–7. Epub 1985/02/01. https://doi.org/10.1007/BF00393507 PMID: 24249339.
20. Hansmann P, Sitte P. Composition and molecular structure of chromoplast globules of Viola tricolor. Plant Cell Rep. 1982; 1(3):111–4. Epub 1982/04/01. https://doi.org/10.1007/BF00272366 PMID: 24259022.
21. Deruère J, Römer S, d'Harlingue A, Backhaus RA, Kuntz M, Camara B. Fibril assembly and carotenoid overaccumulation in chromoplasts: a model for supramolecular lipoprotein structures. Plant Cell. 1994; 6(1):119–33. Epub 1994/01/01. https://doi.org/10.1105/tpc.6.1.119 PMID: 8130642.
22. Camara B, Hugueney P, Bouvier F, Kuntz M, Monéger R. Biochemistry and molecular biology of chromoplast development. Int Rev Cytol. 1995; 163:175–247. Epub 1995/01/01. https://doi.org/10.1016/s0074-7696(08)62211-1 PMID: 8522420.
23. Egea I, Barsan C, Bian W, Purgatto E, Latché A, Chervin C, et al. Chromoplast differentiation: current status and perspectives. Plant Cell Physiol. 2010; 51(10):1601–11. Epub 2010/08/31. https://doi.org/10.1093/pcp/pcq136 PMID: 20801922.
24. Lippold F, vom Dorp K, Abraham M, Hölzl G, Wewer V, Yilmaz JL, et al. Fatty acid phytyl ester synthesis in chloroplasts of Arabidopsis. Plant Cell. 2012; 24(5):2001–14. Epub 2012/05/25. https://doi.org/10.1105/tpc.112.095588 PMID: 22623494.
25. Liu L, Shao Z, Zhang M, Wang Q. Regulation of carotenoid metabolism in tomato. Mol Plant. 2015; 8 (1):28–39. Epub 2015/01/13. https://doi.org/10.1016/j.molp.2014.11.006 PMID: 25578270.
26. Nogueira M, Mora L, Enfissi EM, Bramley PM, Fraser PD. Subchromoplast sequestration of carotenoids affects regulatory mechanisms in tomato lines expressing different carotenoid gene combinations. Plant Cell. 2013; 25(11):4560–79. Epub 2013/11/20. https://doi.org/10.1105/tpc.113.116210 PMID: 24249831.
27. Pozueta-Romero J, Rafia F, Houlné G, Cheniclet C, Carde JP, Schantz ML, et al. A ubiquitous plant housekeeping gene, PAP, encodes a major protein component of bell pepper chromoplasts. Plant Physiol. 1997; 115(3):1185–94. Epub 1997/12/09. https://doi.org/10.1104/pp.115.3.1185 PMID: 9390444.
28. Hiltbrunner A, Bauer J, Vidi PA, Infanger S, Weibel P, Hohwy M, et al. Targeting of an abundant cytosolic form of the protein import receptor at Toc159 to the outer chloroplast membrane. J Cell Biol. 2001; 154(2):309–16. Epub 2001/07/27. https://doi.org/10.1083/jcb.200104022 PMID: 11470820.
29. Martinis J, Kessler F, Glauser G. A novel method for prenylquinone profiling in plant tissues by ultra-high pressure liquid chromatography-mass spectrometry. Plant Methods. 2011; 7(1):23. Epub 2011/07/23. https://doi.org/10.1186/1746-4811-7-23 PMID: 21777468.
30. Eugeni Piller L, Glauser G, Kessler F, Besagni C. Role of plastoglobules in metabolite repair in the tocopherol redox cycle. Front Plant Sci. 2014; 5:298. Epub 2014/07/16. https://doi.org/10.3389/fpls.2014.00298 PMID: 25018761.
31. Alba R, Payton P, Fei Z, McQuinn R, Debbie P, Martin GB, et al. Transcriptome and selected metabolite analyses reveal multiple points of ethylene control during tomato fruit development. Plant Cell. 2005; 17 (11):2954–65. Epub 2005/10/26. https://doi.org/10.1105/tpc.105.036053 PMID: 16243903.
32. Bhuiyan NH, Friso G, Rowland E, Majsec K, van Wijk KJ. The Plastoglobule-Localized Metallopeptidase PGM48 Is a Positive Regulator of Senescence in Arabidopsis thaliana. Plant Cell. 2016; 28 (12):3020–37. Epub 2016/11/30. https://doi.org/10.1105/tpc.16.00745 PMID: 27895226.

33. Espinoza-Corral R, Heinz S, Klingl A, Jahns P, Lehmann M, Meurer J, et al. Plastoglobular protein 18 is involved in chloroplast function and thylakoid formation. J Exp Bot. 2019; 70(15):3981–93. Epub 2019/04/13. https://doi.org/10.1093/jxb/erz177 PMID: 30976809.

34. Shanmugabalaji V, Grimm B, Kessler F. Characterization of a Plastoglobule-Localized SOUL4 Heme-Binding Protein in Arabidopsis thaliana. Front Plant Sci. 2020; 11:2. Epub 2020/02/23. https://doi.org/10.3389/fpls.2020.00002 PMID: 32076429.

35. Szklarczyk D, Franceschini A, Wyder S, Forslund K, Heller D, Huerta-Cepas J, et al. STRING v10: protein-protein interaction networks, integrated over the tree of life. Nucleic Acids Res. 2015; 43(Database issue):D447–52. Epub 2014/10/30. https://doi.org/10.1093/nar/gku1003 PMID: 25352553.

36. Szklarczyk D, Gable AL, Nastou KC, Lyon D, Kirsch R, Pyysalo S, et al. The STRING database in 2021: customizable protein-protein networks, and functional characterization of user-uploaded gene/measurement sets. Nucleic Acids Res. 2021; 49(D1):D605–d12. Epub 2020/11/26. https://doi.org/10.1093/nar/gkaa1074 PMID: 33237311.

37. Lois LM, Rodríguez-Concepción M, Gallego F, Campos N, Boronat A. Carotenoid biosynthesis during tomato fruit development: regulatory role of 1-deoxy-D-xylulose 5-phosphate synthase. Plant J. 2000; 22(6):503–13. Epub 2000/07/08. https://doi.org/10.1046/j.1365-313x.2000.00764.x PMID: 10886770.

38. Martinis J, Glauser G, Valimareanu S, Kessler F. A chloroplast ABC1-like kinase regulates vitamin E metabolism in Arabidopsis. Plant Physiol. 2013; 162(2):652–62. Epub 2013/05/02. https://doi.org/10.1104/pp.113.218644 PMID: 23632854.

39. Lohmann A, Schöttler MA, Bréhélin C, Kessler F, Bock R, Cahoon EB, et al. Deficiency in phylloquinone (vitamin K1) methylation affects prenyl quinone distribution, photosystem I abundance, and anthocyanin accumulation in the Arabidopsis AtmenG mutant. J Biol Chem. 2006; 281(52):40461–72. Epub 2006/11/04. https://doi.org/10.1074/jbc.M609412200 PMID: 17082184.

40. Manara A, DalCorso G, Guzzo F, Furini A. Loss of the Atypical Kinases ABC1K7 and ABC1K8 Changes the Lipid Composition of the Chloroplast Membrane. Plant Cell Physiol. 2015; 56(6):1193–204. Epub 2015/03/27. https://doi.org/10.1093/pcp/pcv046 PMID: 25809944.

41. Manara A, DalCorso G, Leister D, Jahns P, Baldan B, Furini A. AtSIA1 AND AtOSA1: two Abc1 proteins involved in oxidative stress responses and iron distribution within chloroplasts. New Phytol. 2014; 201(2):452–65. Epub 2013/10/15. https://doi.org/10.1111/nph.12533 PMID: 24117441.

42. Vishnevetsky M, Ovadis M, Itzhaki H, Levy M, Libal-Weksler Y, Adam Z, et al. Molecular cloning of a carotenoid-associated protein from Cucumis sativus corollas: homologous genes involved in carotenoid sequestration in chromoplasts. Plant J. 1996; 10(6):1111–8. Epub 1996/12/01. https://doi.org/10.1046/j.1365-313x.1996.10061111.x PMID: 9011091.

43. Kilambi HV, Kumar R, Sharma R, Sreelakshmi Y. Chromoplast-specific carotenoid-associated protein appears to be important for enhanced accumulation of carotenoids in hp1 tomato fruits. Plant Physiol. 2013; 161(4):2085–101. Epub 2013/02/13. https://doi.org/10.1104/pp.112.212191 PMID: 23400702.

44. Suzuki M, Takahashi S, Kondo T, Dohra H, Ito Y, Kiriiwa Y, et al. Plastid Proteomic Analysis in Tomato Fruit Development. PLoS One. 2015; 10(9):e0137266. Epub 2015/09/16. https://doi.org/10.1371/journal.pone.0137266 PMID: 26371478.

45. Heitz T, Bergey DR, Ryan CA. A gene encoding a chloroplast-targeted lipoxygenase in tomato leaves is transiently induced by wounding, systemin, and methyl jasmonate. Plant Physiol. 1997; 114(3):1085–93. Epub 1997/07/01. https://doi.org/10.1104/pp.114.3.1085 PMID: 9232884.

46. Lundquist PK, Poliakov A, Giacomelli L, Friso G, Appel M, McQuinn RP, et al. Loss of plastoglobule kinases ABC1K1 and ABC1K3 causes conditional degreening, modified prenyl-lipids, and recruitment of the jasmonic acid pathway. Plant Cell. 2013; 25(5):1818–39. Epub 2013/05/16. https://doi.org/10.1105/tpc.113.111120 PMID: 23673981.

47. Espinoza-Corral R, Herrera-Tequia A, Lundquist PK. Insights into topology and membrane interaction characteristics of plastoglobule-localized AtFBN1a and AtLOX2. Plant Signal Behav. 2021; 16(10):1945213. Epub 2021/06/29. https://doi.org/10.1080/15592324.2021.1945213 PMID: 34180346.

48. Gross J, Cho WK, Lezhneva L, Falk J, Krupinska K, Shinozaki K, et al. A plant locus essential for phylloquinone (vitamin K1) biosynthesis originated from a fusion of four eubacterial genes. J Biol Chem. 2006; 281(25):17189–96. Epub 2006/04/18. https://doi.org/10.1074/jbc.M601754200 PMID: 16617180.

49. Wang L, Patena W, Van Baalen KA, Xie Y, Singer ER, Gavrilenko S, et al. A Chloroplast Protein Atlas Reveals Novel Structures and Spatial Organization of Biosynthetic Pathways. bioRxiv. 2022:2022.05.31.493820. https://doi.org/10.1101/2022.05.31.493820

50. Ariizumi T, Kishimoto S, Kakami R, Maoka T, Hirakawa H, Suzuki Y, et al. Identification of the carotenoid modifying gene PALE YELLOW PETAL 1 as an essential factor in xanthophyll esterification and yellow flower pigmentation in tomato (Solanum lycopersicum). Plant J. 2014; 79(3):453–65. Epub 2014/06/04. https://doi.org/10.1111/tpj.12570 PMID: 24888879.

51. Shumskaya M, Bradbury LM, Monaco RR, Wurtzel ET. Plastid localization of the key carotenoid enzyme phytoene synthase is altered by isozyme, allelic variation, and activity. Plant Cell. 2012; 24 (9):3725–41. Epub 2012/10/02. https://doi.org/10.1105/tpc.112.104174 PMID: 23023170.

52. Morelli L, Torres-Montilla S, Glauser G, Shanmugabalaji V, Kessler F, Rodriguez-Concepcion M. Novel insights on the contribution of plastoglobules and reactive oxygen species to chromoplast differentiation. bioRxiv. 2022:2022.06.20.496796. https://doi.org/10.1111/nph.18585 PMID: 36307969

53. Davidi L, Levin Y, Ben-Dor S, Pick U. Proteome analysis of cytoplasmatic and plastidic β-carotene lipid droplets in Dunaliella bardawil. Plant Physiol. 2015; 167(1):60–79. Epub 2014/11/19. https://doi.org/10.1104/pp.114.248450 PMID: 25404729.

Zita *et al. Plant Methods* (2023) 19:55
https://doi.org/10.1186/s13007-023-01034-w

Plant Methods

METHODOLOGY **Open Access**

A quantitative method to measure geranylgeranyl diphosphate (GGPP) and geranylgeranyl monophosphate (GGP) in tomato (*Solanum lycopersicum*) fruit

Wayne Zita[1], Venkatasalam Shanmugabalaji[1], Miguel Ezquerro[2], Manuel Rodriguez-Concepcion[2], Felix Kessler[1] and Gaetan Glauser[3*]

Abstract

Background Isoprenoids are a very large class of metabolites playing a key role in plant physiological processes such as growth, stress resistance, fruit flavor, and color. In chloroplasts and chromoplasts, the diterpene compound geranylgeranyl diphosphate (GGPP) is the metabolic precursor required for the biosynthesis of tocopherols, plastoquinones, phylloquinone, chlorophylls, and carotenoids. Despite its key role for the plant metabolism, reports on GGPP physiological concentrations in planta have been extremely scarce.

Results In this study, we developed a method to quantify GGPP and its hydrolysis product geranylgeranyl monophosphate (GGP) from tomato fruit, using ultra-high performance liquid chromatography coupled with tandem mass spectrometry (UHPLC–MS/MS). Quantification was done by external calibration and the method was validated in terms of specificity, precision, accuracy, and detection and quantitation limits. We further demonstrate the validity of our approach by analysing GGPP contents in the ripe fruits of wild-type tomatoes and mutants defective in GGPP production. Finally, we also show that the sample preparation is key to prevent GGPP hydrolysis and mitigate its conversion to GGP.

Conclusion Our study provides an efficient tool to investigate the metabolic fluxes required for GGPP supply and consumption in tomato fruit.

Keywords Geranylgeranyl diphosphate, GGPP, Geranylgeranyl monophosphate, GGP, Geranylgeranyl diphosphate synthase, GGPPS, UHPLC–MS/MS, Isoprenoid, Carotenoid

Background

In plants, isoprenoids (terpenes or terpenoids) are a large family of primary and secondary metabolites essential for a multitude of physiological and biological functions [1, 2]. Geranylgeranyl diphosphate (GGPP) is a C20 diterpene synthesised through the head-to-tail condensation of three isopentenyl diphosphate (IPP) groups and the head dimethylallyl diphosphate (DMAPP) by the geranylgeranyl diphosphate synthase (GGPPS) [3]. Plant cells synthesise IPP and DMAPP using the mevalonic

---

*Correspondence:
Gaetan Glauser
gaetan.glauser@unine.ch
[1] Plant Physiology Laboratory, University of Neuchâtel, 2000 Neuchâtel, Switzerland
[2] Institute for Plant Molecular and Cell Biology (IBMCP), CSIC-Universitat Politècnica de València, 46022 Valencia, Spain
[3] Neuchâtel Platform of Analytical Chemistry, University of Neuchâtel, 2000 Neuchâtel, Switzerland

acid (MVA) pathway in the cytosol or the methylerythritol 4-phosphate (MEP) pathway in plastids, where GGPP is most needed (Fig. 1) [2, 3]. Plastidial GGPP is a key component in plants as it is required for the biosynthesis of many photosynthesis-related terpenoids such as carotenoids, chlorophylls, tocopherols, phylloquinone, and plastoquinones [2–4]. MEP-derived GGPP is also used for the production of gibberellins and diterpenes (Fig. 1). In tomato (*Solanum lycopersicum*), five genes encode GGPPS-like enzymes. Among them, paralogs SlGGPPS1/SlG1 (Solyc11g011240), SlGGPPS2/SlG2 (Solyc04g079960) and SlGGPPS3/SlG3 (Solyc02g085700) have been localized in plastids and are required for GGPP biosynthesis [5, 6]. A recent study concluded that SlG2 and SlG3 are the main isoforms supplying GGPP in shoot tissues. Consistently, ripe fruit from *slg2* and *slg3* tomato knockouts showed decreased levels of lycopene, the red carotenoid that gives the characteristic colour to tomatoes [7].

Despite its central role in plants and other organisms, there is no commonly accepted method to measure GGPP at physiological levels. GGPP measurement represents a challenge due to its amphiphilic nature [8]. GGPP is not volatile, which makes its direct analysis by gas chromatography or gas chromatography–mass spectrometry impossible. In addition, the presence of phosphate groups complicates separation by conventional reversed-phase HPLC methods and may require ion-pairing chromatography or pre-column derivatization of the sample [9]. In addition, GGPP as an essential biosynthetic precursor in plant tissues is rapidly converted by enzymes to downstream secondary metabolites, complicating its detection. For these reasons, in most studies, instead of directly analysing GGPP, researchers have measured its downstream products such as carotenoids, quinones or other derived terpenoids [5, 6, 10, 11]. While some studies have proposed methods to detect GGPP in human plasma and cells using HPLC–MS or HPLC-fluorescence detection [12–14], we are unaware of any validated method able to measure GGPP physiological levels in plants. McCaskill et Croteau reported a complex and time-consuming procedure for the isolation and quantification of radiolabelled intermediates of the MVA pathway by ion-pairing chromatography coupled to radiodetection [15]. Recently, Ma et al. reported endogenous levels of GGPP in Arabidopsis leaves and inflorescences by UHPLC–MS/MS, however information on the methodology employed was limited [16].

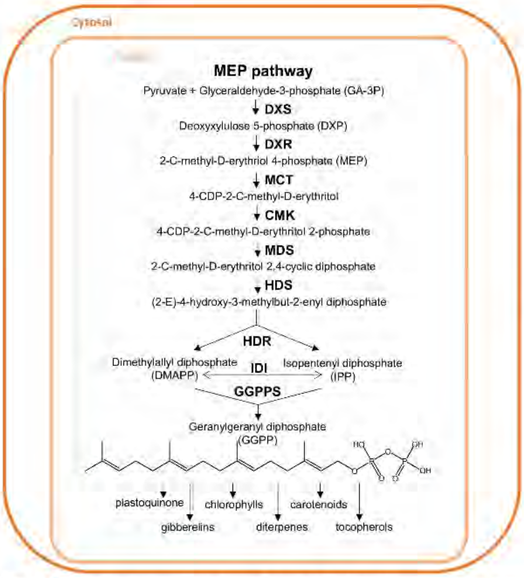

Fig. 1 Schematic representation of the MEP pathway. Here, enzymes required for the biosynthesis of GGPP are represented. Enzymes: 1-deoxy-D-xylulose-5-phosphate synthase (DXS), 1-deoxy-D-xylulose-5-phosphate reductoisomerase (DXR), 4-(cytidine 5′-diphospho)-2-C-methyl-D-erythritol synthase (MCT), 4-(cytidine 5′-diphospho)-2-C-methyl-D-erythritol kinase (CMK), 2-C-methyl-D-erythritol 2,4-cyclodiphosphate synthase (MDS), 4-hydroxy-3-methylbut-2-enyl diphosphate synthase (HDS), 4-hydroxy-3-methylbut-2-enyl diphosphate reductase (HDR), isopentenyl diphosphate isomerase (IDI), geranylgeranyl diphosphate synthase (GGPPS)

In this work, we developed a simple but efficient method to measure GGPP and its hydrolysis product GGP in tomato fruit. The method is based on a single extraction step after quenching and lyophilisation of the fruits followed by reversed-phase UHPLC–MS/MS at alkaline pH. The method was validated according to standard guidelines and applied to the analysis of wild-type and GGPPS-defective *slg2* and *slg3* tomato fruits.

Results and discussion

Optimisation of HPLC–MS/MS conditions

Due to the concomitant presence of a hydrophilic head (phosphate groups) and a lipophilic tail on their structures, there is no clearly defined scheme for the chromatographic separation of GGPP and GGP. Our aim was to find appropriate separation conditions without the need for ion-pairing or derivatisation agents, which may reduce detection sensitivity and lengthen the extraction process. During our trials, we found that hydrophilic interaction chromatography (HILIC) was not conclusive and thus focused on reverse-phase chromatography. Using an ethylene-bridged C18 column with a wide pH range, we observed a very strong dependency on the pH: at pH 2.7, using 0.05% formic acid as an additive in the aqueous mobile phase, the peaks for GGPP and GGP were extremely wide and almost indistinguishable from the baseline (Fig. 2A, D). By increasing the pH to 5.8 using a combination of 20 mM ammonium acetate and

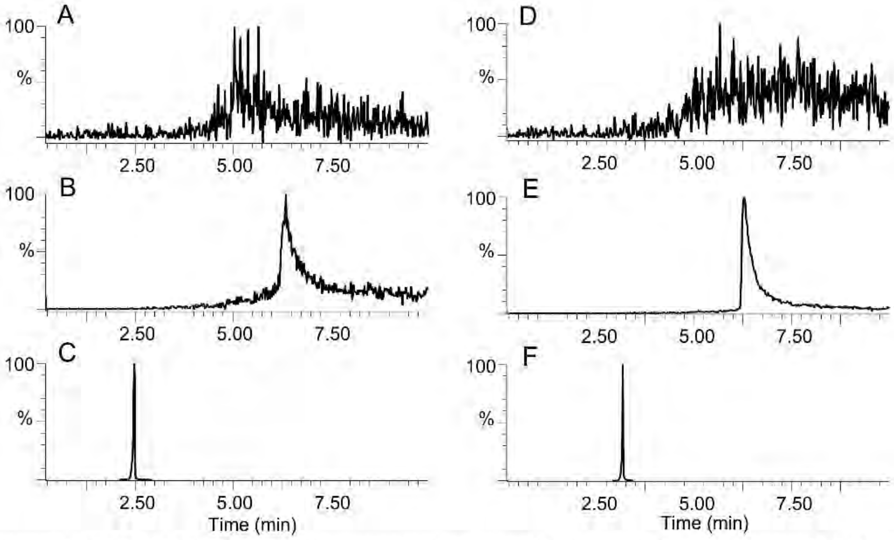

Fig. 2 Chromatograms for GGPP and GGP at different pHs using an ethylene-bridged C18 column. **A**, **D** Chromatograms for GGPP and GGP at pH 2.7 (formic acid 0.05%); **B**, **E** chromatograms for GGPP and GGP at pH 5.8 (acetic acid 0.01% + 20 mM ammonium acetate); **C**, **F** chromatograms for GGPP and GGP at pH 10.0 (ammonia 0.05%). The organic mobile phase was acetonitrile in all cases

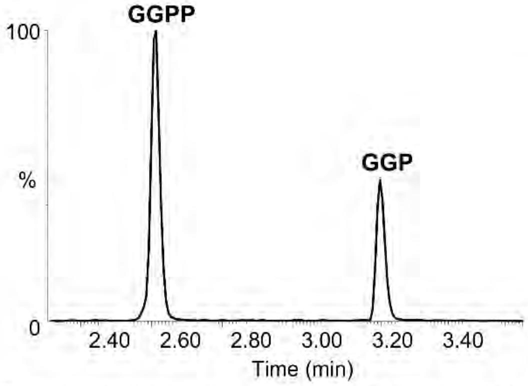

Fig. 3 Representative chromatograms for standard solutions of GGPP and GGP. The concentrations of GGPP and GGP were 10 ng/mL and 1 ng/mL, respectively, both in acetonitrile:water (50:50, v/v). The MRM transition was *m/z* 369.2 > 79.0 for both molecules. A gradient of H_2O + 0.05% NH_4OH and acetonitrile + 0.05% NH_4OH was applied

0.01% acetic acid, the peak shapes improved but were still not acceptable to allow reliable quantitation (Fig. 2B, E). At pH 10.0, using 0.05% NH_4OH as additive, the peaks became much thinner, although a slight fronting persisted (Fig. 2C, F). Adding 0.05% NH_4OH to both aqueous and organic phases minimized peak fronting and enabled sharp and symmetrical peaks for both GGPP (RT 2.56 min, composition at elution 22.6%) and GGP (RT 3.20 min, composition at elution 28.4%) (Fig. 3). Acetonitrile as an organic solvent gave narrower peaks and slightly higher signal-to-noise ratios than methanol and was therefore preferred. The effect of the injection volume was also investigated. Using an injection solvent composed of 50–80% ACN, we found that peak distortion started to occur above 2 µL injections. We thus selected an injection volume of 2 µL as the best compromise between peak shape and sensitivity. Noteworthily, these conditions are valid for an Acquity UPLC system with a fixed loop injector in the partial loop with needle overfill mode. Preliminary assays using identical injection parameters on a flow-through needle (FTN) autosampler indeed revealed some peak distortion and further optimisation would be required when using this type of autosampler.

Mass spectrometric detection was performed on a triple quadrupole instrument (TQ-XS) of the last generation. We tested electrospray (ESI) and atmospheric pressure chemical ionization (APCI) sources, both in positive and negative ionisation modes. Not surprisingly, ESI and APCI positive ionisation gave no detectable peak. By contrast, the negative mode generated strong signals thanks to deprotonation of the phosphate group. Negative ESI was largely superior to APCI, with signals for GGPP and GGP approximately 10 and 15-fold higher, respectively. We tested different parameters of the ESI source, namely capillary voltage, source temperature, desolvation gas flow and temperature, nebulisation gas flow and cone gas flow. Only capillary voltage, desolvation gas temperature and cone gas flow had a significant impact on the signal-to-noise ratios, with optimal values at -2 kV, 500 °C and 350 L/h, respectively. After having optimised source conditions, we determined MRM parameters. We found that GGPP readily lost a phosphate group in the MS source giving a prominent *m/z* 369.2 ion, corresponding to deprotonated GGP. The $(M-H)^-$ ion at *m/z* 449 was also present, albeit at a lower intensity. We thus selected *m/z* 369.2 > 79.0 as the quantitative transition for both GGPP and GGP, with no risk of interference between them since the two molecules were well separated in the chromatographic dimension (Fig. 3). One and two additional qualitative transitions were found for GGP (*m/z* 369.2 > 97.0) and GGPP (*m/z* 369.2 > 97.0 and 449.2 > 97.0), respectively. Cone voltage and collision energies were tuned for maximal sensitivity and under optimized conditions, injections as low as 500 and 100 fg on column could be detected for GGPP and GGP, respectively.

Sample preparation

Once we had an analytical method which was able detect trace levels of GGPP and GGP, we attempted to optimize their extraction from plant tissues. We used wild-type tomato fruits and first tested different extraction solvents: acetonitrile:water (80:20, v/v), ethylacetate (in this particular case with evaporation and reconstitution in acetonitrile:water (80:20, v/v) since ethylacetate was incompatible as an injection solvent), methanol and methanol:water:NH_4OH (70:30:0.05, v/v/v) (Fig. 4). Unanticipatedly, results were very different, with acetonitrile:water (80:20, v/v) being the solvent which seemed to best preserve GGPP and ethylacetate the one which led to highest conversion to GGP (possibly due to the evaporation step). Furthermore, acetonitrile:water (80:20, v/v) was the solvent which provided the best extraction yield, determined as the sum of GGPP and GGP peaks. Based on these considerations, we selected acetonitrile:water (80:20, v/v) as the solvent of choice for GGPP extraction.

The observation that different solvents may lead to different rates of conversion from GGPP to GGP during extraction prompted us to test whether the typical sample preparation steps of quenching, drying and solvent evaporation could also have an impact on the GGPP/GGP ratio. Using acetonitrile:water (80:20, v/v) as extraction solvent in all cases, we observed that quenching the fresh fruits in liquid nitrogen prior to grinding and extraction had a significant effect in preserving GGPP (Fig. 5; *t*-test calculated on GGPP/GGP ratios, n = 3, p = 0.002). By contrast, after quenching there was no difference if frozen or lyophilised tissues were used (*t*-test,

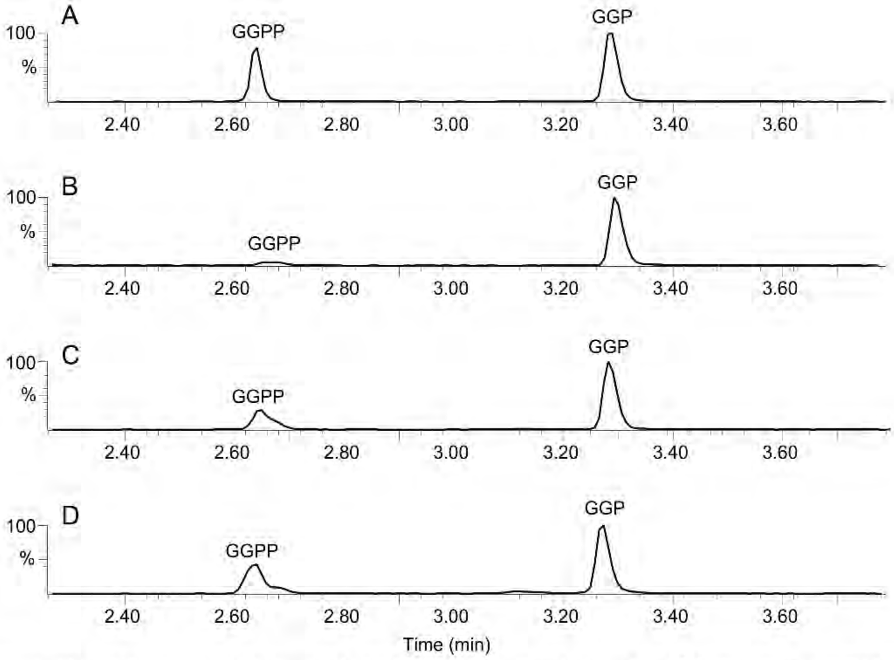

Fig. 4 Chromatograms for wild-type tomato fruits extracted with different solvents or solvent mixtures. **A** Acetonitrile:water (80:20, v/v); **B** ethylacetate; **C** methanol; **D** methanol:water:NH_4OH (70:30:0.05, v/v/v). For this experiment, fruits were not quenched in liquid N_2 prior to extraction

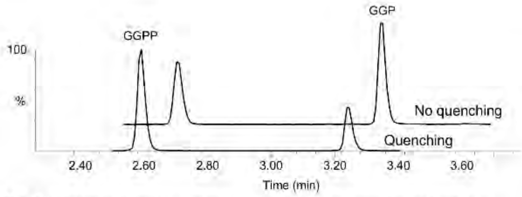

Fig. 5 Chromatograms for wild-type tomato fruits submitted to quenching in liquid N_2 immediately after sample collection or direct extraction in acetonitrile:water (80:20, v/v)

n = 3, p = 0.12). It should however be noted that, from a practical viewpoint, we found it much easier to grind lyophilised than fresh tissues using stainless steel beads in a tissue lyser. In addition, since GGPP and GGP have phosphate groups which may bind to metal cations, we tested the use of metal versus glass beads and found no difference between them. Finally, evaporation at 40 °C of the extraction solvent followed by reconstitution in the same solvent, namely acetonitrile:water (80:20, v/v), caused partial degradation of GGPP into GGP (*t*-test, n = 3, p = 0.02). Taken together, we thus recommend to quench the fruits as soon as they have been collected, lyophilise them as it makes subsequent steps easier, and avoid any evaporation during sample preparation to best preserve GGPP.

Method calibration and validation

Spiking experiments with known concentrations of GGPP and GGP in plant extracts showed that matrix effects were negligible in tomato fruits. Therefore, the external calibration approach was selected and further evaluated during the method validation. Using linear calibration models, the r^2 were > 0.99 for both GGPP and GGP and back-calculated concentrations were always within ± 10% of the true concentrations (Additional file 1: Tables S1 and S2). Specificity was excellent in fruit samples (Figs. 4 and 5). Precision and accuracy were determined at 4 different concentrations which were expected to cover the physiological concentrations in different mutants. RSD% (for precision) and deviations (for accuracy) always fell within 10% and 90–115%, respectively (Table 1). The fact that accuracy values were within acceptable ranges for both GGPP and GGP indicate that no significant conversion from GGPP to GGP occurred during the sample preparation process. The method's limits of quantitation were 1 ng/mL (or 50 ng/g DW) and 0.17 ng/mL (or 8.5 ng/g DW) for GGPP and GGP, respectively. The limits of detection were 0.2 ng/mL and 0.03 ng/mL for GGPP and GGP, respectively. Taken together, these results demonstrate that the developed method is reliable and can be applied to the analysis of tomato fruits from various backgrounds.

Application to tomato fruits

To further validate our approach, we applied the developed method to the analysis of fruits from three "Micro-Tom" tomato genotypes: WT and two knockout mutants which lack one functional GGPPS (*slg2* and *slg3*). Fruits from these lines were tagged in the plant at the breaker (B) stage, i.e. when the first symptoms of colour change due to chlorophyll loss and carotenoid accumulation were visually detected. Ten days later, all fruits had acquired the characteristic red colour of ripe fruit. At this point (B + 10), fruits were collected from the plant and pericarp samples were snap-frozen in liquid nitrogen for subsequent lyophilisation. Levels of GGPP and GGP were significantly reduced in lyophilised fruit samples from *slg2* and *slg3* samples as compared to the WT (Fig. 6). Regarding GGPP levels specifically, WT, *slg2* and *slg3* contained 1.35, 0.50 and 0.36 µg/g DW, respectively. One-way ANOVA revealed significant differences between genotypes ($F_{2,7} = 181.77$, $p < 0.001$). Moreover, a Holm-Sidak post-hoc test showed that the levels of GGPP were significantly higher in *slg2* than in *slg3* (p = 0.037). This is consistent with the reported phenotype of carotenoid accumulation in these mutants, as described by Barja et al. [7]. These findings are interesting as they shed light on the role of different GGPPS paralogs in tomato fruit ripening [7]. Our results hence confirm the predominant role of SlG3 for the synthesis of GGPP required for the burst of carotenoids that changes the fruit colour from green to red when ripe. GGP levels were much lower than those of GGPP, with 0.087, 0.041 and 0.039 µg/g DW in the WT, *slg2* and *slg3*, respectively. This represents less than 10% of the actual GGPP levels

Table 1 Precision and accuracy values obtained for GGPP and GGP in tomato fruits

	Precision (RSD%, n = 4)				**Accuracy (%, n = 4)**			
	C1	**C2**	**C3**	**C4**	**C1 (%)**	**C2 (%)**	**C3 (%)**	**C4 (%)**
GGPP	9.8	6.6	7.6	4.7	105	99	90	114
GGP	8.9	6.9	3.3	2.1	95	93	92	90

See "Methods" section for details about the actual concentrations corresponding to C1–C4

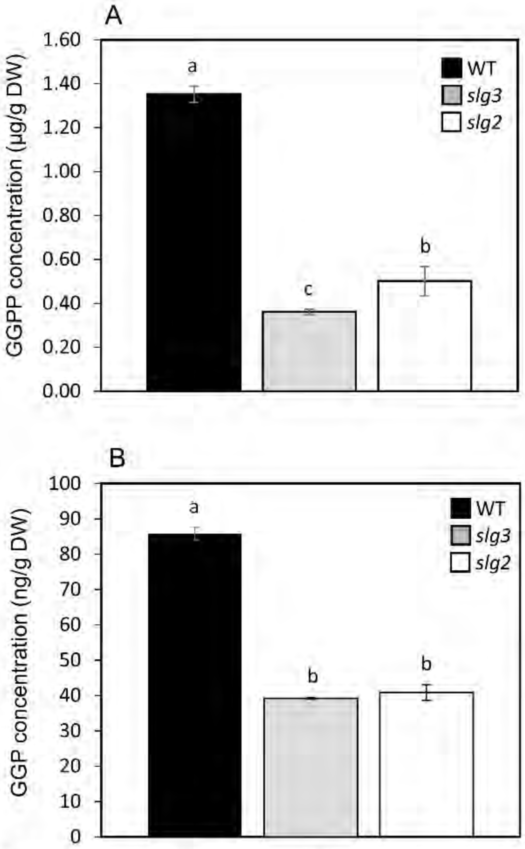

Fig. 6 GGPP and GGP levels in *slg2* and *slg3* compared to WT tomato fruit. **A** GGPP absolute concentrations in WT, *slg2*, *slg3* B + 10 fruits; **B** GGP absolute concentrations in WT, *slg2*, *slg3* B + 10 fruits. Data are the means of three to four biological replicates (± SE). a–c significant differences between genotypes as detected by one-way ANOVA followed by post-hoc tests ($p < 0.05$)

and confirms that our method is gentle enough to prevent GGPP hydrolysis to a large extent.

Conclusion

Our study establishes appropriate separation and detection conditions for GGPP and GGP without the need for ion-pairing or derivatization agents which may impact sensitivity and lengthen the extraction process. We show that reversed-phase chromatography at alkaline pH coupled to tandem mass spectrometry provides good peak shapes and sufficient sensitivity to enable the precise and accurate quantification of low levels of GGPP and GGP *in planta*. We applied our method to the analysis of ripe fruit from wild-type tomato and two knockout mutants of the main plastid-localised GGPPS isoforms. As expected, levels in the mutants were significantly lower than in the wild-type, thereby confirming the validity of our approach. Our method will be useful to identify new proteins and enzyme functions in a panoply of GGPP-dependent isoprenoid biosynthetic pathways with a view to improving tomato fruit quality and nutrition. In addition, the method may be extended to the detection of other prenyldiphosphates from the terpenoid pathway such as GPP and FPP to monitor new biotechnological approaches for plant and fruit fortification.

Methods

Chemicals

GGPP and GGP were purchased from Echelon Biosciences and Larodan, respectively. For HPLC–MS analyses, milli-Q water, LC–MS grade acetonitrile from VWR, and LC–MS grade NH_4OH solution (25%) from Merck were used. For sample preparation, HPLC grade acetonitrile from Merck (Supelco) was employed.

Plants

Tomato used in this study was *Solanum lycopersicum*, cv. Micro-Tom. Three genetic backgrounds were used, the wild-type (WT), as well as the CRISPR mutant alleles *slg2-1* and *slg3-1* [7]. Plants were grown in a chamber under controlled conditions (14 h under white light—150 µmol m^{-2} s^{-1}—at 25 ± 1 °C and 10 h in the dark at 22 ± 1 °C). Fruits were tagged at the breaker (B) stage, harvested at B + 10 and quenched immediately in liquid nitrogen according to [17]. The samples were then stored at −80 °C until lyophilisation in a Labconco benchtop freeze-dryer.

Sample preparation

GGPP and GGP were extracted from lyophilised tomato fruits pericarp. Twenty mg of dry tissues were ground with 3 stainless steel UFO-beads (3.5 mm diameter) in a 2.0 mL microcentrifuge tube. Then, fifty volumes of acetonitrile:water (80:20, v/v) were added and the mixture was shaken in a tissue lyser (TissueLyser LT, QIAGEN) with a frequency of 50 Hz for 5 min. The homogenate was sonicated at 60 Hz for 1 min and centrifuged at 16,000×*g* for 10 min at room temperature. After centrifugation, 200 µL of supernatant was collected and transferred to glass vials for HPLC–MS/MS analysis.

HPLC–MS/MS conditions

GGPP and GGP analysis was performed on a binary pump Acquity UPLC connected to a TQ-XS triple quadrupole (Waters), both controlled by MassLynx 4.2 (Waters). An Acquity UPLC BEH C18 column (2.1 × 50 mm, 1.7 µm, Waters) was used for the separation. The flow rate was set to 0.4 mL/min. Mobile phases consisted of milli-Q water + 0.05% NH_4OH (phase A) and acetonitrile (ACN) + 0.05% NH_4OH (phase B). The gradient started at 5% phase B and increased linearly to 41% B in 4.0 min, then to 100% B in 0.5 min. At the end of the run, a 2.0 min wash at 100% B for 2.0 min followed by re-equilibration at 5% B for 2.0 min was implemented. The column was maintained at 25 °C. The injection volume was of 2 µL (fixed loop injector, partial loop with needle overfill mode) and the autosampler temperature was kept at 15 °C. The strong needle wash was a mix of ACN:H_2O (90:10, v/v) and the weak needle wash a mix of ACN:H_2O (10:90, v/v).

The mass spectrometer was operated in electrospray negative ionisation using a capillary voltage of -2 kV, a source temperature of 150 °C, a desolvation temperature of 500 °C, a desolvation gas flow of 1000 L/h, a cone gas flow of 350 L/h, and a nebuliser gas flow of 7 bars. The StepWave was set to normal transmission values. The multiple reaction monitoring (MRM) mode was employed to maximize sensitivity. MRM transitions for both GGPP and GGP were *m/z* 369.2 > 79.0 (quantitative, Q) and *m/z* 369.2 > 97.0 (qualitative, q1). For GGPP, an additional qualitative transition (q2, *m/z* 449.2 > 79.0, q2) was set. Cone and collision energy voltages for Q, q1 and q2 transitions were 15 and 21 V, 15 and 19 V, and 10 and 20 V, respectively. The dwell time was fixed to 136 ms. The HPLC flow was diverted to the waste from 0.0 to 2.25 min, and from 3.8 min to the end of the run.

Quantification and method validation

Quantification was done by external calibration using standard concentrations in acetonitrile:water (50:50, v/v) at 1, 2, 4, 8, 16 and 32 ng/mL for GGPP, and 0.125, 0.25, 0.5, 1, 2 and 4 ng/mL for GGP. A linear calibration with the origin excluded and weighted by 1/x was applied. The response function of the calibration curve was assessed by back-calculating the concentrations based on the linear model and accepting it if the deviation was within 15% for all calibration points. Selectivity was evaluated by analysing non-spiked samples and samples spiked with a mixture of GGPP and GGP at 15 and 3 ng/mL, respectively. Intra-day precision and accuracy were expressed as percentage of relative standard deviation (%RSD) and percentage of deviation from true values, respectively, and were determined from samples of the *slg3* mutant spiked at 1, 3, 6 and 12 ng/mL (respectively C1–C4) for GGPP and 0.17, 0.5, 1, and 2 ng/mL (respectively C1–C4) for GGP (n = 4 for each concentration). Since GGPP and GGP are constitutively present in plants, including the *slg3* mutant, unspiked samples were also analysed and their concentrations subtracted from those of the spiked samples. Limits of quantification (LOQ) were determined as the smallest spiked concentration which gave precision and accuracy values within 15% and 80–120%, respectively. The instrumental detection limit was evaluated on standard solutions which gave signal-to-noise ratios of 3. Data processing was performed in TargetLynx XS (Waters).

Statistics

All data in this study were the means of two independent experiments and the result of three to four technical or biological replicates, except the comparison of extraction solvents for which only two technical replicates were performed. No data were excluded from the analysis. The results were analyzed and compared for statistical differences by a two-sample, unequal variance (heteroscedastic) Student's t-test (Excel 2016), or by one-way ANOVA followed by Holm-Sidak post-hoc tests for pair-wise comparisons (SigmaPlot v.15).

Supplementary Information

The online version contains supplementary material available at https://doi.org/10.1186/s13007-023-01034-w.

Additional file 1: Table S1. Response function for GGPP with calibration equation y = 274.40x − 46.08 (R = 0.9990). **Table S2.** Response function for GGP with calibration equation y = 1405.94x − 4.6 (R = 0.9990).

Acknowledgements
The authors wish to thank Mrs. Sylvie Guinchard for her technical assistance.

Author contributions

WZ and GG conceived the original research. WZ, ME and GG carried out the research and data analysis. WZ and GG wrote the original draft. All authors contributed to draft editing and approved the manuscript.

Funding
This work was funded by the Swiss National Science Foundation (Project 310030_208000 to F.K.) and by the University of Neuchâtel.

Data availability

The datasets used for the current study are available from the corresponding author on reasonable request.

Declarations

Ethics approval and consent to participate

Not applicable.

Consent for publication

Not applicable.

Competing interests

The authors declare that they have no competing interests.

Received: 4 April 2023 Accepted: 1 June 2023

References

1. Gershenzon J, Dudareva N. The function of terpene natural products in the natural world. Nat Chem Biol. 2007;3(7):408–14.
2. Tholl D. Biosynthesis and biological functions of terpenoids in plants. Adv Biochem Eng Biotechnol. 2015;148:63–106.

3. Beck G, Coman D, Herren E, Ruiz-Sola MA, Rodríguez-Concepción M, Gruissem W, Vranová E. Characterization of the GGPP synthase gene family in *Arabidopsis thaliana*. Plant Mol Biol. 2013;82(4–5):393–416.
4. Ruiz-Sola M, Coman D, Beck G, Barja MV, Colinas M, Graf A, Welsch R, Rütimann P, Bühlmann P, Bigler L, et al. *Arabidopsis* GERANYLGERANYL DIPHOSPHATE SYNTHASE 11 is a hub isozyme required for the production of most photosynthesis-related isoprenoids. New Phytol. 2016;209(1):252–64.
5. Zhou F, Pichersky E. The complete functional characterisation of the terpene synthase family in tomato. New Phytol. 2020;226(5):1341–60.
6. Barja MV, Rodriguez-Concepcion M. Plant geranylgeranyl diphosphate synthases: every (gene) family has a story. aBIOTECH. 2021;2(3):289–98.
7. Barja MV, Ezquerro M, Beretta S, Diretto G, Florez-Sarasa I, Feixes E, Fiore A, Karlova R, Fernie AR, Beekwilder J, et al. Several geranylgeranyl diphosphate synthase isoforms supply metabolic substrates for carotenoid biosynthesis in tomato. New Phytol. 2021;231(1):255–72.
8. Zhou F, Wang C-Y, Gutensohn M, Jiang L, Zhang P, Zhang D, Dudareva N, Lu S. A recruiting protein of geranylgeranyl diphosphate synthase controls metabolic flux toward chlorophyll biosynthesis in rice. Proc Natl Acad Sci. 2017;114(26):6866–71.
9. Nürenberg G, Volmer DA. The analytical determination of isoprenoid intermediates from the mevalonate pathway. Anal Bioanal Chem. 2012;402(2):671–85.
10. Martinis J, Kessler F, Glauser G. A novel method for prenylquinone profiling in plant tissues by ultra-high pressure liquid chromatography–mass spectrometry. Plant Methods. 2011;7(1):23.
11. Zita W, Bressoud S, Glauser G, Kessler F, Shanmugabalaji V. Chromoplast plastoglobules recruit the carotenoid biosynthetic pathway and contribute to carotenoid accumulation during tomato fruit maturation. PLoS ONE. 2022;17(12): e0277774.
12. Sugimoto H, Iguchi M, Jinno F. Bioanalysis of farnesyl pyrophosphate in human plasma by high-performance liquid chromatography coupled to triple quadrupole tandem mass spectrometry and hybrid quadrupole Orbitrap high-resolution mass spectrometry. Anal Bioanal Chem. 2017;409(14):3551–60.
13. Chhonker YS, Haney SL, Bala V, Holstein SA, Murry DJ. Simultaneous quantitation of isoprenoid pyrophosphates in plasma and cancer cells using LC–MS/MS. Molecules. 2018;23(12):3275.
14. Henneman L, van Cruchten AG, Denis SW, Amolins MW, Placzek AT, Gibbs RA, Kulik W, Waterham HR. Detection of nonsterol isoprenoids by HPLC–MS/MS. Anal Biochem. 2008;383(1):18–24.
15. McCaskill D, Croteau R. Procedures for the isolation and quantification of the intermediates of the mevalonic acid pathway. Anal Biochem. 1993;215(1):142–9.
16. Ma Y, Chen Q, Wang Y, Zhang F, Wang C, Wang G. Heteromerization of short-chain trans-prenyltransferase controls precursor allocation within a plastidial terpenoid network. J Integr Plant Biol. 2023;65(5):1170–82.
17. Alba R, Payton P, Fei Z, McQuinn R, Debbie P, Martin GB, Tanksley SD, Giovannoni JJ. Transcriptome and selected metabolite analyses reveal multiple points of ethylene control during tomato fruit development. Plant Cell. 2005;17(11):2954–65.

Publisher's Note